UNIVERSITY OF CALIFORNIA,
IRVINE

Statistical modeling of climate change impacts on ecosystems and wildfire in the Western U.S.

DISSERTATION

submitted in partial satisfaction of the requirements
for the degree of

DOCTOR OF PHILOSOPHY

in Earth System Science

by

Shane Riley Coffield

Dissertation Committee:
Professor James T. Randerson, Chair
Professor Efi Foufoula-Georgiou
Professor Michael L. Goulden
Professor Padhraic Smyth

2022

DEDICATION

To the activists, leaders, and fellow scientists fighting for our future. May an improved understanding of the Earth system help build a more sustainable and just society.

TABLE OF CONTENTS

LIST OF FIGURES

LIST OF TABLES

ACKNOWLEDGEMENTS

My PhD research was supported by the National Science Foundation Graduate Research Fellowship Program (grant DGE-1839285). I am also grateful to the Jenkins Family for their financial support to the Department of Earth System Science at UC Irvine. I appreciate the scientific journals *(International Journal of Wildland Fire*, *AGU Advances*, and *Global Change Biology*) and publishers (CSIRO and Wiley) which have allowed me to share my work Open Access with the community. I have also greatly benefitted from professional engagements with NSF Machine Learning and Physical Sciences (MAPS) research traineeship, the California Ecosystem Futures project funded by UC Lab Fees, and the Center for Ecosystem Climate Solutions funded by the California Strategic Growth Council.

I also acknowledge my presence on the unceded territories of the Acjachemen and Tongva peoples, the original inhabitants and stewards of present-day Irvine, many of whom maintain strong ties to this area. I strongly advocate for the inclusion of Native perspectives and traditional knowledge in addition to the Western scientific knowledge presented in this dissertation, particularly regarding the protection and stewardship of ecosystems.

I would like to express my deep gratitude to the advisors on my committee. My primary advisor, Dr. Jim Randerson, has been a constant source of scientific inspiration and guidance. I truly admire him as a scholar whose expertise spans many disciplines across Earth system science and ecology. This dissertation absolutely would not have been possible without his continued enthusiasm, encouragement, positivity, and ideas which have motivated me over the past five years. His genuine passion for science is infectious and will surely have a lasting impact on me.

My co-advisors and committee members Drs. Mike Goulden, Efi Foufoula-Georgiou, and Padhraic Smyth have also provided immeasurable guidance. I greatly appreciate their perspectives across ecology, statistics, engineering, and computer science, which have helped make this a truly multidisciplinary research endeavor. I am grateful for their expertise and consistently positive character.

It has been a great privilege to have been a part of the ESS community at UCI. My fellow lab members and graduate students have provided invaluable social support and a sense of belonging which have been critical to my success in the department. Aside from my research, I have learned so much from being involved in the Inclusive Excellence Committee, graduate student leadership, and the CLEAN Education organization.

Finally, I am extremely privileged to have felt supported as a scientist throughout my educational career both before and during my PhD. I have consistently been surrounded by family, friends, and mentors who believe in me and encourage me. My parents have always

enabled me to pursue my interests, buying me books and a telescope as a kid and teaching me that I could achieve whatever I set my mind to. I'm grateful to my brother, aunts and uncles, grandparents, and friends who have consistently supported me and shown interest in my pursuits. I also appreciate the teachers who went above and beyond to provide opportunities for me, especially in math and science. I strive to pay it forward and help more young people have the opportunities and support that I had. Most importantly, I am incredibly grateful for my partner, Matt, who has been my biggest supporter for the past five years. He has been by my side every day of my PhD, and I am continually inspired by his work ethic, kind heart, and passion for making the world a better place.

The text of chapter 1 in this dissertation is a reprint of the material adapted from "Machine learning to predict final fire size at the time of ignition." *International Journal of Wildland Fire*, 28, 861–873, 2019, used with permission from CSIRO. The co-authors listed in this publication are C.A. Graff, Y. Chen, P. Smyth, E. Foufoula-Georgiou, and J.T. Randerson.

The text of chapter 2 in this dissertation is a reprint of the material adapted from "Climate-driven limits to future carbon storage in California's wildland ecosystems." *AGU Advances*, 2(3), e2021AV000384, 2021, used with permission from Wiley. The co-authors listed in this publication are C.A. Graff, Y. Chen, P. Smyth, E. Foufoula-Georgiou, and J.T. Randerson.

The text of chapters 3 and 4 in this dissertation are currently unpublished material used with the permission of co-authors C.D. Vo, J.A. Wang, M.L. Goulden, G. Badgley, D. Cullenward, W.R.L. Anderegg, J.T. Randerson, C.A. Graff, V. Bhoot, E. Foufoula-Georgiou, and P. Smyth.

VITA

Shane Riley Coffield

EDUCATION

Ph.D. Earth System Science, University of California, Irvine — Aug 2022
Dissertation: Statistical modeling of climate change impacts on ecosystems and wildfire in the Western US.
Thesis advisor: Dr. James Randerson
Committee members: Dr. Michael Goulden, Dr. Efi Foufoula-Georgiou, Dr. Padhraic Smyth

M.S. Earth System Science, University of California, Irvine — Dec 2019

B.S. Geophysical Sciences with Honors, The University of Chicago — June 2017
B.S. Environmental Science, The University of Chicago — June 2017

PROFESSIONAL EXPERIENCE

University of California, Irvine - Teaching Assistant in Earth System Science — Irvine, CA
Food & Water Systems — Sep 2018 - Dec 2018
Professor: Dr. Nathan Mueller

Programming for Environmental Science — Jan 2019 - Mar 2019
Professor: Dr. James Randerson

On Thin Ice — Mar 2019 - Jun 2019
Professor: Dr. Julie Ferguson

NASA Marshall Space Flight Center - Research Intern — Huntsville, AL
Earth Sciences Branch — Jun 2016 - Aug 2017
Advisor: Dr. Mohammad Al-Hamdan

The University of Chicago - Undergraduate Research — Chicago, IL
Satellite monitoring of water quality in the Great Lakes — Sep 2016 - Jun 2017
Advisor: Dr. Maureen Coleman

IBM Almaden Research Center - Research Intern — San Jose, CA
Machine learning with Hierarchical Temporal Memory — Jun 2015 - Aug 2015
Advisor: Dr. Wayne Imaino

PEER-REVIEWED PUBLICATIONS

PUBLISHED

Chen, Y., Hantson, S., Andela, N., Coffield, S.R., Graff, C.A., Morton, D.C., Ott, L.E., Foufoula-Georgiou, E., Smyth, P., Goulden, M.L., Randerson, J.T. (2022). California wildfire spread derived using VIIRS observations and an object-based tracking system. *Scientific Data, 9*(1), 1-15. https://doi.org/10.1038/s41597-022-01343-0

Coffield, S.R., Hemes, K.S., Koven, C.D., Goulden, M.L., Randerson, J.T. (2021) Climate-driven limits to future carbon storage in California's wildland ecosystems. *AGU Advances, 2*(3), e2021AV000384. https://doi.org/10.1029/2021AV000384

Chen, Y., Randerson, J. T., Coffield, S. R., Foufoula-Georgiou, E., Smyth, P., Graff, C. A., ... & Ott, L. E. (2020). Forecasting global fire emissions on sub-seasonal to seasonal (S2S) timescales. *Journal of Advances in Modeling Earth Systems*, *12*(9), e2019MS001955. https://doi.org/10.1029/2019MS001955

Graff, C. A., Coffield, S. R., Chen, Y., Foufoula-Georgiou, E., Randerson, J. T., & Smyth, P. (2020). Forecasting daily wildfire activity using Poisson regression. *IEEE Transactions on Geoscience and Remote Sensing, 58*(7), 4837-4851. https://doi.org/10.1109/TGRS.2020.2968029

Coffield, S.R., Graff, C.A., Chen, Y., Smyth, P., Foufoula-Georgiou, E., Randerson, J.T. (2019) Machine learning to predict final fire size at the time of ignition. *International Journal of Wildland Fire*, *28*, 861–873. https://doi.org/10.1071/WF19023

Al-Hamdan, M., Crosson, W., Burrows, E., Coffield, S.R., & Crane, B. (2019). Development and validation of improved PM2.5 models for public health applications using remotely sensed aerosol and meteorological data. *Environmental Monitoring and Assessment*, *191*(2), 1-16. https://doi.org/10.1007/s10661-019-7414-3

IN PRESS

Coffield, S.R., Vo, C.D., Wang, J.A., Goulden, M.L., Badgley, G., Cullenward, D., Anderegg, W.R.L., Randerson, J.T. Using remote sensing to quantify the additional climate benefits of California forest carbon offset projects. *Global Change Biology.*

IN REVIEW

Wu, C, Coffield, S.R., Goulden, M.L., Randerson, J.T., Trugman, A.T., Anderegg, W.R.L. Diverging estimates in US forest carbon storage potential from climate risks. *Nature*.

Graff, C. A., Coffield, S. R., Chen, Y., Foufoula-Georgiou, E., Randerson, J. T., Smyth, P. Forecasting daily wildfire spread with convolutional neural networks. *IEEE Transactions on Geoscience and Remote Sensing.* (in revision)

Gorris, M., Randerson, J.T., Coffield, S.R., Treseder, K.T., Zender, C.S., Xu, C., Manore, C.A. Climate controls on the spatial pattern of West Nile virus incidence in the United States. *Environmental Health Perspectives*. (in revision)

AWARDS AND HONORS

Finalist for the UC President's Postdoctoral Fellowship — June 2022

Outstanding Contributions to the Earth System Science Department — June 2021

NSF Graduate Research Fellowship — Sep 2018 - Aug 2022

NASA Earth and Space Science Fellowship (Award declined) — Mar 2018

Honorary Fellow, NSF Machine Learning & Physical Sciences NRT — Sep 2017 - Jun 2021

UC Irvine Diversity Recruitment Fellowship — Sept 2017

PRESENTATIONS

Coffield, S.R. Statistical modeling of climate change impacts on ecosystems and wildfire in the Western US. Invited oral presentation at the University of Utah School of Biological Sciences, Salt Lake City, UT. Apr 2022.

Chinowsky, C. Clark, K., Coffield, S.R., Dye, A., O'Connor, J. Data and policies to increase LGBT+ retention in STEM. Workshop at the AAAS Annual Meeting, virtual. Feb 2022.

Coffield, S.R., Vo, C., Wang, J., Anderegg., W.R.L., Goulden, M.L., Randerson, J.T. Remote sensing-based evaluation of California's forest carbon offset projects. Poster presentation at the American Geophysical Union Fall Meeting, New Orleans, LA. Dec 2021.

Coffield, S.R., O'Connor, J., Dye, A., Chinowsky, C., Clark, K. Improving LGBTQ+ retention in STEM: A transatlantic perspective on current barriers and best practices. Poster presentation at the American Geophysical Union Fall Meeting, New Orleans, LA. Dec 2021.

Chinowsky, C. Clark, K., Coffield, S.R., Dye, A., O'Connor, J. Data and policies to increase LGBT+ retention in STEM. Workshop at the National Science Policy Network Symposium, virtual. Nov 2021.

Coffield, S.R., Hemes, K.S., Koven, C.D., Goulden, M.L., Randerson, J.T. Climate-driven limits to future carbon storage in California's wildland ecosystems. NASA JPL Carbon Cycle Group meeting, Pasadena, CA. Jan 2021.

Coffield, S.R., Hemes, K.S., Koven, C.D., Goulden, M.L., Randerson, J.T. Climate-driven limits to future carbon storage in California's wildland ecosystems. Poster presentation at the American Geophysical Union Fall Meeting, virtual. Dec 2020.

Coffield, S.R., Graff, C., Chen, Y., Smyth, P., Foufoula-Georgiou, E., Randerson, J.T. Machine learning to predict final fire size at the time of ignition. Invited oral presentation at the UC Irvine Center for Occupational and Environmental Healthy Symposium, Irvine, CA. Feb 2020.

Coffield, S.R., Graff, C., Chen, Y., Smyth, P., Foufoula-Georgiou, E., Randerson, J.T. Machine learning to predict final fire size at the time of ignition. Poster presentation at the American Geophysical Union Fall meeting, San Francisco, CA. Dec 2019

Coffield, S.R., Graff, C., Chen, Y., Smyth, P., Foufoula-Georgiou, E., Randerson, J.T. Machine learning to predict final fire size at the time of ignition. Invited oral presentation at the UC Irvine Machine Learning Nexus, Irvine, CA. Oct 2019.

Coffield., S.R. Crosson, W.L., Al-Hamdan, M.Z., Barik, M.G. Satellite remote sensing for modeling and monitoring of water quality in the Great Lakes. Poster presentation at the American Geophysical Union Fall Meeting, New Orleans, LA. Dec 2017.

PROFESSIONAL AFFILIATIONS

American Geophysical Union — Dec 2017 - Present
Voices for Science, 2020 cohort

National Science Policy Network — Sep 2020 - Present
Science Diplomacy Exchange and Learning (SciDEAL) fellow
Co-founder of UC Irvine chapter

Phi Beta Kappa Honor Society — June 2017 - Present
The University of Chicago

POPULAR PRESS

Coffield, S. Climate change impacts on California ecosystems. *NPR Academic Minute*. Oct 2021.

Brazil, B. Decline in carbon-eating vegetation will make it even harder for California to combat climate change. *LA Times Daily Pilot*. Jul 2021.

Nguyen, L. UCI researchers develop algorithm to help predict the final size of a wildfire. *LA Times Daily Pilot*. Oct 2019.

Martinez, A. UCI Fire Algorithm. *Take Two*, NPR KPCC. Sep 2019.

Riley, G. How A.I. can help predict wildfire outcomes. *The Jefferson Exchange*, Jefferson Public Radio. Sep 2019

Grove, C. Can artificial intelligence help predict Alaska wildfire growth? *Alaska Public Media.* Sep 2019.

EXTRACURRICULAR ACTIVITIES

Journal Referee: *Stochastic Environmental Research and Risk Assessment* (2020), *Science of the Total Environment* (2020, 2022)

Climate, Literacy, Empowerment, And iNquiry (CLEAN) Oct 2017 - May 2022
K-12 Outreach, Board Member

Undergraduate student mentorship Jun 2020 - Sep 2021
Cassandra Vo, UC Irvine, B.A. Environmental Science and Policy

UC Irvine Earth System Science Student Mentor Sep 2020 - June 2022

UC Irvine Earth System Science Graduate Student Representative Sep 2020 - June 2021

American Geophysical Union Voices for Science fellow Apr 2020 - Mar 2021

National Science Policy Network Sep 2020 - Present
Science Diplomacy Exchange and Learning (SciDEAL) fellow, Co-founder of UC Irvine chapter

Seed Consulting Group Mar 2021 - May 2021
Received “Innovation Award”

Diverse Educational Community & Doctoral Experience (DECADE) Oct 2018 - Sep 2020
Student Representative

Inclusive Excellence Committee, UC Irvine Earth System Science Jun 2020 - Jun 2022

ABSTRACT OF THE DISSERTATION

Statistical modeling of climate change impacts
on ecosystems and wildfire in the Western U.S.

by

Shane Riley Coffield

Doctor of Philosophy in Earth System Science

University of California, Irvine, 2022

Professor James T. Randerson, Chair

Ecosystems in the Western US face a combination of climate-driven threats including warming temperature, drought, and wildfire. How ecosystems respond to these threats is directly relevant for human health, water availability, and carbon storage toward climate mitigation, among other services. However, there currently exist large uncertainties regarding the impact of a changing climate on ecosystems and the reliability of these ecosystems to serve as carbon sinks going forward.

In my dissertation I used statistical and machine learning techniques along with large-scale geospatial datasets to explore several questions at the intersection of climate change and ecosystems. In my first study, I developed a new framework for wildfire prediction. I found that vapor pressure deficit at the time of ignition and the density of black spruce trees surrounding ignition sites could be used to predict in Alaskan ecosystems whether a fire would become large. These two pieces of information could help managers triage wildfires to protect vulnerable ecosystems given limited resources. In my second chapter, I quantified the future impacts of climate change on carbon storage in

California ecosystems, finding that warming temperatures are likely to drive a net loss of carbon and increase the challenges associated with meeting the State's climate mitigation goals. Projected losses were greatest for the mid-elevation mountains, northern coast region, and locations of current forest carbon offset projects. This study also revealed the largest sources of uncertainty to future ecosystem projections, most notably the uncertainty in future precipitation for California and uncertainty in tree species migration rates relative to the climate velocity. In my third chapter, I focused on California's forest carbon offset projects and used remote sensing datasets to assess whether these projects have led to additional carbon sequestration in the 5-10 years since their initiation. Five lines of evidence related to carbon trends, harvest rates, and species composition in projects relative to similar forests suggested that in general our portfolio of projects has not led to detectable carbon sequestration beyond what would have otherwise occurred. Finally, in my fourth chapter, I quantified future wildfire risk across California based on climate and vegetation projections from my second chapter. I found that California is likely to see substantial increases in wildfire over this century, especially in scenarios with increased precipitation and/or shrub cover.

The collective results of my research highlight key scientific uncertainties related to the future of ecosystems, particularly the uncertainty in future precipitation. The results of each chapter also offer insights which are relevant for effective ecosystem management in a rapidly changing climate. These insights include (1) predicting large fires from the time of ignition, (2) identifying areas of ecosystem vulnerability for carbon sequestration and conservation goals, (3) building a more reliable and systematic framework for assessing

additionality of carbon offsets, and (4) identifying areas of greatest future fire risk, where fuels management could have the greatest impact on reducing extreme wildfire outcomes.

INTRODUCTION

Climate change and Western US ecosystems

Recent decades have been characterized by rapid ecosystem changes in the Western US, especially in response to predominantly climate-driven disturbances like wildfire, drought, and biotic agents (Anderegg et al., 2020). Some direct human factors are also at play - for example, fuel buildup due to fire suppression, changes in agriculture and grazing, and expansion of the wildland-urban interface - and can compound climate-driven impacts (Buckley Biggs & Huntsinger, 2021; Calkin et al., 2005; Li et al., 2022; Steel et al., 2015). Of these changes, arguably the most obvious and consequential has been the substantial increase in burned area, both in boreal Alaska and the semi-arid forests and shrublands of the lower Western US. These wildfires expose millions of people to poor air quality and have economic impacts in the billions of dollars for California alone (Burke et al., 2021; D. Wang et al., 2020). The increased fire activity is largely related to rising temperatures, and particularly periods of resulting high vapor pressure deficit (VPD) (Abatzoglou & Williams, 2016; Faivre et al., 2016; Gutierrez et al., 2021; Juang et al., 2022; Wiggins et al., 2016). In the case of Alaska, increased lightning has also been identified as a driver (Veraverbeke et al. 2017). In Alaska as well as 2008 and 2020 in California, extreme lightning events have led to hundreds of concurrent fires. These growing threats to ecosystems, particularly extreme wildfire, underscore the importance of improved fire prediction and optimized use of limited resources to protect vulnerable ecosystems and human populations.

Understanding and predicting the impacts of climate on ecosystems is particularly important given that these ecosystems are also a large potential resource for climate

mitigation through carbon sequestration. Globally, terrestrial ecosystems are known to be a substantial carbon sink, absorbing nearly a third of anthropogenic emissions (Friedlingstein et al., 2019). However, the strength of this carbon sink is much weaker and uncertain in the semi-arid ecosystems of the Western US, given the prevalence of recent wildfires and droughts (Gonzalez et al. 2015; California Air Resources Board, 2019; Fellows & Goulden, 2008). It is also unknown whether these ecosystems will be a source or sink for carbon in the future, especially due to uncertainties in future fire and drought, nutrient availability, CO_2 effects, and adaptation and migration capacity (Anderegg et al. 2020; McDowell et al. 2020). Old-growth forests, including giant sequoia and coastal redwood in California, are large carbon reservoirs that are at high risk due to the rapid rate of climate change relative to particularly long life cycles (Fernández et al., 2015; Shive et al., 2022).

These threats and uncertainties to carbon storage are directly relevant for climate mitigation policies such as California's Climate Change Scoping Plan, including ambitious goals for natural and working lands (California Air Resources Board, 2019) as Natural Climate Solutions (NCS). Through improved land management, the State hopes to reverse the current trend of land carbon emissions and make the land sector a net sink for carbon by mid-century. California also leads one of the world's largest carbon offset programs, with over 100 improved forest management (IFM) projects across the US (37 of which are within California's northern forests). A lack of rigorous accounting of future climate risks in these policies could lead to unmet targets and limited climate benefits while emissions remain high in other sectors.

Two central concepts in carbon offsetting explored in this dissertation are *permanence* and *additionality*. Permanence refers to the lifetime of sequestered carbon,

required to be at least 100 years in California's Cap and Trade system (California Air Resources Board, 2019). Forest offset projects receive risk ratings for carbon reversal back to the atmosphere across categories including disease and wildfire. Currently wildfire risk is chosen as either 2% or 4% for each project over its entire lifetime. This risk calculation does not rigorously account for how wildfire risk may increase in the future in response to changing climate as well as fire impacts on vegetation (e.g., Abatzoglou et al., 2021).

Additionality refers to carbon sequestration being additional to what would otherwise occur in a business-as-usual scenario (CCR 17 § 98 95973), currently defined by a static baseline based on regionally averaged carbon stocks for different forest types. Protocol could be improved by more systematically quantifying both permanence risks and additionality in order to accurately credit carbon offset projects and calculate net emissions.

Modeling of ecosystems

A variety of tools exist to simulate and predict how ecosystems interact with climate and climate change. At a high level these can be grouped into two categories of models: mechanistic/dynamic/process-based models and statistical/data-driven/empirical models. In general, there are pros and cons to each, regarding their reliability for extracting different insights and making predictions. The first category, mechanistic or process-based models, explicitly represents physical or biological processes and responses - for example, the physics equations governing fire spread (Rothermel, 1972) or the physiology of temperature, gas exchange, and water use in plants (Finney et al., 2012). In fire prediction, the FIRETEC model is computationally expensive but commonly used for research purposes

to understand the interactions between fuels, meteorology, and fire behavior (Linn et al., 2002). In terms of simulating ecosystem change more broadly, one example is the Functionally Assembled Terrestrial Ecosystem Simulator, or FATES (Koven et al. 2020; Fisher et al., 2015). These models are particularly useful for illuminating causality in ecosystem change, and making ecosystem predictions in non-analog future conditions where purely data-driven models would otherwise extrapolate.

The second category, statistical or empirical models, are well-suited to leverage the huge quantities of geospatial data available from an increasing proliferation of remote sensing missions such as Landsat. Statistical and/or machine learning techniques can be used to detect changes in time series data (e.g., Linn et al., 2002; Zhu & Woodcock, 2014) and identify relationships between environmental drivers and ecosystem properties. Random forests (RF) are one form of machine learning which have received increasing attention for ecological applications, given their flexibility to capture non-linear relationships, minimize overfitting, and make semi-interpretable predictions (e.g., Belgiu & Drăguţ, 2016; Breiman, 2001; Prasad et al., 2006).

In this dissertation I applied statistical and machine learning techniques to explore patterns in historical data, understand controls on ecosystems, and make predictions about near-term or long-term future change. The selected modeling approaches allowed for unique insights into climate-ecosystem relationships, including quantification of uncertainties from different sources. The use of large-scale datasets also enabled systematic spatial and temporal analyses of change which are otherwise limited to specific field studies or inventory datasets. As a whole, the research reveals the impacts of changing climate on Western US ecosystems which could enable optimized land management and

policies to mitigate further climate outcomes.

Organization of research

In Chapter 1, I focused on boreal Alaska, which is responding to particularly rapid climate warming (Kasischke and Turetsky 2006; Kasischke et al. 2010; Veraverbeke et al. 2017). Given the observed increases in lightning and wildfire in a region where wildfires are typically unmitigated, I developed a simple machine learning-based system for predicting the final size of a fire given the time and location of ignition. I found that two environmental variables - vapor pressure deficit and the fraction of black spruce trees around the ignition site - could be used to classify fires as small, medium, or large with 50% accuracy. Predictability was highest for large fires, with model-predicted large fires ultimately accounting for 75% of burned area. This prediction framework could serve as a decision-support tool for fire management given limited resources, especially as large fires pose an increasing threat to humans, ecosystems, and the climate. This research was published in the *International Journal of Wildland Fire* as:

"Coffield, S.R., Graff, C.A., Chen, Y., Smyth, P., Foufoula-Georgiou, E., Randerson, J.T. (2019) Machine learning to predict final fire size at the time of ignition. *International Journal of Wildland Fire*, *28*, 861–873. https://doi.org/10.1071/WF19023"

In Chapter 2, I developed a set of eco-statistical models to describe the current spatial distribution of aboveground carbon stocks in California, which are increasingly at risk of climate-driven threats. Applying end-of-century future climate to these models, I found that most of the state's natural lands may face a net loss of carbon on the order of 9-16%, directly at odds with State goals to increase total land carbon stocks by 4-5%.

Particularly vulnerable areas include the mid-elevation Sierra Nevada, the northern coastal region, and locations of forest carbon offset projects. Conifers were more vulnerable to future loss than hardwoods, and climate scenarios with net drying of the state led to substantially larger losses than climate scenarios with net increases in precipitation. This study identified a few key scientific bottlenecks and uncertainties to future ecosystem projections in California, including the uncertainty in future precipitation and migration, and the developed risk maps could help inform where different types of management are most needed to preserve existing carbon pools. This research was published in *AGU Advances* as:

"Coffield, S.R., Hemes, K.S., Koven, C.D., Goulden, M.L., Randerson, J.T. (2021) Climate-driven limits to future carbon storage in California's wildland ecosystems. *AGU Advances, 2 (3),* e2021AV000384. https://doi.org/10.1029/2021AV000384"

In Chapter 3, I further investigated the improved forest management (IFM) carbon offset projects discussed in Chapter 2, this time through the lens of *additionality* rather than *permanence* of carbon stocks. "Additionality" refers to offset projects leading to carbon sequestration which would not otherwise occur. I developed a framework with five hypotheses to test whether there was evidence of additionality across the portfolio of 37 IFMs in California, which began as early as 2012. I compared carbon stocks, harvest rates, and species composition for offset projects relative to similar forests, and looked for evidence of change once projects began. In general, I found a lack of sufficient evidence of additionality, suggesting that the current California protocol could be improved to incentivize real carbon gains. This work is currently in press at *Global Change Biology*:

"Coffield, S.R., Vo, C.D., Wang, J.A., Goulden, M.L., Badgley, G., Cullenward, D.,

Anderegg, W.R.L., Randerson, J.T. Using remote sensing to quantify the additional climate benefits of California forest carbon offset projects. *Global Change Biology* (in press)."

Lastly, in Chapter 4, I returned to the concept of fire risk from Chapter 1 and used the modeling framework from Chapter 2 to understand the historical drivers and future probability of fire occurrence in California. I found that the spatial pattern of wildfire over 1990-2021 could be explained by variables such as the mean annual precipitation, fractional shrub cover, and slope. Fire risk is likely to increase substantially in the future, on the order of 40-50%, especially for the mid-elevation Sierra Nevada and northern coastal regions. This is especially important to quantify in the context of prioritized fire risk mitigation and risk accounting for carbon offset projects. This work is currently in preparation for publication:

"Coffield, S.R., Graff, C.A., Wang, J.A., Bhoot, V., Goulden, M.L., Foufoula-Georgiou, E., Smyth, P., Randerson, J.T. Projecting future wildfire risk in California from changing climate and vegetation composition. (in prep)."

Together the four chapters of my dissertation improve our understanding of how climate controls ecosystems, especially in terms of carbon storage and fire risk, and how they will respond to continued climate change. In doing so I have also suggested how decision-makers can better account for these risks to increase ecosystem resilience and achieve climate goals.

Chapter 1

Machine learning to predict final fire size at the time of ignition

Adapted from:

Coffield, S.R., Graff, C.A., Chen, Y., Smyth, P., Foufoula-Georgiou, E., Randerson, J.T. (2019) Machine learning to predict final fire size at the time of ignition. *International Journal of Wildland Fire*, *28*, 861–873. https://doi.org/10.1071/WF19023

1.1 Introduction

Globally, fire prediction has received increasing attention because of the health and climate impacts of fires and the fact that fire regimes have been changing. First, in terms of public health, fire aerosols contribute to over 300,000 premature deaths each year (Johnston et al. 2012). They are also associated with increased hospitalisations due to respiratory and cardiovascular illness (Johnston et al. 2007; Delfino et al. 2009; Liu et al. 2017; Cascio 2018). Second, in terms of climate, fires are responsible for both positive and negative feedbacks with the climate system. Fires contribute significantly to the global carbon cycle, emitting 2.2 Pg of carbon annually (van der Werf et al. 2017). Deposition of black carbon aerosols increases the absorbed solar energy, melting snow and ice at high latitudes (Flanner et al. 2007; Mouteva et al. 2015; Hao et al. 2016; Sand et al. 2016). As a competing feedback, direct changes to the local landscape may increase reflected radiation, resulting in surface cooling on timescales of years to decades (Randerson et al. 2006; Rogers et al. 2013; Liu et al. 2019). Third, fire regimes have been changing around the globe because of human management and climate change. On average, global fire activity has been declining, largely driven by land use in grassland, savanna, and tropical ecosystems (Andela et al. 2017). However, areas such as the northern boreal forests and Western USA

have seen increased fire activity due to climate change and human-caused ignitions, with climate change threatening to exacerbate this trend in the future (Westerling et al. 2006; Liu et al. 2012; Liu and Wimberly 2016; Veraverbeke et al. 2017).

In the Alaskan boreal forests in particular, the impact of a changing climate has been pronounced. The region has experienced warmer summers, longer growing seasons and an increase in lightning. Because Alaska's burn area has historically been lightning-limited, the increase in lightning has resulted in recent years having some of the most frequent ignitions and most burned area on record (Kasischke and Turetsky 2006; Kasischke et al. 2010; Veraverbeke et al. 2017). Kasischke et al. (2010) reported that for the first decade of the 21st century, the boreal region of Alaska had an average annual burned area of 7670 km^2 , the largest in a 150-year record. With an area of 516,000 km^2 for the boreal interior region, this corresponds to a fire return frequency of ~70 years – at least 30 years less than estimates of variability for the Holocene (Lynch et al. 2002). Increasing lightning and fire trends are expected to continue with future climate warming (Flannigan et al. 2005; Krawchuk et al. 2009; Romps et al. 2014; French et al. 2015; Young et al. 2017), with one study predicting a doubling of burned area by 2050 relative to 1991–2000 (Balshi et al. 2009). Such a changing fire regime threatens both the native peoples and ecosystems that are maladapted to modern fire frequencies. The huge fires and their impacts in recent years may warrant a rethinking of fire management; lands that have previously been limited-suppression zones could now require increased suppression effort to maintain contemporary burning levels and mitigate impacts to humans and vulnerable ecosystems.

Previous work has illuminated the environmental controls on fires and fire size in boreal forests. The controls are typically a combination of topography, vegetation,

meteorology and human activity (Kasischke et al. 2002; Flannigan et al. 2005; DeWilde and Chapin 2006; Parisien et al. 2011a; Parisien et al. 2014; Sedano and Randerson 2014; Rogers et al. 2015). Topography has been shown to be relevant both in terms of slope and aspect. Steep slopes can help with rapid upward spread of fires. Aspect is relevant as it relates to tree species and the thickness of the surface duff layer; black spruce, for example, is more likely to dominate north-facing slopes. This species is more flammable than other conifers and has been shown to influence fire intensity and size (Kasischke et al. 2002; Rogers et al. 2015). The structure of the vegetation as fuel can also control the spatial structure of burn probability, with large areas of contiguous conifer forest more likely to burn (Parisien et al. 2011b). In terms of meteorology, the Canadian Forest Service has developed the Canadian Forest Fire Weather Index (FWI) System to rate fire danger, using weather parameters to represent moisture content in various fuel layers. The weather parameters include 1200 hours local standard time (LST) temperature, relative humidity, 24-h precipitation and 10-m wind speed (Van Wagner 1987). Although the FWI has been used as a predictor of fire size and emissions (Di Giuseppe et al. 2018), simpler variables such as vapor pressure deficit (VPD) and temperature can explain regional variability in fire activity, including fire size (Wiggins et al. 2016). VPD appears to be important in setting both ignitions and spread in boreal forests, with VPD anomalies explaining 45% of the variance in annual burned area (Sedano and Randerson 2014). This is likely because of the importance of VPD in determining the moisture content in dead vegetation (fuels) on short timescales, especially in fine fuels like standing dead grass and live mosses (Miller 2019). Extreme temperature has been found to be a major control on boreal fire size at many different spatial scales, whereas relationships between burned area and other variables,

including wind, fuel type, fuel moisture, topography and road density, often vary considerably with spatial and temporal scale (Parisien et al. 2011a; Parisien et al. 2014). Road density is important because it regulates access to wildlands, shaping patterns of both ignition and suppression. Fires near human-populated areas are more likely to be suppressed and less likely to become large (DeWilde and Chapin 2006). The presence of flammable fine fuels near roads may also allow lightning strikes to cause more fires in those areas (Arienti et al. 2009).

Numerous types of fire prediction models exist, including both dynamical physical-based spread models and statistical models. Two examples of dynamical spread models that are commonly used by Alaskan fire management agencies are FARSITE (Finney 1998) and the Fire Spread Probability Simulator (FSPro) (Finney et al. 2011). FSPro is a geospatial probabilistic model for predicting fire growth over many days. FARSITE is a deterministic modeling system used on shorter timescales (1–5 days) with a single weather scenario. In terms of rapid prediction of fire growth from ignition with minimal training, a few tools exist, such as REDapp from the Canadian Interagency Forest Fire Centre (http://redapp.org/, accessed 20 August 2019) and the Fire Behaviour Prediction (FBP) Calculator (Forestry Canada Fire Danger Group 1992). Even these are quite complex in comparison to the models we present, relying on information about fuel composition and mechanistic equations for fire spread.

Several studies have investigated statistical models for fire spread and size, primarily based on meteorological indices (Preisler et al. 2009; Faivre et al. 2014, 2016; Butler et al. 2017; Di Giuseppe et al. 2018). One study used machine learning techniques, including random forests, to predict burned area in Portugal with instantaneous weather

conditions at ignition (Cortez and Morais 2007). The models relied on ground station data and were most accurate for predicting the area of small fires. Less research has focussed specifically on the conditional probability of a large fire given information available at the time of ignition. One study used logistic regression with a fire potential index to predict the probability of fires exceeding a specified threshold in the contiguous USA (Preisler et al. 2009). This work examined the fraction of fires that would become large, but did not attempt to identify which specific ignition events were most likely to become large. Also, machine learning classification techniques have rarely been evaluated in the context of fire prediction. One example is a study in Brazil that used machine learning classification to predict the risk of ignitions in different areas, but similarly did not attempt to identify which ignitions were most likely to become large (de Souza et al. 2015).

In this study, we present and evaluate a new framework for fire prediction: using machine learning classification to identify specific ignitions that are most likely to become large fires. This is accomplished with two simple driver variables, extracted near the time and place of each ignition point. The final model is a decision tree that can efficiently classify ignition events. This approach may be especially promising for predicting fires and their impacts in the boreal forests of Alaska, where many ignitions occur and suppression resources are limited. In preparing for a future with more and larger fires, this type of simple prediction system may prove useful for fire and ecosystem management.

1.2 Methods

1.2.1 Data

We chose as a study area the state of Alaska. The interior portion of Alaska is primarily a mixture of boreal forests and taiga which experience substantial burning (Wein

and Maclean 1983; Kasischke et al. 2002). For example, in the large fire year of 2015, 20,800 km^2 of land burned. We chose a 17-year study period of 2001–2017, based on the availability of satellite and ground-based fire data as described below (Fig. 1). For each year, we considered the fire season of 1 May through 31 August, which contains fires accounting for 99.5% of the annual burned area according to data obtained from the Alaska Large Fire Database (ALFD, http://fire. ak.blm.gov/incinfo/aklgfire.php, accessed 5 October 2018).

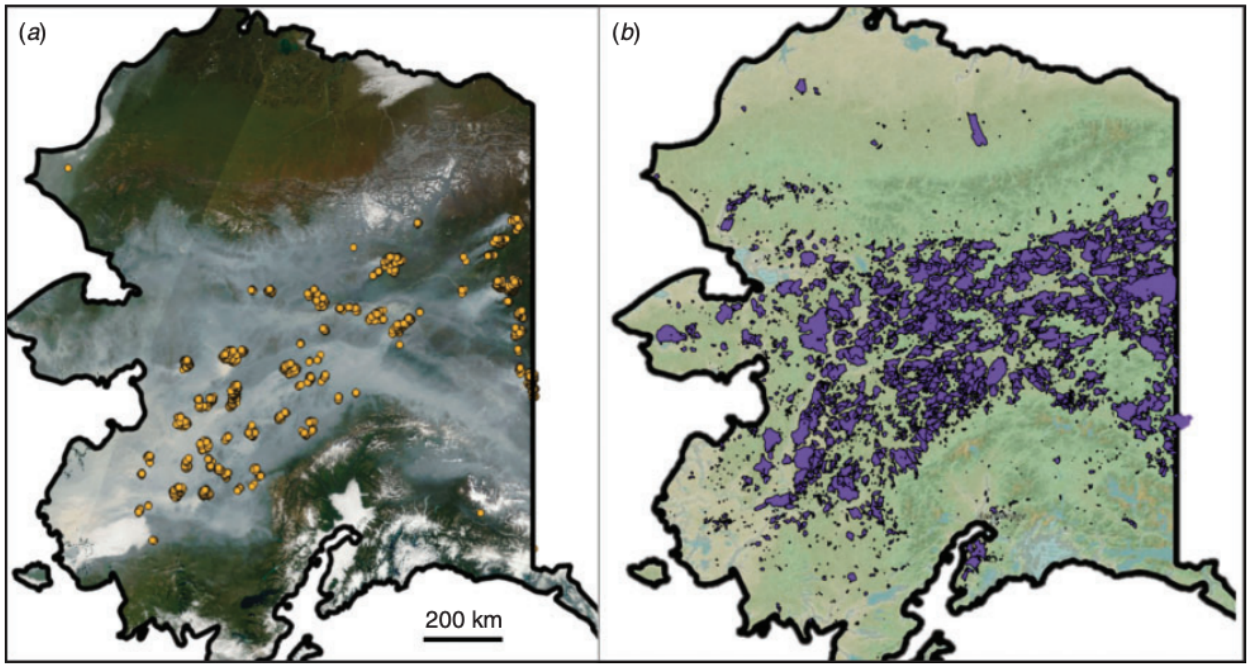

Figure 1.1. Study area of mainland Alaska, USA. In panel (a), Moderate Resolution Imaging Spectroradiometer (MODIS) active fire detections for 14 August 2005 are overlaid on a satellite optical image taken the same day (NASA EOSDIS). In panel (b), all fire perimeters from the Alaska Large Fire Database (ALFD) for 2001–2017 are overlaid on a background landscape map from QGIS Open Layers.

Fires

We obtained historical fire perimeter data from the ALFD available through the Bureau of Land Management's Alaska Interagency Coordination Center. The ALFD fire-history data compile information from satellite and ground-based records, reporting

fire points, perimeters, start dates and management options back to 1939. For our time period, this gave a set of 1771 fires. The management options are determined by the Alaska Interagency Fire Management Plan (https://agdc.usgs.gov/data/ projects/fhm/index.html, accessed 5 October 2018). They include 'limited', 'modified', 'full' and 'critical', in order of increasing priority for suppression resources (Fig. 2). Fires occurring in a modified, full, or critical zone are threatening to high-valued cultural or historical sites, high-valued natural resource areas, human property, or human life. Here, we selected only fires occurring in the 'limited' fire-management zone, which receives very minimal suppression, for two reasons. First, this set of fires had final fire perimeters that were more likely controlled by natural landscape and climate processes, and less by human intervention, making the modeling problem more tractable. Second, there is likely more flexibility in managing fires in this zone, making it an important potential target for efforts to maintain historical fire regions as a part of broader climate adaptation efforts. Considering fires only in this zone narrowed our dataset of fires from 1771 to 1224 fires.

We used active fire data from the Moderate Resolution Imaging Spectroradiometer (MODIS) to further filter the ALFD fire perimeter dataset. The MODIS Collection 6 Monthly Fire Location Product (MCD14ML) was obtained from the Department of Geographical Sciences at the University of Maryland (Giglio et al. 2016). Comparison of the ALFD and MODIS fire data revealed some spatial and temporal disagreement. In some cases, large fires in the ALFD had no corresponding fire detections from MODIS, and in other cases, the timing of fire events disagreed by multiple weeks. Since the start dates for some fires may be uncertain given the way multiple data sources are compiled in the ALFD, we compared start days with MODIS active fire detections to screen out potential outliers. We removed

fires that were large (>4 km^2) but had no associated MODIS detection within 10 km and 5 days, applying a reasonably wide temporal window for agreement as sometimes cloud or smoke cover can obscure fires for a few days. We did not filter out any fires in June 2001 when there was a gap in MODIS data. Our filtering further narrowed our dataset of fires from 1224 to 1168 fires.

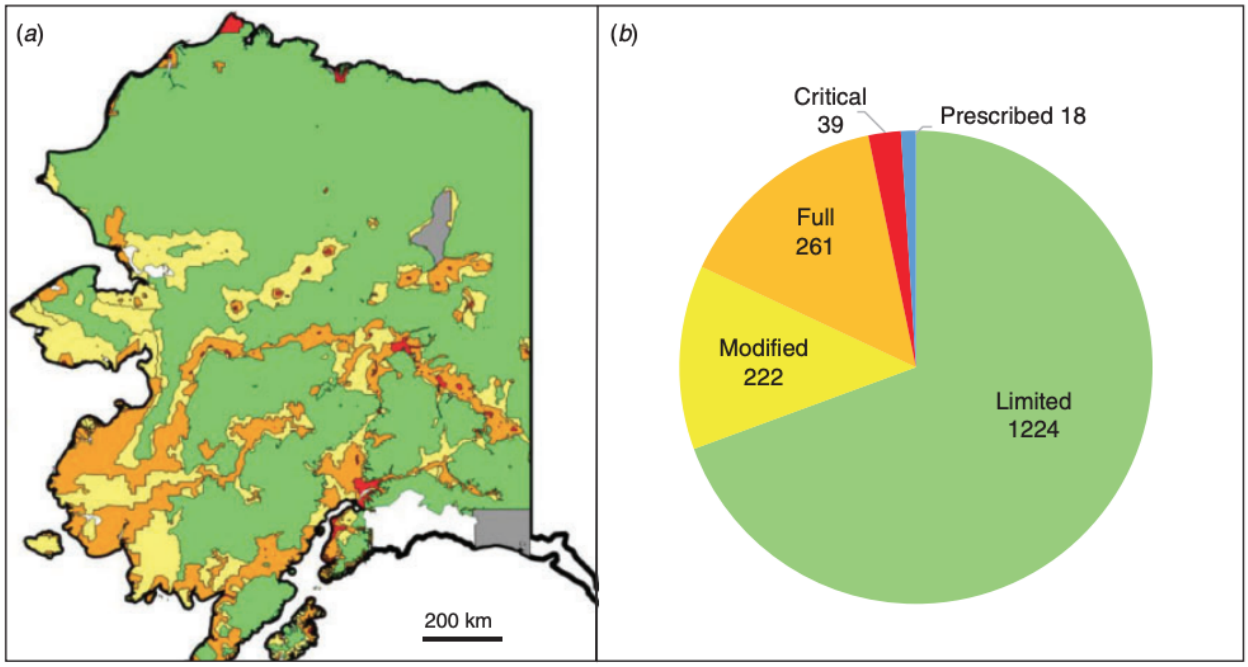

Figure 1.2. Prevalence of fires in different fire management zones. Panel (a) shows the fire management zones established by the Alaska Fire Service. Panel (b) shows the number of fires in the ALFD database that occurred in each zone during May–August of 2001–2017. In total, 1224 out of 1771 fires (69%) occurred in the limited management zone, where fires are more likely to be controlled by the natural environment and not suppression efforts. Out of the 1224 fires in the limited management zone, 1168 passed through an additional filter using satellite observations to corroborate the start date. This latter set was used in our model analysis.

Meteorology

We accessed daily meteorological data for 2-m air temperature, relative humidity, precipitation, 10-m wind speed and surface air pressure from the European Centre for Medium-Range Weather Forecasts (ECMWF) ERA5 reanalysis (Copernicus Climate Change Service 2017). The data are available at a 0.258° resolution. We used temperature and

relative humidity to derive VPD. This deficit is the difference between the saturation vapor pressure and the actual vapor pressure; we calculated saturation vapor pressure using the Tetens equation (Tetens 1930). We also created a temperature anomaly variable by subtracting the mean temperature for each day over 2001–2017 from the observed temperature.

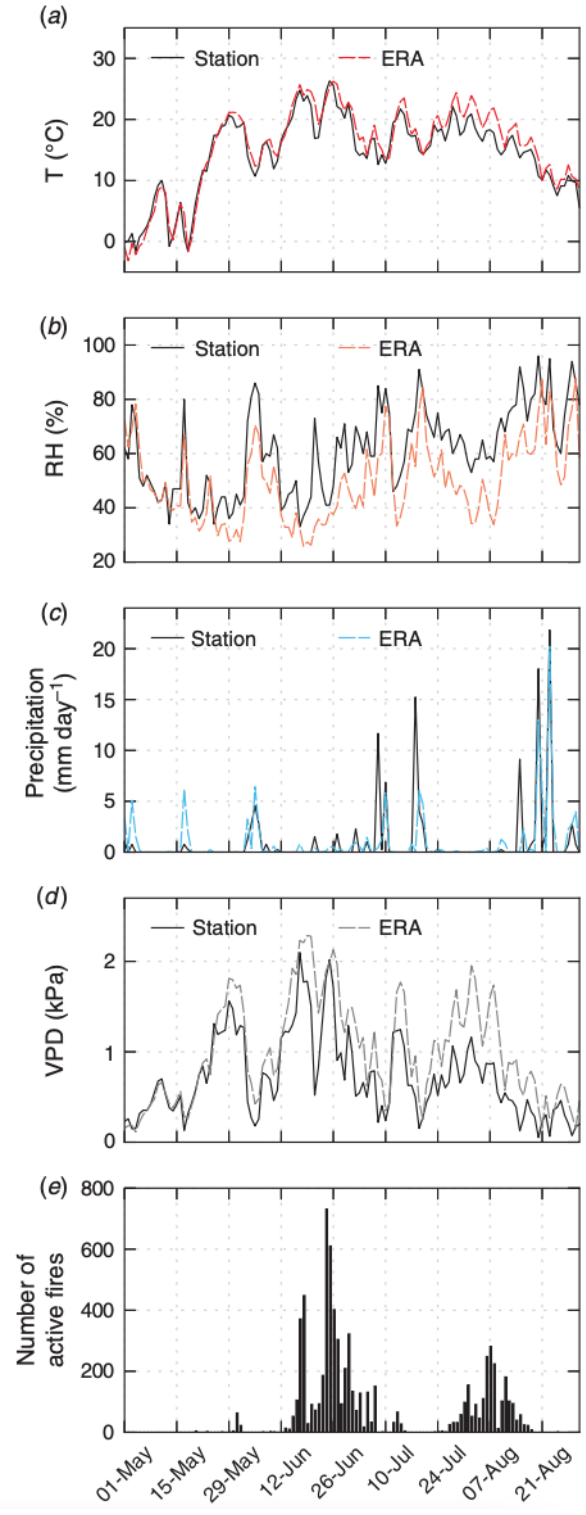

Figure 1.3. Time series of reanalysis weather data, ground station weather data, and fire activity for an example year, 2013. Panels (a–d) show the daily weather data from the European Center for Medium-Range Weather Forecasts (ECMWF) ERA5 reanalysis for the grid cell at Fairbanks along with in situ measurements from Fairbanks Airport station (from the Western Regional Climate Center). Despite the difference in spatial scale, total Moderate Resolution Imaging Spectroradiometer (MODIS) fire detections over interior Alaska (e) show a correspondence to weather, especially vapor pressure deficit (VPD).

As a preliminary validation of the ERA5 meteorology products, we plotted temperature, relative humidity, precipitation and VPD at Fairbanks through time for comparison against groundtruth weather data from the Western Regional Climate Center (https://raws.d.ri.edu, accessed 7 December 2018) (Fig. 1.3). The ERA5 global reanalysis appears to capture the local

variability measured by the Fairbanks station. We also included a time series of the number of total fire detections in the interior region of Alaska (Fig. 1.3e). Total fire activity shows a strong correspondence to VPD in particular, despite the difference of spatial scales, given that Fairbanks is centrally located and the ERA5 data are spatially correlated across interior Alaska.

Vegetation

We included vegetation data from the LANDFIRE Existing Vegetation Type product, which is a Landsat-based classification available at a 30-m resolution for 2001, 2008, 2010, 2012 and 2014 (Rollins 2009). We created two vegetation classes, grouping together several abundant tree species known to influence fire behavior: one class for any black or white spruce (evergreen) forest cover, and one class for any birch or aspen (deciduous) forest cover. For each fire, we considered these vegetation data at that location using the closest previous year that the data were available. We calculated the fraction of spruce forest cover and the fraction of birch–aspen forest cover for several different radii around each ALFD fire starting point.

Topography

Lastly, we included topographical data from the USA Geological Survey's GTOPO30 global digital elevation model (DEM), available at a 30-arc second (~1-km) resolution (Gesch et al. 1999). Similar to the vegetation data, for each fire, we considered slope, elevation and aspect averaged for several different radii around each ALFD starting point.

1.2.2 Model development and selection

We first developed and tested decision tree classifiers predicting final size class using data at the time and place of ignition. In contrast to many machine learning models,

such as random forests or neural networks, decision trees are readily interpretable. Their interpretability and simplicity make them more transparent for applications in decision-support systems. They also allow us to draw more scientific insight than more complex deep learning methods into which variables, and in which combinations, are major controllers of final fire size.

We divided the population of 1168 fires from the ALFD into terciles and labeled them based on final burned area: 'small' corresponds to fires that burned less than 1.2 km^2 , 'medium' to fires between 1.2 and 19.8 km^2, and 'large' to fires greater than 19.8 km^2 . It should also be noted that we briefly investigated using four or five fire size groups instead of three groups. We present only the three-size-group approach, given our fairly limited sample size with 10-fold cross-validation and similar qualitative findings with four or five groups. Choosing three groups also makes the classification accuracy higher, which may be more useful for communicating with managers or the public.

In all cases, we used 10-fold cross-validation to develop and validate trees using the scikit-learn package in Python (Pedregosa et al. 2011). The scikit-learn decision tree classifier uses an optimized version of the Classification and Regression Trees (CART) algorithm, which relies on a standard Gini function to optimize leaf-node purity on the training set, and does not support pruning. More details on the algorithm are provided at https://scikit-learn.org/stable/modules/tree.html (accessed 20 August 2019). In cross-validation, we select models based on highest average accuracy on the test sets. The accuracy is defined as the number of correct classifications relative to the total number of classifications.

Because scikit-learn CART does not support pruning, for our analysis, we needed to

specify the maximum size of the tree. In total, there were three dimensions to analyze in finding the optimal model: the tree shape, the timespan around ignitions to average weather data, and which variables to include.

As a starting point, we built decision tree classifiers based only on VPD averaged over a 5-day period from the day of ignition (t = 0) to 5 days in the future (t = 5). This window represents the idealized data that would be available in a standard weather forecast. We adjusted the size of the trees, allowing for up to 20 leaf nodes, and chose the tree shape with the highest accuracy in validation.

Next, we found the optimal timespan (around ignitions) over which to average weather data. We held the tree shape constant and varied the timespans of weather data, starting 10 days before ignition and ending 7 days after. Once the optimal timespan was selected, we analyzed the information content in different input variables. We allowed the tree shape to change, and we report the highest accuracy of validation achieved (with error bars) using different combinations of weather variables.

In addition to the weather variables, we explored vegetation, topography and day-of-year (DOY) as model inputs. For the vegetation, we considered a spruce fraction and a birch–aspen fraction, averaged for a 4-km radius around each ignition point. We chose a 4-km radius because 4 km gave the largest correlation in a preliminary linear regression analysis between vegetation and burned area.

We tested four other machine learning classification algorithms in comparison to decision trees, all available through the same scikit-learn package in Python: random forests, k-nearest neighbors, gradient boosting and a multi-layer perceptron (MLP). For each, we manually searched over a range of relevant parameters and report model accuracy

for the optimal parameter values.

1.2.3 Model analysis

We chose a 'best model' based on highest validation accuracy and computed other statistics, including recall and precision, for large fires in particular. We developed and present a metric for the improvement in 'weighted error' over a null (random) classification model. This metric captures more information about misclassification. We defined accurate classification as error = 0, misclassification by 1 size class as error = 1, and misclassification by 2 size classes as error = 2. A random classification would have an average weighted error of (1/3)(0) + (1/3)(1) + (1/3)(2) = 1.

As another method of assessing model performance, we considered the cumulative burned area fraction accounted for when fires are ranked according to model prediction. Each fire in each test set was assigned a predicted probability of being in each size class. This allowed us to rank the fires in each test group by their predicted probability of being large. We show the mean and range of cumulative burned area fraction, derived from the 10 folds of data used in the cross-validation. We compare this modeled ranking to 10 simulated random rankings as well as the observed ranking based on observed fire size.

To assess whether the model could capture interannual variability in fire dynamics, we tested whether the best model was able to reproduce year-to-year differences in the fraction of large fires. In this case, we redeveloped models using each year as a hold-one-out fold for cross-validation (instead of 10 equal-sized groups) and calculated the correlation between the observed and predicted fraction of large fires each year.

We also quantified the information content in the spatial v. temporal variability of the weather data. In one scenario, we used the climatological mean weather data for every

grid cell as the input, regardless of when each ignition occurred. In a second scenario, we used the spatially averaged weather data for each day as the input, regardless of where on the landscape each ignition occurred. We report and compare the classification accuracies of these scenarios.

To explore the footprint of human fire management, we applied our best model, developed on fires in the 'limited' management zone, to fires occurring in other management zones where fires are more actively suppressed. By comparing fire sizes and quantifying the model's overprediction of large fires in the other zones, we inferred how burned area was being modified by current fire management practices.

1.3 Results

For our first set of models, we considered VPD averaged for each fire from the date of ignition through 5 days in the future. Allowing for trees with up to 20 leaf nodes, our 'baseline' best classification accuracy was 46.1 ± 6.7% using trees with 3 nodes. This represents the mean and standard deviation of accuracy across the 10 folds.

Next, specifying three-node trees, we averaged VPD data over different timespans. We found the optimal time window to be 1–5 days after the ignition, with an average accuracy of 49.2 ± 4.7% (Fig. 1.4). Going forward, we considered weather data over only this timespan for each fire.

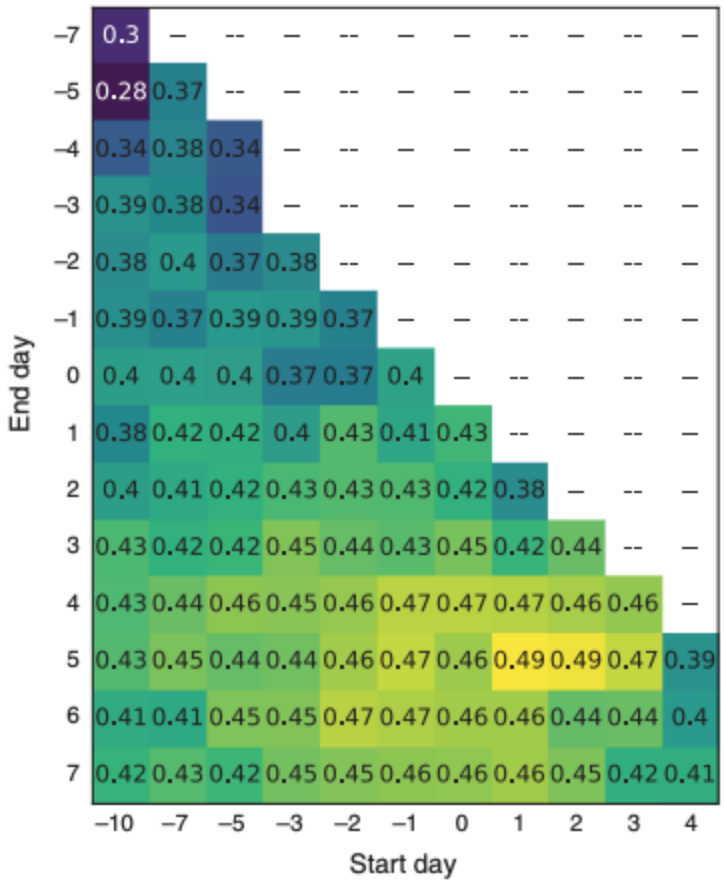

Figure 1.4. Classification accuracy with varying time window of weather data. Each cell shows the mean validation accuracy across the 10-fold cross-validation, using weather data averaged over different timespans. The timespans start up to 10 days before ignition (-10) and extend up through 7 days after ignition (+7). In all cases, classification models used only vapor pressure deficit (VPD) with 3 leaf nodes. From this analysis, the optimal time window for classification is from 1 to 5 days after ignition.

Our analysis of weather variables is presented in Table 1.1. We found that VPD was the best predictor of final fire size at the time of ignition. Models including other weather variables did not outperform the VPD-only model. In addition to accuracy, we report *P*-values in Table 1.1, each representing a t-test comparing models with different variables against a random classification. All models except three (wind, surface pressure and temperature anomaly) significantly outperformed a random classification at a $P = 0.05$

level. It should also be noted that no models with combinations of variables significantly outperformed the models with only VPD or only relative humidity (RH).

Table 1.1. Information in different weather variables Decision trees are developed and validated including different combinations of variables. The mean and standard deviation of validation accuracy across the 10 folds are reported. Asterisks (*) indicate significantly higher accuracy than a random classification, and bold type indicates the highest-accuracy model. Tree shapes vary with up to 5 leaf nodes. RH, relative humidity; T, 2-m air surface temperature; Pr, total daily precipitation; VPD, vapor pressure deficit; W, wind speed; SP, surface pressure; Tanom, temperature anomaly from climatology.

Variables included	Accuracy of best model	*P*-value
	Random classification	
None	$33.3 \pm 4.4\%$	–
	One-variable models	
RH	$47.2 \pm 4.9\%$	<0.001*
T	$39.4 \pm 6.4\%$	0.013*
Pr	$45.7 \pm 5.0\%$	<0.001*
VPD	**$49.2 \pm 4.7\%$**	<0.001*
W	$29.6 \pm 9.0\%$	0.868
SP	$31.6 \pm 9.7\%$	0.689
T_{anom}	$37.6 \pm 6.7\%$	0.055
	Two-variable models	
VPD, T	$49.2 \pm 4.7\%$	<0.001*
VPD, Pr	$48.8 \pm 5.5\%$	<0.001*
VPD, RH	$47.8 \pm 3.8\%$	<0.001*
T, Pr	$44.4 \pm 5.6\%$	<0.001*
T, RH	$44.0 \pm 5.6\%$	<0.001*
Pr, RH	$45.2 \pm 4.3\%$	<0.001*
	Three-variable models	
VPD, T, Pr	$48.8 \pm 5.5\%$	<0.001*
VPD, T, RH	$45.7 \pm 5.8\%$	<0.001*
VPD, Pr, RH	$47.8 \pm 3.8\%$	<0.001*
T, Pr, RH	$43.1 \pm 5.3\%$	<0.001*
	Four-variable model	
VPD, T, Pr, RH	$45.5 \pm 5.9\%$	<0.001*

Our analysis of other variables (day-of-year, vegetation and topography) is presented in Table 1.2. We tested all possible combinations of variables and report a select summary. Among the other variables, only two were statistically significant: day-of-year

and spruce fraction. For the day-of-year variable, fires ignited in late June and early July were most likely to become large. However, including day-of-year did not improve the VPD model. For the spruce-fraction variable, fires with a low fraction of spruce forest around the ignition point were less likely to develop into the largest size class. This agrees with previous research highlighting the importance of black spruce trees in regulating fire intensity and severity in North America (Rogers et al. 2015). Including spruce fraction did improve the VPD model, although not significantly, with an accuracy of 50.4 ± 5.2%. For the remainder of this paper, we refer to this VPD plus spruce fraction model as our 'best model'.

None of the more complex machine learning classifiers outperformed the simpler decision tree model (Table 1.3). For each classifier, we present the highest validation accuracy achieved, along with descriptions of the optimal parameters. Any parameters not specified were left at their default values.

For our best decision tree model, we present a representative tree (Fig. 1.5) and summary statistics (Table 1.4). In the tree, ignitions occurring during a period of low VPD were classified as small fires, and ignitions occurring during a period of moderate VPD were classified as medium fires. For ignitions occurring during a period of high VPD, most were classified as large fires. A subset of the high-VPD ignitions had a very low spruce fraction and were classified as small fires. Fig. 1.6 is a visualization of the variation across the 10 folds. Our best model yields a weighted error of 0.637 ± 0.059, or an improvement (reduction) of 36.3 ± 5.9% over a random classification.

Table 1.2. Information in other variables (vegetation type, day of year, and topography). We tested all possible combinations of all variables and present a selected summary below. Asterisks (*) indicate significantly higher accuracy than a random classification, and bold type indicates the highest-accuracy model. 'Spruce fraction' is the proportion of black or white spruce cover in a 4-km radius around ignition; 'Birch–aspen fraction' is the proportion of birch or aspen cover in a 4-km radius around ignition. VPD, vapor pressure deficit.

Variables included	Accuracy of best model	*P*-value
	Random classification	
None	33.3 ± 4.4%	–
	One-variable models	
Spruce fraction	40.7 ± 7.1%	0.007*
Birch-aspen fraction	29.4 ± 4.8%	0.962
Day of year	39.1 ± 7.3%	0.025*
Slope	36.2 ± 7.1%	0.145
Aspect	26.4 ± 7.6%	0.989
Elevation	34.7 ± 6.0%	0.280
	Combination models	
Spruce, birch-aspen	40.4 ± 7.2%	0.009*
VPD, spruce	**50.4 ± 5.2%**	<0.001*
VPD, birch/aspen	49.2 ± 4.7%	<0.001*

Table 1.3. Comparison of machine learning classification methods. In addition to decision trees, we tested several machine learning classification methods. In each case, we manually searched over different combinations of relevant parameters and report the most accurate parameter settings for each model below. Performance of decision trees was effectively indistinguishable from that of random forests, and so we focus on the simpler model in this paper.

Algorithm	Best accuracy	Variables included	Parameter description
Decision tree	50.4 ± 5.2%	VPD, spruce	4 leaf nodes
Random forest	50.0 ± 4.2%	VPD, spruce	6 leaf nodes, 32 trees
K-nearest neighbours	47.7 ± 2.8%	VPD	60 neighbours
Gradient boosting	49.5 ± 4.3%	VPD, spruce	50 estimators, 0.01 learning rate; depth 2
Multi-layer perceptron	48.0 ± 3.6%	VPD, spruce	0.001 learning rate; single hidden layer with 50 units; 200 iterations; batch size 20

Table 1.4 Statistics for the best model. Models used vapor pressure deficit (VPD) and the fraction of spruce cover, with VPD averaged for the time interval of 1–5 days after the ignition event and spruce fraction averaged for a 4-km radius. We present the mean statistics across the 10-fold cross-validation. Recall is defined as the number of true positives divided by the sum of true positives and false negatives TP ÷ (TP + FN). It represents the proportion of observed large fires that were accurately identified by the model. Precision is defined as the number of true positives divided by the sum of true and false positives TP ÷ (TP + FP). It represents the proportion of fires the model predicted would be large that were observed large.

Confusion matrix

		Predicted		
		Small	Medium	Large
Observed	Small	22.2%	4.1%	7.1%
	Medium	16.2%	6.2%	11.0%
	Large	7.0%	4.2%	22.1%

Summary

Accuracy	$50.4 \pm 5.2\%$
Recall for large fires	$65.2 \pm 8.4\%$
Precision for large fires	$52.5 \pm 11.8\%$
Burned area accounted for by fires classified as large	$74.9 \pm 12.6\%$
Improvement in weighted error over a null model	$36.3 \pm 5.9\%$

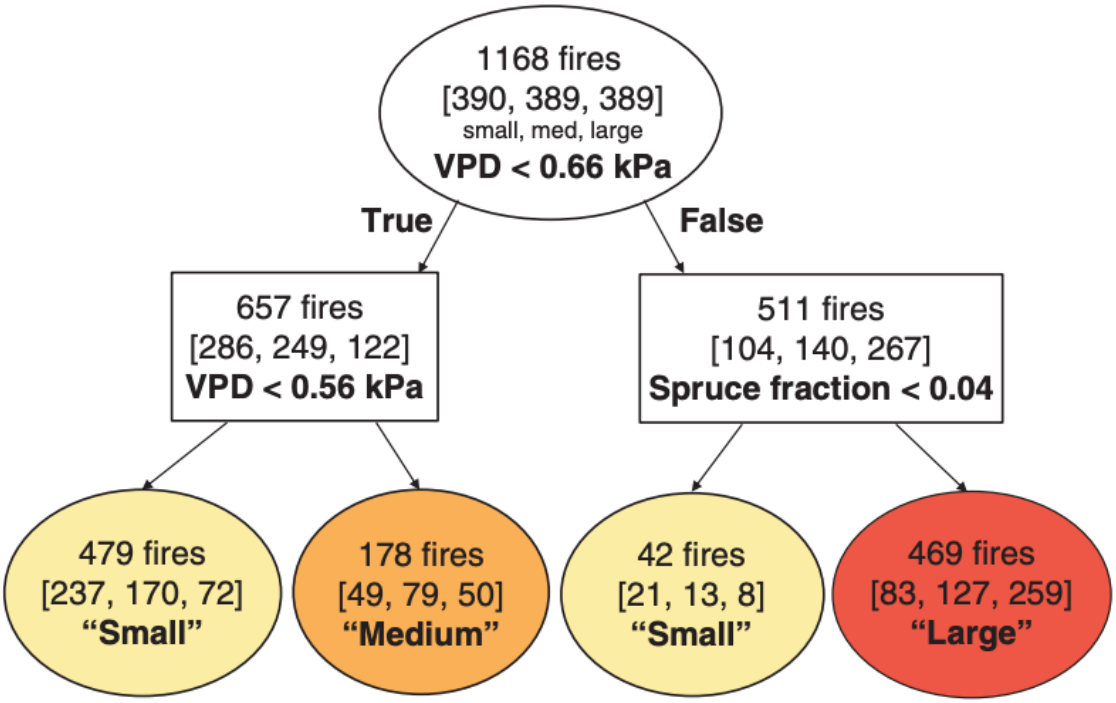

Figure 1.5. Example of a classification tree using vapor pressure deficit (VPD) averaged for 5 days after ignitions and the fraction of spruce cover in a 4-km radius. This representative tree results from training the entire dataset of 1168 fires. Thresholds for the splits are selected by the training algorithm, optimizing leaf node purity. Color coding with yellow, orange and red respectively indicates classification as small, medium or large fires. The numbers in brackets indicate the observed number of fires falling in each size class.

Figure 1.6. Performance of decision trees. Fires are separated into 10 columns representing the 10-fold cross-validation, with 116 samples in each fold. Fires are sorted vertically by the observed size from largest at top to smallest at bottom, and colored based on model classification (red for large, orange for medium, and yellow for small).

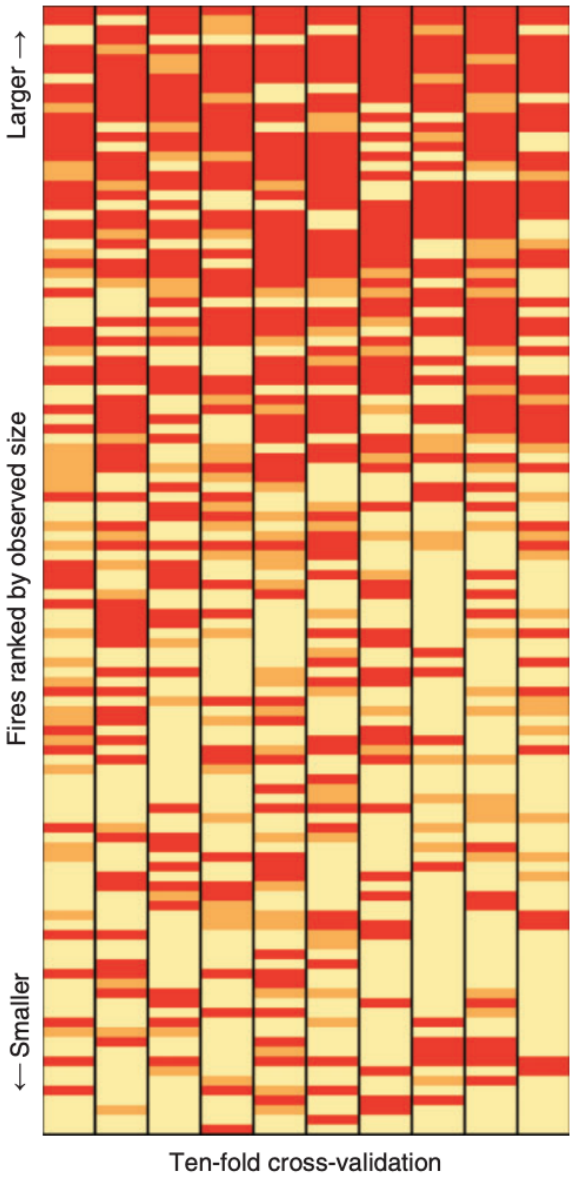

The model performed particularly accurately for the large fire class, with a recall of 65.2 ± 8.4% and a precision of 52.5 ± 11.8%. The model predicted that 40% of ignitions would become large fires. In reality, those 40% of ignitions became fires that accounted for 75% of the total burned area. In Fig. 1.7, we rank fires based on their modeled predicted probability of being large. This shows, for example, that half of the total burned area could be accounted for by the top 29% of fires identified by the model.

Fig. 1.8 shows two more model assessments, investigating the role of (a) the number of fires in the dataset and (b) the number of leaf nodes in the decision trees. The number of

fires in the dataset did not appear to be limiting model performance, as maximum accuracy approached 50% for as few as 200 fires. Also, overfitting did not appear to be limiting model performance, given that we selected our model based on optimal accuracy in the test group. A perfectly fit tree for the training dataset required 480 leaf nodes, but best performance for the test group was achieved with 11 or fewer nodes.

On interannual timescales, the VPD plus spruce fraction decision tree model was able to capture year-to-year variations in the fraction of large fires (Fig. 1.9). The model correctly predicted the fraction of large fires increases during large fire years (Fig. 1.9c), as indicated by a significant correlation between predictions and observations during 2001–2017 ($r^2 = 0.50$, $P = 0.001$).

We quantified the information in the spatial v. temporal variability of weather with the best model (Table 1.5). We found that these two components were comparable, with the 'space-only' model achieving an accuracy of 40% and the 'time-only' model achieving an accuracy of 41%. However, the two models varied significantly in which fire size classes were accurately captured; the 'space-only' model had higher recall for large fires, while the 'time-only' model had higher recall for small fires.

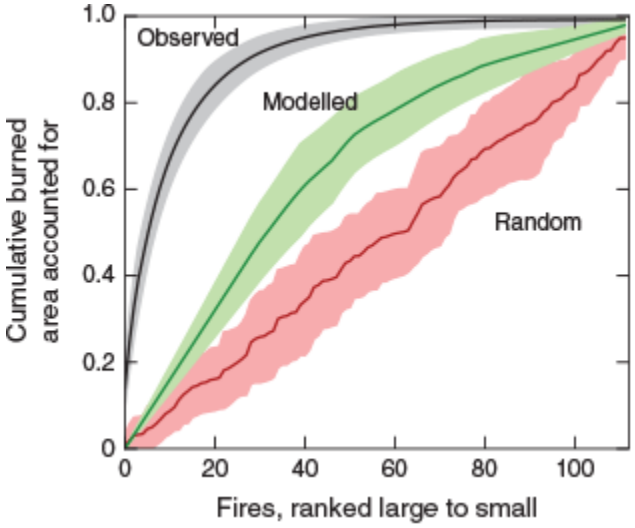

Figure 1.7. Cumulative burned area comparing observed, modeled, and random rankings of fires. Each line is a ranking of 116 fires on the x-axis. The errors about each line represent the variation from the 10-fold cross-validation. The 'modeled' line uses the vapor pressure deficit and spruce fraction model, ranking based on the predicted probability of each fire being large, as determined by the decision tree for that fold. The 'random' ranking is a numerical simulation in which all the fires are shuffled. In all three cases, the y-axis is the cumulative area that would be accounted for by each ranking system.

Figure 1.8. Learning curve and overfitting analysis. For (a), we randomly selected subsets of our fire dataset for model development and validation, and these subsets are ordered by size on the x-axis. The y-axis reflects the mean and standard deviation of model accuracy across 100 simulations. In each simulation, models were developed and validated using vapor pressure deficit and spruce fraction as inputs. The upper limit of accuracy with these parameters appears to be ~50%. The shape of the curve indicates that the accuracy of our model is not strongly constrained by data availability. For (b), we allowed the number of leaf nodes to increase until each was pure. We chose the 4-leaf-node model as our 'best model'.

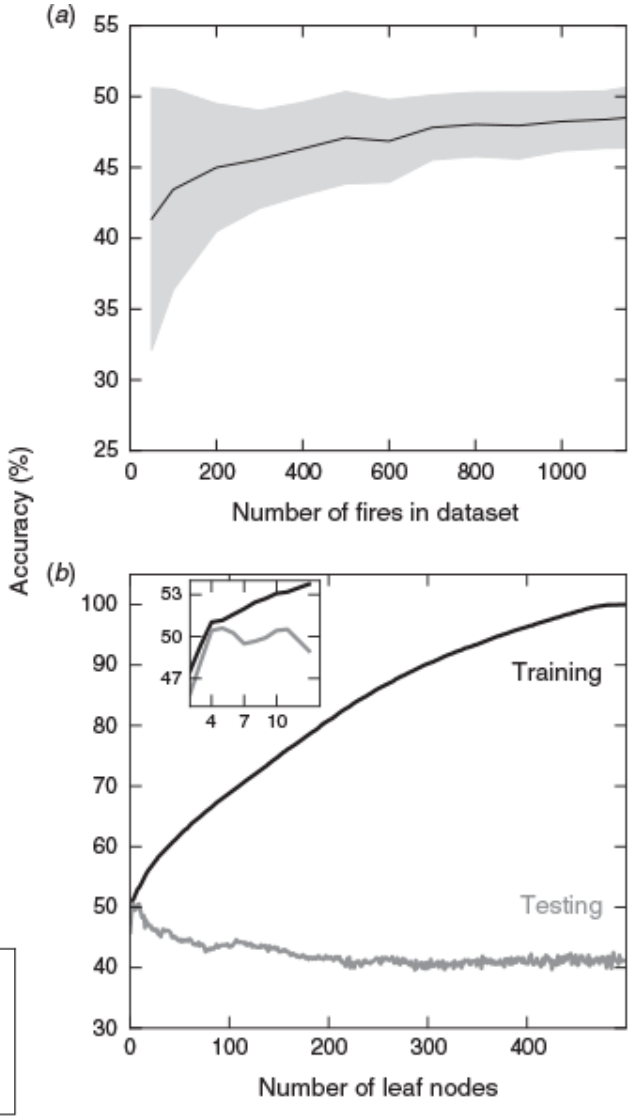

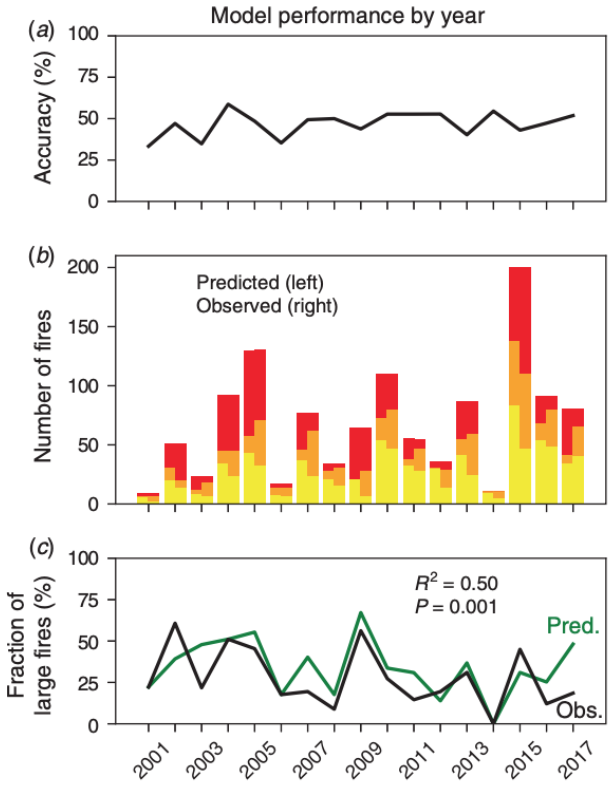

← **Figure 1.9.** Model performance by year. We reran our best model using each year as a hold-one-out fold for cross-validation (instead of 10 equal-sized groups). Panel (a) shows model accuracy when tested on each year. Panel (b) shows the predicted (left) v. observed (right) fires falling into each size class each year (yellow for small, orange for medium, and red for large). Panel (c) shows the predicted (green) v. observed (black) fraction of large fires each year. The model generally captures the interannual variability of fires, predicting a larger proportion of large fires in 2004, 2005 and 2009, but under predicting large fires in 2015.

Table 1.5. Information in spatial v. temporal variability of weather

Input data	Accuracy	Recall for small fires	Recall for large fires
Climatology for each cell (space only)	$40.2 \pm 5.8\%$	$33.9 \pm 24.8\%$	$59.0 \pm 8.3\%$
Region-wide daily weather (time only)	$41.1 \pm 7.0\%$	$68.5 \pm 21.3\%$	$40.4 \pm 22.5\%$
Daily weather for each cell	$50.4 \pm 5.2\%$	$65.7 \pm 8.3\%$	$65.4 \pm 8.4\%$

To quantify human impacts on Alaska's fire regime, we considered fires in the other management zones that have a higher suppression priority. Specifically, we considered the combination of fires in the 'modified', 'full' and 'critical' management options. More fires in the high suppression zone were small (43%), and fewer became large (25%) (Fig. 1.10). Although there were 8% more ignitions per unit area in the high suppression zones, there was also 28% less annual burned area per unit area (Table 1.6). The increased fire frequency was likely explained by the higher density of roads, which allowed more ignitions by both humans and lightning, according to previous research (DeWilde and Chapin 2006; Arienti et al. 2009). Using Table 1.6, we estimated that the total human footprint on the fire regime in interior Alaska was to increase the frequency of fires by 3.4% but to decrease annual burned area by 7.5% during 2001–2017. The higher frequency of fires was more than offset by the increased suppression effort.

When applied to the other management zones (critical, full and modified), our model (using VPD and spruce fraction) overpredicted large fires. Accuracy decreased from 50.4 to 43.0%. Precision for large fires decreased from to 52.5 to 34.0%; however, recall for large fires stayed approximately the same, decreasing only slightly from 65.2 to 64.3% (Table 1.7). This drop in precision but not in recall aligned with intuition and supported the

robustness of our model; the model did not predict large fires as precisely in these zones, as many of the fires that would have naturally become large were actively suppressed. However, the model still identified with the same success rate the fires that did become large, based on VPD and spruce fraction.

Moreover, we found that the overprediction of large fires in the more managed zones was disproportionate; for this set of ignitions, the model predicted 48.2% would become large (Table 1.7) rather than 40.2% (Table 1.4). Ignitions in the more managed zones were more often human-caused and occurred during periods of higher VPD, on average, than did those in the limited management zone (0.70 v. 0.66 kPa respectively). Using the mean fire size for each size class from the limited management zone, we found that our model predicted an average fire size of 1.8 times that which was observed for fires in the more managed zones. This suggests that suppression efforts decreased burned area in more managed zones by ~44%.

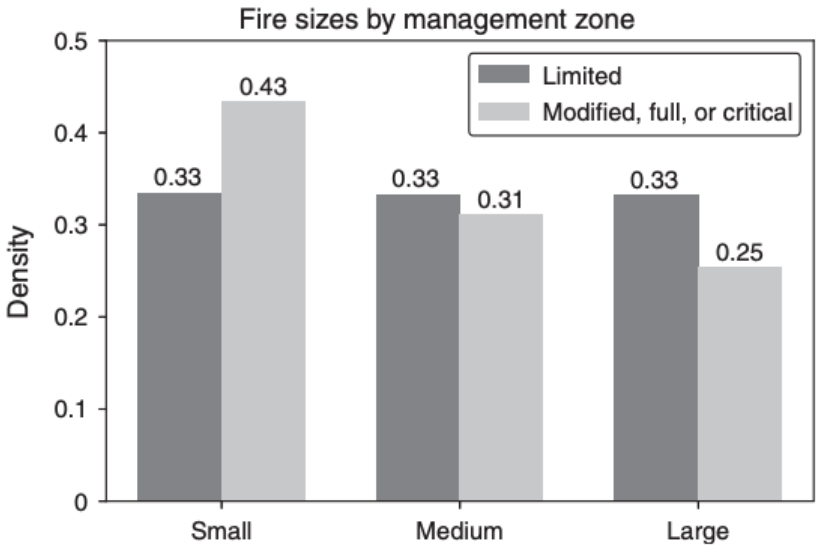

Figure 1.10. Fire sizes by management zone. The terciles of fires in the 'limited' management zone were used to define small (<1.2 km^2), medium (1.2–19.8 km^2) and large (>19.8 km^2). Fires in other management zones are less likely to become large, indicating the impact of suppression effort and human fragmentation of the landscape.

Table 1.6. Summary of burned area and fire density across more managed zones. Fires in the critical, full or modified management options of interior Alaska are more frequent but burn less area annually, per unit area. If the entire interior region followed the fire density and burn area density of the limited management zone, we estimate there would be (1.19×10^{-4} fires year^{-1} km^{-2}) (633 581 km^2) = 75.4 fires annually and (9.61×10^{-3} km^2 year^{-1} km^{-2}) (633 581 km^2) = 6089 km^2 burned area annually. By comparing against the observed values of 78.0 fires year^{-1} and 5631 km^2 year^{-1}, we infer that the human footprint is to increase the total number of fires only slightly, by 3.4%, but to decrease the total annual burned area by 7.5%.

	Management option		
	Critical, full, or modified	Limited	All
Mean fire size (km^2)	52.0	79.9	71.8
Burned area per year (km^2 year^{-1})	1183	4449	5631
Fires per year	22.0	55.0	78.0
Area (km^2)	170543	463038	633581
Burned area per year per area (km^2 year^{-1} km^{-2})	6.94×10^{-3}	9.61×10^{-3}	8.89×10^{-3}
Fires per year per area (n year^{-1} km^{-2})	1.29×10^{-4}	1.19×10^{-4}	1.23×10^{-4}

Table 1.7. Statistics for best model applied to other management zones. Models used vapor pressure deficit (VPD) and spruce fraction, with VPD averaged for the time interval of 1–5 days after the ignition event and spruce fraction averaged for a 4-km radius. This sample of 507 fires included management zones 'critical', 'full' and 'modified'

Confusion matrix

		Predicted		
		Small	Medium	Large
Observed	Small	22.2%	6.1%	15.0%
	Medium	9.9%	4.4%	16.8%
	Large	5.7%	3.4%	16.4%

Summary

Accuracy	43.0%
Recall for large fires	64.3%
Precision for large fires	34.0%
Burned area accounted for by fires classified as large	70.6%
Improvement in weighted error over a null model	22.2%

1.4 Discussion

We present and evaluate a novel approach for fire prediction: decision tree classification with weather and vegetation cover data to predict final fire size at the time of ignition. We found that VPD alone, over the period of a standard weather forecast, could be used to classify ignitions into three groups with ~49% accuracy. VPD combined with one vegetation parameter, spruce fraction, improved accuracy to just over 50%. Further research could scale-up the complexity of the vegetation and topography variables to better capture the fuel structure and barriers to fire spread in the area around ignition.

Our findings suggest that weather, specifically VPD, early in a fire's life can determine if a fire will be extinguished early or will be able to grow large. Further investigation is needed to compare the duration of fires in the small, medium and large classes in relation to the 5-day window used here. It may be that very dry conditions in the first few days allow the fires to grow large enough to persist through wet intervals, so that they can grow again during hot and dry intervals, as suggested by Sedano and Randerson (2014).

Our results are particularly promising for early identification of large fires. Accuracy was highest for the large fire class, with a recall of 65% and precision of 53%. The framework presented in Fig. 1.7 allows for a cost–benefit analysis of fire suppression. In theory, if it were possible to suppress fires at the instant of ignition, it may be possible to save 50% of the burned area by targeting only the top 29% of ignitions identified by our model. This type of information could offer substantial benefits for human health and preservation of vulnerable ecosystems as further climate warming increases burned area (Westerling et al. 2006; Liu et al. 2012; Liu and Wimberly 2016; Veraverbeke et al. 2017).

It is likely that weather forecasts would be a key limiting factor for model accuracy, as forecasts tend to degrade rapidly after a few days into the future. We did not investigate the degradation of model accuracy when using archived weather forecasts in place of reanalysis, primarily due to the cost of these ECMWF datasets. We speculate that the primary factor limiting accuracy to 50% is the incomplete characterisation of biology, fuels and barriers with our vegetation cover variables, which do not mechanistically account for fire spread. Information was also lost in our temporal averaging of weather and the inability of coarser-scale reanalysis products to capture very localized variations in precipitation. The number of fires in the dataset did not appear to be limiting the accuracy, based on a learning curve analysis (Fig. 1.8a).

With our approach focusing on information available at the time of ignition, we found that decision trees, a simple and readily interpretable method, performed similarly to other machine learning classifiers (namely, random forests, k-nearest neighbors, gradient boosting and multi-layer perceptrons). Incorrect application of any of these methods may yield overfitting, and so we provided an analysis of the training v. testing accuracy for our selected decision tree model (Fig. 1.8b). Although perfect training accuracy requires nearly 500 leaf nodes for a dataset of 1168 fires, testing accuracy is optimized for 11 or fewer leaf nodes. We did not include an analysis of more complex or deep learning methods (e.g. recurrent neural network), given our fairly small dataset and lack of indication that more complex models would outperform simpler models. However, future research in fire size prediction should investigate more methodologies, especially at larger scales with more data and more complex input variables.

In our comparison of fire sizes and model results for different management zones,

we also inferred the footprint of human suppression effort on burned area. As expected, our model overpredicts large fires in zones that are more actively managed. However, the model still had similar recall for the fires that did become large. Our model also allowed us to estimate the impacts of fire suppression, taking into account that human ignitions in these areas tended to occur during periods with hotter and drier weather.

Our models differed in structure and purpose from other fire size prediction methods and were not intended to compete with more complex models used for fire management. Rather, we view our analysis as a useful framework for investigating the major controls on fires using information available at the time of ignition. The insight gained may be useful in other regions beyond boreal forests of Alaska, where the early information could help inform management strategies in vulnerable ecosystems responding to strong trends in climate.

1.5 Acknowledgements

This work is based upon support received from the National Science Foundation (NSF) Graduate Research Fellowship Program under grant number DGE-1839285 (for S. R. Coffield), by NSF under grant number 1633631 (for C. A. Graff, J. T. Randerson, P. Smyth) as part of the University of California, Irvine (UCI) NSF Research Traineeship (NRT) Machine Learning and Physical Sciences (MAPS) Program, by NASA under award NNX15AQ06A as part of the California State University-Los Angeles (CSULA)/UCI Data Intensive Research and Education Center (DIRECT)- STEM project (for P. Smyth), by NSF under award CNS-1730158 (for P. Smyth), by the Department of Energy Office of Science's Reducing Uncertainty in Biogeochemical Interactions through Synthesis and Computation (RUBISCO) Science Focus Area and NASA's Soil Moisture Active Passive (SMAP), Interdisciplinary

Research in Earth Science (IDS) and Carbon Monitoring System (CMS) programs (for J. T. Randerson, Y. Chen), by the NSF under grant number DMS-1839336 (for E. Foufoula-Georgiou, J. T. Randerson, P. Smyth) as part of the Transdisciplinary Research in Principles of Data Science (TRIPODS) program, and by NASA under grant number NNX16AO56G (for E. Foufoula-Georgiou) as part of the Global Precipitation Measurement (GPM) program. The authors declare no conflicts of interest.

Chapter 2

Climate-driven limits to future carbon storage in California's wildland ecosystems

Adapted from:

Coffield, S.R., Hemes, K.S., Koven, C.D., Goulden, M.L., Randerson, J.T. (2021) Climate-driven limits to future carbon storage in California's wildland ecosystems. *AGU Advances, 2*(3)*,* e2021AV000384. https://doi.org/10.1029/2021AV000384

2.1 Introduction

Terrestrial ecosystems are currently large carbon sinks, sequestering approximately 30% of anthropogenic emissions globally over 1850–2018 (Friedlingstein et al., 2019). Their past and present ability to sequester carbon, as well as the many other ecosystem services they provide, make "natural climate solutions" an appealing class of climate mitigation strategies (Anderegg et al., 2020; Griscom et al., 2017). In fact, enhanced ecosystem carbon storage in forests is a key component of many climate mitigation pathways that keep global temperature rise below 1.5°C or 2°C (Roe et al., 2019).

A prime example of using terrestrial ecosystems toward natural climate solutions can be found in California, home to one the most ambitious climate change mitigation policies globally. The state's Natural and Working Lands Climate Change Implementation Plan (California Air Resources Board, 2019) seeks to contribute carbon dioxide removal consistent with the statewide goal of carbon neutrality by 2045. The plan involves reversing the net land carbon flux, which is currently positive (i.e., a source of carbon) (California Air Resources Board, 2019; Sleeter et al., 2019), such that the land will sequester an additional 23 MtC by 2045 and 230 MtC by 2100. For reference, 230 MtC

corresponds to approximately 4.2% of the estimated current total ecosystem carbon stock of 5,500 MtC in California (California Air Resources Board, 2019).

Despite this reliance on forests for climate change mitigation, there is considerable uncertainty regarding the future ability of forests to take up and store carbon due to changing temperature and precipitation regimes, disturbance, and other indirect climate change feedbacks (Anderegg et al., 2020; Sperry et al., 2019). Many of these climate-related threats are already apparent in observations. For example, over the twentieth century, as a result of fire suppression management as well as climatic shifts, California forests generally became denser, with smaller trees, less biomass, and an increase in the dominance of oaks relative to pines (McIntyre et al., 2015). More rapid climate change and intense drought stress in this century have caused shifts in plant communities, including widespread mortality (Anderegg et al., 2013; Breshears et al., 2005; Goulden & Bales, 2019), range contractions (Kelly & Goulden, 2008), and shifts in hydraulic trait composition (Trugman et al., 2020). It is estimated that California's 2012–2015 drought killed 41% (Stovall et al., 2019) to 49% (Fettig et al., 2019) of trees in the central and southern Sierra Nevada, disproportionately ponderosa pines and larger trees at lower elevations. The result has been a shift in forest composition and redistribution of major species. These direct climate-driven changes, along with the effects of land management and increasing severity of wildfires, have caused California's total terrestrial carbon stocks to decrease (California Air Resources Board, 2019; Fellows & Goulden, 2008) and they pose continued risks to carbon storage into the future (Anderegg et al., 2020; Galik & Jackson, 2009; Lalonde et al., 2018; McDowell et al., 2020). Moreover, future climate change-driven shifts to carbon storage capacity have direct implications for the long-term success of current carbon

sequestration projects. Strategies that assume the carbon carrying capacity will remain static across the landscape risk sequestering carbon into vulnerable ecosystems that may undergo a transition to a lower carbon state. Likewise, these strategies may miss opportunities to accelerate storage into locations where the carbon carrying capacity will become more favorable in the future.

Future ecosystem projections based on climate broadly fall into two categories: statistical models and dynamical (or processed-based) models. Statistical models often leverage the tight spatial relationships between climate and vegetation, which are typically described by bioclimate schemes (Holdridge, 1947; Whittaker, 1975). These spatial relationships can be extrapolated temporally to model past or future vegetation. An early example of this is by Prentice and Fung, who applied a bioclimate scheme to estimate vegetation biomass globally during the last glacial maximum, assuming steady state, i.e., that vegetation is in equilibrium with climate (Prentice & Fung, 1990). More recent examples often use machine learning methods such as random forests (RF) (Gómez-Pineda et al., 2020; Iverson et al., 2004; Prasad et al., 2006; Rehfeldt et al., 2012; Rogers et al., 2017) or the Maxent model (Phillips et al., 2006) to capture climate niches and make projections based on future climate (e.g., Loarie et al., 2008). Decision tree-based statistical methods including random forests can be useful in ecological modeling by uncovering hidden structures in the data and outperforming simpler regression techniques, especially at larger geographic scales (Prasad et al., 2006). Decision trees assume no underlying relationship between response and predictor variables (linear, quadratic, etc.) but instead construct decision rules, which optimally parse and partition the data based on predictor variables. Additionally, techniques like cross-validation and pruning can be used to find

optimal tree size and avoid overfitting. Ensemble methods based on randomized collections of trees, that is, random forests, further protect against overfitting and bias by randomly subsetting the out-of-sample test data and candidate variables across individual trees (Breiman, 2001). In general, these methods allow easier interpretation and visualization than more complex or deep learning methods, allowing insight into the key predictors and underlying relationships.

Another statistical approach relevant for ecological forecasting is the calculation of climate analogs, which involves connecting present and future climates by nearest distance in multidimensional climate space (Koven, 2013; Mahony et al., 2017; Williams et al., 2007). This approach allows for identification of particularly novel future climates, and the geographic distance between analogs can inform whether species' migration may be able to keep pace with expected climate change. Areas of highly novel future climates require particularly large levels of extrapolation for statistical niche models, and may indicate locations where process-based model approaches need to be prioritized.

Process-based models offer some advantages over statistical ecological niche models because they are able to represent dynamic processes such as establishment and mortality, competitive interactions, wildfire, effects of carbon dioxide on water use, and climate change impacts on net primary productivity and decomposition (Fisher et al., 2018). Statistical models have received criticism for not representing these processes explicitly (Hampe, 2004; Jackson et al., 2009), but in many cases statistical models have been shown to perform similarly to (or better than) process-based models (Hijmans & Graham, 2006; Kearney et al., 2010; Keenan et al., 2011; Morin & Thuiller, 2009). Even dynamical models have been criticized for the credibility of their representation of complex ecological

processes, especially due to limited quantitative understanding of the factors that control species range limits, competition, dispersal, migration, and the long-term physiological impacts of rising CO2 (Bachelet et al., 2008; Neilson et al., 2005; Rehfeldt et al., 2012). Statistical approaches informed by species abundance observations have the potential to capture the combined interactions of drought and fire that might be contained in the structure of vegetation. They can also constrain some aspects of other processes, for example, by considering migration rates, which to our knowledge have not yet been rigorously integrated into process-based models.

Regardless of approach, previous research has disagreed about the direction and magnitude of terrestrial carbon change in response to future climate in the Western United States (Foster et al., 2019; Lenihan et al., 2003; Rogers et al., 2011), though there appears to be a growing consensus of high vulnerability especially in California (Lenihan et al., 2008a; Loarie et al., 2008; Sleeter et al., 2019; Thorne et al., 2017). What makes this area of research especially challenging is the many possible trajectories of, and interactions between, land management (Cameron et al., 2017; Thorne et al., 2017), wildfires (Westerling & Bryant, 2007), climate scenarios and precipitation change (Thorne et al., 2017), impacts of biotic agents on tree mortality (Stephenson et al., 2019; Trugman et al., 2021), and migration potential (Higgins et al., 2003; Rogers et al., 2017).

In this study, we use a variety of eco-statistical approaches to project end-of-century aboveground live (AGL) carbon storage in California's wildland ecosystems, isolating the impact of climate change from other global change drivers. Our work builds upon multiple previous studies quantifying climate-driven vulnerability, and through our statistical approaches we offer a more comprehensive analysis of uncertainty arising from different

dimensions—namely (a) eco-statistical approach, (b) climate scenarios, (c) climate models, and (d) tree migration rates. The fourth component, migration, is often not accounted for in the current generation of process-based models, and is typically only accounted for in statistical models in the simplest of terms (assuming either no migration or unlimited migration). The uncertainties associated with future wildland carbon distributions and the spatial patterns of vulnerability that we quantify may allow policymakers to identify where multi-decadal carbon sequestration in aboveground biomass is an appropriate part of a climate mitigation portfolio, and where it may be a liability in a future climate.

2.2 Methods

2.2.1 Data

Climate Data

We obtained the downscaled modeled climate data for 2006–2099 from the Bias-Corrected Spatially Downscaled (BCSD) CMIP5 Climate Projections data set (Brekke et al., 2013; Maurer et al., 2007). This 1/8° resolution data set was chosen for its monthly temporal resolution and inclusion of all 32 CMIP5 models for RCP4.5 and RCP8.5. We used the mean daily precipitation and temperature variables and averaged them each to four seasons, giving us eight input variables to our models (Fig. 2.1). With all models, we used 2006–2015 average as "present" and 2090–2099 average as "future." Because there is substantial variability in precipitation change across the models (Fig. 2.2), we also grouped the 32 models into three moisture availability scenarios: "dry" (average of the eight models showing the greatest precipitation decrease for California), "mean" (of all 32 models), and "wet" (average of the eight models showing the greatest precipitation increase for California). On average for California, these moisture response scenarios correspond to a

precipitation decrease of 95 mm/y (−16%) for the dry scenario, an increase of 50 mm/y (+9%) for the mean of all models, and an increase of 227 mm/y (+39%) for the wet scenario with RCP8.5 (Fig. A1).

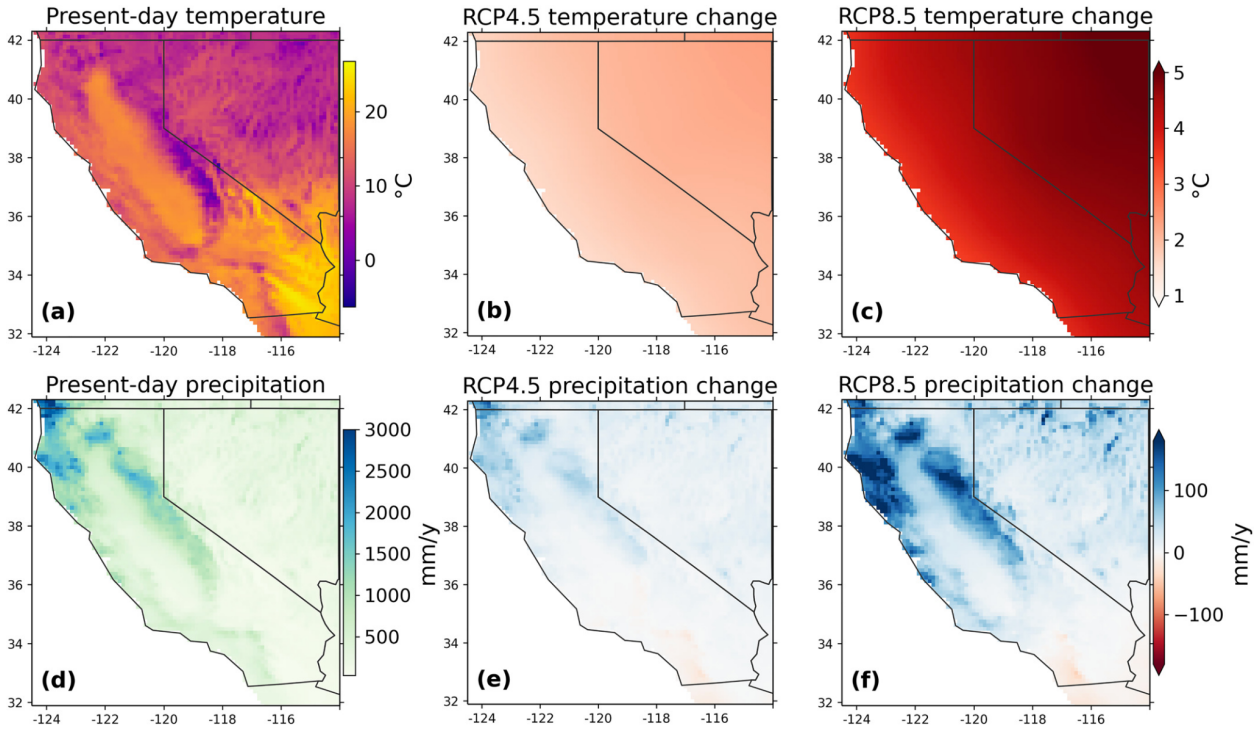

Figure 2.1. Average climate data from 32 downscaled CMIP5 climate models. The Bias-Corrected Spatially Downscaled (BCSD) climate data were the basis for the eight predictor variables in our models: four seasons of temperature and precipitation. For simplicity here, we show only the annual averages of temperature (a) and precipitation (d) for 2006–2015. Both RCP4.5 (middle) and RCP8.5 (right) show similar patterns of warming (b, c) and wetting (e, f), with different magnitudes. Under the more extreme RCP8.5 warming scenario, by 2090–2099, the state experiences approximately 4°C of warming, and slight wetting in the north and slight drying in the south. However, there is large disagreement over the direction and magnitude of precipitation across the 32 models (Fig. 2.2).

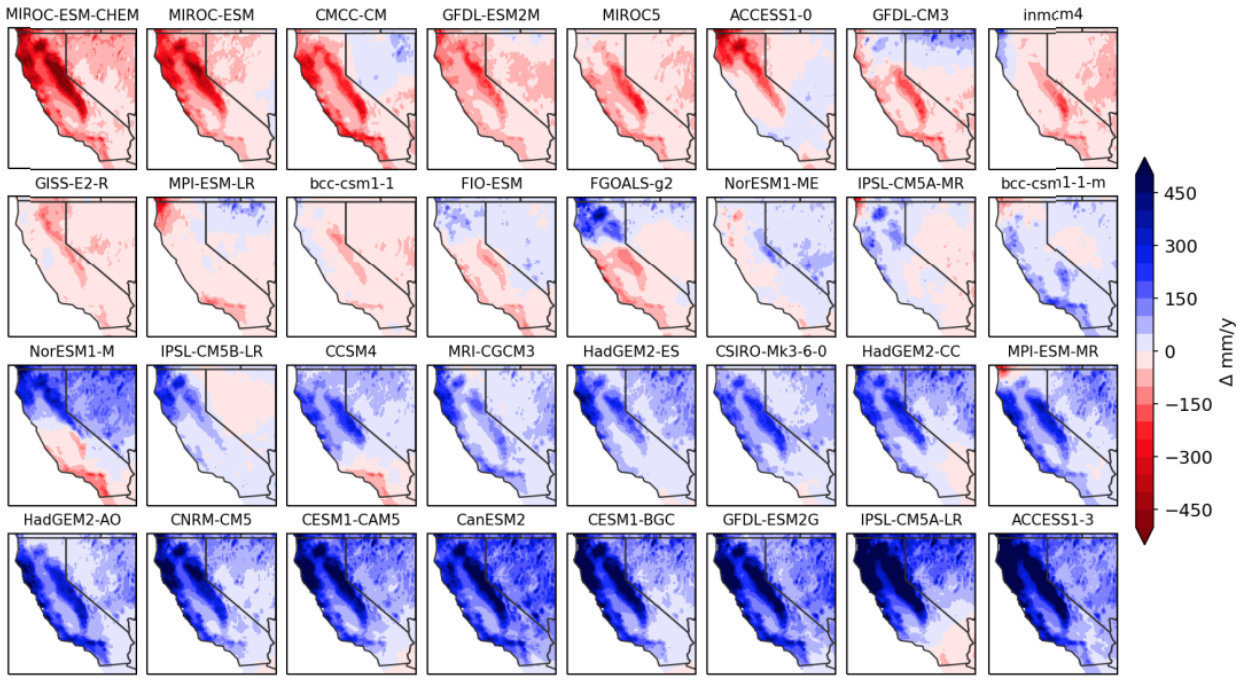

Figure 2.2. Model-to-model differences in projected changes in precipitation across the state of California during the 21st century. These maps were created by taking the difference between decadal means during 2090-2099 and 2006-2015 from 32 downscaled CMIP5 models for RCP8.5. Models are sorted from most drying to most wetting, with the first eight models (top row) comprising our "dry" scenario and the last eight models (bottom row) comprising our "wet" scenario (see Fig. A1).

Vegetation and Carbon Data

We incorporated data for vegetation or carbon from several different data sets, depending on what was most appropriate for each eco-statistical approach (Table 2.1). Our main quantity of interest throughout the study was aboveground live wildland carbon density, which we obtained upon request from the California Air Resources Board. This data set was available for California at 30 m for 2014 (California Air Resources Board, 2018) and is a direct extension of the data set described in Gonzalez et al., 2015 for years 2001 and 2010. For one of our approaches, we also first partitioned California's wildlands into two groups: forest versus shrubland or grassland, based on 30 m land cover data from the US Geological Survey National Land Cover Database (NLCD) for 2016 (Homer et al., 2020). For

another approach where we searched for present-day analogs to future climates, we needed carbon data that extended beyond California, including the Western United States and Mexico. For this larger domain we used a global product for 100 m aboveground biomass from the European Space Agency's Climate Change Initiative, available for the year 2017 (Santoro & Cartus, 2019). We scaled these biomass data by 47% to represent carbon, following common practice (Gonzalez et al., 2015). Finally, in our last approach, we modeled carbon densities separately for different tree species. Those species-level data were obtained from Oregon State University Landscape Ecology, Modeling, Mapping & Analysis (LEMMA), available at 30 m for 2012 (Kennedy et al., 2018). The LEMMA data set is based on a nearest neighbors approach, matching all pixels to their most similar inventory plot in terms of spectral and environmental characteristics. We considered the top 39 species in California by biomass, which account for 99% of aboveground forest biomass.

2.2.2 Data processing

In all cases, our study area was the wildland areas of California at an eighth-degree resolution, matching the resolution of the climate data set. We excluded any 1/8° pixels that were less than 50% wildland land cover for the purpose of our analysis. Here we considered "wildland" as forest, shrub, grass, or barren cover and excluded urban, agriculture, or water cover as classified by the NLCD. The remaining data set contained 2258 pixels (approximately 345,000 km^2 or 81% of California). For the pixels that were kept in the analysis, we also kept track of the valid subpixel land cover fraction, which we used to scale back our model estimates for total carbon. For those calculations, we also excluded barren areas, effectively preventing our models from adding biomass carbon to

rock-covered areas at high elevations in the Sierra Nevada mountains (or to other areas, such as deserts, which we assumed will not support biomass in the future).

Table 2.1. Summary of eco-statistical approaches. Each approach is fundamentally distinct, requiring different data sources based on the spatial domain and quantities of interest. In the third and fourth approaches, we also explored dispersal and establishment as factors limiting future carbon densities. In every approach, we compared results for RCP4.5 versus RCP8.5 and for dry versus wet climate models.

Eco-statistical approach	*Description*	*Data sources*
1. RF regression of carbon density	Random forest regression to project future carbon density based on seasonal climate predictors	CA Air Resources Board aboveground wildland carbon density (California Air Resources Board, 2018; Gonzalez et al., 2015)
2. RF classification of dominant vegetation type	Random forest classification to project future vegetation type (forest or shrubland/grassland) based on seasonal climate predictors; translated to carbon based on ecoregion averages	USGS National Land Cover Database (Homer et al., 2020); CA Air Resources Board aboveground wildland carbon density (California Air Resources Board, 2019)
3. Climate analogs	Assigned future carbon density equal to the carbon density from the location of the most similar climate in the present	ESA Climate Change Initiative biomass (Santoro & Cartus, 2019)
4. Tree species niche models	Random forest regression to project future carbon density for each of 39 species based on seasonal climate predictors	LEMMA species-level biomass (Kennedy et al., 2018)

As a supplementary analysis, we also explored the sensitivity of our eighth-degree carbon and land cover data sets to disturbance history (including fire and harvest) in California. We used fire and harvest polygons from the California Department of Forestry and Fire Protection (CALFIRE, 2021; FRAP, 2019) for 1995–2014 to filter our data at a 30-m resolution before averaging to the final eighth-degree resolution. The purpose of the analysis was to quantify whether our training data, and the resulting model projections described below, would be substantially different if we excluded young, recently disturbed

forest stands, which could have low carbon density or be classified as grass or shrublands in the NLCD map.

Data availability

The data that support the findings of this study were derived from the following resources available in the public domain. We appreciate the insight and data development work of our colleague Klaus Scott at the California Air Resources Board, who provided the California AGL carbon data layer. https://ww2.arb.ca.gov/nwl-inventory; https://lemma.forestry.oregonstate.edu/data; https://www.mrlc.gov/data/nlcd-2016-land-cover-conus; https://catalogue.ceda.ac.uk/uuid/bedc59f37c9545c981a839eb552e4084; ftp://gdo-dcp.ucllnl.org/pub/dcp/archive/cmip5/bcsd. All input data, model projections, and Python and Google Earth Engine scripts are available in a public repository via Dryad: https://doi.org/10.7280/D1568Z. Data include observations and model estimates of AGL carbon density on a 0.125° × 0.125° grid. The AGL carbon density data set at its original resolution of 30 m is available upon request from CARB.

2.2.3 Eco-statistical approaches

RF regression of carbon density

In our first and simplest eco-statistical modeling approach, we fit random forest regression models to estimate the present spatial distribution of aboveground live carbon density as a function of eight predictor climate variables: four seasons of temperature and precipitation averaged for 2006–2015. Random forest models were developed using the scikit-learn machine learning package in Python (Pedregosa et al., 2011) and validated with tenfold cross validation. We used the default forest size of 100 decision trees and chose a

maximum number of 25 leaf nodes, which optimized outgroup performance as measured by root mean square error (RMSE). We then fit a single random forest model to all 2258 data points, explored error structure and variable importance, and applied the model to the 2090s climate data. We report a total percent change based on the difference between the sum of modeled present and future AGL carbon density. We repeated this analysis (and all others below) to compare RCP4.5 versus RCP8.5 and dry versus wet models.

For this RF approach to modeling aboveground live carbon density, we also added an analysis of the contributions of temperature versus precipitation to carbon change under RCP8.5. We compared the spread of total projected biomass change across the 32 CMIP5 models when (a) temperature changes but precipitation is held constant, (b) precipitation changes but temperature is held constant, and (c) both temperature and precipitation change.

RF classification of dominant vegetation type

In our second approach, we chose a categorical variable of dominant vegetation type (namely, forest or shrub) as our target variable and repeated the methodology of the previous approach, with random forest classification models in place of regression models. The dominant vegetation type came from the NLCD, where deciduous, evergreen, and mixed forests were grouped together as “forest," and shrub/scrub and grassland/herbaceous were grouped together as “shrub." Instead of RMSE, we considered classification accuracy (number of correct classifications as a fraction of total number of classifications) as our performance metric. To estimate total carbon change from this approach, we applied the mean carbon density across the forest or shrub pixels in the corresponding ecoregion from the present. For this averaging step, we used the Level III

Ecoregions as defined by the EPA, helping to account for the different carbon densities of different forest regions in California.

Climate analogs

Our third approach leveraged the concept of climate analogs, first introduced by Williams et al., 2007 and then revised by Mahony et al., 2017, to project changes in carbon. The main idea is to find, for every pixel under 2090s climate, the most similar ("analog") pixel from the present climate. In the original Williams et al., 2007 approach, the distances between future and present climates were expressed as a standardized Euclidean distance (SED) in climate space (in our case, an eight-dimensional space of our eight variables). A more statistically robust metric presented by Mahony et al., 2017 is the Mahalanobis distance, which also accounts for the number of dimensions and correlation between variables. The Mahalanobis distance D_{ji}, between the future climate of a focal point, j, and another point, i, in the present, is described as

$$D_{ji} = \sqrt{D_{ji}^2} = \sqrt{[b'_j - a'_i]^T [R_j]^{-1} [b'_j - a'_i]} \quad (1)$$

where a' is a row vector of present climate data averages (in our case, of length 8), and b' is a row matrix of future climate data averages. Both a'_i and b'_j are normalized by the interannual climatic variability of the present climate at location j. $[R_j]$ is the correlation matrix of the eight climate variables at j in the present, calculated across 10 years of data. We then assigned a carbon density to each pixel in the future equal to that of its best present analog indicated by the minimum D_{ji}.

In using the future climate as the reference, the minimum Mahalanobis distance represents the novelty of the future climate at a given point. This novelty can then be

interpreted in a more meaningful way as a “sigma dissimilarity," that is, a multivariate z-score from a chi-square distribution with eight degrees of freedom. The sigma dissimilarity represents the departure of the future climate from historical variability (Mahony et al., 2017).

The climate analog analyses also allow determination of a climate analog velocity as the distance between the reference point and the geographical point that minimizes Mahalanobis distance divided by the time interval between the means of the two periods considered. By enlarging or decreasing the search area for the two points, a climate velocity limit can be applied to the metric, to capture dispersal limitations to ecosystem change. We thus explored the sensitivity of this approach to a maximum climate velocity by varying the search area over which a potential analog could be found for a given pixel. We calculated and compared carbon change for three different search areas: within 100 km of a given pixel, within 500 km of a given pixel, or within the entire domain of the climate data set (United States and Mexico, north of 25°). These different search areas roughly represent different magnitudes of dispersal limitation, the first being the most restrictive. The third and broadest domain is the most permissive, allowing for California ecosystems to reassemble and resemble ecosystems anywhere in the United States or northern Mexico if climatically favorable. While perhaps unrealistic, we include this third, unrestricted scenario in our final results as an end-member for comparison against the more restricted scenarios.

Tree species niche models

In our fourth and final approach, we developed random forest regression models separately for the AGL carbon of each of 39 tree species, accounting for 99% of

aboveground live forest carbon. Our RF regression models followed the training and testing methodology outlined in the first approach, RF regression of carbon density. As with the climate analogs, we explored a few "sub-approaches" to test the model sensitivity and the equilibrium assumption. In the first "equilibrium" sub-approach, we added together 20 different models for 20 species that account for 94% of AGL forest carbon (species 21–39 were ultimately excluded due to poor model performance). We also verified whether adding together 20 separate models led to any projections of carbon that were higher than anywhere observed in the present, in which case we might need to consider competition. In the second sub-approach, we grouped the 39 various species together into functional types, modeling conifer versus hardwood species (see Table S1 for full details on the species and their groupings). These first two sub-approaches assume equilibrium with future climate, that is, that the tree species are given infinite time to migrate and fully establish. In the final two sub-approaches, we added a consideration of migration—a fast (500 m/y) and slow (50 m/y) scenario. These migration rates were chosen based on previous studies which estimate rates of tree dispersal and establishment on similar orders of magnitude (Davis, 1983; Higgins et al., 2003; Huntley, 1991; Settele et al., 2015; Solomon, 1997). For simplicity, each migration rate provided a threshold where, for each future pixel, we forced a given species' biomass to zero if there was no present-day presence within a distance of (migration rate) × (85 years). For reference, those distances are 43 km for the fast scenario, and 4.3 km (effectively one 1/8° pixel in any direction) for the slow scenario. These simple calculations are intended to provide a first-order estimation of the magnitude of variation arising from a tenfold increase in migration capacity in comparison to infinite migration capacity. As a whole, the comparison across these sub-approaches allows us to highlight

specific vulnerable species/groups and to quantify the impact that management such as assisted migration could have in increasing California's total carbon storage.

2.3 Results

We developed, tested, and applied a variety of statistical models to project future aboveground carbon stocks in response to climate change (Table 2.1). In all cases, models were driven by eight climate predictors: four seasons of temperature and precipitation (Fig. 2.1). We report performance metrics for the different approaches (Table 2.2) and spatial patterns of error (Fig. A2). Each eco-statistical approach revealed important insights about future carbon stocks, and on average projected losses of 8.8% ± 5.3% due to RCP4.5 climate change and 16.1% ± 7.5% due to RCP8.5 climate change (Table 2.3). We found high agreement in both magnitude and spatial patterns across the various approaches. The largest sources of variation, in order, were between (a) the dry and wet climate models, (b) the slow migration and equilibrium runs in the tree species niche models, and (c) RCP4.5 and RCP8.5.

Table 2.2. Summary of models' performance. Models are fundamentally different approaches to describing future vegetation and carbon storage, with different relevant metrics for each. For the random forest regression type models (approaches 1 and 4), we report the average root mean square error (RMSE) and the coefficient of determination (R^2) between the predictions and observations at present-day. Both represent performance on out-of-sample data during cross-folding validation. For the random forest classification of forest-vs-shrub, we report the classification accuracy (expressed as a percent representing the number of correct classifications relative to the total number of classifications) and confusion matrix. For the third, climate analogs approach, there is not a singular model being fit to the present-day data for which to report a performance metric, but the goodness of fit of the analogs is described by the climatic novelty map shown in Fig A7.

Eco-statistical approach	*Performance*	
(1) RF regression of carbon density	RMSE = 13.4	R^2 = 0.85
(2) Classification of dominant veg. type	Classification accuracy = 90.1%	
	Confusion matrix	
	Pred. shrub	Pred. forest
Obs. shrub	66.0%	5.2%
Obs. forest	4.6%	24.2%
(4) Tree species niche models		
· 20 species models' average	RMSE = 2.0	R^2 = 0.66
· Conifer model average	RMSE =12.4	R^2 = 0.80
· Hardwood model average	RMSE = 5.7	R^2 = 0.80

Table 2.3. Projected change in aboveground live carbon. We estimated net carbon losses from climate change for several different scenarios and statistical modeling approaches. For comparison, the total change aligning with the State's carbon sequestration goals is +4.2%. The largest differences, in order, are (1) between the dry and wet climate models, (2) the slow migration and equilibrium runs in the tree species niche models, (3) between RCP4.5 and RCP8.5.

	RCP4.5			*RCP8.5*		
Eco-statistical approach	*Dry*	*Mean*	*Wet*	*Dry*	*Mean*	*Wet*
(1) RF regression of carbon density	-20.7%	-5.0%	+7.4%	-33.2%	-15.5%	+1.6%
(2) RF classification of dominant veg. type	-17.6%	-6.3%	+1.1%	-27.4%	-18.5%	-15.0%
(3) Climate analogs						
· Full domain	-26.0%	-14.0%	-6.7%	-32.7%	-23.2%	-6.0%
· Restricted to 500 km	-25.2%	-13.8%	-6.6%	-30.8%	-21.4%	-4.6%
· Restricted to 100 km	-25.7%	-16.5%	-11.7%	-32.6%	-24.9%	-14.1%
(4) Tree species niche models						
· 20 species, equilibrium	-23.2%	-2.8%	+20.8%	-29.9%	-2.8%	+30.3%
· Conifer vs hardwood, equilibrium	-20.3%	-2.0%	+13.7%	-30.9%	-7.4%	+14.1%
· 20 species, fast migration (500 m/yr)	-25.8%	-6.9%	+13.2%	-33.8%	-11.3%	+9.6%
· 20 species, slow migration (50 m/yr)	-29.7%	-11.7%	+6.5%	-40.0%	-20.0%	-4.5%
Average	**-23.8%**	**-8.8%**	**4.2%**	**-32.4%**	**-16.1%**	**1.3%**
Standard deviation	3.7%	5.3%	11.0%	3.5%	7.5%	14.6%

2.3.1 Four statistical approaches to project future carbon stocks

In our first, simplest RF regression approach, the most important predictors of carbon density were fall, winter, and spring precipitation, with an average R^2 of 0.85 between out-of-sample predicted and observed carbon density (Table 2.2, Figure A3). While less important than fall, winter, and spring precipitation, temperature also enhanced model performance. The importance of summer and winter temperature in particular indicates that climate warming will cause changes in the distribution of carbon stocks. In agreement with other approaches, this RF regression revealed largest losses in the Northern California Coast ecoregion and foothills of the Sierra Nevada, with some potential for gain at high elevations (Figs. 2.3, A4).

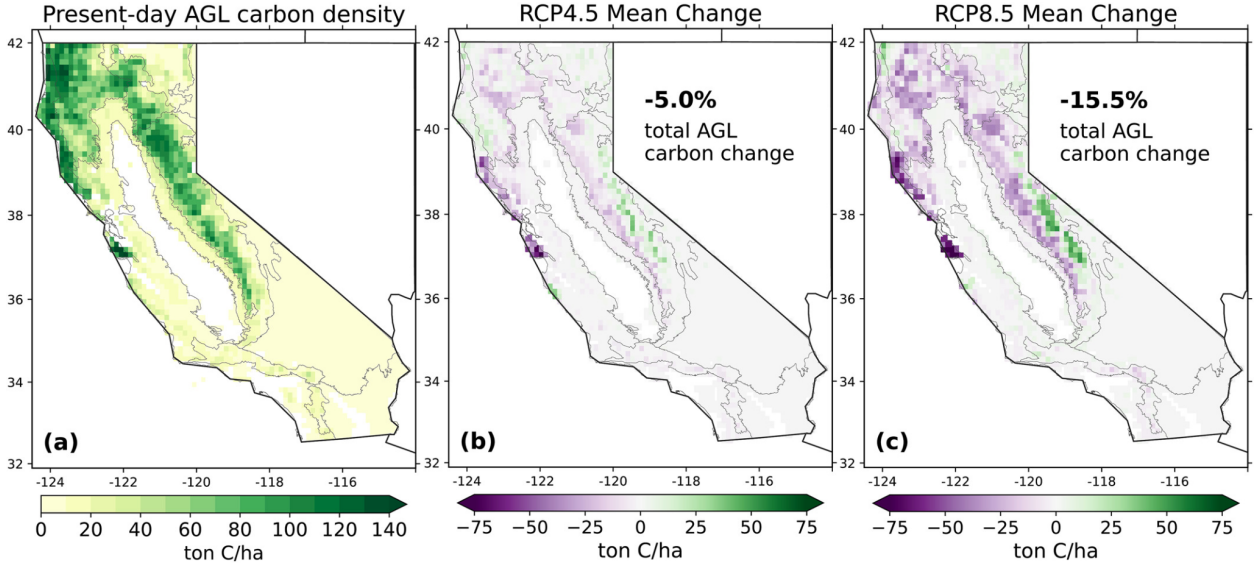

Figure 2.3. Present observed aboveground live carbon density (a) and our modeled change with (b) RCP4.5 and (c) RCP8.5 climate change from the random forest regression. Areas of greatest vulnerability to climate-driven carbon loss are the northern coasts and low/mid-elevation Sierras, with some potential for carbon gain at high elevations. See Figure S5 for similar maps showing wet and dry models.

The RF classification approach identified specific areas of major plant type transitions, namely, between forest and shrubland ecosystems due to climate change. We

found widespread conversion of forest to shrubland, even in wetting scenarios, especially in the lower elevation areas of the Sierra Nevada and Southern Cascades (Figure 2.4). With RCP8.5 mean warming, our RF classification model projected a loss of 28.0% of forested area. This loss of forest area corresponded to a smaller decrease of 18.5% for AGL carbon density, given that these are on average less carbon-dense forest areas, and persistent shrublands account for a non-negligible amount of the state's carbon stocks.

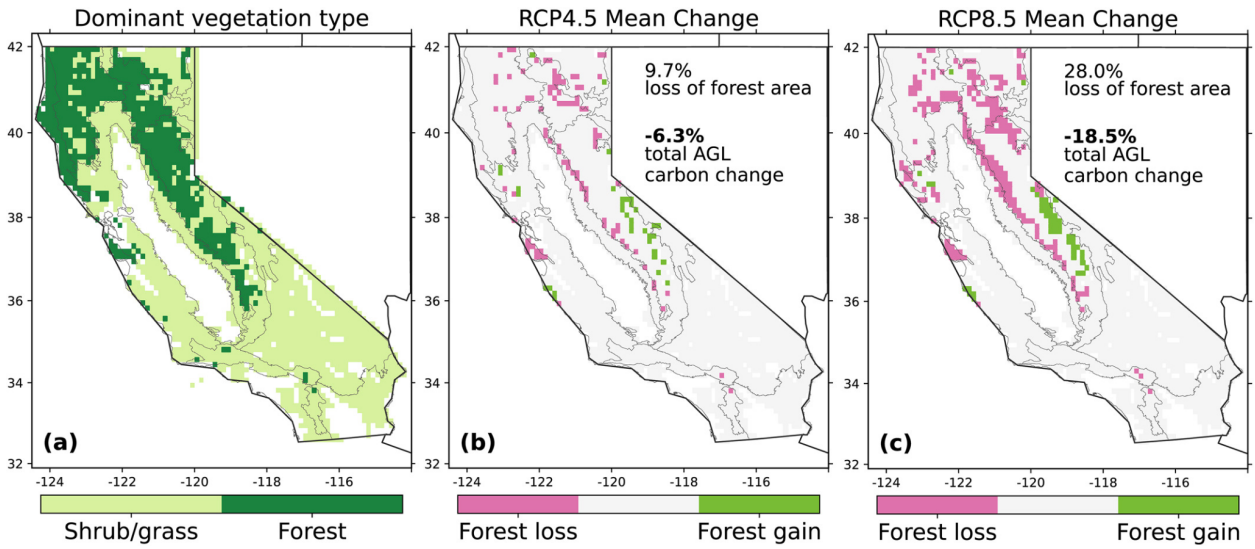

Figure 2.4. Results from RF classification of dominant vegetation type. Both RCP4.5 and RCP8.5 scenarios result in a net conversion of forest into shrubland, especially in the foothills of the Sierra Nevada and central coast. This type conversion is relevant as it would likely be associated with increased fire risk. Total loss of aboveground live carbon is approximately three times larger with the more extreme warming scenario of RCP8.5.

The climate analogs approach provided similar patterns of change as the previous two approaches, with mean carbon loss of 14.0% for RCP4.5 and 23.2% for RCP8.5. We found no clear evidence that the magnitude of carbon change was sensitive to the restriction in search radius (in some, but not all climate scenarios, further restricting the search radius led to more carbon loss). Also, in quantifying how future climates will compare to present climates (Figures A5 and A6), we found that specific areas of California

like the southern deserts, northern coasts, and Central Valley may have little resemblance to any present-day areas of the United States or Mexico (Figure A7).

Finally, our fourth approach with tree species niche models using RF regression quantified how specific tree species could be impacted by varying degrees of climate change, and how migration capacity could substantially limit total carbon stocks (Figs. 2.5, A8). The niche models projected carbon density declines of 30.7% for conifer species such as Douglas fir and Ponderosa pine with RCP8.5 climate change. On the other hand, oak species such as canyon live oak were projected to increase their total AGL carbon density by 43.7%. This replacement occurred especially in the low-to-mid elevation areas of the Sierra Nevada and Southern Cascades, and the general pattern of climate change favoring oaks over conifers agrees with previous research (McIntyre et al., 2015). Coast redwoods in particular showed high vulnerability at the southern ends of their range (south of San Francisco), in agreement with Fernández et al. (2015).

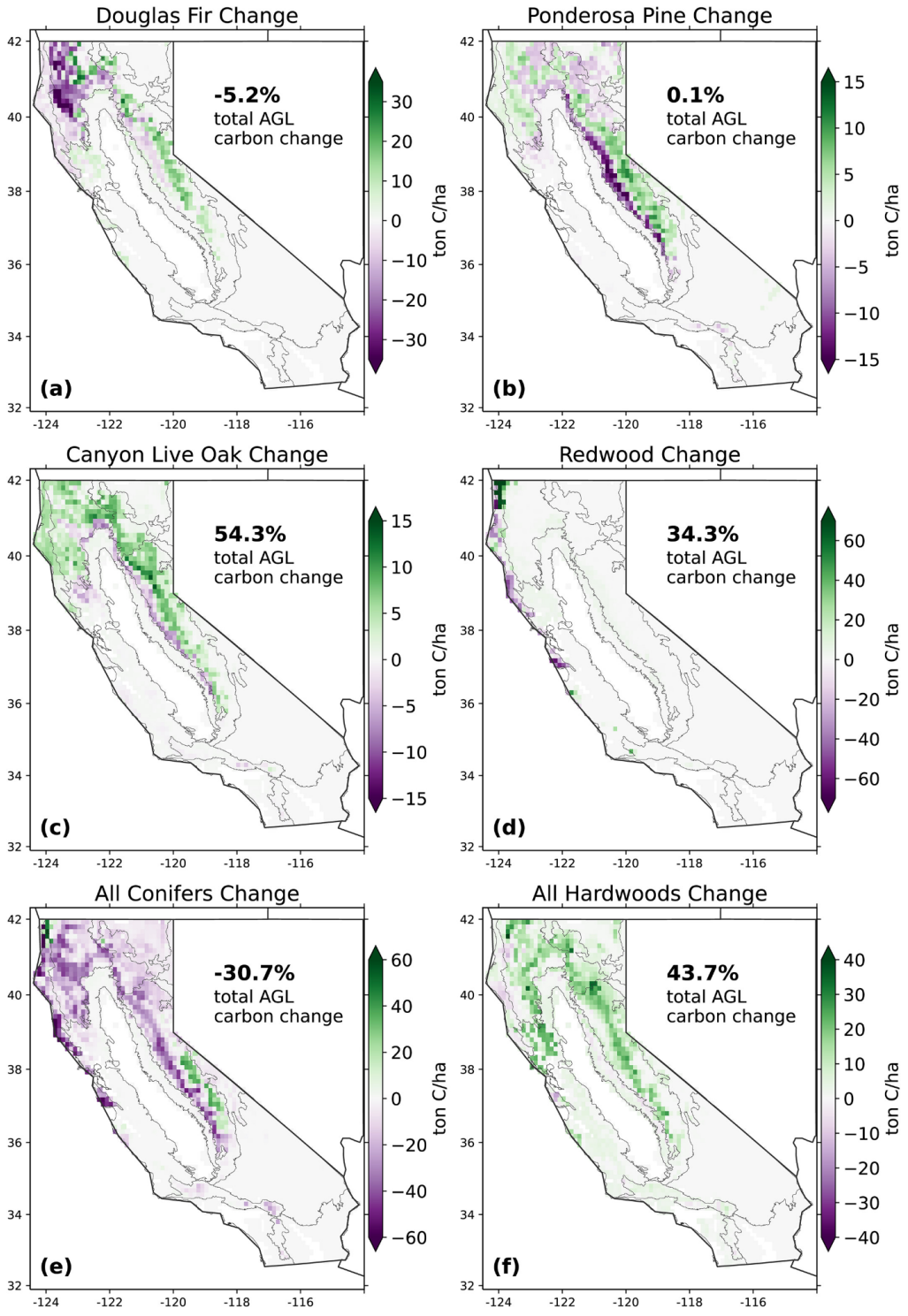

Figure 2.5. Selected results from tree species niche models, for the equilibrium scenario and RCP8.5 multi-model mean. Several species shift from low elevation to high elevation in the Sierra Nevada. Coast redwood shows high vulnerability in the southern part of its range, which may be compensated for by large increases in density in the north. In general, conifer species show future carbon losses while hardwood species show carbon gains.

Migration strongly constrained our projections of total future ecosystem carbon. When we assumed that all tree species would be able to geographically adjust to reach equilibrium with future climate, carbon loss was only 2.8% for either RCP4.5 or RCP8.5. Carbon loss increased to 11.3% for RCP8.5 when we imposed a limit to migration consistent with an upper bound on tree migration rate observations (500 m/y), and to 20.0% using a more conservative estimate of possible migration rates (50 m/y).

2.3.2 Climate drivers and uncertainty

We also explored the role of uncertainty in future precipitation, and the entangled effects of temperature and precipitation. Across all approaches, wet models resulted in less carbon loss, and often carbon gain. On average, for RCP8.5, we projected 32.4% carbon loss with dry models and 1.3% carbon gain with wet models (Table 2.3). The carbon gain in the latter case suggests that the increased moisture availability in these wettest eight climate models is sufficient to compensate for the effects of 3–4°C of warming on water demand. To further understand the sensitivity of carbon density to climate controls, we compared RF regression model projections with RCP8.5 mean climate change but with temperature or precipitation held constant. We found that rising temperatures systematically drive carbon loss, while the variation in future precipitation contributes substantial uncertainty to the magnitude of loss (Fig 2.6). This finding was true for species-specific approaches as well, where temperature change explained most of the spatial patterns including large losses of coastal redwood in the south and increased favorability of hardwoods over conifers.

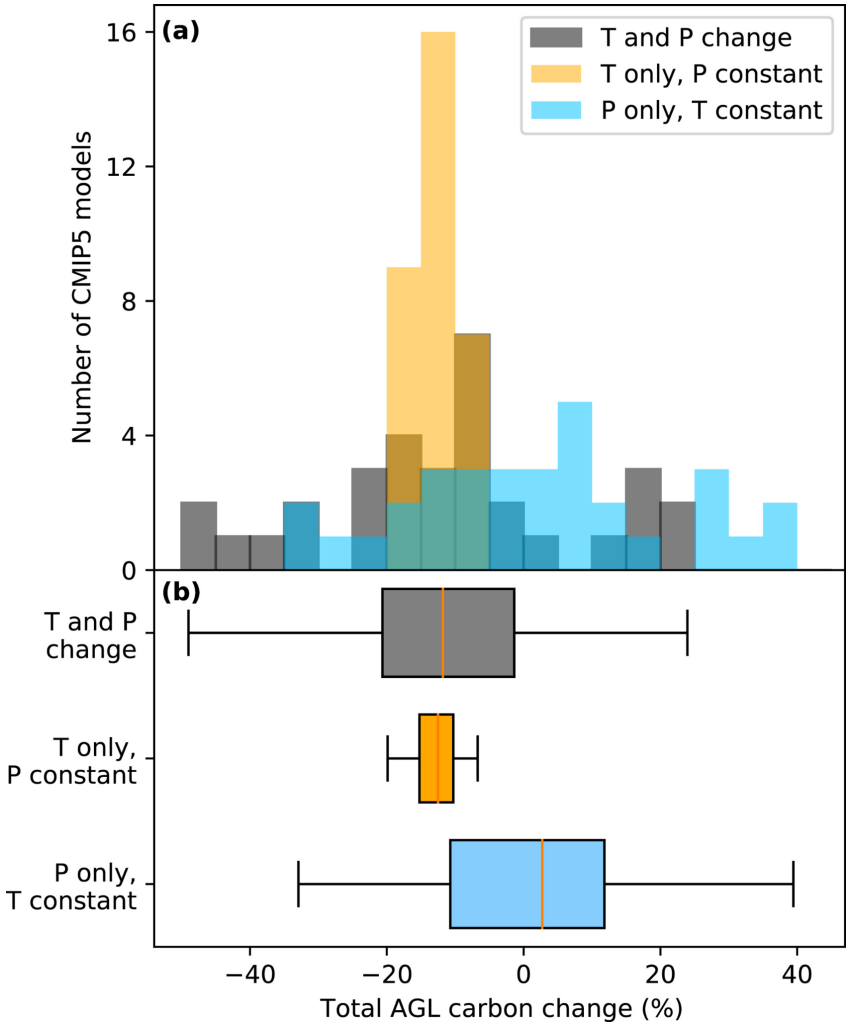

Figure 2.6. Contribution of temperature versus precipitation change to carbon change. The range represents the spread across carbon projections using the 32 different CMIP5 models under RCP8.5 in our RF carbon regression approach. Rising temperature systematically drives declines in carbon storage, while the uncertainty in precipitation change adds large variability to the magnitude of carbon change.

2.3.3 Spatial patterns of vulnerability

Lastly, we quantified several aspects of the spatial pattern of vulnerability (Figs. 2.3 and 2.77), most notably with respect to elevation. Coastal areas and low-to-mid-elevation areas of the Sierra Nevada showed the greatest future carbon declines, whereas high elevation areas may offer the most potential for increased carbon storage. Based on our

tree species niche models, these losses are largely explained by the shifts in redwood range on the coast and loss of conifers in favor of oaks in the Sierra Nevada (Fig. 2.5).

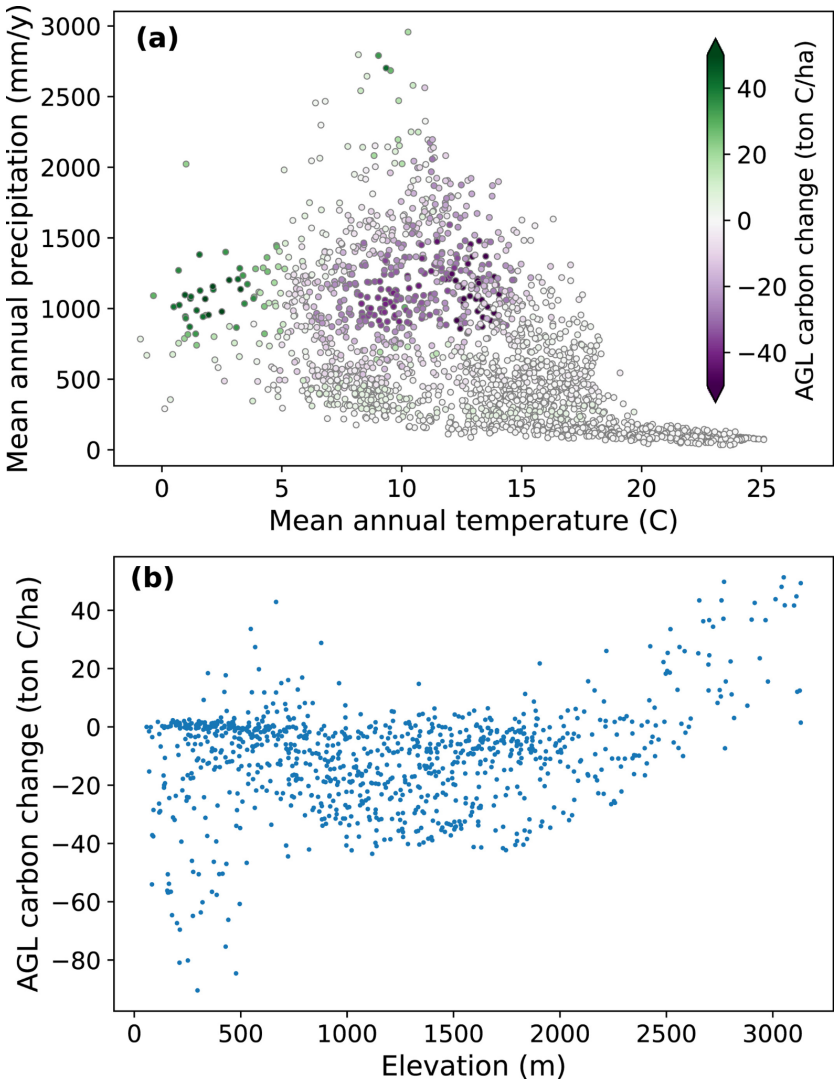

Figure 2.7. Correlation between aboveground live (AGL) carbon change and present-day climate (a) and elevation (b). Vulnerability to carbon loss decreases for presently cooler climate regions (a) or with elevation for forested grid cells (b). Cool and high-elevation regions greater than approximately 2200 m show increased AGL carbon with warming, while the greatest losses are in low elevation, moderately warm climates.

The implications of carbon storage changes over the coming century in California will have important economic and policy impacts. We observed particular vulnerability in some of the areas where there are existing forest carbon offset projects as a part of

California's Cap-and-Trade system (California Air Resources Board, 2015) (Fig. 2.8). The offset project protocol legally requires landowners to measure and verify carbon permanence for 100 years after any credits are issued. Credits are calculated by comparing carbon stocking to a 100-year modeled baseline, which could only evolve based on climate-driven risk if the crediting period were renewed every 25 years. We found that offset projects are located in disproportionately vulnerable parts of the state, such as the low-elevation regions of the Southern Cascades and Northern Coast ecoregions. With RCP8.5 mean climate change for our first RF regression approach, the average offset area loses 23.1% AGL carbon, while the state total projected loss is 15.5% across all ecosystems or 10.4% for forests (Fig 2.8b). Anticipation of these projected changes could inform more realistic baselines in order to minimize losses to such vulnerable areas and constrain expectations around forest management policy.

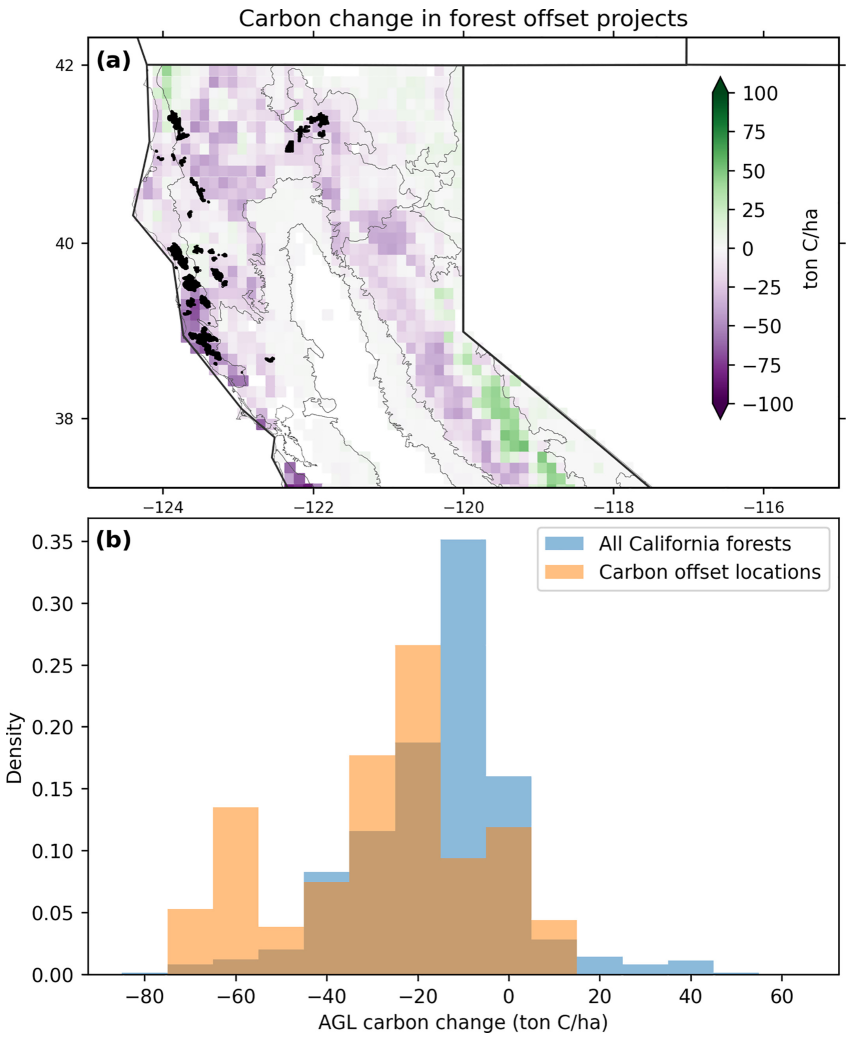

Figure 2.8. Vulnerability of California forest carbon offset projects to RCP8.5 mean climate change. Thirty-two forest carbon offset projects are based in California, in the Northern California Coast and Southern Cascades ecoregions (black polygons in panel (a)). For RCP8.5 mean climate change, grid cells where projects are located are projected to lose 23.1% of AGL carbon (orange, b), while the average forested grid cell loses 10.4% of aboveground live (AGL) carbon (blue, b), and the total statewide expected loss is 15.5% (Table 2.3). For RCP4.5 mean climate change, project grid cells are projected to lose 6.5% of AGL carbon compared to average forest loss of 3.1%. The disproportionate vulnerability of these critical areas is likely to impede their capacity to store carbon for 100+ years as required per the forest carbon offset protocol.

2.4 Discussion

2.4.1 Climate change effects

Several important insights emerge from some of our key findings, especially where

there is consistency across approaches. These insights can help build a more resilient future for California despite great climate uncertainties. The first is that a reduction in emissions from RCP8.5 to RCP4.5 leads to approximately half the end-of-century carbon losses from ecosystems. This result emphasizes how global emissions, the vast majority of which are not in California's jurisdictional control, will determine the fate of California's natural and working land carbon stocks. The second insight is that uncertainty in wet season precipitation regimes (Fig 2.2), under either climate scenario, will drive the majority of the variability in carbon storage. Investments in science that yield more robust, multi-decadal precipitation projections for the state will not only benefit the state's water-strapped economy, but also our understanding of its natural and working land carbon future. Third, these results allow the state to consider climate mitigation portfolios that do not assume carbon storage stationarity. Doing so could result in proactive strategies that involve minimizing carbon losses in vulnerable areas, adding biomass in areas that will become more favorable for carbon storage (particularly high elevations), and assisting with the redistribution of key species. These projections could also be leveraged to establish more appropriate future baseline scenarios against which carbon sequestration projects, like those featured in California's Cap & Trade Offset program, could be assessed.

The individual modeling approaches also provided complementary perspectives and insight. For example, one major conclusion from our RF classification of vegetation type is the substantial loss of forest cover (28%) with RCP8.5 mean climate change. Such large-scale conversion of forest to shrub or grasslands may be driven by climate-related disturbances such as wildfire (Abella & Fornwalt, 2015; Coop et al., 2016; Lauvaux et al., 2016; Rother & Veblen, 2016; Savage & Mast, 2005; Tepley et al., 2017) and drought- and

insect-driven mortality (Anderegg et al., 2013, 2020; Stephenson et al., 2019; Trugman et al., 2021), which have already been documented as important drivers of vegetation change across the Western United States.

Another set of insights comes from the climate analogs approach, which quantifies the degree of novelty of the emerging climate regimes across the state. The spatial pattern of novelty highlights the areas where the emerging climate regime is most novel as compared to the historical climate regime (Figures A7b and A7c). The less novel areas are where historically informed statistical approaches are interpolating within the existing climate variability and thus most likely to have some predictive power. In contrast, the more novel areas (in particular, along the Northern California Coast and central part of the Southern Cascades) are where statistical approaches are fundamentally extrapolating and may require approaches based on process representation to understand their future trajectories.

From the separate species niche models, we projected that certain tree types like oaks will be favored over conifers. Certain key tree species like redwood were projected to see substantial range shifts, with total carbon density being limited by migration capacity as a result. The pattern of increasing total carbon loss with lower migration potential supports the idea that the velocity of climate change is a source of ecosystem vulnerability (Ackerly et al., 2010; Loarie et al., 2009), and that management activities such as assisted migration could have a large impact on carbon storage and conservation of key species. For coast redwood in particular, large increases in density at the northern end of its coastal range and even expansion toward the Sierra Nevada could theoretically offset losses at the southern end of its range, but only if migration rates do not become limiting. Realistically,

redwoods take hundreds of years to grow, so range shifts resulting in net carbon gains are implausible on the timescale of this century. In addition, our methodology does not explicitly capture coastal fog as a moisture source, and there is evidence of declining fog frequency in the last century (Johnstone & Dawson, 2010), highlighting the importance of considering a broader set of climate drivers in future work.

2.4.2 Assumptions and limitations

This study was based on a few major assumptions. First, we chose a fairly simple representation of environmental drivers, that is, four seasons of temperature and precipitation, and focused on exploring the influence of different statistical approaches and climate scenarios. We did not explicitly represent other drivers as input variables—such as other hydrological variables, soil characteristics, or vulnerability to insects—although many of these processes are implicitly represented in the climate-carbon relationships derived from our statistical models. Regarding hydrology, our approach captured some of the seasonal structure and aspects of water balance (e.g., length and intensity of the dry season, high temperature limits) but did not explicitly account for other hydrological variables like drought indices (Madakumbura et al., 2020) and vapor pressure deficit which should be explored in future studies. We also did not consider the potential increasing interannual variability of precipitation with climate change (Swain et al., 2018), which may be another source of ecosystem vulnerability and additional decreases in carbon stocks.

Second, our methodology involving fairly coarse spatial resolution and fitting of climate drivers to empirical data is an imperfect representation of finer scale ecological dynamics. Due to limitations in both data and modeling, we cannot capture the exact fundamental niches of different species and vegetation types as a function of landscape and

watershed position, but rather estimate the realized climate niches at an eighth-degree within California. In the results presented in the main text, we also have not explicitly accounted for land use legacy, disturbance history, or forest age. We provide a supplemental analysis (Table A2 and Fig. A9) showing that an initial attempt to account for post-fire and post-harvest impacts on carbon stocks in our random forest regression or classification had only a minimal impact on our carbon density projections. While the supplemental analysis does not change any of our major conclusions, which are more focused on comparison of different climate scenarios and statistical approaches, it highlights the importance of regarding with caution the interpretation of individual grid cell changes given the heterogeneity of fire and harvest effects. Relatedly, embedded in our projections is an assumption of a set of climate-fire-management interactions which do not change markedly over the next century. If the State undertakes a fundamentally different approach to fire and land management, like widespread forest fuel reduction treatments (Agee & Skinner, 2005) or fire regimes intensify beyond the current range of observations, these could dampen or amplify some of our projected changes.

Third, we assumed that other potential factors to mitigate carbon loss (i.e., CO_2 fertilization and acclimation), would be negligible compared to the scale of spatial reorganization of vegetation represented in our models. Regarding CO_2, there is a lack of agreement in the literature on the extent to which carbon storage will be enhanced by rising CO_2, especially considering the concurrent changes to drought frequency (Birami et al., 2020; Jiang et al., 2020; Lenihan et al., 2008b; Needham et al., 2020; Sperry et al., 2019; Swann et al., 2016) and declining nitrogen availability in some cases (Luo et al., 2004; Wamelink et al., 2009). For example, one study found that 55–71% of climate projections

have enough CO_2 increase to offset the temperature-driven mortality, depending on the extent of acclimation (Sperry et al., 2019), whereas another found that heat and drought erased any benefits of increased CO_2 (Birami et al., 2020). Acclimation may play a substantial role, though the extent of which is uncertain (Sperry et al., 2019). Due to this uncertainty and the lack of elevated CO2 experiments in semi-arid forest ecosystems, our analysis targeted only the climate-driven ecosystem response. Our scenarios may be representative of the full ecosystem response, including CO2 fertilization, if changes in water use efficiency due to CO_2 are small in comparison to the effects of effects of 3°–4° of warming. During the historical era, the accelerating effects of large-scale drought and fire mortality and across California and the western United States seem to suggest that, so far, the magnitude of climate impacts on forests is substantially larger than the benefits from rising CO_2.

Finally, our analysis considered aboveground live carbon and did not attempt to model dead or belowground carbon pools, which account for a majority (83%) of ecosystem carbon in California (California Air Resources Board, 2019). In order to compensate for a projected aboveground live loss of 11.3% and meet state goals of 4.2% total ecosystem carbon increase, these other pools would have to increase by 6.1%. There is considerable uncertainty in the carbon dynamics of the dead pools and whether changes in these pools could compensate for losses in aboveground biomass. Drier conditions may slow decomposition and minimize carbon losses of litter and coarse woody debris; however, the buildup of these pools would also increase fire risk. The direct effects of warming, in contrast, may accelerate decomposition, increasing losses from litter and soil carbon pools (Davidson et al., 1998; Davidson & Janssens, 2006).

2.4.3 Implications for land management

Land management strategies have the potential to mitigate some of the projected carbon losses reported here. A study by Cameron et al., 2017 found that extremely ambitious implementation of conservation, restoration, and forest management could contribute up to 26 MMTCO_2e/y by 2050, or 135 MtC (2.5%) to total ecosystem carbon by 2050, not considering climate change. Another found that a low population growth and land-use scenario could contribute 215 MtC (3.9%) by 2100, even with RCP8.5 climate change (Sleeter et al., 2019). These potential increases to total ecosystem carbon would be enough to offset our projected loss of aboveground live carbon alone, but likely not enough to offset potential losses in the other larger carbon pools.

More broadly, our spatial patterns of climate-stable and climate-unstable carbon stocks (and habitat types) are relevant for management as they could inform where different actions would be most effective over this century. The current one-size-fits-all strategy to maximize carbon stocks across California forests appears poorly suited to the projected shifting mosaic of carbon with climate change. We suggest a more climate-aware approach—for example, in climate-unstable locations such as the low-mid elevation Sierra Nevada and central and northern coastal ranges, management should focus on stabilizing existing carbon stocks against inevitable climate-driven transitions, rather than incentivizing carbon gain. In these areas, the priorities could be to reduce the risk of catastrophic fire, and thinning and restoration to promote large trees and reduce water stress. Management to increase carbon stocks would be most valuable in select climate-stable locations such as above 2,000 m elevation in the Sierra Nevada and in the northwestern coastal Klamath range. In addition, assisted migration and establishment,

though difficult and controversial, could allow key species like coast redwood to relocate to or increase density in climate-favorable habitat regions (McLachlan et al., 2007; Millar & Stephenson, 2015). These species take decades or centuries to reach maturity, and so early action in anticipation of climate change is essential for both conservation and achieving California's long-term carbon goals.

Our results provide actionable insights about the likely magnitude and uncertainties of terrestrial carbon change over this century. We present a comprehensive statistical analysis showing widespread agreement in the direction and relative magnitude of change across different approaches. We also included a consideration of migration which is often not well accounted for in other modeling approaches. Our findings highlight that the uncertainty in this migration component, as well as in future precipitation, are major scientific bottlenecks for long-term ecological forecasting. Overall, we estimate that rapid warming in the coming decades will drive large declines in aboveground biomass, especially in coastal and low-elevation areas. The losses are in stark contrast to California's goals of markedly increasing the land carbon sink toward carbon neutrality by 2045. The projected losses also suggest that climate-driven vulnerability should be an important point of continued research in the context of natural climate solution strategies, such as California's forest carbon offsets program, which rely heavily on sustained carbon dioxide removal by ecosystems.

2.5 Acknowledgments

This work is based upon support received from the National Science Foundation (NSF) Graduate Research Fellowship Program under grant number DGE-1839285 (for S. R. Coffield), by the UCOP National Laboratory Fees Research Program under grant number

LFR-18-542511 (for S. R. Coffield, J. T. Randerson, C. D. Koven, M. L. Goulden), by the California Strategic Growth Council's Climate Change Research Program with funds from California Climate Investments as part of the Center for Ecosystem Climate Solutions (for M. L. Goulden, J. T. Randerson, S. R. Coffield, and K. S. Hemes), by NSF under grant number 1633631 (for J. T. Randerson) as part of the University of California, Irvine (UCI) NSF Research Traineeship (NRT) Machine Learning and Physical Sciences (MAPS) Program, by the Department of Energy (DOE) Office of Science's Reducing Uncertainty in Biogeochemical Interactions through Synthesis and Computation (RUBISCO) Science Focus Area (for J. T. Randerson and C.D. Koven), by the DOE Early Career Research Program (for C. D. Koven), by the Regents of the University of California under prime contract number DE-AC02-05CH11231 for management and operation of LBNL (for C. D. Koven), and by the Stanford Woods Institute for the Environment (for K.S. Hemes). M. L. Goulden reports grants from the California Strategic Growth Council, and K. S. Hemes had an occasional scientific advising relationship with the California Forest Carbon Coalition. Neither of these impacted the scientific analysis presented in this publication.

Chapter 3

Using remote sensing to quantify the additional climate benefits of California forest carbon offset projects

Adapted from:

Coffield, S.R., Vo, C.D., Wang, J.A., Goulden, M.L., Badgley, G., Cullenward, D., Anderegg, W.R.L., Randerson, J.T. Using remote sensing to quantify the additional climate benefits of California forest carbon offset projects. *Global Change Biology* (in press).

3.1 Introduction

Nature-based climate solutions (NCS) include land management, reforestation, and conservation activities to sequester carbon, and are a component of most pathways to keep the planet below 1.5-2°C of warming (Roe et al., 2019; Smith et al., 2016). Compared to other carbon dioxide removal technologies, NCS are comparatively low cost (Psarras et al., 2017), immediately ready for large-scale deployment (Minx et al., 2018), not reliant on energy inputs (Smith et al., 2016), and frequently come with environmental and social co-benefits (Seddon et al., 2020). NCS have received increasing attention in the US and internationally, for example through the U.S. Department of Energy's Carbon Negative Earthshot initiative to remove carbon, discussed at the 2021 COP26 summit (Gardner, 2021).

Among NCS, improved forest management (IFM) is estimated to have the greatest potential to sequester carbon. Surveys report IFM sequestration potential of up to 16 Gt CO_2 yr^{-1} of negative emissions globally by 2030 (Griscom et al., 2017) or about half of total NCS sequestration (Fargione et al., 2018). Forest management practices that improve carbon storage include extending time between harvests, thinning to increase productivity,

or increasing the stocking of trees. However, recent research has also highlighted the need for improved estimation and verification of the carbon potential of IFM (Kaarakka et al., 2021), which may be overestimated (Reise et al., 2022).

NCS, and IFM in particular, are a prominent component of California's climate mitigation policies. Administered by the California Air Resources Board (CARB), the California cap-and-trade program sets a cumulative carbon emissions limit, with tradable annual budgets that shrink each year, for large entities responsible for about 75% of the State's emissions. Emitters can use verified carbon offsets to comply with program requirements, subject to a set volumetric limit between 4 and 8% of their covered emissions (Haya et al., 2020). Offset projects occur across the continental United States and Alaska, in six categories: forestry, urban forestry, dairy digesters, destruction of ozone-depleting substances, mine methane capture, and rice cultivation. While forestry offsets represent only 29% of all CARB offset projects, they account for 85% of all carbon credits issued so far (California Air Resources Board, 2021). Of the forestry projects, most (91%) are IFM projects, which are the focus of this study. According to state law, a central principle of these carbon offsets is that they must be "real, permanent, quantifiable, verifiable, and enforceable" as well as "in addition to" any climate benefits that would otherwise occur (California Health and Safety Code § 38562(d), 2011).

Determining whether carbon sequestration is *additional* is a central challenge for offset programs such as California's. Additionality is defined broadly in the Intergovernmental Panel on Climate Change (IPCC) 5th Assessment Report as "beyond a business-as-usual level, or baseline" which is "difficult to establish in practice due to the counterfactual nature of the baseline" (Allwood et al., 2014). Baselines can be defined by a

variety of approaches, usually involving estimation of average carbon stocking and expected economic constraints for the given land type and species assemblage; projects are thought to be providing *additional* benefits if they accrue carbon beyond the baselines' average rate. Some studies have criticized the counterfactual and hypothetical nature of baselines, which are impossible to prove (Murray et al., 2007). California has defined the term additionality in a way that is similar to the IPCC definition, referring to activities that "result in GHG removal enhancements [that] are not required by law, regulation, or any legally binding mandate applicable in the offset project's jurisdiction, and would not otherwise occur in a conservative business-as-usual scenario." A "conservative" scenario is one that is "more likely than not to understate net [climate benefits]" (CCR 17 § 95973, CCR 17 § 95802); in other words, a conservative baseline should err toward higher baseline carbon stocks in forests to avoid over-crediting.

CARB's offset program operationalizes these requirements through its Compliance Offset Protocol for U.S. Forest Projects (California Air Resources Board, 2015). According to the Protocol, additionality is quantified relative to a 100-year static business-as-usual baseline calculated based on either (1) regional- and species-aggregated U.S. Forest Service (USFS) Forest Inventory and Assessment (FIA) stocking levels, or (2) a project's on-site carbon stocking, depending on the condition of the project timberlands when the project enters the program. Projects are then issued carbon credits for any sustained carbon stocking above the baseline, usually a combination of the initial stocking above the baseline plus incremental growth in subsequent years (Fig. 3.1). This approach for carbon crediting assumes that any carbon accumulation above the counterfactual baseline scenario would not have occurred without the offsets program; in other words, the protocol treats the

baseline as true and assumes that landowners would otherwise reduce carbon stocks to baseline levels.

CARB's system of quantifying additionality has received scrutiny around how baselines are determined and whether carbon stocking above a baseline represents carbon accumulation that would not have otherwise occurred. Because for most projects the baseline depends on regional average carbon stocks, crediting is therefore sensitive to how those regions ("supersections" and "assessment areas") are defined. Badgley et al. (2021) point out that strategic placement of projects on lands whose species composition is not well-represented by the assessment area average has led to an average over-crediting of nearly 30% (Badgley et al., 2021). Recent reports from investigative journalists suggest that some projects are non-additional in their entirety, for example because they preserve forests that are not in danger of logging (Elgin, 2020; Song & Temple, 2021). Quantifying additionality is necessarily an imperfect process, based on unobservable counterfactual scenarios, and these examples support the idea that closer scrutiny and analyses, beyond what exists in CARB's protocol, could be implemented to help ensure true climate benefits (Anderson-Teixeira & Belair, 2021).

In this study, we present a robust framework for systematically assessing additionality based on remote sensing ecosystem observations, and use it to investigate the climate benefits of the 37 IFM carbon offset projects within California. By comparing carbon and disturbance trends in offset project lands to those of nearby forest areas over the same period, we can infer whether the carbon being sequestered in project lands is additional to what may have been sequestered without the offsets program. This analysis also allows us to investigate CARB's IFM protocol assumption that, absent offset payments,

carbon stocks would follow the baseline scenario. We present hypotheses regarding the signal expected from the presence of additionality in Table 3.1, considering information about pre-project stand conditions (Hypotheses 1-3) and post-project changes (Hypotheses 4-5). The first and fourth hypotheses are aimed at capturing evidence of carbon-positive management practices; i.e., management to directly increase the rate of carbon accumulation from what it would otherwise be. The second, third, and fifth hypotheses are aimed at capturing evidence of management to prevent degradation; i.e., by extending rotation lengths or protecting existing carbon stocks in stands that would otherwise be at risk of harvesting.

Through our analysis we also demonstrate the potential utility of remote sensing-based geospatial data products as components of large-scale carbon accounting and offset verification, especially as these products continue improving. Remote sensing products have been increasingly used for climate mitigation applications in the USA, (e.g., H. Tang et al., 2021) and for tracking Reducing Emissions from Deforestation and Forest Degradation (REDD+) in the tropics (Bullock et al., 2020; Sangermano et al., 2012; X. Tang et al., 2019; West et al., 2020). The forest carbon and disturbance datasets we use here offer spatially extensive coverage, frequent temporal sampling, increased measurement transparency, and the potential for near-real-time monitoring of changes on the ground. Therefore, remote sensing could enable reliable, independent tracking and carbon accounting in offset projects, lower costs and barriers to entry for smaller landowners, and provide greater confidence and accountability toward large-scale deployment of carbon offsets in and beyond California.

Table 3.1. IFM forest offset additionality hypotheses. These hypotheses describe the general characteristics of a portfolio of IFM projects that generate carbon additionality in an idealized offset program, considering rates of carbon accumulation, disturbance, and species composition.

Quantity	If carbon is additional	If carbon is not additional	Exceptions/caveats
1. Pre-project **carbon** accumulation	Long-term historical carbon accumulation rate has been near-zero or negative; flat baseline is a realistic and conservative "business-as-usual"	Historical carbon accumulation rate has been positive; flat baseline likely underestimates the current "business-as-usual"	Historical carbon accumulation rate has been positive but is no longer expected to remain positive for most forests
2. Pre-project **harvest**	Project areas were harvested at similar rates as other similar forests over recent decades	Harvest rates were high in project areas relative to similar lands before projects began, and forests are now recovering	Project lands are particularly productive and naturally have high harvest and high growth rates
3. Pre-project **species composition**	Project areas have similar tree species to nearby forests, or have more high-value species, indicating average or high risk of timber harvest	Project areas have less valuable species than nearby forests, making them less valuable and less likely to be at risk of timber harvest.	Project lands have less valuable species but would otherwise be replanted with high-value species; which species are considered "high-value" may change over time
4. Post-project change in **carbon** accumulation	Carbon accumulation rate after project initiation is greater than the pre-project rate and greater than the rate for similar forests	Carbon accumulation rate after project initiation is similar or less than the pre-project rate and the rate for similar forests	Carbon accumulation slows in the short-term due to management like thinning to reduce fire risk
5. Post-project change in **harvest**	Harvesting rate has decreased relative to pre-project levels and relative to similar forests	Harvesting has stayed the same or increased relative to pre-project levels for similar forests	Some carbon that will remain stored in wood products over 100 years is still additional

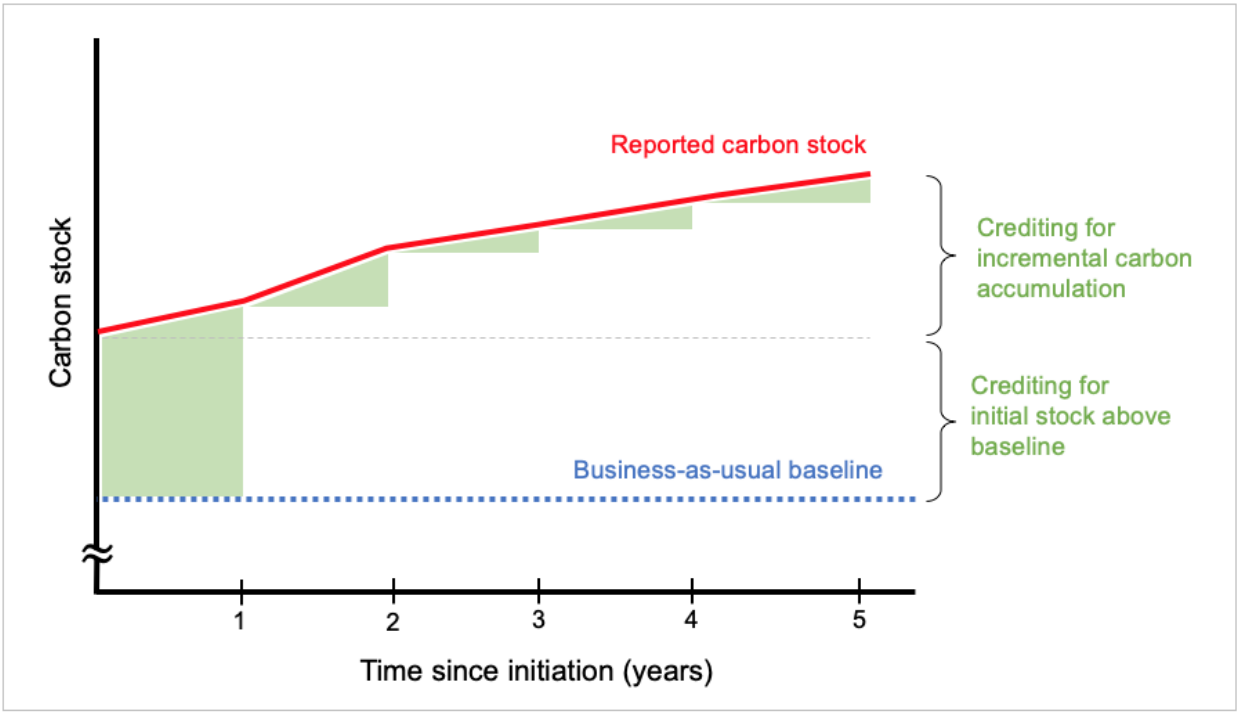

Figure 3.1. Conceptual diagram of carbon crediting following project initiation. CARB issues credits to offset projects after each reporting period. For the majority of IFM projects, the first set of credits issued is mostly for initial carbon stocking above the baseline in the first reporting period, with incremental credits awarded thereafter based on carbon accumulation (minus estimated secondary effects and leakage which we do not discuss here). In this example, assuming negligible secondary effects and leakage, the project would receive a similar number of credits attributable to initial stocking and incremental accumulation after 5 years.

3.2 Methods

3.2.1 Datasets

IFM offset projects

We compiled documentation for all 37 active or previously active IFM compliance offset projects in California from two CARB-approved registries: the American Carbon Registry (ACR) (https://acr2.apx.com/myModule/rpt/myrpt.asp?r=111, accessed Sep 1, 2021) and the Climate Action Reserve (CAR) (https://thereserve2.apx.com/myModule/rpt/myrpt.asp?r=111, accessed Sep 1, 2021).

Access to offset project documentation is also available through the Air Resources Board Offset Credits (ARBOCs) issuance map (https://webmaps.arb.ca.gov/ARBOCIssuanceMap/, accessed Sept 1, 2021). From these registries, we obtained project landowner information, geographic information system (GIS) polygons of project boundaries, the number of credits issued, and total carbon stocks for years where estimates are provided. We used the American Climate Registry (ACR) and Climate Action Reserve (CAR) project IDs to label projects in this study.

The carbon stocks provided in project documentation are self-reported by offset project landowners who often work with carbon developers, consulting foresters, and third-party carbon verifiers on implementation and reporting. Carbon stocks for each reporting period come from a combination of forest inventory and an approved set of empirical-based forest growth models, as described in Appendices A-B of the Compliance Offset Protocol for U.S. Forest Projects (California Air Resources Board, 2015). Inventory methodology varies across projects, with CARB providing minimum requirements for field measurements which must take place every 12 years while providing detailed documentation of methodology. The aboveground live carbon is estimated using CARB-provided allometric equations based on diameter and height measurements. Between inventories, projects may apply approved models such as the USFS Forest Vegetation Simulator (FVS) to grow tree diameter and height from the most recent inventory data. These growth models generally apply empirically-derived rates of succession for different tree species following disturbance and management but do not incorporate climate impacts such as the ongoing drought on growth projections (e.g.,

https://www.fs.fed.us/fvs/). Given that current offset projects are less than 12 years of age, we expect most documented carbon changes to be based on these growth models.

We converted carbon stocks from units of ton CO_2 to ton C by scaling by the molar ratio of 12.01/44.01. To compare against remote sensing data, our primary variable of interest from the registries was the aboveground live (AGL) carbon component, but AGL was not consistently available. For the 12 projects that did provide AGL carbon stocks, the AGL carbon stocks were on average a factor of 0.806 ± 0.002 of the total carbon stocks (Table B1). Therefore, we scaled total carbon stocks by 0.806 to estimate the AGL component in the other 25 projects. Projects begin as early as 2012, with credit issuance beginning in 2013. The 37 project boundaries span four different "supersections", defined by CARB based on ecosections or combinations of ecosections from the U.S. Forest Service (McNab et al., 2007) (Fig. 3.2).

Remote sensing-based carbon and harvest

We obtained and compared data for AGL forest carbon from two related geospatial data products which leverage remote sensing data and were available annually at 30m × 30m for 1986-2017 in California. The first dataset, from the Environmental Monitoring, Analysis and Process Recognition (eMapR) lab (Kennedy et al., 2018) is described as an "observation-based, empirical carbon monitoring system" derived from a mix of field measurements, airborne lidar data, Landsat time series imagery, and statistical modeling. According to eMapR documentation, a time series algorithm (LandTrendr, Kennedy et al., 2010) was used first to detect changes in annually aggregated Landsat imagery and build maps of disturbance and stabilized surface reflectance imagery. The time series increments of stabilized surface reflectance imagery were then matched with Forest Inventory Analysis

(FIA) plot data using a gradient nearest neighbor (GNN) algorithm based on similar spectral, climate, topographical, and disturbance history characteristics to create yearly maps of FIA-based forest metrics. Metrics including canopy height were then converted to aboveground biomass using allometric equations. The system was prototyped in the conifer-dominated forests of the Western Cascades region of western Oregon and a small portion of northern California, but the final data are available across the contiguous US. The authors note little bias in tracking biomass densities, until high densities beyond 450-500 Mg/ha (210-235 ton C/ha) where biomass begins to be underestimated. They also show that the eMapR biomass estimates generally agreed well with inventory plot data at broad scales, with some noise at the 30m × 30m pixel level. For our study, we aggregated the data to compute project-level means, with a mean project size of approximately 46 km^2 (or 51,000 individual 30m pixels).

The second dataset, from the Landscape Ecology Modeling Mapping & Analysis (LEMMA) lab (Bell et al., 2018; Ohmann & Gregory, 2002), is based on a similar approach as eMapR, using LandTrendr and a GNN model to match 30m x 30m pixels to similar inventory plots based on environmental variables (climate, geology, topography) and three Landsat Tasseled Cap indices. LEMMA varies slightly from eMapR in the spectral and environmental indices used, and the area over which the dataset was developed – in the case of the LEMMA California biomass product, over all of California and western Oregon.

The raw data for both eMapR and LEMMA have units of aboveground forest biomass per hectare, which we converted to units of carbon using a scaling factor of 0.47, following CARB's guidance (Gonzalez et al., 2015) and allowing us to match the carbon units in the offset project documentation. The LEMMA product also provides biomass by individual tree

species at 30 m for a single year, 2012, which allowed us to compare the species composition of different areas.

To quantify the harvest history in offset projects and in other areas used as controls, we used a Landsat-derived record of disturbance for California from 1985-2021 (J. A. Wang et al., 2022). Due to challenges in detecting disturbances at the beginning of the time series, we omit estimates from the year 1985 and analyze disturbances from 1986 to 2021, aligning with the start year of the eMapR and LEMMA biomass datasets. This disturbance dataset uses the Continuous Change Detection and Classification (CCDC) algorithm (Zhu & Woodcock, 2014) to identify abrupt changes in land surface characteristics across California based on time series surface reflectance at each 30m x 30m pixel from Collection 2 Landsat imagery (Masek at al., 2020). These changes are then attributed to disturbance causes (fire, harvest, or die-off) using a random forest model trained on archival geospatial datasets of disturbance. For this study we extracted the harvest component specifically, giving us a record of where forest harvest occurred each year from 1986-2021. These data provide a binary layer of harvest/no-harvest for each pixel but do not quantify harvest intensity. We present "harvest rate" as a percentage representing the fraction of area harvested per year in a given region of interest.

We systematically evaluated the three datasets for the purposes of this study, i.e., to track relative changes in carbon and harvest across the landscape for different regions of interest. We quantitatively compared eMapR and LEMMA against project-reported carbon stocks and trends. We also visualized eMapR carbon, LEMMA carbon, and harvest changes for one example project with high rates of disturbance, CAR1066, to qualitatively assess agreement over the time period of 1986-2017 when all three datasets are available. For all

relevant figures, we show results based on both eMapR and LEMMA. Due to a lack of eMapR and LEMMA data development beyond 2017, we were restricted to this smaller time window and could not address our carbon hypotheses (#1, 4) as robustly as the harvest hypotheses (#2, 5) for which data are available through 2021.

Land ownership

In several of our analyses, we compared offset project lands to other privately-owned forestlands in California by excluding public lands labeled by the California Department of Forestry and Fire Protection. We obtained these public lands data from the California State Geoportal (https://gis.data.ca.gov/datasets/f73858e200634ca888b19ca8c78e3aed_0/explore, accessed Sep 1, 2021). For other analyses, we compared specific timber companies' offset project lands against their other land holdings, using private land ownership data provided by the CalLands database (Macaulay & Butsic, 2017), available at https://callands.ucanr.edu/.

3.2.2 Comparison of carbon stocks and accumulation rates

In the first stage of our analysis, we explored both eMapR and LEMMA records of aboveground forest biomass as largely independent sources to corroborate the carbon stocks and trends reported in the offset project documentation. We used Google Earth Engine (Gorelick et al., 2017) to extract and average eMapR and LEMMA data for each project polygon over the same period that each project has reported carbon stocks (up to 2017, after which eMapR and LEMMA data are not available). We then plotted time series comparing the three datasets and calculated mean stocks and trends. For carbon stocks, carbon trends, and mean harvest rates, we report metrics by project as well as a mean and

standard error across the 37 projects, weighted by the area of each project. We also provide validation of the three datasets in the Supporting Information, comparing eMapR vs. LEMMA stocks and trends against project documentation, and assessing qualitative agreement in relative changes between eMapR, LEMMA, and harvest for an example project, CAR1066.

To gain insight into the incentives and long-term strategies of these carbon offset projects, we calculated the ratio of credits earned at the beginning of the project from the initial stock above baseline to the credits earned during the project from incremental carbon accumulation (Fig. 3.1). This ratio allowed us to identify the dominant source of crediting to date and to estimate the amount of time required for crediting from incremental carbon accumulation to exceed the initial payout.

3.2.3 Spatio-temporal comparison of projects to similar lands

As a method of estimating the additionality of carbon in offset project lands, we compared time series of carbon and harvest in offset project lands to time series of carbon and harvest in similar privately-owned forestlands. We used three different methods to delineate similar but non-offset lands, representing alternative business-as-usual scenarios or approximate control groups. These control groups allowed us to infer the presence of additionality along the hypotheses presented in Table 3.1, i.e., whether carbon sequestration and harvest in the offset projects were different from what they would otherwise be.

In the first method of defining an approximate spatial control group, we drew a 2-km surrounding buffer region around each project, excluding urban or agricultural lands as defined by the National Land Cover Database for 2016 (Homer et al., 2020) and

publicly-owned lands as defined by the California Department of Forestry and Fire Protection. This 2-km surrounding region represents a land area similar in size to most projects. The approach has been used by previous forestry studies (e.g., Yang et al., 2021) to design controls in a systematic way, with geographic adjacency between test (i.e., project) and control regions ensuring that environmental, climate, and ecological conditions are on average likely to be similar.

In the second method, we defined larger (regional) control groups: all private forestlands in either the "coastal region" or "interior region" of northern California. The coastal region consists of the Northern California Coast supersection plus the western part of the Southern Cascades supersection (USFS ecosections 263A and M261B). The interior region consists of the eastern Southern Cascades (excluding M261B), Modoc Plateau, and Sierra Nevada supersections north of 39.7 °N. We found it appropriate to consider these two regions separately given their substantial ecological differences and diverging patterns of carbon and harvest over time.

In the third method (presented in the Supporting Information), we followed the approach of several previous studies using covariate matching to identify control groups for each project (e.g., Stuart 2010; Andam et al. 2008; Ferraro et al. 2011). We used three covariates: PRISM mean annual temperature and precipitation normals for 1990-2020 (Daly et al., 2008) and "site productivity class", a metric for forest productivity provided by the USFS from Forest Inventory and Analysis data (obtained from B. Wilson, cited in Tubbesing et al., 2020). For this approach, all data were regridded to 800 m to match the PRISM climate data. Then, we calculated the Mahalanobis distance between each project mean and all other pixels of the same region (coastal or interior) in the three-dimensional

standardized space of temperature, precipitation, and site class. Each project's "control" carbon and harvest time series consisted of the average of the most similar *n* number of pixels, where n is chosen for each project to approximate the same area as the project (mean = 53 pixels, ranging from 7 to 225).

Finally, we also provide case studies quantifying differences in carbon accumulation, harvest, and species composition for two large timber companies' offset vs. non-offset land holdings. Sierra Pacific Industries (SPI) is one of the largest timber companies and landowners in the United States, and has submitted approximately 30.5% of its California land area for active or proposed IFM projects. Green Diamond Resource Company owns primarily coastal redwood timberlands and owns one active IFM project in California, CAR1339, representing 11.9% of its land holdings in California. We investigated whether active or proposed offset lands have statistically distinct amounts of carbon or harvest compared to other lands by each owner (thus evaluating hypotheses 2 and 3). Preferential selection of lands that have most recently been harvested, for example, could allow the company to continue harvesting as business-as-usual on other lands while earning credits for lands it has recently harvested, profited from, and is now waiting to regenerate regardless of the offsets program.

Hypotheses 1 & 2: Assessing pre-project carbon accumulation and harvest

We first considered the available historical record of carbon and harvest leading up to the offset program initiation (1986-2012), comparing carbon stocks, carbon accumulation, and harvest rates for project areas versus control areas. We report the mean quantities and standard error over the 27 years. For harvest rates, which are highly variable

year-to-year, we also performed a paired (relative) t-test across years to assess whether the projects' harvest rates are consistently above or below those of the control areas.

Hypothesis 3: Assessing pre-project species composition

Next, we investigated the species composition of projects versus the spatial controls, using the species-level biomass data provided by LEMMA. This allowed us to quantify whether project areas had a higher or lower density of particularly valuable timber species like redwood and Douglas-fir prior or at the time of project initiation in 2012. For an analysis of redwood composition, we focused on the Northern California Coast supersection (USFS ecosection 263A, green in Fig. 3.2) which is characterized by redwood stands. We performed paired t-tests comparing the density of a given species in each project to its density in the projects' surroundings. This tree species comparison allowed us to estimate whether there is otherwise high demand for harvest in the projects. Because the species data were only available for 2012, we were not able to compare species composition longitudinally or for before-vs-after project initiation in this study; hence there is no Hypothesis 6 for post-project changes in species composition.

Hypotheses 4 & 5: Assessing post-project change in carbon accumulation and harvest

We then quantified how much carbon accumulation and harvest was occurring in offset project lands compared to the spatial controls, before and after different projects were initiated. For these before-and-after comparisons, we only considered the 16 projects which started by 2014; this allowed for at least 3 points of eMapR or LEMMA data (2015-2017), and 7 points of harvest data (2015-2021) after project initiation. These 16 projects accounted for 37% of all project area and 41% of credits issued to date from the full set of 37 projects. We calculated after-minus-before changes, testing for statistical

significance using a Chow test on differences in carbon slope and a paired t-test on differences between average harvest rates for each project.

Data and code availability

All data come from publicly accessible sources described above. We have compiled and packaged the specific CARB, eMapR, LEMMA, and harvest data we used into an online Dryad repository at https://doi.org/10.7280/D17D6W. Python and Google Earth Engine code is provided in the repository as well as Github https://github.com/scoffiel/carbon_offsets/.

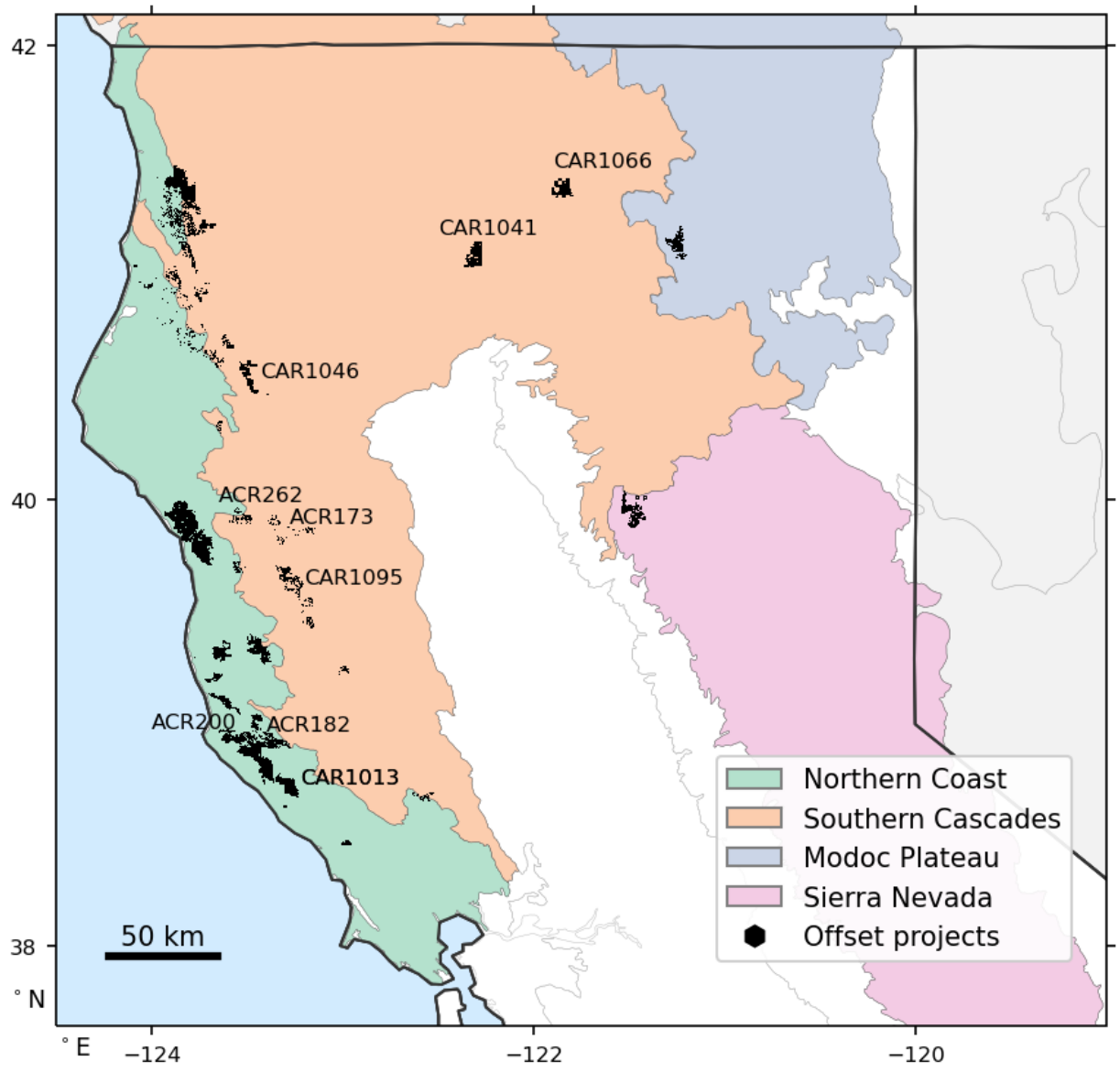

Figure 3.2. Study area encompassing improved forest management (IFM) compliance projects in California. We tracked 37 projects spanning four supersections as defined by CARB using US Forest Service ecosections: Northern Coast (green), Southern Cascades (orange), Modoc Plateau (blue), and Sierra Nevada (pink). Nine of the largest and longest-running projects are labeled.

3.3 Results

3.3.1 Comparison of carbon stocks and accumulation rates

Across the 37 IFM projects in California, we found that eMapR and LEMMA records of average carbon stocks varied from those reported in project documentation (RMSE = 30.9 and 29.2 ton C/ha, respectively) (Fig. B1). However, the remote sensing products did not show a clear bias in terms of consistent over- or underestimation relative to project-reported carbon stocks for individual projects. One exception was for projects with high reported carbon densities, where we did find a slight underestimation, as expected.

For carbon accumulation rates, the remote sensing-derived estimates were considerably different from the project-reported inventories. Specifically, projects reported 2.4 times higher rates of carbon accumulation than eMapR or LEMMA, with the average project-reported rate (weighted by project area) being 1.97 ± 0.54 ton C/ha/y versus 0.83 ± 0.16 ton C/ha/y for eMapR and 0.82 ± 0.22 for LEMMA (see Table B2 for full details by project). Here error is reported as standard error across the sample of 37 projects. Projects' rates of carbon accumulation were variable and likely dependent on stand age, with some as high as 4-5% per year averaged over the past 4-6 years according to project documentation. The carbon time series for nine of the largest and longest-running offset projects highlights the discrepancy in carbon accumulation rate among data sources (Fig. 3.3). As described in the Methods, the Landsat-derived estimates of carbon accumulation used here may have a low bias at high AGL carbon (and high leaf area), contributing in part to the difference with the project documentation; further quantitative assessment of potential absolute differences may require next-generation remote sensing products that are currently in development, leveraging new observations from GEDI and other lidar products (Dubayah et al., 2020). However, despite the differences between eMapR, LEMMA, and project-reported carbon, the eMapR and LEMMA products show relatively high levels

of agreement in being able to track relative changes associated with harvest disturbance patches at a landscape scale (Fig B2).

Excluding CAR1046 (terminated due to fire) and seven other projects that began as early action projects prior to 2012, the initial credits issued to IFM projects in California were on average 26.5 ± 5.9 times greater than the number of credits issued annually thereafter. Thus we can expect that if current forest growth rates continue, it would take 26.5 years on average for the incremental growth to become the dominant source of payment. Since this estimate is comparable to the project crediting period of 25 years, we expect that the subsequent trajectory of carbon accumulation may serve an important (non-negligible) revenue stream for many projects, and potentially a dominant term for several projects. This variation in growth rate versus initial stocks is demonstrated in Fig B3. Large timber companies (i.e., Sierra Pacific Industries, Green Diamond Resource Company, and Mendocino Redwood Company) are more likely to have high growth rates but lower initial stocks, with an average of 23.1 ton C/ha above the baseline compared to 39.2 ton C/ha above the baseline for other projects. The break-even times for accumulation credits equaling initial above-baseline credits varied from 3 years to 93 years for different projects.

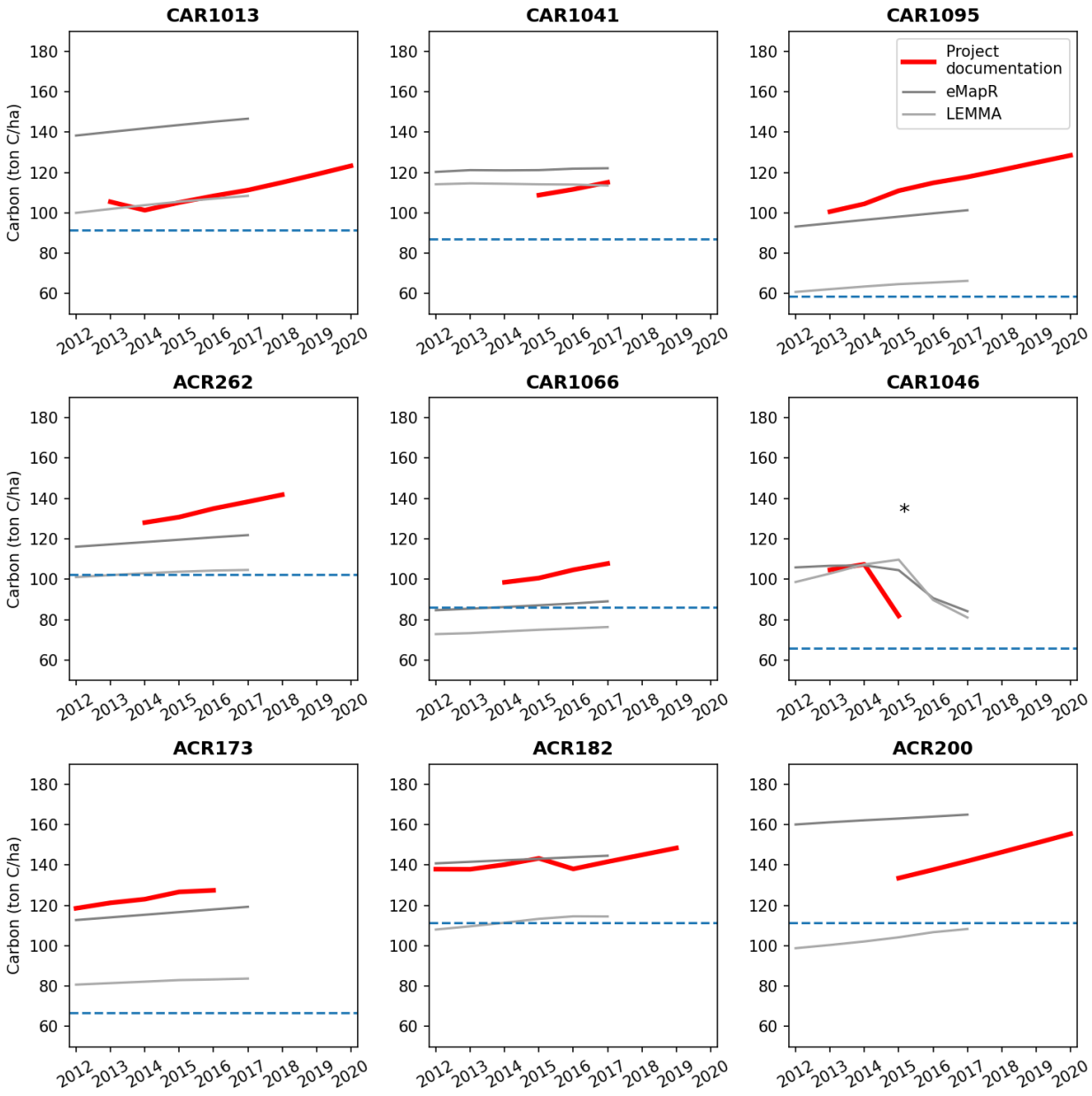

Figure 3.3. Three datasets of carbon stocks in IFM projects. Here we show comparisons of three different data sources for a sample of the nine largest projects that started between 2013 and 2015 (labeled in Fig. 3.2). Baseline carbon stocks as reported in project documentation are indicated by horizontal dashed lines. Remote sensing-derived estimates of aboveground carbon stocks (gray) show slower rates of carbon accumulation than those reported in project documentation (red), with approximately half of the total carbon accumulation over time. The asterisk* in CAR1046 indicates the Route Complex Fire in 2015 which ultimately led to the project being terminated.

3.3.2 Spatio-temporal comparison of projects to similar lands

Using carbon data from eMapR and LEMMA, and harvest data from Wang et al. 2022, we quantified differences in the time series for offset project lands compared to three control groups: a 2-km surrounding region around projects, a broader region of either coastal or interior northern California (Fig. 3.4a-b), and a set of covariate-matched 800 m pixels. We found broadly consistent patterns of carbon accumulation between eMapR and LEMMA and between the "surrounding" and "covariate-matched" controls. Therefore, for conciseness in the main text, we focus our primary analysis on eMapR and the first two systems of controls, with results for LEMMA and the matched controls system presented in the Supporting Information (Fig B3-B5).

Hypotheses 1 & 2: Pre-project carbon accumulation and harvest

Most offset projects, located in the coastal region, have relatively high carbon stocks and have been accumulating carbon over the past three decades, both before and after the offset program began (Fig. 3.4c). Over the pre-project period of 1986-2012, project areas had consistently higher carbon stocks than control groups. For coastal projects the mean carbon stock was 123.0 ± 1.9 ton C/ha, which was higher than the surrounding areas (97.5 ± 1.4) and coastal region (78.0 ± 1.2). Similarly, for interior projects, the mean carbon stock was 91.2 ± 0.3 ton C/ha, which was higher than the surrounding areas (66.5 ± 0.2) and interior region (50.6 ± 0.06). Here the reported errors represent standard error in stocks over the 27-year record.

The pre-project carbon accumulation rate for the combined projects area was different (in absolute units) than the rate in nearby forests (1.30 ton C/ha/y for coastal projects vs. 0.95 for surroundings or 0.82 for coastal region; -0.22 for interior projects vs. -0.15 for surroundings or -0.04 for interior region). However, as a percent change, all three

coastal areas - i.e., projects, surroundings, and the full region - were growing at 1.0-1.1% per year, and all three interior areas showed negligible ($\leq$ 0.2%) change per year. Therefore, as a percent change, the total carbon added in projects beyond what would be expected based on these regional average rates of accumulation is effectively zero. The finding of consistently increasing carbon stocks across the coastal region is at odds with Hypothesis 1 regarding the static baseline for carbon.

For harvest, we found a general pattern of decline since the early 2000s, and an especially steep decline starting in 2008, a few years before any projects began (Fig. 3.4e-f). Project areas had mostly higher harvest rates (measured as the fraction of area harvested) than their immediate surroundings prior to 2012, particularly for the interior region. Over the period of 1986-2012 preceding the offsets program, the combined coastal project areas were harvested at about the same rate as their surroundings (harvest rate differences were not statistically significant) and 17% more relative to the broader coastal region (paired t-test across years, p=0.004). The combined interior project areas were harvested 69% more, relative to their surroundings (p=0.12, not statistically significant), and 106% more than (more than twice as much as) the broader interior region (p<0.001). These four interior projects with particularly high harvest are owned by Sierra Pacific Industries (SPI), a large timber company. Looking across SPI lands, we found that areas of active or proposed offset projects were harvested 27% more than the rest of its properties in California during the same period of 1986-2012 (p<0.001), and 31% more during 2008-2012 (p=0.002). This finding of disproportionate rates of historical harvest on project lands is at odds with Hypothesis 2 regarding recovery from harvest.

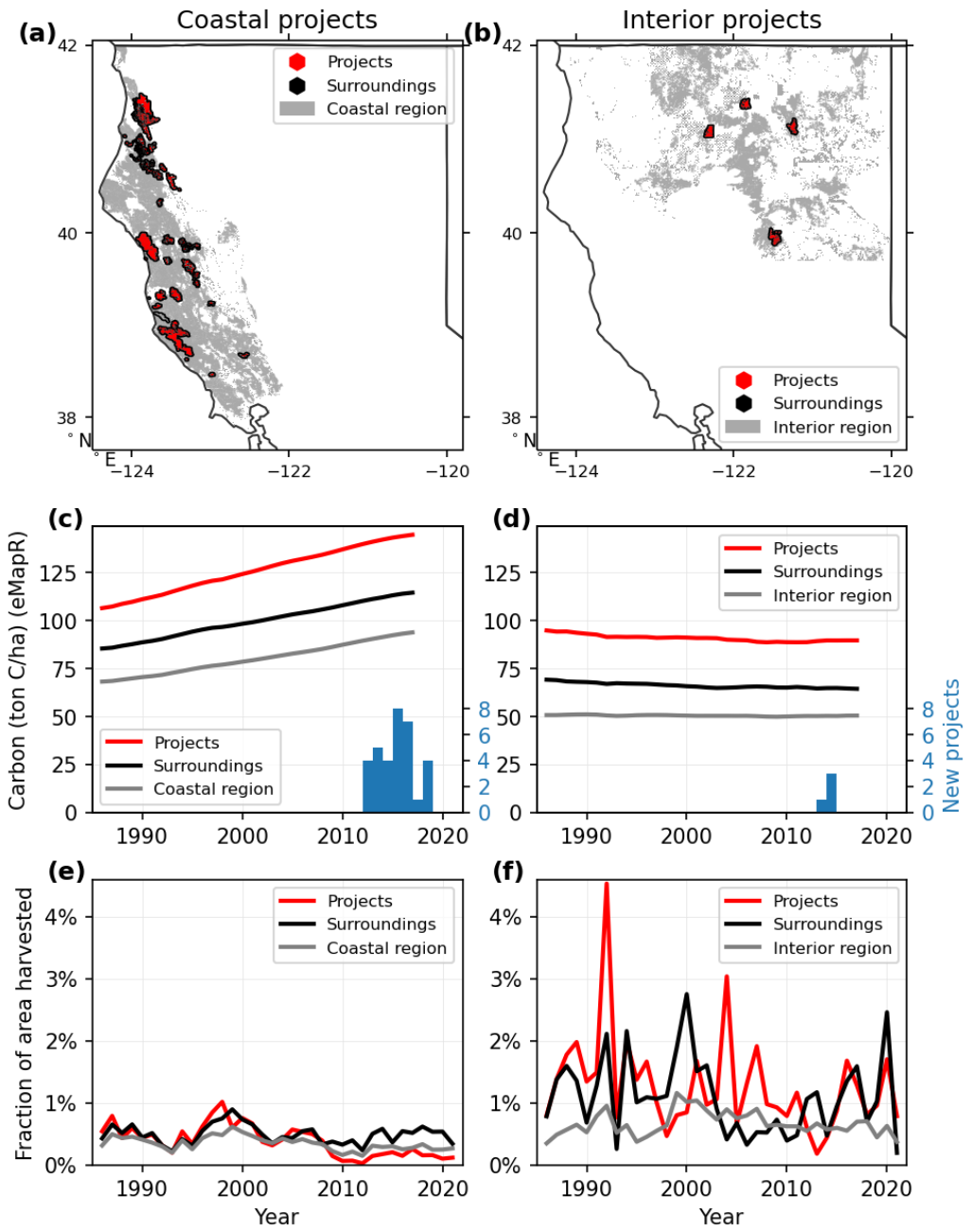

Figure 3.4. Carbon and harvest trends in offset projects and surrounding lands. We divided projects into two groups: 33 projects in the "coastal region" of Northern California Coast plus western Southern Cascades (left panels) and 4 projects in the "interior region" of the eastern Southern Cascades, Modoc Plateau, and northern Sierra Nevada (right). We then compared carbon (eMapR) and harvest data for the combined offset project lands (red), a 2-km surrounding area of private forests around offset projects (black), and all private forests of the broader region (gray). Offset project lands follow carbon trajectories similar to other forests, both before and after projects begin (c-d). Offset project lands have historically been harvested more intensely than surrounding lands, especially in the interior region (e-f). Supporting Fig. B4 includes similar patterns for LEMMA carbon and the third system of matched controls.

Hypothesis 3: Pre-project species composition

Next, we focused on the Northern California Coast supersection for an analysis of tree species composition in offset areas compared to other areas. Much of this region is coast redwood forest which has high harvest value, mixed with tanoak which is a less valuable understory species (Waring & O'Hara, 2008). Using the LEMMA record of species composition available for 2012, at the time that the offset program began, we found statistically significantly higher tanoak density in offset project stands (30.3%) compared to their immediate surroundings (25.4%) or the supersection mean (20.2%) ($p < 0.001$ for both paired t-tests) (Fig. 3.5). The discrepancy was higher for timber company-owned projects, which had 34.7% tanoak compared to their immediate surroundings with 26.1% tanoak. For the Green Diamond Resource Company specifically, their IFM (CAR1339) is drawn around stands with particularly high tanoak density (35%) and low redwood (4%), versus the rest of its properties which are 18% tanoak and 25% redwood by carbon density (Fig 3.6). The project documentation for CAR1339 is consistent with this finding from the LEMMA data, reporting that tanoak constitutes more than half the basal area included in the IFM. In this case study, the Green Diamond project lands were also historically harvested less than their other properties, in contrast to the Sierra Pacific Industries projects discussed previously which were historically harvested more. This finding of projects being drawn around less valuable stands is at odds with Hypothesis #3 regarding projects protecting forests otherwise at risk of harvest.

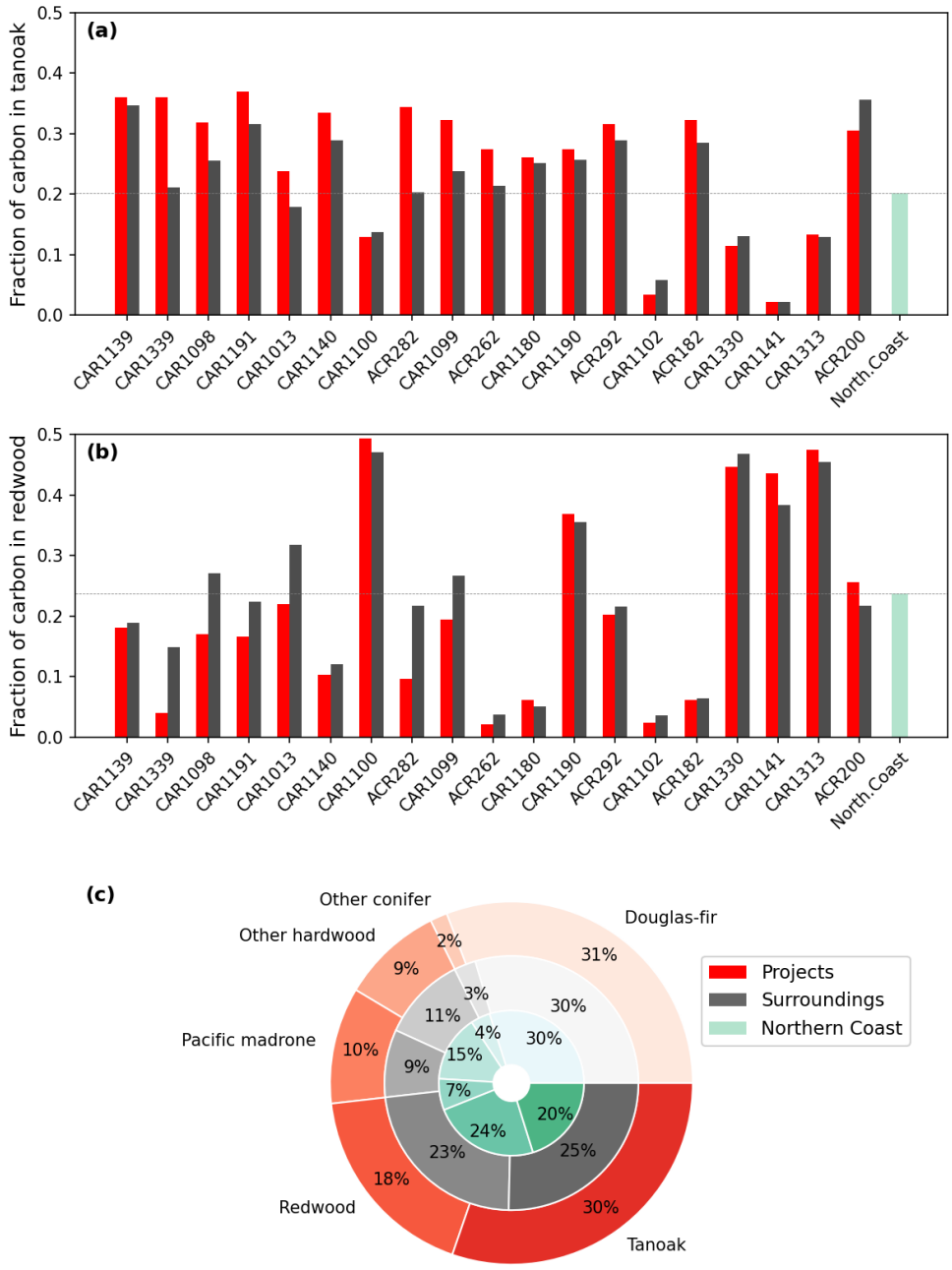

Figure 3.5. Species composition of Northern Coast offset projects. Offset projects in the Northern Coast supersection (Fig. 3.2) have significantly more of their carbon as tanoak and less as redwood, compared to surrounding non-offset areas in 2012. This is particularly true for timber company-owned projects (CAR1339, CAR1191, CAR1190). This suggests that harvest value in project lands was lower than surrounding areas prior to projects' start, and credits issued to many of these projects may not actually be preventing greater harvest.

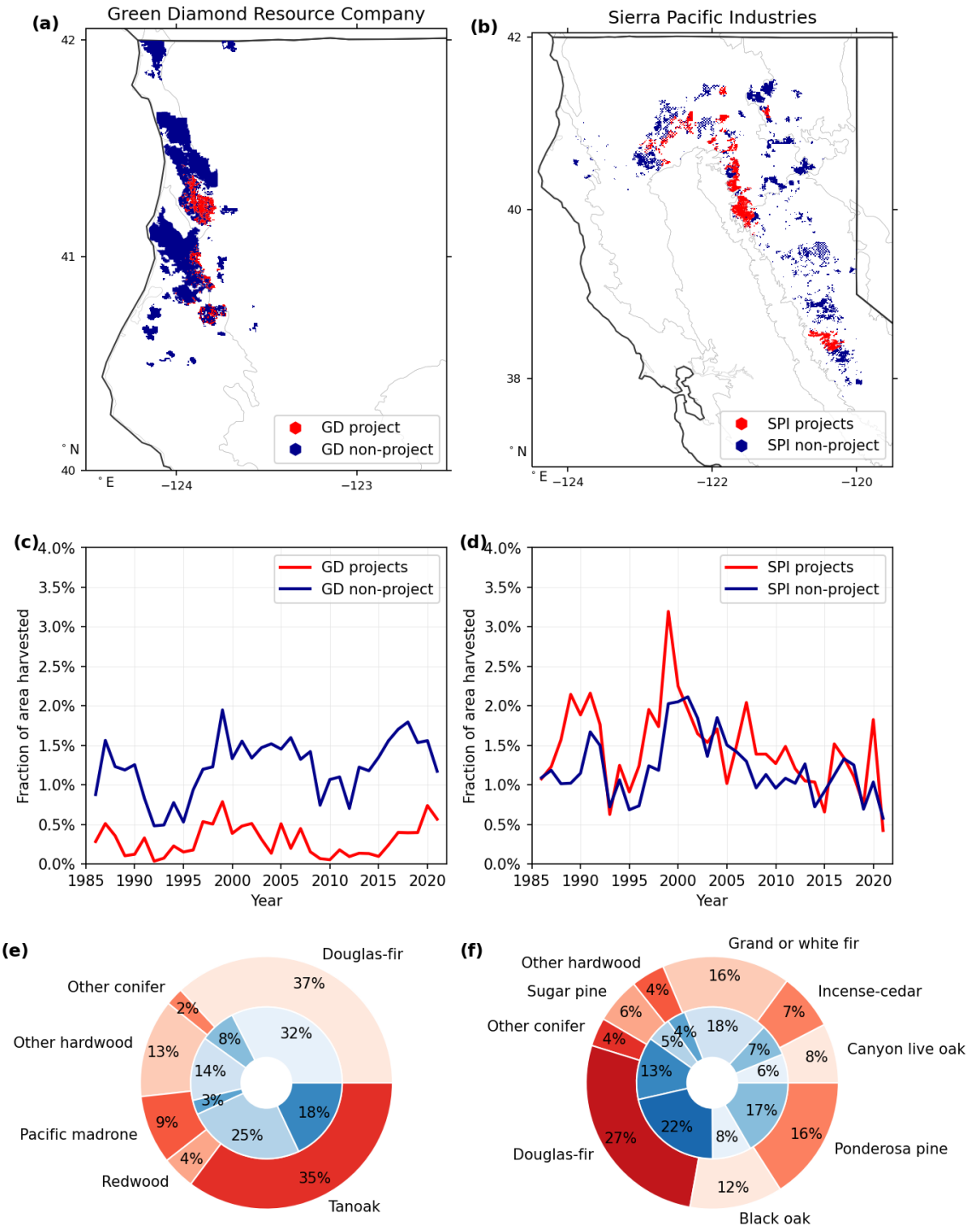

Figure 3.6. Divergent strategies of offset project selection between two large timber companies. Green Diamond Resource Company (GD, left) and Sierra Pacific Industries (SPI, right) demonstrate different strategies in the selection of their lands for proposed or active offset projects (red) vs. the rest of their land holdings (blue). GD lands are located predominantly in the Northern California Coast (a). GD project lands (currently one project, CAR1339) have a very intricate delineation, around areas that have been historically harvested *less* (c), and have nearly double the fraction of

tanoak (a less timber-valuable species) and only one-sixth the redwood of their other properties e). SPI lands, on the other hand, are predominantly in the fir and pine forests of interior California (b), and their offset project lands have been harvested 26% *more* than their other properties over 1986-2012 (d).

Hypotheses 4 & 5: Post-project change in carbon accumulation and harvest

Finally, we compared carbon accumulation and harvest rates for each project over equal time periods before and after project initiation for the 16 projects that started by 2014 (Fig. B5). Regarding carbon, 12 projects showed a decrease in eMapR carbon accumulation rate after initiation, 10 of which were statistically significant as measured by a Chow test with $p<0.05$. Two other projects not included here, CAR1046 (terminated) and CAR1174, have also lost significant amounts of carbon due to fires in 2015 and 2018. The other four projects showed insignificant increases in carbon accumulation rate. One project, CAR1092, showed a significant increase in harvest rate after initiation.

We also compared before-and-after rates of carbon accumulation and harvest for these 16 projects grouped into two landowner categories: large timber companies (Sierra Pacific Industries) and others (Fig. 3.7) (landowner information provided in Table B3). This analysis revealed that carbon accumulation rates have been decreasing across Northern California forests, including offset project lands, which show a statistically significant decline in accumulation rate since initiation ($p < 0.05$) according to eMapR. Harvest rates have increased slightly (not statistically significant) on the large timber companies' offset project lands as well as their surroundings, and have decreased slightly in the combined 12 other projects. These findings of a general lack of increase in carbon accumulation or decrease in harvest are at odds with Hypotheses 4 (carbon) and 5 (harvest) regarding the expected changes after project initiation.

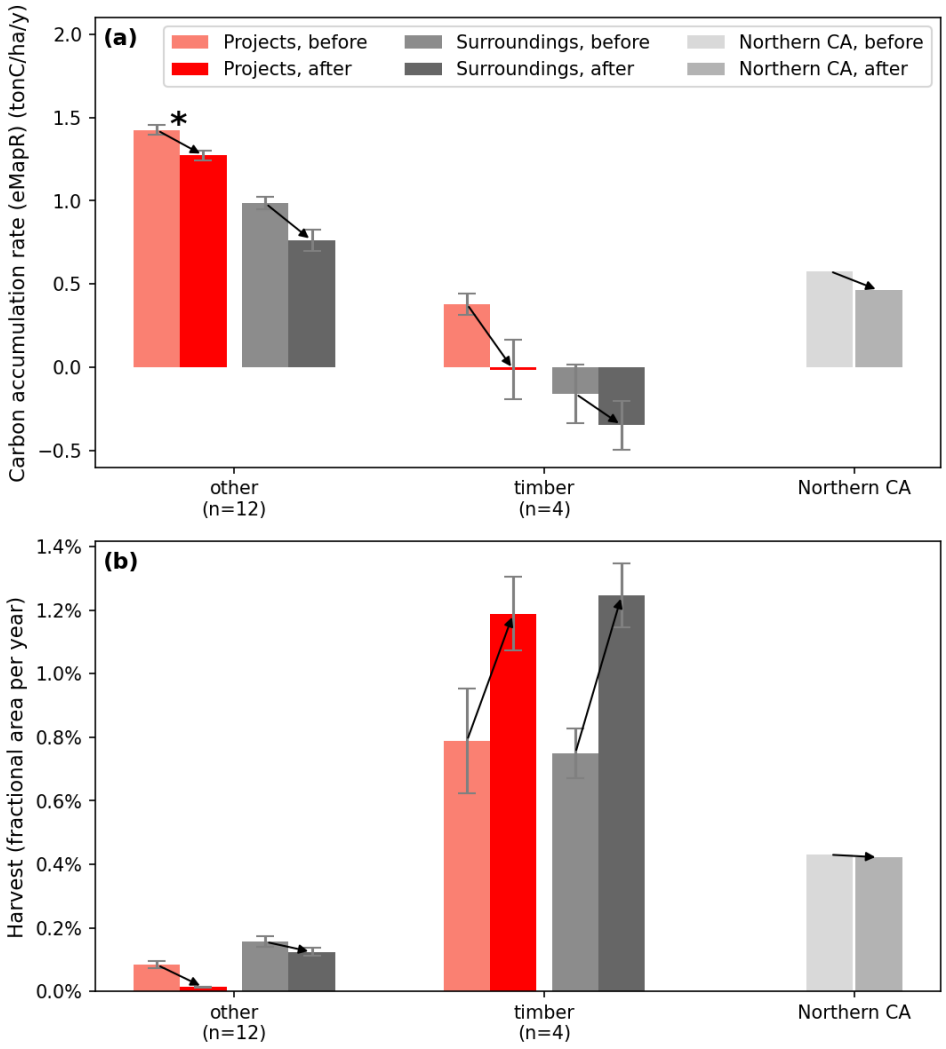

Figure 3.7. Carbon and harvest changes by landowner category. Offset projects are owned by a variety of conservation groups, individuals, timber companies, other for-profit companies, and tribes. Carbon accumulation rate has declined broadly across Northern CA, including in offset projects and nearby areas regardless of landowner type (a). Harvesting rates across Northern CA have remained fairly constant, with no indication of harvest reductions in offset projects. In fact we observe a slight increase in harvest on large timber company-owned offset projects and their surroundings. CAR1046 was excluded since it burned in 2015 and was terminated. Statistical significance in a paired t-test is indicated by an asterisk*; most changes are not statistically significant largely due to small sample size and low power.

3.4 Discussion

In this study we applied three geospatial remote sensing-based data products to systematically assess carbon and harvest in IFM compliance offset projects within

California. Our comparison between eMapR, LEMMA, and project-reported carbon revealed several differences, including projects reporting considerably faster accumulation of carbon than estimates derived from eMapR or LEMMA. Per the IFM protocol, projects may rely on approved forest growth models (which do not incorporate climate impacts on growth projections) to report carbon stocks for up to 12 years at a time, and may adjust those estimates before receiving credits, for which ground-based inventories are required. Our finding about the rate of carbon accumulation contributing a similar number of credits after approximately 26.5 years as those initially awarded for above-baseline stocking suggests that both high initial stocks and high growth rates (perhaps due to recovery from previous harvest and other edaphic factors that accelerate growth) are in the projects' financial interest under existing protocol. For large timber company lands which have historically harvested more intensely and start with a lower initial stock, the greater incentive is for landowners to place offset projects on lands with the greatest potential for sustained growth rather than protecting carbon stocks in already-dense stands.

By comparing carbon and harvest trends in offset project lands to other similar lands, we can infer the extent to which carbon that has accumulated is truly additional to what may have accumulated otherwise. We found five lines of evidence which cast substantial doubt on additionality (project-by-project breakdown in Table B4), with carbon stocks and accumulation that very likely would have occurred regardless of the offsets program.

First, regarding Hypothesis 1, the fact that eMapR and LEMMA show a long-term accumulation over 1986-2017 for all coastal regions suggests that the existing protocol which always draws flat baselines may not be realistic for many California forests; the

real-world baseline in this case would be a slow increase. In other words, the accumulation in these project lands may be attributed to this broader trend for private forestlands recovering from high levels of harvest in the 1950s-1970s (Morgan et al., 2004) and is not necessarily a consequence of specific management on project lands. Although these projects have carbon stocks above baseline levels, the fact that project relative carbon accumulation rates track the rates observed in control regions suggests that credited incremental growth may not be additional. The widespread positive rates of accumulation also weaken the protocol's assumption that offset stocks would otherwise be reduced to baseline levels. This potential over-crediting adds to over-crediting concerns from previous research related to how baselines are defined (Badgley et al., 2021).

Regarding Hypothesis 2, we found that many project areas have been harvested more than other areas over the historical period, especially for large timber companies such as Sierra Pacific Industries in the interior region, and may now be receiving credit for the natural recovery of those forests. Longer-term monitoring would be required to quantify whether these areas will recover and stay recovered beyond the remainder of the expected rotation periods.

Regarding Hypothesis 3, the disproportionately high tanoak density in Northern Coast IFM projects (such as the Green Diamond Resource Company project) suggests that these lands have lower harvest value than nearby private forestlands and are therefore at lower risk of logging. Although theoretically landowners could replace the tanoak with redwood seedlings, the lack of harvest on these tanoak-dense stands such as CAR1339 (Fig 3.6) over recent decades suggests little intention of timber production, such that protecting these areas as offsets would offer limited additional climate benefit. Protecting

disproportionately tanoak stands is likely also not in the best interest of maximizing carbon storage, as the species is much less carbon-dense per area than conifers like redwood.

Regarding Hypothesis 4, none of the projects across our subset of the 16 longest-running projects demonstrated a statistically significant increase in their eMapR carbon accumulation rate after initiation (one project showed a significant increase according to LEMMA). Instead, most projects demonstrated decreases, following a similar pattern as the controls. While protocol rules do not require projects to increase their carbon accumulation rates, as projects can claim to avoid baseline scenarios that significantly degrade carbon stocks instead, the general lack of increases among projects in our sample was striking. We would expect that IFM practices such as increasing rotation length would lead to increased carbon sequestration (due to lack of active carbon removal), observable in the first few years. However, a longer observational record may be required. Decreases in carbon accumulation in the past several years were also observed in non-project lands and coincide with increased disturbances like drought, fire, and the sudden oak death pathogen which could threaten project permanence over the full duration of the projects' lifetime.

Regarding Hypothesis 5, we found no evidence that timber companies are substantially reducing their harvest activity on offset project lands. In fact, we found some indication that harvest *may* be increasing, and carbon accumulation decreasing, in timber company projects and surrounding lands. The offset protocol credits initial stocks above the baseline and considers incremental growth additional, even when the harvest rate increases slightly and carbon accumulation rate decreases but remains positive. However, these inferences are based on only 3-5 years of post-project carbon data and 7-9 years of

post-project harvest data, so longer monitoring is required to more confidently assess additionality by this method. Longer monitoring would also be needed to detect the carbon impacts of extending rotation length in timberlands. Another caveat for timber projects is that the protocol also provides credits for carbon in harvested wood products, which may allow some of the increased harvest activity to still be related to additional and permanent carbon storage (a topic beyond the scope of this study). In general, though, our finding that in most cases, landowners are able to both continue harvesting at previous rates and receive carbon credits suggests that the current protocol may be over-crediting for naturally productive stands.

We acknowledge some well-known uncertainties and limitations in the remote sensing observations, which differ from the uncertainties and limitations in the inventory or modeling approaches used to document a project's stocks. First, eMapR and LEMMA may not accurately capture incremental growth in closed-canopy forests. Both tend to underestimate biomass at high densities (e.g., in the redwood forests, particularly with LEMMA), and eMapR calibration only included a small portion of northern California; however calibration did include diverse conifer-dense stands (Battles et al., 2018; Kennedy et al., 2018). We therefore refrain from drawing any specific conclusions about the exact carbon stocks in project areas, but rather use these products to compare relative differences across the landscape, which are useful for evaluating additionality, and demonstrate the types of analyses that could benefit offset programs going forward. In general, we do not expect biases to impact the project areas differently than the control areas and therefore feel comfortable using them to capture signals of additionality and draw qualitative conclusions even if the exact magnitudes of change are uncertain. These

products have also undergone peer review (Kennedy et al., 2018; Ohmann & Gregory, 2002), have been widely used for many carbon cycle applications at larger spatial scales (Bell et al., 2015, 2021; Zhou et al., 2021), and are demonstrated here to broadly capture the spatial structure of disturbance and post-disturbance recovery (Fig B2). We also expect remote sensing products to continue improving for use at fine scales with IFMs, with support by programs such as NASA's Carbon Monitoring System and new spaceborne lidar observations from the Global Ecosystem Dynamics Investigation (GEDI) (Dubayah et al., 2020). Second, the disturbance history dataset by J. A. Wang et al. (2022) was shown to have a 72% user's accuracy (omission) and 81% producer's accuracy (commission). Based on the nature of the disturbance detection, it is likely to be more accurate for capturing clear-cut harvests as opposed to selective thinning. We may have underestimated the total amount of harvest but do not expect this to present a bias in comparing offset versus non-offset lands. In general and importantly, though, the datasets are largely independent from the project data and enable larger-scale analyses that would otherwise not be possible. The analyses therefore demonstrate the potential value of improved remote sensing observations for offset project verification.

Another caveat is that the spatial control groups we designed are imperfect estimates of a counterfactual scenario, which in reality is impossible to quantify precisely. It is theoretically possible that the offset lands would have otherwise diverged from the controls, for example by being harvested even more. In general, however, our approach for defining controls is systematic, reasonable, transparent, and we would expect these lands to face a similar risk of degradation. Our assessment is also thorough in exploring three distinct definitions of control groups which yield the same broad conclusions of lack of

additionality. Although imperfect, remote sensing tools enable the design of effective controls that make it possible to characterize the counterfactual additionality claims made across the IFM project portfolio as a whole.

We intend this analysis to serve as a constructive criticism for the offsets program, which could benefit by incorporating more geospatial analyses of carbon and harvest trends. A next generation IFM protocol leveraging new remote sensing products and spatial controls could more accurately track additional climate benefits than the current system for defining baselines. By comparing observed trends in projects relative to similar "control" forests, an implicit baseline would be allowed to change over time, such as is the standard for some REDD+ projects and the Duke framework for forest offsets (Willey & Chameides, 2007). Such a system could require evidence of either carbon-positive management or prevention of degradation, for example by documenting a divergence from historical trends or control areas, rather than a hypothetical counterfactual. It could also enable more accurate tracking of harvest risk based on species composition, particularly in coastal forests where harvest potential may vary as a consequence of degradation from previous harvest and land management. More tailored offset rules might involve weighing the benefits of potentially more permanent but less total carbon storage as tanoak as compared to redwood. Finally, a system based on comparison against controls could incentivize more holistic approaches to forest conservation, including resiliency against fire to help maintain carbon stocks that would otherwise decline. Such improvements to make the program more rigorous could help build confidence among credit issuing bodies, policymakers, and the public that climate targets are being met. Otherwise we may be miscalculating net emissions while rewarding projects for little or no change in forest management. Improving

California's crediting scheme could have a large global impact, with California serving as an example system for other offset programs nationally and internationally.

Our findings about declining rates of carbon accumulation and lack of evidence of additionality elucidate a need for more rigorous evaluation of carbon stocks, trends, and risks. The current protocol may be crediting projects on lands that are naturally productive or that feature low harvest potential, rather than inducing new climate mitigation outcomes. Our analyses also demonstrate an important role for geospatially complete, remote-sensing-based, and publicly available data products for monitoring carbon offset projects. These datasets for carbon and harvest allowed us to perform comprehensive comparisons of the trajectories of offset areas relative to other similar areas since the 1980s at a 30m resolution. Such spatial and temporal completeness exceeds what is offered by plot-level forest inventories (which are also often only privately accessible) or county-level datasets. Completeness and public availability could also improve offset program buy-in from smaller landowners and enable more large-scale and transparent deployment of carbon offsetting. However, geospatial data products require continued scientific investment, validation, and annual updates to increase confidence in their accuracy for different forest types and over time.

3.5 Conclusion

We present a novel suite of analyses to (1) demonstrate the potential for remote-sensing based data products in evaluating improved forest management offset projects and to (2) investigate the validity of additionality assumptions embedded in California's forest offset protocol. Although remote sensing-based methods for estimating carbon stocks are not yet reliable replacements for on-the-ground measurements, they

provide a reasonable and systematic basis for detecting changes between trends in lands enrolled in carbon offset projects and nearby control areas. In comparing carbon accumulation rates, harvest patterns, and species composition between project areas and similar private forestlands, we did not find evidence that IFM project carbon stocks are systematically at risk of being managed down to baseline levels, nor that carbon being added in IFM projects is additional to what might have been added in the absence of offset credit incentives. Implementing these types of analyses toward stricter standards in IFM protocol could both increase confidence in carbon additionality and enable the deployment of nature-based climate solutions at larger scales beyond the state of California.

3.6 Acknowledgments

We appreciate the constructive feedback of our colleague, Dr. John Battles at the Department of Environmental Science, Policy, and Management at UC Berkeley, during the development of this manuscript.

This research was funded by the National Science Foundation (NSF) Graduate Research Fellowship Program [grant number DGE-1839285] (for S. R. Coffield), by the UCOP National Laboratory Fees Research Program [grant number LFR-18-542511] (for S. R. Coffield, J. A. Wang, J. T. Randerson, and M. L. Goulden), by the California Strategic Growth Council's Climate Change Research Program with funds from California Climate Investments as part of the Center for Ecosystem Climate Solutions (for M. L. Goulden, C. D. Vo, J. T. Randerson, S. R. Coffield, and J.A. Wang), by the Department of Energy (DOE) Office of Science's Reducing Uncertainty in Biogeochemical Interactions through Synthesis and Computation (RUBISCO) Science Focus Area (for J. T. Randerson), by NASA's Modeling and Analysis Program (for J.T. Randerson). W. R. L. Anderegg acknowledges funding from David

and Lucile Packard Foundation, US National Science Foundation grants 2044937, 1802880 and 2003017, and USDA NIFA AFRI grant 2018-67019-27850. G. Badgley is supported by the Black Rock Forest postdoctoral fellowship in forest ecology. D. Cullenward is Vice Chair of California's Independent Emissions Market Advisory Committee, but does not speak for the Committee here.

Chapter 4

Projecting future wildfire risk in California from changing climate and vegetation composition

Adapted from:

Coffield, S.R., Graff, C.A., Wang, J.A., Bhoot, V., Goulden, M.L., Foufoula-Georgiou, E., Smyth, P., Randerson, J.T. Projecting future wildfire risk in California from changing climate and vegetation composition. (in prep).

4.1 Introduction

Changing wildfire regimes are of key concern for human health, ecosystem function, biodiversity, and climate mitigation (e.g. Johnston et al., 2012, Westerling et al., 2008, Wang et al., 2021, Anderegg et al., 2020). In California, a rapid increase in burned area over recent years has resulted in significant loss of life and economic costs in the billions of dollars per year (CALFIRE Incident Reports https://www.fire.ca.gov/incidents; Wang et al., 2021). Large wildfires have also led to record carbon emissions, with the California Air Resources Board estimating that 2020 wildfires released 110 $MMTCO_2eq$, or roughly a quarter of total emissions from other sectors (California Air Resources Board, 2020). These emissions contribute to the total land sector being a net source of carbon, with forests themselves also declining in total tree cover and biomass and now likely being a net source (Gonzalez et al., 2015, Wang et al., 2022). The loss of carbon presents a substantial challenge to the State's climate mitigation goals, which include managing natural and working lands to become a net sink of carbon by mid-century (California Air Resources Board 2019).

Recent work has helped illuminate the drivers of increasing wildfire in California and the Western US. Ignitions have been found to be heavily controlled by environmental

and human factors, with human ignitions largely explained by precipitation, topography, populations, and roads, and lightning ignitions largely explained by factors like snow water equivalent, lightning density, and fuels (Chen & Jin, 2022). Human-ignited fires also tend to occur during periods of hotter and drier weather, thereby spreading faster than lightning-ignited fires (Hantson et al., 2022). In terms of burned area, similar factors such as human variables, temperature, aridity (specifically vapor pressure deficit), and fuel structures are important drivers on daily to climatic scales (Gutierrez et al., 2021; Jin et al., 2015; Juang et al., 2022; Li & Banerjee, 2021).

The trend of increasing burned area is expected to continue into the future given increasing temperature and aridity which strongly control fire risk and fire size from daily to annual time scales. (Williams et al., 2019, Gutierrez et al., 2019). Several studies have made future projections, with disagreement in the magnitude and areas of greatest change depending on variables included and processes represented e.g., (Abatzoglou et al., 2021; Hurteau et al., 2014; Spracklen et al., 2009; Westerling et al., 2011). For example, not including human factors may lead to overstating future burned area (Mann et al., 2016). In general, though, total increases in fire risk vary, with one recent study projecting burned area increasing by over a factor of four for US forests as a whole (Anderegg et al., 2022). One key uncertainty which is not consistently considered in future projections of wildfire is the feedback effect of fire on vegetation. As burned area and fire severity increase, fuel load could be decreased for subsequent fire. However the extent of this feedback is unclear, and could potentially be positive if frequent and intense fire drives conversion of forests to more fire-prone shrublands and grasslands. One recent study found that future fuel

constraints are unlikely to substantially restrain burned area over this century in the Western US (Abatzoglou et al. 2021).

In this study we investigated the human and environmental factors controlling historical (1990-2021) fire occurrence in California, and made projections for future expected annual burn probability for 2081-2100. We expanded on previous work by using random forest (RF) machine learning models and quantifying uncertainty using different combinations of drivers (including modeled future vegetation), and considering uncertainty in precipitation from downscaled CMIP6 climate models. Our geospatial projections of future fire at a 4-km scale provide new insights into spatial patterns of risk and their uncertainties, which could help inform targeted land management for fuel and risk reduction, particularly in the context of carbon goals.

4.2 Methods

4.2.1 Data

We gathered historical fire perimeters from the California Department of Forestry and Fire Protection (FRAP) GIS dataset for 1990-2021 (California Department of Forestry and Fire Protection, 2021). We aggregated perimeters to an annual resolution, rasterized to 1 km, summed across years, and rescaled to 2.5 min (about 4.5 km) to match the climate datasets discussed below. Our target variable for our models was defined as the sum of burn occurrence divided by 32 years for each pixel, providing a metric of an expected annual burn frequency in percent per year (%/y). We excluded areas from analysis within our domain which were >50% non-wildland (urban or agricultural) as defined by the National Land Cover Database for 2016 (Homer et al. 2020).

We obtained monthly historical climate data at 2.5 min over the same period, 1990-2021, from the PRISM Climate Group at Oregon State University (Daly et al., 2008). We considered two variables, mean temperature and precipitation, averaged over the 32-year period and for individual seasons (winter (DJF), spring (MAM), summer (JJA), and fall (SON)). Future climate projections were collected from the WorldClim dataset (Fick & Hijmans, 2017), which provides downscaled bias-corrected CMIP6 projections for 23 different climate models at the same spatial resolution, 2.5 min, in increments of 20 years. We used the SSP2-4.5 scenario from CMIP6, representing a moderate warming scenario. To calculate climate change, we subtracted the historical climate baseline used by WorldClim - downscaled CRU-TS-4.03 monthly data for 1990-2018 from the Climatic Research Unit at the University of East Anglia (Harris et al., 2014). We then added this change from WorldClim-minus-CRU onto the PRISM data to provide our final dataset of future climate for 2081-2100.

For vegetation, we used 30 m herbaceous, shrub, and tree cover from Wang et al. 2022, constructed based on the National Land Cover Database (Homer et al., 2020) and expanded to cover California annually since 1986 using Landsat 2 spectral indices (Masek et al., 2020). We considered these three vegetation cover variables for the year 1989, prior to the start of our fire record, and averaged to a 2.5 min resolution.

Topographical variables were derived from NASA's SRTM digital elevation data Version 4, originally at 90 m. At a 2.5 min resolution, we calculated mean slope, mean aspect, roughness (standard deviation of 90 m subpixels) and the proportion of southward aspect (subpixels with aspect between 135 and 225°).

Finally, we considered two human variables: population density and road density available through Google Earth Engine (Gorelick et al., 2017). Population density came from the NASA Gridded Population of the World (GPW) for 2020 at 30 arcsecond (~1 km) (Doxsey-Whitfield et al., 2015) and road density was calculated based on TIGER US Census roads for 2016 (data.census.gov).

4.2.2 Modeling framework

For our modeling approach we used Random Forest (RF) regression, a machine learning technique based on an ensemble of decision trees which seeks to find non-linear combinations of predictor variables that can accurately predict a target variable, minimizing the root mean square error (RMSE) (Breiman, 2001). RFs have been commonly used for ecological prediction given their flexibility to capture non-linear relationships and suitability for medium-sized datasets (e.g., Coffield et al., 2021; Iverson et al., 2004; Prasad et al., 2006). We used default settings for the RF regressor from scikit-learn in Python (Pedregosa et al., 2011), and also specified that each tree in the forest use the square root of the number of available predictor variables.

We set up a 10-fold cross-validation framework for model training and testing, holding out a randomly selected 10% of our 18,744 pixel dataset at a time and training the RF model on the remaining 90%. This allowed us to construct validation plots and compare model performance (measured by RMSE) with different combinations of variables included. We also present a second, more rigorous cross-validation scenario where geographically cohesive sets of pixels, sorted by latitude, are held out. This second scheme for cross-validation reduces the effect of spatial dependence which is likely to be present between neighboring pixels that are in the training and test sets.

Once we determined which environmental and human variables most contributed to model performance (in terms of RMSE reduction and variable importance), we trained a single RF model using all of the available data, to be used for future projection. We compared future projections for a 3 × 3 set of scenarios: first, using three different combinations of changing variables (climate only, climate with constant vegetation, and climate and vegetation both changing), and second for three climate scenarios (driest, mean, and wettest). The "driest" and "wettest" scenarios result from driving the RF with only the five climate models which showed the most decrease or most increase in precipitation for California. This framework is presented in Table 4.1 in the Results.

4.3 Results

4.3.1 Historical model results

We built random forest models to predict annual burn probability based on combinations of 20 different explanatory variables: climate (4 seasons and annual mean of temperature and precipitation), topography (slope, aspect, elevation, roughness, and southward aspect), vegetation (herbaceous, shrub, and tree cover), and human factors (population density and road density). A subset of these variables and the target variable is shown in Fig. 4.1.

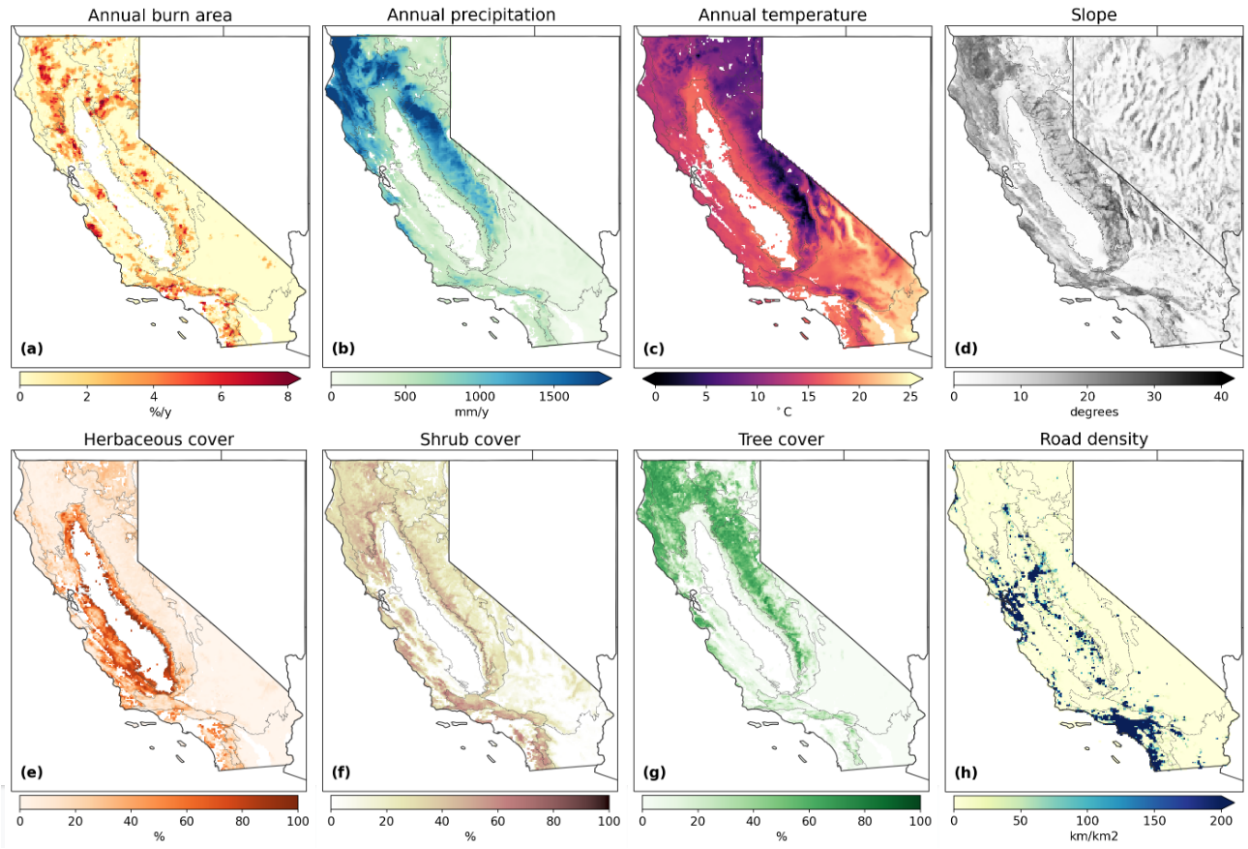

Figure 4.1. Annual burn area (a) and seven example predictors. The most important variables that were retained in our final model are annual precipitation, summer temperature, winter temperature, slope, herbaceous cover, shrub cover, tree cover, and road density.

After cross-validation with all variables, we chose a final model using eight predictor variables: annual precipitation, summer temperature, winter temperature, slope, herbaceous cover, shrub cover, tree cover, and road density (Fig. 4.2). This final model gave an RMSE of 1.01 ± 0.03 percent per year (%/y), with an R^2 of correlation of 0.56 ± 0.03 between predictions and observations (Fig. 4.2b-c). For the second, more rigorous cross-validation scheme with geographically coherent blocks held out, the resulting RMSE was 1.21 ± 0.27 %/y and R^2 = 0.34 ± 0.11 (Fig. 4.2d-e). In both cases the model was slightly biased toward the mean, tending to underestimate high expected burned area. However, the

model qualitatively performs quite well spatially, capturing most of the hotspots of fire occurrence across the state (Fig. 4.3).

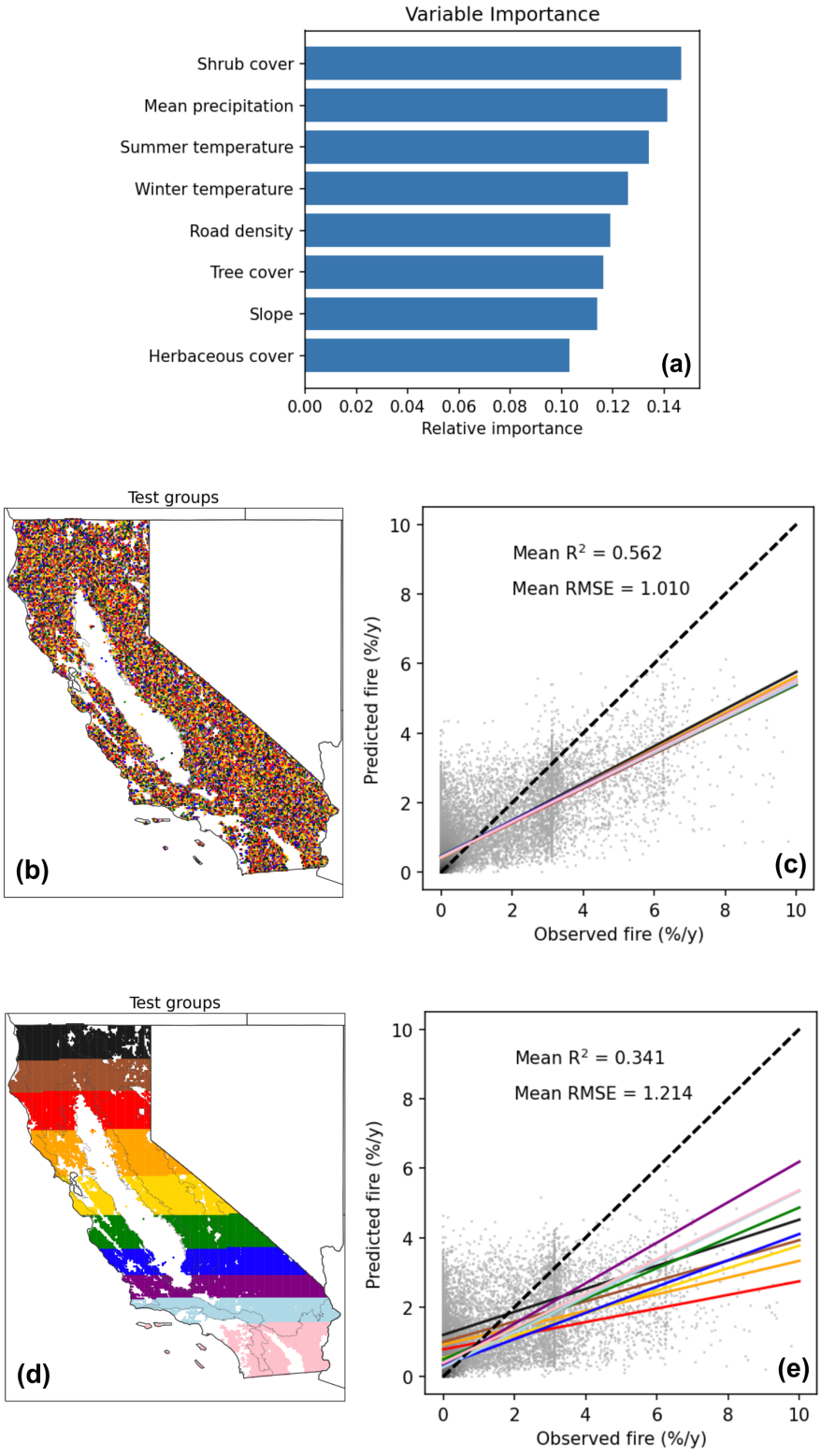

Figure 4.2. RF model variable importance and cross-validation using two difference schemes. In the first scheme, 10 cross-validation groups are assigned randomly. In the second scheme, 10 cross-validation groups are assigned based on latitudinal sorting, such that any of the 10 trained models are then tested in a new geographic area outside of the training domain. In both cases the model tended to underpredict high fire occurrence. The cluster of pixels with observed values near 3.1%/y results from many 4-km pixels in the record that burned once in 32 years.

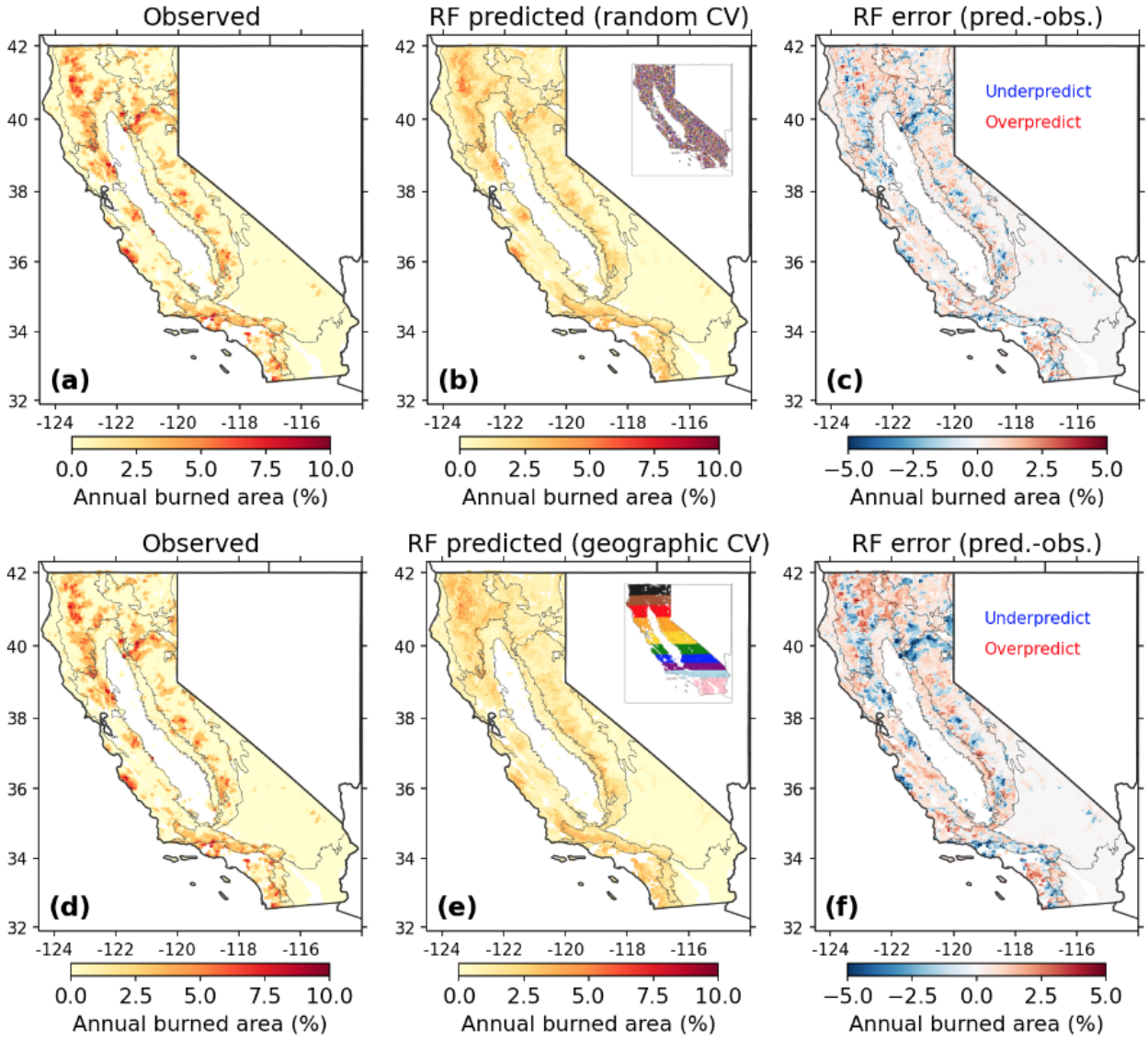

Figure 4.3. Spatial performance of RF model built on eight predictors. The top row depicts the results of the first cross-validation scheme with randomly assigned groups, and the second row depicts the second cross-validation scheme with latitudinally sorted groups. In either case, the "predictions" for a given pixel are shown for when it was in the held-out test group of a model. While the model is conservative, it generally captures the spatial patterns of fire occurrence, with higher probability in the Sierra Nevada foothills, southern ranges, and Klamath mountains in the northwest.

4.3.2 Future projections

The WorldClim downscaled climate projections for SSP2-4.5 show 2-4°C of warming and a slight increase in precipitation on average for California, with disagreement across models especially for precipitation (Fig. 4.4). We combined these climate models into three groups based on precipitation: the 5 models with the least added precipitation ("dry"; GISS-E2-1-G, CNRM-CM6-1, CanESM5, and CanESM5-CanOE), the mean of all 22, and the 5 models with the most added precipitation ("wet"; UKESM1-0-LL, HadGEM3-GC31-LL, FIO-ESM-2-0, and INM-CM4-8).

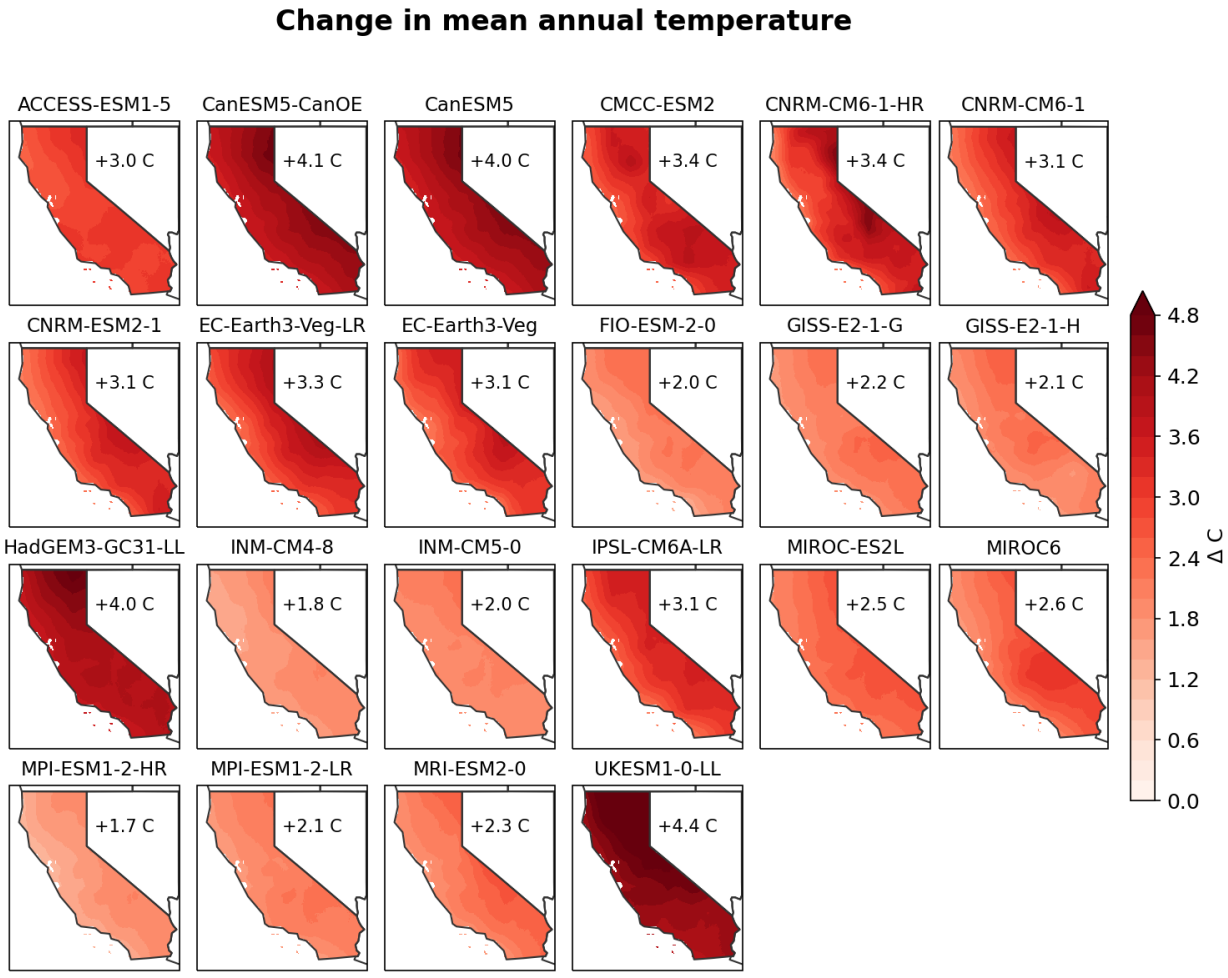

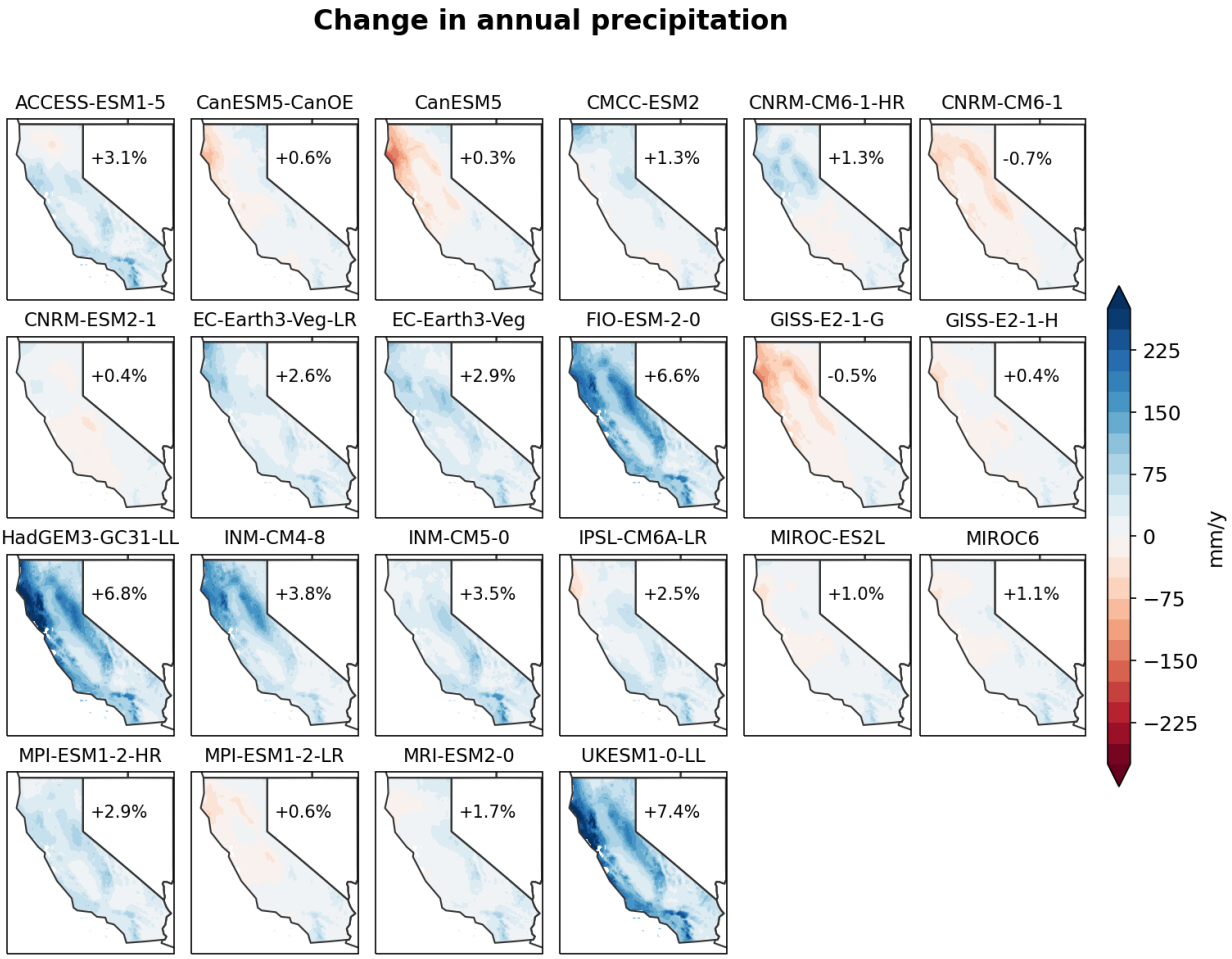

Figure 4.4. Downscaled climate change projections from WorldClim for SSP2-4.5 (2081-2100 minus 1900-2018). Due to model disagreement especially for precipitation, we ran our models with three moisture scenarios: wet, dry, and mean.

Fig. 4.5 provides the results of nine different model runs, with three different sets of changing variables and three future moisture scenarios. In the third set of models, the same RF approach was also first used to project future vegetation based on mean annual precipitation, summer temperature, and winter temperature (Fig. 4.6). Allowing vegetation to respond directly to these three climate change variables led to a 7.6% increase in shrub cover, leading to greater fire risk, along with decreases in herbaceous and tree cover. The relocation of shrub cover upslope toward the mid-elevation of the Sierra Nevada corresponds to a similar shift in fire risk. In general, we found highly consistent patterns of

change across the nine model runs, with increases in burned area ranging from 36-52%. Fire risk appeared to spread out from present-day risk hotspots, with widespread increases in temperature moving those particular areas out of the optimum climate space and applying risk to surrounding areas. Increases were particularly high in the northern coast region, which has less fire than other interior regions at present-day. The peak area of fire risk in the Sierra Nevada shifted slightly eastward (upslope) to mid-elevation regions. Finally, we found that the wettest climate scenarios consistently led to the greatest increases in fire risk.

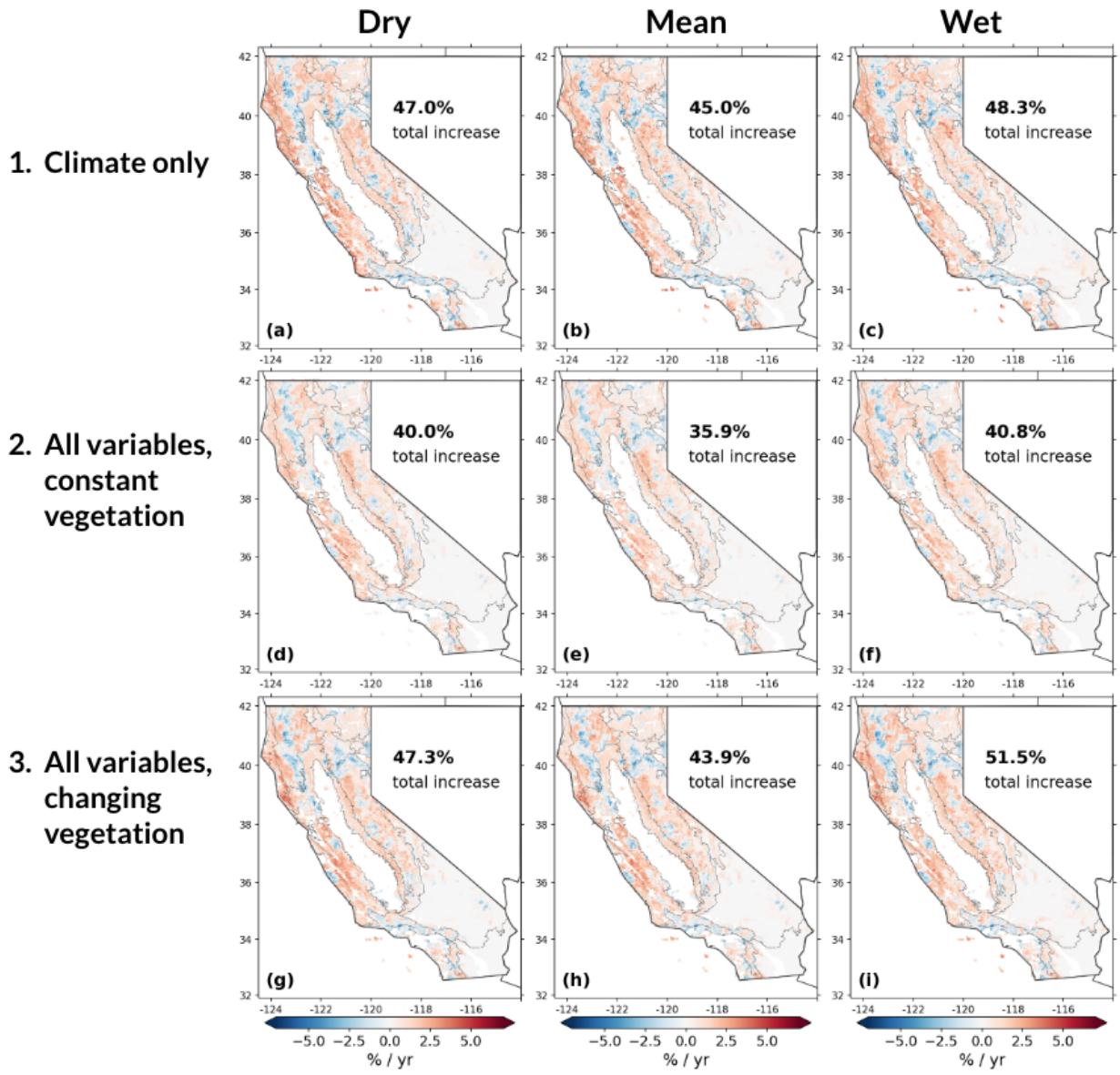

Figure 4.5. Total relative change in expected statewide annual burned area (modeled 2081-2100 minus modeled 1990-2021) for three different sets of changing variables and three future moisture scenarios.

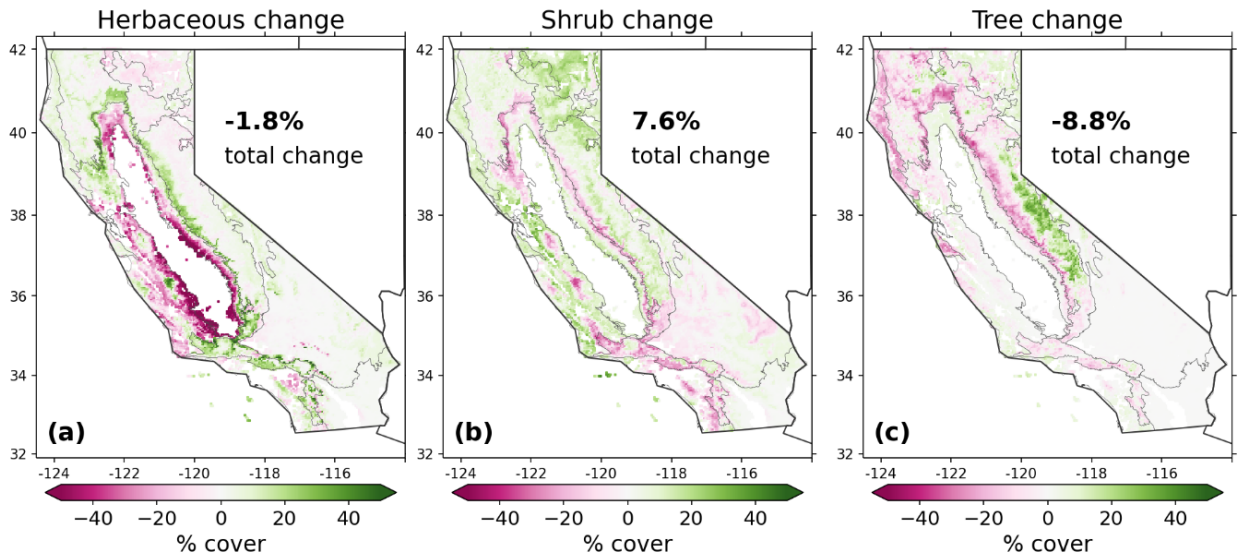

Figure 4.6. Total relative change in statewide vegetation cover. These changes were calculated based on separate RF models trained on climate (mean annual precipitation, summer temperature, and winter temperature) and used for the third set of models (Fig. 4.5 g-i). Shown above are for the "mean" moisture change scenario. The expansion of shrubs in particular largely explains the shifts in fire risk in the projections in Fig. 4.5.

4.4 Discussion

In this study we used random forests to model the historical spatial distribution of wildfire occurrence in California and make projections to end-of-century. We found that the RF model was able to capture spatial patterns of high fire risk, particularly along the foothills of the Sierra Nevada as well as the southern ranges and Klamath Mountains of northwestern California. In the future projections, we found widespread increases in fire and shifts away from present-day hotspots, largely due to the expansion of shrub cover and increase in temperature.

The importance of shrub cover and its positive influence on fire is uniquely highlighted in this study, leveraging the new dataset for statewide land cover types from Wang et al. (2022). The positive relationship between shrub cover and fire risk may be explained mechanistically by shrubs' higher relative proportion of dead biomass and fine

fuels which respond rapidly to drier atmospheric conditions, as well as the high air-to-fuel density allowing for increased oxygen access and fire spread rates (Rothermel 1972, Rollins 2009).

We also highlight the role of future precipitation, which adds some uncertainty to the future projections, although the change is much smaller and less consequential on average than the 2-4°C rise in temperature. We found that the scenarios with greatest increases in precipitation consistently led to the greatest increases in wildfire occurrence. Although previous research has found that drier scenarios led to less fuel as measured by aboveground live carbon (Coffield et al., 2021), we found a positive influence of precipitation on fire risk. We speculate that this positive effect is related to fuel content being less limiting in the wet scenario, specifically for shrub cover which was able to increase more than in dry or mean scenarios.

Future work will involve a fourth set of models, specifically simulating vegetation responses to the projected changes in wildfire. Increased wildfire on the order of 40-50% could somewhat limit future fuels in forests, or could further accelerate subsequent fire by driving type conversion of forests to shrublands. This work should also be compared alongside other process-based models which can capture other factors not considered here - including vegetation responses to increased CO_2, changing nutrients, and competition as species shift geographically (Swann et al., 2016, Birami et al., 2020, Needham et al., 2020, Wamelink et al., 2009, Luo et al., 2004, Lenihan et al., 2008, Svenning & Sandel, 2013). This study may also be improved by removing some of the "hottest" models from our projections, particularly those with > 4°C warming, as previous work has suggested (Hausfather et al., 2022).

Our projected changes in wildfire occurrence with climate change could directly inform targeted land management to mitigate risks, as well as risk assessment for carbon goals and carbon offset programs. The currently assumed fire risk of 2-4% over 100 years in the California protocol for forest offsets is highly unrealistic, particularly for many of the projects located in the northern coastal region where future increases are concentrated. This work could be expanded to the rest of the US and applied to offset project polygons specifically.

In general, our study agrees with previous work which warns of substantial future increases in fire risk across California. Our results are also unique in comparing the role of different future drivers, including models which explicitly represent how future decades may experience an expansion of shrub cover and loss of tree cover throughout most of the state. These projections could serve as a basis for land management and carbon offsetting goals, in order to help maintain fire regimes that are less threatening to human health and vulnerable ecosystems.

4.5 Acknowledgments

This research was funded by the National Science Foundation (NSF) Graduate Research Fellowship Program [grant number DGE-1839285] (for S. R. Coffield), by the UCOP National Laboratory Fees Research Program [grant number LFR-18-542511] (for S. R. Coffield, J. A. Wang, J. T. Randerson, and M. L. Goulden), by the California Strategic Growth Council's Climate Change Research Program with funds from California Climate Investments as part of the Center for Ecosystem Climate Solutions (for M. L. Goulden, J. T. Randerson, S. R. Coffield, and J.A. Wang), by the Department of Energy (DOE) Office of Science's Reducing Uncertainty in Biogeochemical Interactions through Synthesis and

Computation (RUBISCO) Science Focus Area (for J. T. Randerson), by NASA's Modeling and Analysis Program (for J.T. Randerson).

CONCLUSIONS

Summary of results

The goal of my dissertation was to explore the climate and environmental factors governing ecosystem processes such as carbon storage and wildfire in the Western US, and quantify the impacts of future climate change. This was accomplished using a variety of statistical and machine modeling approaches leveraging geospatial data for climate, topography, vegetation, and human factors.

In Chapter 1, I developed a machine learning-based model for predicting final fire size from initial conditions including the fraction of black spruce trees surrounding the ignition site and the vapor pressure deficit over the first five days of a fire. In the context of increasing fire number and burned area in Alaska, this information suggests that large fires could be caught early in their life, before the first few dry days allow them to escape. This information could also help with the design of a natural climate solutions strategy based on suppressing wildfires during extreme fire years, thus maintaining the current fire regime and avoiding loss of vegetation and permafrost carbon. Also in this chapter I was able to estimate the footprint of fire management on total burned area, applying my model to more actively suppressed areas to find that they would have otherwise been larger.

In Chapter 2, I again used machine learning to quantify how seasonal patterns of temperature and precipitation control the observed spatial patterns of aboveground live carbon and species' ranges in California. When applied to the future, I discovered that much of the state is projected to lose carbon, on the order of 9-16%, which is directly at odds with the State's goal of increasing carbon sequestration over this century. Loss of carbon stocks was particularly high in the more extreme warming and drying scenarios. This study also

revealed the uncertainty in future precipitation as the biggest source of uncertainty toward ecological projections of future carbon stocks.

In Chapter 3, I focused on the 37 improved forest management carbon offset projects in California which I had previously identified as hosting particularly climate-vulnerable carbon stocks. I developed a new framework and hypotheses for testing the additionality of carbon that has thus far been added to these offset projects. I found that in general across the portfolio of projects, the time series of projects' carbon and harvest rates did not show a departure from historical trends or from other similar forests over the same time period. Also, in many cases in the northern coastal region, projects appeared to be selectively placed in areas of higher tanoak and less redwood density, suggesting that they were at less risk of logging in the first place. As remote sensing-based carbon monitoring technologies improve and as offsets receive increasing attention for climate mitigation, these types of systematic spatiotemporal analyses could help improve the transparency and reliability of carbon crediting protocols.

In Chapter 4, I returned to the modeling framework from Chapter 2, which I expanded to make projections of future fire occurrence in California. The spatial patterns of historical burned area were a more complex problem to model than the patterns of carbon stocks; however, I found that a random forest trained on eight environmental predictors could explain most of the areas of observed wildfire. In particular, fractional shrub cover was the most important variable and was positively correlated with fire occurrence. Applying the model to the future with different combinations of changing climate and vegetation, I found widespread increases in wildfire risk on the order of 40-50%, particularly in scenarios with increasing shrub cover and moisture.

Together, my research found that Western US ecosystems are highly vulnerable to changes in temperature and moisture availability driven by climate change. This underscores the importance of strong climate mitigation policies, including real emissions reductions and land management to reduce risks.

Implications for land management

Each chapter offers specific insights which are directly relevant for land management decisions or goals. In Chapter 1, the framework for fire prediction from the time of ignition could be useful for triaging fires in regions that are responding to strong trends in climate. My simple model based on thresholds for black spruce cover and vapor pressure deficit could easily be implemented as a computationally inexpensive decision support tool. Both Alaska and California have seen recent years where extreme fire weather conditions lead to hundreds of ignitions within a few days. Particularly in California, these events have overwhelmed suppression resources necessary to protect populated areas. In Alaska, although most fires are remote and not direct threats to human settlements, there could still be value in applying selective suppression effort to wildland fires in order to maintain historical fire regimes, mitigate carbon emissions, and protect vulnerable ecosystems.

In Chapter 2, the geospatial carbon vulnerability layers have been incorporated into the Center for Ecosystem Climate Solutions (CECS) web tool at https://cecs.ess.uci.edu/carbon-vulnerability/ . The tool makes it possible for stakeholders to view the projected carbon changes. This could help inform strategic protection of at-risk carbon pools, particularly in regions such as the mid-elevation Sierra Nevada and Northern Coast. The species vulnerability maps identify key species for conservation purposes, such

as coast redwood which show high risk on the southern end of its range. The vulnerability maps could also inform optimal placement and realistic expectations for carbon offset projects, which are currently located in high-risk areas. Offset policy could be designed with baselines accounting for climate risks, rather than strictly incentivizing increased carbon for all locations.

In Chapter 3, the geospatially systematic analyses for tracking additionality provide a framework for improved carbon crediting protocols. Projects could be incentivized not just to maintain carbon stocks above a static baseline, but to demonstrate departure from carbon and harvest patterns of similar "control" forests. Remote sensing-based carbon and disturbance monitoring provides opportunity for more systematic, transparent, and accessible tracking of forests which could be leveraged for offset protocols, especially as the remote sensing products improve and offsets receive increasing attention at larger scales.

In Chapter 4, similar to Chapter 2, the maps of future fire risks could inform ecosystem management for conservation of certain species, protection of vulnerable populations, or for risk quantification for carbon offset projects. Currently in California's forest offset protocol (California Air Resources Board, 2015), either a 2 or 4% fire risk rating is assigned to all projects, which are required to allocate that many credits toward an insurance pool. My findings suggest that future fire probability is at least that much *per year*, not per 100 years over which permanence is required. Carbon offsetting could be improved with higher insurance allocations, or for explicitly incentivizing fire risk reduction to maintain existing carbon stocks that would otherwise decline. This chapter highlights the importance of pursuing California's ambitious land treatment goals, including expanding implementation of prescribed burning, given the substantial future fire risks.

Future research

This dissertation revealed important patterns of climate risks to ecosystems in Alaska and California. I envision three main areas of related future work: (1) expanding these studies to the entire Western US or other regions, (2) improving model performance and systematically comparing results and insights from these statistical models against those of mechanistic or process-based models, and (3) increased efforts to improve data and research in areas of identified uncertainty. Additional research in these areas would contribute to some of the critical open scientific questions: Will Western US ecosystems be a source or sink for carbon over this century? How will fire weather and drought change in the future? What types and amounts of management practices are needed to maintain historical fire regimes and carbon stocks?

First, my domain was the state of Alaska (Chapter 1) or California (Chapters 2-4), however the themes are relevant for the entire Western US as well as other parts of the globe. In Chapter 1, the triaging framework for fire prediction could be useful in other boreal regions as well as California which has experienced periods of extreme fire weather, requiring fast response and prioritization of suppression resources as well as natural climate solutions frameworks based on fire reduction. The vulnerability maps from Chapters 2 and 4 could be expanded, with work currently in review at *Nature* with colleagues from the University of Utah to quantify carbon changes across US forests. In the cases of Chapters 3 and 4, the domain could be expanded to the US if the Landsat-derived vegetation cover and disturbance datasets (Wang et al., 2022) became available beyond California. It would be especially valuable to look at broader trends of California's forest carbon offset projects, including 80+ other projects beyond the 37 which are geographically

within California.

Second, there is room to continue improving the modeling approaches, particularly in Chapter 4. Fire is a complex ecosystem process connected to changes in fuel which are also responding to climate change over time. A next step would be to probabilistically simulate burned area for 20-year increments into the future using WorldClim climate projections. Based on historical patterns of post-fire vegetation recovery in different ecoregions, a simulation could allow fire to modulate the herbaceous, shrub, and tree cover for the subsequent 20-year timestep. Exploring this system would reveal the importance of potential positive or negative feedbacks between fire and fuels over time. Then, this approach for fire could be compared against dynamic ecosystem models such as The Dynamic Temperate and Boreal Fire and Forest-Ecosystem Simulator (DYNAFFOREST) currently in review at *Environmental Modelling and Software*. Such other approaches which more rigorously represent vegetation responses may show similar or distinct spatial patterns of risk. Also, models such as the Functionally Assembled Terrestrial Ecosystem Simulator (FATES) (Koven et al. 2020; Fisher et al., 2015) are being developed for California to model the future of mixed conifer forests. It would be useful to compare those results to the carbon and species projections from Chapter 2 to identify areas of certainty/uncertainty in ecosystem futures.

Third, these chapters identified several other areas of scientific needs, especially related to data. For example, in Chapter 2 (and to some extent Chapter 4), I identified model uncertainty in future precipitation as a major source of uncertainty for future ecosystem predictions. There is high model-to-model disagreement regarding the *direction* of precipitation change for the Western US, let alone the exact magnitude or the changes in

timing or interannual variability. These factors can all be critical to ecosystem function and fire occurrence. Another key area of uncertainty, which we therefore neglected to represent, was the effect of CO_2 on semi-arid forests. More studies and potentially data collection via free-air carbon enrichment experiments for these ecosystem types would help elucidate whether increased CO_2 will improve plant water use efficiency enough to offset any of the otherwise predicted ecosystem vulnerabilities. There is also a general lack of data regarding the potential migration capacity of key Western tree species, which in Chapter 2 I identified as a major uncertainty.

In Chapter 3, I discussed the limitations of current remote sensing-based biomass products, including some bias at high biomass densities. Continued improvement of these products, for example through new spaceborne lidar observations from the Global Ecosystem Dynamics Investigation (GEDI) (Dubayah et al., 2020) and other efforts from NASA's Carbon Monitoring System, could enable more reliable carbon tracking toward offset crediting.

Finally, in Chapter 4, I also identified the important role of shrubs in controlling fire risk. More research is needed to investigate how shrub cover has changed over time in the Western US, as well as the role of grazing and other potential drivers of change in the past and future. More research is also needed to quantify the effectiveness of different management practices such as prescribed burning to reduce fire, and to make projections of future fire under different management scenarios as well. Continued work in these areas will help increase certainty for future ecosystem predictions relevant for management and climate goals.

REFERENCES

Abatzoglou, J. T., & Williams, A. P. (2016). Impact of anthropogenic climate change on wildfire across western US forests. *Proceedings of the National Academy of Sciences of the United States of America*, *113*(42), 11770–11775. https://doi.org/10.1073/pnas.1607171113

Abatzoglou, J. T., Battisti, D. S., Williams, A. P., Hansen, W. D., Harvey, B. J., & Kolden, C. A. (2021). Projected increases in western US forest fire despite growing fuel constraints. *Communications Earth & Environment*, *2*(1), 1–8. https://doi.org/10.1038/s43247-021-00299-0

Abella, S. R., & Fornwalt, P. J. (2015). Ten years of vegetation assembly after a North American mega fire. *Global Change Biology*, *21*(2), 789–802. https://doi.org/10.1111/gcb.12722

Ackerly, D. D., Loarie, S. R., Cornwell, W. K., Weiss, S. B., Hamilton, H., Branciforte, R., & Kraft, N. J. B. (2010). The geography of climate change: Implications for conservation biogeography. *Diversity and Distributions*, *16*(3), 476–487. https://doi.org/10.1111/j.1472-4642.2010.00654.x

Agee, J. K., & Skinner, C. N. (2005). Basic principles of forest fuel reduction treatments. *Forest Ecology and Management*, *211*, 83–96. https://doi.org/10.1016/j.foreco.2005.01.034

Allwood, J. M., Bosetti, V., Dubash, N. K., Gomez Echeverri, L., & von Stechow, C. (2014). Glossary. Climate Change 2014: Mitigation of Climate Change. Contribution of Working Group III to the Fifth Assessment Report of the Intergovernmental Panel on Climate Change. http://pure.iiasa.ac.at/id/eprint/11110/1/ipcc_wg3_ar5_annex-i.pdf

Andam, K. S., Ferraro, P. J., Pfaff, A., Sanchez-Azofeifa, G. A., & Robalino, J. A. (2008). Measuring the effectiveness of protected area networks in reducing deforestation. Proceedings of the National Academy of Sciences of the United States of America, 105(42), 16089–16094. https://doi.org/10.1073/pnas.0800437105

Andela N, Morton DC, Giglio L, Chen Y, van der Werf GR, Kasibhatla PS, DeFries RS, Collatz GJ, Hantson S, Kloster S, Bachelet D, Forrest M, Lasslop G, Li F, Mangeon S, Melton JR, Yue C, Randerson JT (2017) A human-driven decline in global burned area. *Science* 356, 1356–1362. doi:10.1126/SCIENCE.AAL4108

Anderegg, W. R. L., Chegwidden, O. S., Badgley, G., Trugman, A. T., Cullenward, D., Abatzoglou, J. T., Hicke, J. A., Freeman, J., & Hamman, J. J. (2022). Future climate risks from stress, insects and fire across US forests. *Ecology Letters*, *25*(6), 1510–1520. https://doi.org/10.1111/ele.14018

Anderegg, W. R. L., Kane, J. M., & Anderegg, L. D. L. (2013). Consequences of widespread tree mortality triggered by drought and temperature stress. *Nature Climate Change*, *3*(1),

30–36. https://doi.org/10.1038/nclimate1635

Anderegg, W. R. L., Trugman, A. T., Badgley, G., Anderson, C. M., Bartuska, A., Ciais, P., et al. (2020). Climate-driven risks to the climate mitigation potential of forests. *Science*, *368*(6497). https://doi.org/10.1126/science.aaz7005

Anderson-Teixeira, K. J., & Belair, E. P. (2021). Effective forest-based climate change mitigation requires our best science. Global Change Biology, 28(4). https://doi.org/10.1111/gcb.16008

Arienti MC, Cumming SG, Krawchuk MA, Boutin S (2009) Road network density correlated with increased lightning fire incidence in the Canadian western boreal forest. *International Journal of Wildland Fire* 18, 970–982. doi:10.1071/WF08011

Bachelet, D., Lenihan, J., Drapek, R., & Neilson, R. (2008). VEMAP vs VINCERA: A DGVM sensitivity to differences in climate scenarios. *Global and Planetary Change*, *64*, 38–48. https://doi.org/10.1016/j.gloplacha.2008.01.007

Badgley, G., Freeman, J., Hamman, J. J., Haya, B., Trugman, A. T., Anderegg, W. R. L., & Cullenward, D. (2021). Systematic over-crediting in California's forest carbon offsets program. *Global Change Biology*, *28*(4). https://doi.org/10.1111/gcb.15943

Balshi MS, McGuire AD, Duffy P, Flannigan MD, Walsh J, Melillo J (2009) Assessing the response of area burned to changing climate in western boreal North America using a Multivariate Adaptive Regression Splines (MARS) approach. *Global Change Biology* 15, 578–600. doi:10. 1111/J.1365-2486.2008.01679.X

Battles, J. J., Bell, D. M., Kennedy, R. E., Saah, D. S., Collins, B. M., York, R. A., Sanders, J. E., & Lopez-Ornelas, F. (2018). *Innovations in measuring and managing forest carbon stocks in California: A report for California's Fourth Climate Change Assessment*. California Natural Resources Agency. https://www.energy.ca.gov/sites/default/files/2019-12/Forests_CCCA4-CNRA-2018-014_ada.pdf

Belgiu, M., & Drăguţ, L. (2016). Random forest in remote sensing: A review of applications and future directions. *ISPRS Journal of Photogrammetry and Remote Sensing: Official Publication of the International Society for Photogrammetry and Remote Sensing* , *114*, 24–31. https://doi.org/10.1016/j.isprsjprs.2016.01.011

Bell, D. M., Acker, S. A., Gregory, M. J., Davis, R. J., & Garcia, B. A. (2021). Quantifying regional trends in large live tree and snag availability in support of forest management. *Forest Ecology and Management*, *479*, 118554. https://doi.org/10.1016/j.foreco.2020.118554

Bell, D. M., Gregory, M. J., & Ohmann, J. L. (2015). Imputed forest structure uncertainty varies across elevational and longitudinal gradients in the western Cascade Mountains, Oregon, USA. *Forest Ecology and Management*, *358*, 154–164. https://doi.org/10.1016/j.foreco.2015.09.007

Bell, D. M., Gregory, M. J., Kane, V., Kane, J., Kennedy, R. E., Roberts, H. M., & Yang, Z. (2018). Multiscale divergence between Landsat- and lidar-based biomass mapping is related to regional variation in canopy cover and composition. *Carbon Balance and Management*, *13*(1), 15. https://doi.org/10.1186/s13021-018-0104-6

Birami, B., Nägele, T., Gattmann, M., Preisler, Y., Gast, A., Arneth, A., & Ruehr, N. K. (2020). Hot drought reduces the effects of elevated CO2 on tree water-use efficiency and carbon metabolism. *New Phytologist*, *226*(6), 1607–1621. https://doi.org/10.1111/nph.16471

Breiman, L. (2001). Random forests. *Machine Learning*, *45*(1), 5–32. https://doi.org/https://doi.org/10.1023/A:1010933404324

Brekke, L., Thrasher, B. L., Maurer, E., & Pruitt, T. (2013). *Downscaled CMIP3 and CMIP5 climate projections: release of downscaled CMIP5 climate projections, comparison with preceding information, and summary of user needs*. Denver, CO.

Breshears, D. D., Cobb, N. S., Rich, P. M., Price, K. P., Allen, C. D., Balice, R. G., et al. (2005). Regional vegetation die-off in response to global-change-type drought. *Proceedings of the National Academy of Sciences of the United States of America*, *102*(42), 15144–15148. https://doi.org/10.1073/pnas.0505734102

Buckley Biggs, N., & Huntsinger, L. (2021). Managed Grazing on California Annual Rangelands in the Context of State Climate Policy. *Rangeland Ecology & Management*, *76*, 56–68. https://doi.org/10.1016/j.rama.2021.01.007

Bullock, E. L., Woodcock, C. E., & Olofsson, P. (2020). Monitoring tropical forest degradation using spectral unmixing and Landsat time series analysis. *Remote Sensing of Environment*, *238*, 110968. https://doi.org/10.1016/j.rse.2018.11.011

Burke, M., Driscoll, A., Heft-Neal, S., Xue, J., Burney, J., & Wara, M. (2021). The changing risk and burden of wildfire in the United States. *Proceedings of the National Academy of Sciences of the United States of America*, *118*(2). https://doi.org/10.1073/pnas.2011048118

Butler Z, Chen Y, Randerson JT, Smyth P (2017) Fire event prediction for improved regional smoke forecasting. In 'Proceedings of the 7th International Workshop on Climate Informatics: CI 2017', 20–22 September 2017, Boulder, CO, USA. (Eds V Lyubchich, N Oza, A Rhines, E Szekely) NCAR Technical Note NCAR/TN-536þPROC. doi:10.5065/D6222SH7. (National Center for Atmospheric Research: Boulder, CO, USA)

CALFIRE. (2021). Timber Harvesting Plans TA83. Retrieved April 1, 2021, from https://hub-calfire-forestry.hub.arcgis.com/datasets/cal-fire-timber-harvesting-plans-all-ta83

California Air Resources Board. (2015, June 25). Compliance Offset Protocol, U.S. Forest Projects.

https://ww2.arb.ca.gov/sites/default/files/classic/cc/capandtrade/protocols/usforest/forestprotocol2015.pdf

California Air Resources Board. (2018). *Technical Support Document for the Natural & Working Lands Inventory*. Retrieved from https://ww2.arb.ca.gov/nwl-inventory

California Air Resources Board. (2019). *January 2019 Draft California 2030 Natural and Working Lands Climate Change Implementation Plan*. Retrieved from https://ww3.arb.ca.gov/cc/natandworkinglands/draft-nwl-ip-040419.pdf

California Air Resources Board. (2020). *Greenhouse Gas Emissions of Contemporary Wildfire, Prescribed Fire, and Forest Management Activities*. https://ww3.arb.ca.gov/cc/inventory/pubs/ca_ghg_wildfire_forestmanagement.pdf

California Air Resources Board. (2021). ARB Offset Credit Issuance Table. https://ww2.arb.ca.gov/our-work/programs/compliance-offset-program/arb-offset-credit-issuance

California Department of Forestry and Fire Protection. (2021). *Fire perimeters*. https://frap.fire.ca.gov/frap-projects/fire-perimeters/

California Code of Regulations § 95802 (2012). Definitions. https://govt.westlaw.com/calregs/Document/IAB809A46C9794E3EAA751C21B72AE536?viewType=FullText&originationContext=documenttoc&transitionType=CategoryPageItem&contextData=(sc.Default)

California Health and Safety Code § 38562(d), § 38562(d) (2011). https://leginfo.legislature.ca.gov/faces/codes_displaySection.xhtml?sectionNum=38562.&nodeTreePath=30.4&lawCode=HSC

Calkin, D. E., Gebert, K. M., Jones, J. G., & Neilson, R. P. (2005). Forest Service Large Fire Area Burned and Suppression Expenditure Trends, 1970–2002. *Journal of Forestry*, *103*(4), 179–183. https://doi.org/10.1093/jof/103.4.179

Cameron, D. R., Marvin, D. C., Remucal, J. M., & Passero, M. C. (2017). Ecosystem management and land conservation can substantially contribute to California's climate mitigation goals. *Proceedings of the National Academy of Sciences of the United States of America*, *114*(48), 12833–12838. https://doi.org/10.1073/pnas.1707811114

Cascio WE (2018) Wildland fire smoke and human health. *The Science of the Total Environment* 624, 586–595. doi:10.1016/J.SCITOTENV. 2017.12.086

Chapin III, F. S., Matson, P. A., & Vitousek, P. (2011). *Principles of terrestrial ecosystem ecology* (Second). New York: Springer Science & Business Media.

Chen, B., & Jin, Y. (2022). Spatial patterns and drivers for wildfire ignitions in California. *Environmental Research Letters: ERL [Web Site]*, *17*(5), 055004. https://doi.org/10.1088/1748-9326/ac60da

Coffield, S. R., Hemes, K. S., Koven, C. D., Goulden, M. L., & Randerson, J. T. (2021). Climate-driven limits to future carbon storage in California's wildland ecosystems. *AGU Advances*, *2*(3). https://doi.org/10.1029/2021av000384

Coop, J. D., Parks, S. A., McClernan, S. R., & Holsinger, L. M. (2016). Influences of prior wildfires on vegetation response to subsequent fire in a reburned Southwestern landscape. *Ecological Applications*, *26*(2), 346–354. https://doi.org/10.1890/15-0775

Copernicus Climate Change Service (C3S) (2017) ERA5: Fifth generation of ECMWF atmospheric reanalyses of the global climate. Copernicus Climate Change Service Climate Data Store (CDS). Available at https:// cds.climate.copernicus.eu/cdsapp#!/home [Verified 20 Aug 2019]

Cortez P, Morais A (2007) A data mining approach to predict forest fires using meteorological data. In 'Proceedings of the 13th Portuguese Conference on Artificial Intelligence', 3–7 December 2007, Guimares, Portugal. (Eds J Neves, M Santos, J Machado) pp. 512–523. (SpringerVerlag, Berlin). Guimaraes, Portugal) http://www3.dsi.uminho.pt/ pcortez/fires.pdf [Verified 20 August 2019]

Daly, C., Halbleib, M., Smith, J. I., & Gibson, W. P. (2008). Physiographically sensitive mapping of climatological temperature and precipitation across the conterminous United States. *Journal of Applied Meteorology and Climatology*. https://rmets.onlinelibrary.wiley.com/doi/abs/10.1002/joc.1688

Davidson, E. A., & Janssens, I. A. (2006). Temperature sensitivity of soil carbon decomposition and feedbacks to climate change. *Nature*, *440*(7081), 165–173. https://doi.org/10.1038/nature04514

Davidson, E. A., Belk, E., & Boone, R. D. (1998). Soil water content and temperature as independent or confounded factors controlling soil respiration in a temperate mixed hardwood forest. *Global Change Biology*, *4*(2), 217–227. https://doi.org/10.1046/j.1365-2486.1998.00128.x

Davis, M. B. (1983). Quaternary History of Deciduous Forests of Eastern North America and Europe, *70*(3), 550–563.

de Souza FT, Koerner TC, Chlad R (2015) A data-based model for predicting wildfires in Chapada das Mesas National Park in the State of Maranhao. *Environmental Earth Sciences* 74, 3603–3611. doi:10. 1007/S12665-015-4421-8

Delfino RJ, Brummel S, Wu J, Stern H, Ostro B, Lipsett M, Winer A, Street DH, Zhang L, Tjoa T, Gillen DL (2009) The relationship of respiratory and cardiovascular hospital admissions to the southern California wildfires of 2003. *Occupational and Environmental Medicine* 66, 189–197. doi:10.1136/OEM.2008.041376

DeWilde L, Chapin FS (2006) Human impacts on the fire regime of interior Alaska: interactions among fuels, ignition sources, and fire suppression. *Ecosystems* 9,

1342–1353. doi:10.1007/S10021-006-0095-0

Di Giuseppe F, Remy S, Pappenberger F, Wetterhall F (2018) Using the Fire Weather Index (FWI) to improve the estimation of fire emissions from fire radiative power (FRP) observations. *Atmospheric Chemistry and Physics* 18, 5359–5370. doi:10.5194/ACP-18-5359-2018

Doxsey-Whitfield, E., MacManus, K., Adamo, S. B., Pistolesi, L., Squires, J., Borkovska, O., & Baptista, S. R. (2015). Taking Advantage of the Improved Availability of Census Data: A First Look at the Gridded Population of the World, Version 4. *Papers in Applied Geography*, *1*(3), 226–234. https://doi.org/10.1080/23754931.2015.1014272

Dubayah, R., Blair, J. B., Goetz, S., Fatoyinbo, L., Hansen, M., Healey, S., Hofton, M., Hurtt, G., Kellner, J., Luthcke, S., Armston, J., Tang, H., Duncanson, L., Hancock, S., Jantz, P., Marselis, S., Patterson, P. L., Qi, W., & Silva, C. (2020). The Global Ecosystem Dynamics Investigation: High-resolution laser ranging of the Earth's forests and topography. *Egyptian Journal of Remote Sensing and Space Sciences*, *1*, 100002. https://doi.org/10.1016/j.srs.2020.100002

Elgin, B. (2020, December 9). These Trees Are Not What They Seem: How the Nature Conservancy, the world's biggest environmental group, became a dealer of meaningless carbon offsets. *Bloomberg Green*. https://www.bloomberg.com/features/2020-nature-conservancy-carbon-offsets-trees/

Faivre NR, Jin Y, Goulden ML, Randerson JT (2014). Controls on the spatial pattern of wildfire ignitions in Southern California. *International Journal of Wildland Fire* 23, 799–811. doi:10.1071/WF13136

Faivre, N. R., Jin, Y., Goulden, M. L., & Randerson, J. T. (2016). Spatial patterns and controls on burned area for two contrasting fire regimes in Southern California. *Ecosphere* , *7*(5), 1–25. https://doi.org/10.1002/ecs2.1210

Fargione, J. E., Bassett, S., Boucher, T., Bridgham, S. D., Conant, R. T., Cook-Patton, S. C., Ellis, P. W., Falcucci, A., Fourqurean, J. W., Gopalakrishna, T., Gu, H., Henderson, B., Hurteau, M. D., Kroeger, K. D., Kroeger, T., Lark, T. J., Leavitt, S. M., Lomax, G., McDonald, R. I., … Griscom, B. W. (2018). Natural climate solutions for the United States. *Science Advances*, *4*(11), eaat1869. https://doi.org/10.1126/sciadv.aat1869

Fellows, A. W., & Goulden, M. L. (2008). Has fire suppression increased the amount of carbon stored in western U.S. forests? *Geophysical Research Letters*, *35*(12), L12404. https://doi.org/10.1029/2008GL033965

Fernández, M., Hamilton, H. H., & Kueppers, L. M. (2015). Back to the future: Using historical climate variation to project near-term shifts in habitat suitable for coast redwood. *Global Change Biology*, *21*(11), 4141–4152. https://doi.org/10.1111/gcb.13027

Ferraro, P. J., Hanauer, M. M., & Sims, K. R. E. (2011). Conditions associated with protected

area success in conservation and poverty reduction. Proceedings of the National Academy of Sciences of the United States of America, 108(34), 13913–13918. https://doi.org/10.1073/pnas.1011529108

Fettig, C. J., Mortenson, L. A., Bulaon, B. M., & Foulk, P. B. (2019). Tree mortality following drought in the central and southern Sierra Nevada, California, U.S. *Forest Ecology and Management*, *432*, 164–178. https://doi.org/https://doi.org/10.1016/j.foreco.2018.09.006

Fick, S. E., & Hijmans, R. J. (2017). WorldClim 2: new 1-km spatial resolution climate surfaces for global land areas. *International Journal of Climatology*, *37*(12), 4302–4315. https://doi.org/10.1002/joc.5086

Finney MA (1998) FARSITE: Fire Area Simulator-Model development and evaluation. USDA Forest Service, Rocky Mountain Research Station, Research Paper RMRS-RP-4. (Ogden, UT, USA)

Finney MA, Grenfell IC, McHugh CW, Seli RC, Trethewey D, Stratton RD, Brittain S (2011) A method for ensemble wildland fire simulation. *Environmental Modeling and Assessment* 16, 153–167. doi:10.1007/ S10666-010-9241-3

Finney, M. A., Cohen, J. D., McAllister, S. S., & Jolly, W. M. (2012). On the need for a theory of wildland fire spread. *International Journal of Wildland Fire*, 22(1), 25-36.

Fisher, R. A., Koven, C. D., Anderegg, W. R. L., Christoffersen, B. O., Dietze, M. C., Farrior, C. E., et al. (2018). Vegetation demographics in Earth System Models: A review of progress and priorities. *Global Change Biology*, *24*(1), 35–54. https://doi.org/10.1111/gcb.13910

Flanner MG, Zender CS, Randerson JT, Rasch PJ (2007) Present-day climate forcing and response from black carbon in snow. *Journal of Geophysical Research – D. Atmospheres* 112, D11202. doi:10.1029/ 2006JD008003

Flannigan MD, Logan KA, Amiro BD, Skinner WR, Stocks BJ (2005) Future area burned in Canada. *Climatic Change* 72, 1–16. doi:10.1007/ S10584-005-5935-Y

Forestry Canada Fire Danger Group (1992) Development and structure of the Canadian forest fire behavior prediction system. Forestry Canada, Science and Sustainable Development Directorate, Information Report ST-X-3. (Ottawa, ON, Canada)

Foster, A. C., Armstrong, A. H., Shuman, J. K., Shugart, H. H., Rogers, B. M., Mack, M. C., et al. (2019). Importance of tree- and species-level interactions with wildfire, climate, and soils in interior Alaska: Implications for forest change under a warming climate. *Ecological Modelling*, *409*(March), 108765. https://doi.org/10.1016/j.ecolmodel.2019.108765

FRAP. (2019). California Department of Forestry - Fire and Resource Assessment Program GIS database of fire perimeter polygons. Retrieved April 1, 2021, from https://frap.fire.ca.gov/frap-projects/fire-perimeters/

French NHF, Jenkins LK, Loboda TV, Flannigan M, Jandt R, BourgeauChavez LL, Whitley M (2015) Fire in arctic tundra of Alaska: past fire activity, future fire potential, and significance for land management and ecology. *International Journal of Wildland Fire* 24, 1045–1061. doi:10. 1071/WF14167

Friedlingstein, P., Jones, M. W., O'Sullivan, M., Andrew, R. M., Hauck, J., Peters, G. P., et al. (2019). Global carbon budget 2019. *Earth System Science Data*, *11*(4), 1783–1838. https://doi.org/10.5194/essd-11-1783-2019

Galik, C. S., & Jackson, R. B. (2009). Risks to forest carbon offset projects in a changing climate. *Forest Ecology and Management*, *257*(11), 2209–2216. https://doi.org/10.1016/j.foreco.2009.03.017

Gardner, T. (2021, November 5). U.S. sets goal to drive down cost of removing CO2 from atmosphere. *Reuters*. https://www.reuters.com/business/cop/us-sets-goal-drive-down-cost-removing-co2-atmosphere-2021-11-05/

General Requirements for ARB Offset Credits and Registry Offset Credits, 17 California Code of Regulations (CCR) § 95970 (2012). https://govt.westlaw.com/calregs/Document/I222DEBA09A3011E4A28EDDF568E2F8A2?viewType=FullText&originationContext=documenttoc&transitionType=DocumentItem&contextData=%28sc.Default%29&bhcp=1

Gesch DB, Verdin KL, Greenlee SK (1999) New land surface digital elevation model covers the Earth. *Eos* 80, 69–71. doi:10.1029/ 99EO00050

Giglio L, Schroeder W, Justice CO (2016) The collection 6 MODIS active fire detection algorithm and fire products. *Remote Sensing of Environment* 178, 31–41. doi:10.1016/J.RSE.2016.02.054

Gómez-Pineda, E., Sáenz-Romero, C., Ortega-Rodríguez, J. M., Blanco-García, A., Madrigal-Sánchez, X., Lindig-Cisneros, R., et al. (2020). Suitable climatic habitat changes for Mexican conifers along altitudinal gradients under climatic change scenarios. *Ecological Applications*, *30*(2), 1–17. https://doi.org/10.1002/eap.2041

Gonzalez, P., Battles, J. J., Collins, B. M., Robards, T., & Saah, D. S. (2015). Aboveground live carbon stock changes of California wildland ecosystems, 2001-2010. *Forest Ecology and Management*, *348*, 68–77. https://doi.org/10.1016/j.foreco.2015.03.040

Gorelick, N., Hancher, M., Dixon, M., Ilyushchenko, S., Thau, D., & Moore, R. (2017). Google Earth Engine: Planetary-scale geospatial analysis for everyone. *Remote Sensing of Environment*, *202*, 18–27. https://doi.org/10.1016/j.rse.2017.06.031

Goulden, M. L., & Bales, R. C. (2019). California forest die-off linked to multi-year deep soil drying in 2012–2015 drought. *Nature Geoscience*, *12*(8), 632–637. https://doi.org/10.1038/s41561-019-0388-5

Griscom, B. W., Adams, J., Ellis, P. W., Houghton, R. A., Lomax, G., Miteva, D. A., et al. (2017).

Natural climate solutions. *Proceedings of the National Academy of Sciences of the United States of America*, *114*(44), 11645–11650. https://doi.org/10.1073/pnas.1710465114

Gutierrez, A. A., Hantson, S., Langenbrunner, B., Chen, B., Jin, Y., Goulden, M. L., & Randerson, J. T. (2021). Wildfire response to changing daily temperature extremes in California's Sierra Nevada. *Science Advances*, *7*(47), eabe6417. https://doi.org/10.1126/sciadv.abe6417

Hampe, A. (2004). Bioclimate envelope models: what they detect and what they hide. *Global Ecology and Biogeography*, *13*(5), 469–476.

Hantson, S., Andela, N., Goulden, M. L., & Randerson, J. T. (2022). Human-ignited fires result in more extreme fire behavior and ecosystem impacts. *Nature Communications*, *13*(1), 2717. https://doi.org/10.1038/s41467-022-30030-2

Hao WM, Petkov A, Nordgren BL, Corley RE, Silverstein RP, Urbanski SP, Evangeliou N, Balkanski Y, Kinder BL (2016) Daily black carbon emissions from fires in northern Eurasia for 2002–2015. *Geoscientific Model Development* 9, 4461–4474. doi:10.5194/GMD-9-4461-2016

Harris, I., Jones, P. D., Osborn, T. J., & Lister, D. H. (2014). Updated high-resolution grids of monthly climatic observations - the CRU TS3.10 Dataset. *International Journal of Climatology*, *34*(3), 623–642. https://doi.org/10.1002/joc.3711

Hausfather, Z., Marvel, K., Schmidt, G. A., Nielsen-Gammon, J. W., & Zelinka, M. (2022, May 4). *Climate simulations: recognize the "hot model" problem*. Nature Publishing Group UK; nature.com. https://doi.org/10.1038/d41586-022-01192-2

Haya, B., Cullenward, D., Strong, A. L., Grubert, E., Heilmayr, R., Sivas, D. A., & Wara, M. (2020). Managing uncertainty in carbon offsets: insights from California's standardized approach. *Climate Policy*, *20*(9), 1112–1126. https://doi.org/10.1080/14693062.2020.1781035

Higgins, S. I., Clark, J. S., Nathan, R., Hovestadt, T., Schurr, F. M., Fragoso, J. M. V, et al. (2003). Forecasting plant migration rates: managing uncertainty for risk assessment. *Journal of Ecology*, *91*, 341–347.

Hijmans, R. J., & Graham, C. H. (2006). The ability of climate envelope models to predict the effect of climate change on species distributions. *Global Change Biology*, *12*, 2272–2281. https://doi.org/10.1111/j.1365-2486.2006.01256.x

Holdridge, L. R. (1947). Determination of World Plant Formations From Simple Climatic Data. *Science*, *105*(2727), 367–368. https://doi.org/10.1126/science.105.2727.367

Homer, C., Dewitz, J., Jin, S., Xian, G., Costello, C., Danielson, P., et al. (2020). Conterminous United States land cover change patterns 2001–2016 from the 2016 National Land Cover Database. *ISPRS Journal of Photogrammetry and Remote Sensing*, *13*, 025004. https://doi.org/10.1016/j.isprsjprs.2020.02.019

Huntley, B. (1991). How plants respond to climate change: Migration rates, individualism and the consequences for plant communities. *Annals of Botany*, *67*, 15–22.

Hurteau, M. D., Westerling, A. L., Wiedinmyer, C., & Bryant, B. P. (2014). Projected Effects of Climate and Development on California Wildfire Emissions through 2100. In *Environmental Science & Technology* (p. 140203132416003). https://doi.org/10.1021/es4050133

Iverson, L. R., Prasad, A. M., & Liaw, A. (2004). New machine learning tools for predictive vegetation mapping after climate change: Bagging and Random Forest perform better than regression tree analysis. In Smithers & Richard (Eds.), *Landscape ecology of trees and forests, proceedings of the twelfth annual IALE conference* (pp. 317–320). Cirencester, UK. Retrieved from https://lib.unnes.ac.id/17153/1/1201408017.pdf

Jackson, S. T., Betancourt, J. L., Booth, R. K., & Gray, S. T. (2009). Ecology and the ratchet of events: Climate variability, niche dimensions, and species distributions. *Proceedings of the National Academy of Sciences of the United States of America*, *106*(suppl. 2), 19685–19692. https://doi.org/10.1073/pnas.0901644106

Jiang, M., Medlyn, B. E., Drake, J. E., Duursma, R. A., Anderson, I. C., Barton, C. V. M., et al. (2020). The fate of carbon in a mature forest under carbon dioxide enrichment. *Nature*, *580*(7802), 227–231. https://doi.org/10.1038/s41586-020-2128-9

Jin, Y., Goulden, M. L., Faivre, N., Veraverbeke, S., Sun, F., Hall, A., Hand, M. S., Hook, S., & Randerson, J. T. (2015). Identification of two distinct fire regimes in Southern California: implications for economic impact and future change. *Environmental Research Letters: ERL [Web Site]*, *10*(9), 094005. https://iopscience.iop.org/article/10.1088/1748-9326/10/9/094005/meta

Johnston FH, Bailie RS, Pilotto LS, Hanigan IC (2007) Ambient biomass smoke and cardio-respiratory hospital admissions in Darwin, Australia. *BMC Public Health* 7, 240. doi:10.1186/1471-2458-7-240

Johnston FH, Henderson SB, Chen Y, Randerson JT, Marlier M, DeFries RS, Kinney P, Bowman DMJS, Brauer M (2012) Estimated global mortality attributable to smoke from landscape fires. *Environmental Health Perspectives* 120, 695–701. doi:10.1289/EHP.1104422

Johnstone, J. A., & Dawson, T. E. (2010). Climatic context and ecological implications of summer fog decline in the coast redwood region. *Proceedings of the National Academy of Sciences of the United States of America*, *107*(10), 4533–4538. https://doi.org/10.1073/pnas.0915062107

Juang, C. S., Williams, A. P., Abatzoglou, J. T., Balch, J. K., Hurteau, M. D., & Moritz, M. A. (2022). Causes of exponentially increasing burned area with rising aridity in the Western United States. *In Review at Geophysical Research Letters*.

Kaarakka, L., Cornett, M., Domke, G., Ontl, T., & Dee, L. E. (2021). Improved forest

management as a natural climate solution: A review. *Ecological Solutions and Evidence*, *2*(3). https://doi.org/10.1002/2688-8319.12090

Kasischke ES, Turetsky MR (2006) Recent changes in the fire regime across the North American boreal region – spatial and temporal patterns of burning across Canada and Alaska. *Geophysical Research Letters* 33, L09703. doi:10.1029/2006GL025677

Kasischke ES, Verbyla DL, Rupp TS, McGuire AD, Murphy KA, Jandt R, Barnes JL, Hoy EE, Duffy PA, Calef M, Turetsky MR (2010) Alaska's changing fire regime – implications for the vulnerability of its boreal forests. *Canadian Journal of Forest Research* 40, 1313–1324. doi:10. 1139/X10-098

Kasischke ES, Williams D, Barry D (2002) Analysis of the patterns of large fires in the boreal forest region of Alaska. *International Journal of Wildland Fire* 11, 131–144. doi:10.1071/WF02023

Kearney, M. R., Wintle, B. A., & Porter, W. P. (2010). Correlative and mechanistic models of species distribution provide congruent forecasts under climate change. *Conservation Letters*, *3*(3), 203–213. https://doi.org/10.1111/j.1755-263X.2010.00097.x

Keenan, T., Maria Serra, J., Lloret, F., Ninyerola, M., & Sabate, S. (2011). Predicting the future of forests in the Mediterranean under climate change, with niche- and process-based models: CO2 matters! *Global Change Biology*, *17*(1), 565–579. https://doi.org/10.1111/j.1365-2486.2010.02254.x

Kelly, A. E., & Goulden, M. L. (2008). Rapid shifts in plant distribution with recent climate change. *Proceedings of the National Academy of Sciences of the United States of America*, *105*(33), 11823–11826. https://doi.org/10.1073/pnas.0802891105

Kennedy, R. E., Ohmann, J., Gregory, M., Roberts, H., Yang, Z., Bell, D. M., et al. (2018). An empirical, integrated forest biomass monitoring system. *Environmental Research Letters*, *13*(2), 025004. https://doi.org/10.1088/1748-9326/aa9d9e

Kennedy, R. E., Yang, Z., & Cohen, W. B. (2010). Detecting trends in forest disturbance and recovery using yearly Landsat time series: 1. LandTrendr - Temporal segmentation algorithms. Remote Sensing of Environment, 114(12), 2897–2910. https://doi.org/10.1016/j.rse.2010.07.008

Koven, C. D. (2013). Boreal carbon loss due to poleward shift in low-carbon ecosystems. *Nature Geoscience*, *6*(6), 452–456. https://doi.org/10.1038/ngeo1801

Krawchuk MA, Cumming SG, Flannigan MD (2009) Predicted changes in fire weather suggest increases in lightning fire initiation and future area burned in the mixedwood boreal forest. *Climatic Change* 92, 83–97. doi:10.1007/S10584-008-9460-7

Lalonde, S. J., Mach, K. J., Anderson, C. M., Francis, E. J., Sanchez, D. L., Stanton, C. Y., et al. (2018). Forest management in the Sierra Nevada provides limited carbon storage potential: an expert elicitation. *Ecosphere*, *9*(7), e02321.

https://doi.org/10.1002/ecs2.2321

Lauvaux, C. A., Skinner, C. N., & Taylor, A. H. (2016). High severity fire and mixed conifer forest-chaparral dynamics in the southern Cascade Range, USA. *Forest Ecology and Management*, *363*, 74–85. https://doi.org/10.1016/j.foreco.2015.12.016

Lenihan, J. M., Bachelet, D., Neilson, R. P., & Drapek, R. (2008a). Response of vegetation distribution, ecosystem productivity, and fire to climate change scenarios for California. *Climatic Change*, *87*, 215–230. https://doi.org/10.1007/s10584-007-9362-0

Lenihan, J. M., Bachelet, D., Neilson, R. P., & Drapek, R. (2008b). Simulated response of conterminous United States ecosystems to climate change at different levels of fire suppression, CO2 emission rate, and growth response to CO2. *Global and Planetary Change*, *64*, 16–25. https://doi.org/10.1016/j.gloplacha.2008.01.006

Lenihan, J. M., Drapek, R., Bachelet, D., & Neilson, R. P. (2003). Climate change effects on vegetation distribution, carbon, and fire in California. *Ecological Applications*, *13*(6), 1667–1681. https://doi.org/10.1890/025295

Li, S., & Banerjee, T. (2021). Spatial and temporal pattern of wildfires in California from 2000 to 2019. *Scientific Reports*, *11*(1), 8779. https://doi.org/10.1038/s41598-021-88131-9

Li, S., Dao, V., Kumar, M., Nguyen, P., & Banerjee, T. (2022). Mapping the wildland-urban interface in California using remote sensing data. *Scientific Reports*, *12*(1), 5789. https://doi.org/10.1038/s41598-022-09707-7

Linn, R., Reisner, J., Colman, J. J., & Winterkamp, J. (2002). Studying wildfire behavior using FIRETEC. *International Journal of Wildland Fire*, *11*(4), 233–246. https://doi.org/10.1071/wf02007

Liu JC, Wilson A, Mickley LJ, Dominici F, Ebisu K, Wang Y, Sulprizio MP, Peng RD, Yue X, Son JY, Anderson GB, Bell ML (2017) Wildfire-specific fine particulate matter and risk of hospital admissions in urban and rural counties. *Epidemiology* 28, 77–85. doi:10.1097/EDE. 0000000000000556

Liu Z, Ballantyne AP, Cooper LA (2019) Biophysical feedback of global forest fires on surface temperature. *Nature Communications* 10, 214. doi:10.1038/S41467-018-08237-Z

Liu Z, Wimberly MC (2016) Direct and indirect effects of climate change on projected future fire regimes in the western United States. *The Science of the Total Environment* 542, 65–75. doi:10.1016/J.SCITOTENV.2015. 10.093

Liu Z, Yang J, Chang Y, Weisberg PJ, He HS (2012) Spatial patterns and drivers of fire occurrence and its future trend under climate change in a boreal forest of Northeast China. *Global Change Biology* 18, 2041– 2056. doi:10.1111/J.1365-2486.2012.02649.X

Loarie, S. R., Carter, B. E., Hayhoe, K., McMahon, S., Moe, R., Knight, C. A., & Ackerly, D. D. (2008). Climate change and the future of California's endemic flora. *PLoS ONE*, *3*(6), e2502. https://doi.org/10.1371/journal.pone.0002502

Loarie, S. R., Duffy, P. B., Hamilton, H., Asner, G. P., Field, C. B., & Ackerly, D. D. (2009). The velocity of climate change. *Nature*, *462*(7276), 1052–1055. https://doi.org/10.1038/nature08649

Luo, Y., Su, B., Currie, W. S., Dukes, J. S., Finzi, A., Hartwig, U., et al. (2004). Progressive nitrogen limitation of ecosystem responses to rising atmospheric carbon dioxide. *BioScience*, *54*(8), 731–739. https://doi.org/10.1641/0006-3568(2004)054[0731:PNLOER]2.0.CO;2

Lynch JA, Clark JS, Bigelow NH, Edwards ME, Finney BP (2002) Geographic and temporal variations in fire history in boreal ecosystems of Alaska. *Journal of Geophysical Research* 107, FFR8-1–FFR8-17. doi:10.1029/2001JD000332

Macaulay, L., & Butsic, V. (2017). Ownership characteristics and crop selection in California cropland. *California Agriculture*, *71*(4), 221–230. https://doi.org/10.3733/ca.2017a0041

Madakumbura, G. D., Goulden, M. L., Hall, A., Fu, R., Moritz, M. A., Koven, C. D., et al. (2020). Recent California tree mortality portends future increase in drought-driven forest die-off. *Environmental Research Letters*, *15*, 124040. https://doi.org/10.1088/1748-9326/abc719

Mahony, C. R., Cannon, A. J., Wang, T., & Aitken, S. N. (2017). A closer look at novel climates: new methods and insights at continental to landscape scales. *Global Change Biology*, *23*(9), 3934–3955. https://doi.org/10.1111/gcb.13645

Mann, M. L., Batllori, E., Moritz, M. A., Waller, E. K., Berck, P., Flint, A. L., Flint, L. E., & Dolfi, E. (2016). Incorporating Anthropogenic Influences into Fire Probability Models: Effects of Human Activity and Climate Change on Fire Activity in California. *PloS One*, *11*(4), e0153589. https://doi.org/10.1371/journal.pone.0153589

Masek, J. G., Wulder, M. A., Markham, B., McCorkel, J., Crawford, C. J., Storey, J., & Jenstrom, D. T. (2020). Landsat 9: Empowering open science and applications through continuity. *Remote Sensing of Environment*, *248*, 111968. https://doi.org/10.1016/j.rse.2020.111968

Maurer, E. P., Brekke, L., Pruitt, T., & Duffy, P. B. (2007). Fine-resolution climate projections enhance regional climate change impact studies. *Eos, Transactions American Geophysical Union*, *88*(47), 504. https://doi.org/https://doi.org/10.1029/2007EO470006

McDowell, N. G., Allen, C. D., Anderson-Teixeira, K., Aukema, B. H., Bond-Lamberty, B., Chini, L., et al. (2020). Pervasive shifts in forest dynamics in a changing world. *Science*, *368*(6494). https://doi.org/10.1126/science.aaz9463

McIntyre, P. J., Thorne, J. H., Dolanc, C. R., Flint, A. L., Flint, L. E., Kelly, M., & Ackerly, D. D. (2015). Twentieth-century shifts in forest structure in California: Denser forests, smaller trees, and increased dominance of oaks. *Proceedings of the National Academy of Sciences of the United States of America*, *112*(5), 1458–1463. https://doi.org/10.1073/pnas.1410186112

McLachlan, J. S., Hellmann, J. J., & Schwartz, M. W. (2007). A framework for debate of assisted migration in an era of climate change. *Conservation Biology*, *21*(2), 297–302. https://doi.org/10.1111/j.1523-1739.2007.00676.x

McNab, W. H., Cleland, D. T., Freeouf, J. A., Keys, J. E., Nowacki, G. J., & Carpenter, C. (2007). Description of ecological subregions: sections of the conterminous United States. *General Technical Report WO-76B*, *76*, 1–82. https://www.fs.usda.gov/treesearch/pubs/48669

Millar, C. I., & Stephenson, N. L. (2015). Temperate forest health in an era of emerging megadisturbance. *Science*, *349*(6250), 823–826. https://doi.org/10.1126/science.aaa9933

Miller E (2019) Moisture sorption models for fuel beds of standing dead grass in Alaska. *Fire* 2, 2. doi:10.3390/FIRE2010002

Minx, J. C., Lamb, W. F., & Callaghan, M. W. (2018). Negative emissions—Part 1: Research landscape and synthesis. *The Environmentalist*, *13*(6). https://iopscience.iop.org/article/10.1088/1748-9326/aabf9b/meta

Morgan, T. A., Keegan, C. E., Dillon, T., Chase, A. L., Fried, J. S., & Weber, M. N. (2004). California's forest products industry: A descriptive analysis (Vol. 615). U.S. Department of Agriculture, Pacific Northwest Research Station. https://www.fs.fed.us/pnw/pubs/pnw_gtr615.pdf

Morin, X., & Thuiller, W. (2009). Comparing niche- and process-based models to reduce prediction uncertainty in species range shifts under climate change. *Ecology*, *90*(5), 1301–1313. https://doi.org/10.1890/08-0134.1

Mouteva GO, Czimczik CI, Fahrni SM, Wiggins EB, Rogers BM, Veraverbeke S, Xu X, Santos GM, Henderson J, Miller CE, Randerson JT (2015) Black carbon aerosol dynamics and isotopic composition in Alaska linked with boreal fire emissions and depth of burn in organic soils. *Global Biogeochemical Cycles* 29, 1977–2000. doi:10.1002/2015GB005247

Murray, B. C., Sohngen, B., & Ross, M. T. (2007). Economic consequences of consideration of permanence, leakage and additionality for soil carbon sequestration projects. *Climatic Change*, *80*(1), 127–143. https://doi.org/10.1007/s10584-006-9169-4

Needham, J. F., Chambers, J., Fisher, R., Knox, R., & Koven, C. D. (2020). Forest responses to simulated elevated CO2 under alternate hypotheses of size- and age-dependent mortality. *Global Change Biology*, *26*, 5734–5753.

https://doi.org/10.1111/gcb.15254

Neilson, R. P., Pitelka, L. F., Solomon, A. M., Nathan, R., Midgley, G. F., Fragoso, J. M. V., et al. (2005). Forecasting regional to global plant migration in response to climate change. *BioScience*, *55*(9), 749–759. https://doi.org/10.1641/0006-3568(2005)055[0749:FRTGPM]2.0.CO;2

Ohmann, J. L., & Gregory, M. J. (2002). Predictive mapping of forest composition and structure with direct gradient analysis and nearest- neighbor imputation in coastal Oregon, U.S.A. *Canadian Journal of Forest Research. Journal Canadien de La Recherche Forestiere*, *32*(4), 725–741. https://doi.org/10.1139/x02-011

Parisien MA, Parks SA, Krawchuk MA, Flannigan MD, Bowman LM, Moritz MA (2011a) Scale-dependent controls on the area burned in the boreal forest of Canada, 1980–2005. *Ecological Applications* 21, 789–805. doi:10.1890/10-0326.1

Parisien MA, Parks SA, Krawchuk MA, Little JM, Flannigan MD, Gowman LM, Moritz MA (2014) An analysis of controls on fire activity in boreal Canada: comparing models built with different temporal resolutions. *Ecological Applications* 24, 1341–1356. doi:10.1890/ 13-1477.1

Parisien MA, Parks SA, Miller C, Krawchuk MA, Heathcott M, Moritz MA (2011b) Contributions of ignitions, fuels, and weather to the spatial patterns of burn probability of a boreal landscape. *Ecosystems* 14, 1141–1155. doi:10.1007/S10021-011-9474-2

Pedregosa F, Varoquaux G, Gramfort A, Michel V, Thirion B, Grisel O, Blondel M, Prettenhofer P, Weiss R, Dubourg V, Vanderplas J, Passos A, Cournapeau D, Brucher M, Perrot M, Duchesnay E (2011) Scikit-learn: machine learning in Python. *Journal of Machine Learning Research* 12, 2825–2830.

Pedregosa, F., Varoquaux, G., Gramfort, A., Michel, V., Thirion, B., Grisel, O., et al. (2011). Scikit-learn: Machine Learning in Python. *Journal of Machine Learning Research*, *12*, 2825–2830.

Phillips, S. J., Anderson, R. P., & Schapire, R. E. (2006). Maximum entropy modeling of species geographic distributions. *Ecological Modelling*, *6*(190), 231–259. https://doi.org/10.1016/j.ecolmodel.2005.03.026

Prasad, A. M., Iverson, L. R., & Liaw, A. (2006). Newer classification and regression tree techniques: Bagging and random forests for ecological prediction. *Ecosystems* , *9*(2), 181–199. https://doi.org/10.1007/s10021-005-0054-1

Preisler HK, Burgan RE, Eidenshink JC, Klaver JM, Klaver RW (2009) Forecasting distributions of large federal-lands fires utilizing satellite and gridded weather information. *International Journal of Wildland Fire* 18, 508–516. doi:10.1071/WF08032

Prentice, K. C., & Fung, I. Y. (1990). The sensitivity of terrestrial carbon storage to climate

change. *Nature*, *346*(6279), 48–51. https://doi.org/10.1038/346048a0

Psarras, P., Krutka, H., Fajardy, M., Zhang, Z., Liguori, S., Dowell, N. M., & Wilcox, J. (2017). Slicing the pie: how big could carbon dioxide removal be? *Wiley Interdisciplinary Reviews Energy and Environment*, *6*(5), e253. https://doi.org/10.1002/wene.253

Randerson JT, Liu H, Flanner MG, Chambers SD, Jin Y, Hess PG, Pfister G, Mack MC, Treseder KK, Welp LR, Chapin FS, Harden JW, Goulden ML, Lyons E, Neff JC, Schuur EAG, Zender CS (2006) The impact of boreal forest fire on climate warming. *Science* 314, 1130–1132. doi:10.1126/SCIENCE.1132075

Rehfeldt, G. E., Crookston, N. L., Sáenz-Romero, C., & Campbell, E. M. (2012). North American vegetation model for land-use planning in a changing climate: A solution to large classification problems. *Ecological Applications*, *22*(1), 119–141. https://doi.org/10.1890/11-0495.1

Reise, J., Siemons, A., Böttcher, H., Herold, A., Urrutia, C., & Schneider, L. (2022). *Nature-based solutions and global climate protection*. German Environment Agency. https://www.umweltbundesamt.de/sites/default/files/medien/1410/publikationen/2022-01-03_climate-change_01-2022_potential_nbs_policy_paper_final.pdf

Roe, S., Streck, C., Obersteiner, M., Frank, S., Griscom, B., Drouet, L., et al. (2019). Contribution of the land sector to a 1.5 °C world. *Nature Climate Change*, *9*(11), 817–828. https://doi.org/10.1038/s41558-019-0591-9

Rogers BM, Randerson JT, Bonan GB (2013) High-latitude cooling associated with landscape changes from North American boreal forest fires. *Biogeosciences* 10, 699–718. doi:10.5194/BG-10-699-2013

Rogers BM, Soja AJ, Goulden ML, Randerson JT (2015) Influence of tree species on continental differences in boreal fires and climate feedbacks. *Nature Geoscience* 8, 228–234. doi:10.1038/NGEO2352

Rogers, B. M., Jantz, P., & Goetz, S. J. (2017). Vulnerability of eastern US tree species to climate change. *Global Change Biology*, *23*(8), 3302–3320. https://doi.org/10.1111/gcb.13585

Rogers, B. M., Neilson, R. P., Drapek, R., Lenihan, J. M., Wells, J. R., Bachelet, D., & Law, B. E. (2011). Impacts of climate change on fire regimes and carbon stocks of the U.S. Pacific Northwest. *Journal of Geophysical Research: Biogeosciences*, *116*(3), G03037. https://doi.org/10.1029/2011JG001695

Rollins MG (2009) LANDFIRE: a nationally consistent vegetation, wildland fire, and fuel assessment. *International Journal of Wildland Fire* 18, 235–249. doi:10.1071/WF08088

Romps DM, Seeley JT, Vollaro D, Molinari J (2014) Projected increase in lightning strikes in the United States due to global warming. *Science* 346, 851–854. doi:10.1126/SCIENCE.1259100

Rother, M. T., & Veblen, T. T. (2016). Limited conifer regeneration following wildfires in dry ponderosa pine forests of the Colorado Front Range. *Ecosphere*, *7*(12), e01594. https://doi.org/10.1002/ecs2.1594

Rothermel, R. C. (1972). A mathematical model for predicting fire spread in wildland fuels (Vol. 115). Intermountain Forest & Range Experiment Station, Forest Service, US Department of Agriculture.

Sand M, Berntsen TK, Von Salzen K, Flanner MG, Langner J, Victor DG (2016) Response of Arctic temperature to changes in emissions of shortlived climate forcers. *Nature Climate Change* 6, 286–289. doi:10.1038/NCLIMATE2880

Sangermano, F., Toledano, J., & Eastman, J. R. (2012). Land cover change in the Bolivian Amazon and its implications for REDD+ and endemic biodiversity. Landscape Ecology, 27(4), 571–584. https://doi.org/10.1007/s10980-012-9710-y

Sangermano, F., Toledano, J., & Eastman, J. R. (2012). Land cover change in the Bolivian Amazon and its implications for REDD+ and endemic biodiversity. *Landscape Ecology*, *27*(4), 571–584. https://doi.org/10.1007/s10980-012-9710-y

Santoro, M., & Cartus, O. (2019). ESA Biomass Climate Change Initiative (Biomass_cci): Global datasets of forest above-ground biomass for the year 2017, v1. Centre for Environmental Data Analysis. https://doi.org/http://dx.doi.org/10.5285/bedc59f37c9545c981a839eb552e4084

Savage, M., & Mast, J. N. (2005). How resilient are southwestern ponderosa pine forests after crown fires? *Canadian Journal of Forest Research*, *35*(4), 967–977.

Sedano F, Randerson JT (2014). Multi-scale influence of vapor pressure deficit on fire ignition and spread in boreal forest ecosystems. *Biogeosciences* 11, 3739–3755. doi:10.5194/BG-11-3739-2014

Seddon, N., Chausson, A., Berry, P., Girardin, C. A. J., Smith, A., & Turner, B. (2020). Understanding the value and limits of nature-based solutions to climate change and other global challenges. *Philosophical Transactions of the Royal Society of London. Series B, Biological Sciences*, *375*(1794), 20190120. https://doi.org/10.1098/rstb.2019.0120

Settele, J., Scholes, R., Betts, R. A., Bunn, S., Leadley, P., Nepstad, D., et al. (2015). Terrestrial and inland water systems. In *Climate change 2014 impacts, adaptation and vulnerability: Part A: Global and sectoral aspects* (pp. 271–360). Cambridge University Press.

Shive, K. L., Wuenschel, A., Hardlund, L. J., Morris, S., Meyer, M. D., & Hood, S. M. (2022). Ancient trees and modern wildfires: Declining resilience to wildfire in the highly fire-adapted giant sequoia. *Forest Ecology and Management*, *511*, 120110. https://doi.org/10.1016/j.foreco.2022.120110

Sleeter, B. M., Marvin, D. C., Cameron, D. R., Selmants, P. C., Westerling, A. L. R., Kreitler, J., et

al. (2019). Effects of 21st-century climate, land use, and disturbances on ecosystem carbon balance in California. *Global Change Biology*, *25*(10), 3334–3353. https://doi.org/10.1111/gcb.14677

Smith, P., Davis, S. J., Creutzig, F., Fuss, S., Minx, J., Gabrielle, B., Kato, E., Jackson, R. B., Cowie, A., Kriegler, E., van Vuuren, D. P., Rogelj, J., Ciais, P., Milne, J., Canadell, J. G., McCollum, D., Peters, G., Andrew, R., Krey, V., … Yongsung, C. (2016). Biophysical and economic limits to negative CO2 emissions. *Nature Climate Change*, *6*(1), 42–50. https://doi.org/10.1038/nclimate2870

Solomon, A. M. (1997). Natural migration rates of trees: Global terrestrial carbon cycle implications BT - Past and Future Rapid Environmental Changes. In B. Huntley, W. Cramer, A. V Morgan, H. C. Prentice, & J. R. M. Allen (Eds.) (pp. 455–468). Berlin, Heidelberg: Springer Berlin Heidelberg.

Song, L., & Temple, J. (2021, May 10). A Nonprofit Promised to Preserve Wildlife. Then It Made Millions Claiming It Could Cut Down Trees. *ProPublica and MIT Technology Review*. https://www.propublica.org/article/a-nonprofit-promised-to-preserve-wildlife-then-it-made-millions-claiming-it-could-cut-down-trees

Sperry, J. S., Venturas, M. D., Todd, H. N., Trugman, A. T., Anderegg, W. R. L., Wang, Y., & Tai, X. (2019). The impact of rising CO2 and acclimation on the response of US forests to global warming. *Proceedings of the National Academy of Sciences of the United States of America*, *116*(51), 25734–25744. https://doi.org/10.1073/pnas.1913072116

Spracklen, D. V., Mickley, L. J., Logan, J. A., Hudman, R. C., Yevich, R., Flannigan, M. D., & Westerling, A. L. (2009). Impacts of climate change from 2000 to 2050 on wildfire activity and carbonaceous aerosol concentrations in the western United States. *Journal of Geophysical Research*, *114*(D20). https://doi.org/10.1029/2008jd010966

Steel, Z. L., Safford, H. D., & Viers, J. H. (2015). The fire frequency-severity relationship and the legacy of fire suppression in California forests. *Ecosphere* , *6*(1), 1–23. https://doi.org/10.1890/es14-00224.1

Stephenson, N. L., Das, A. J., Ampersee, N. J., Bulaon, B. M., & Yee, J. L. (2019). Which trees die during drought? The key role of insect host-tree selection. *Journal of Ecology*, *107*(5), 2383–2401. https://doi.org/10.1111/1365-2745.13176

Stovall, A. E. L., Shugart, H., & Yang, X. (2019). Tree height explains mortality risk during an intense drought. *Nature Communications*, *10*(1), 1–6. https://doi.org/10.1038/s41467-019-12380-6

Stuart, E. A. (2010). Matching methods for causal inference: A review and a look forward. Statistical Science: A Review Journal of the Institute of Mathematical Statistics, 25(1), 1–21. https://doi.org/10.1214/09-STS313

Svenning, J. C., & Sandel, B. (2013). Disequilibrium vegetation dynamics under future

climate change. *American Journal of Botany*, 100(7), 1266-1286.

Swain, D. L., Langenbrunner, B., Neelin, J. D., & Hall, A. (2018). Increasing precipitation volatility in twenty-first-century California. *Nature Climate Change*, *8*(5), 427–433. https://doi.org/10.1038/s41558-018-0140-y

Swann, A. L. S., Hoffman, F. M., Koven, C. D., & Randerson, J. T. (2016). Plant responses to increasing CO2 reduce estimates of climate impacts on drought severity. *Proceedings of the National Academy of Sciences of the United States of America*, *113*(36), 10019–10024. https://doi.org/10.1073/pnas.1604581113

Tang, H., Ma, L., Lister, A., & O'Neill-Dunne, J. (2021). High-resolution forest carbon mapping for climate mitigation baselines over the RGGI region, USA. *The Environmentalist*, *16*(3). https://iopscience.iop.org/article/10.1088/1748-9326/abd2ef/meta

Tang, X., Bullock, E. L., Olofsson, P., Estel, S., & Woodcock, C. E. (2019). Near real-time monitoring of tropical forest disturbance: New algorithms and assessment framework. *Remote Sensing of Environment*, *224*, 202–218. https://doi.org/10.1016/j.rse.2019.02.003

Tepley, A. J., Thompson, J. R., Epstein, H. E., & Anderson-Teixeira, K. J. (2017). Vulnerability to forest loss through altered postfire recovery dynamics in a warming climate in the Klamath Mountains. *Global Change Biology*, *23*(10), 4117–4132. https://doi.org/10.1111/gcb.13704

Tetens O (1930) Uber einige meteorologische Begriffe. Zeitschrift fur Geophysik 6, 297–309.

Thorne, J. H., Choe, H., Boynton, R. M., Bjorkman, J., Whitneyalbright, W., Nydick, K., et al. (2017). The impact of climate change uncertainty on California's vegetation and adaptation management. *Ecosphere*, *8*(12). https://doi.org/10.1002/ecs2.2021

Trugman, A. T., Anderegg, L. D. L., Anderegg, W. R. L., Das, A. J., & Stephenson, N. L. (2021). Why is Tree Drought Mortality so Hard to Predict? *Trends in Ecology and Evolution*, 1–13. https://doi.org/10.1016/j.tree.2021.02.001

Trugman, A. T., Anderegg, L. D. L., Shaw, J. D., & Anderegg, W. R. L. (2020). Trait velocities reveal that mortality has driven widespread coordinated shifts in forest hydraulic trait composition. *Proceedings of the National Academy of Sciences*, *117*(15), 8532–8538. https://doi.org/10.1073/pnas.1917521117

Tubbesing, C. L., York, R. A., Stephens, S. L., & Battles, J. J. (2020). Rethinking fire-adapted species in an altered fire regime. Ecosphere , 11(3). https://doi.org/10.1002/ecs2.3091

van der Werf GR, Randerson JT, Giglio L, Van Leeuwen TT, Chen Y, Rogers BM, Mu M, Van Marle MJE, Morton DC, Collatz GJ, Yokelson RJ, Kasibhatla PS (2017) Global fire emissions estimates during 1997– 2016. *Earth System Science Data* 9, 697–720. doi:10.5194/ESSD-9-697- 2017

Van Wagner CE (1987) Development and structure of the Canadian Forest Fire Weather Index System. Canadian Forestry Service, Petawawa National Forest Institute, Forestry Technical Report 35. (Chalk River, ON, Canada)

Veraverbeke S, Rogers BM, Goulden ML, Jandt RR, Miller CE, Wiggins EB, Randerson JT (2017) Lightning as a major driver of recent large fire years in North American boreal forests. *Nature Climate Change* 7, 529–534. doi:10.1038/NCLIMATE3329

Wamelink, G. W. W., Wieggers, H. J. J., Reinds, G. J., Kros, J., Mol-Dijkstra, J. P., van Oijen, M., & de Vries, W. (2009). Modelling impacts of changes in carbon dioxide concentration, climate and nitrogen deposition on carbon sequestration by European forests and forest soils. *Forest Ecology and Management*, *258*(8), 1794–1805. https://doi.org/10.1016/j.foreco.2009.05.018

Wang, D., Guan, D., Zhu, S., Kinnon, M. M., Geng, G., Zhang, Q., Zheng, H., Lei, T., Shao, S., Gong, P., & Davis, S. J. (2020). Economic footprint of California wildfires in 2018. *Nature Sustainability*, *4*(3), 252–260. https://doi.org/10.1038/s41893-020-00646-7

Wang, J. A., Knight, C., Goulden, M. L., Battles, J. B., & Randerson, J. T. (2022). Remote sensing reveals multi-decadal losses of tree cover in California driven by increasing fire disturbance and climate stress. *AGU Advances*, *In press*.

Waring, K. M., & O'Hara, K. L. (2008). Redwood/tanoak stand development and response to tanoak mortality caused by Phytophthora ramorum. *Forest Ecology and Management*, *255*(7), 2650–2658. https://doi.org/10.1016/j.foreco.2008.01.025

Wein RW, Maclean DA (1983) An overview of fire in northern ecosystems. In 'The Role of Fire in Northern Circumpolar Ecosystems'. (Eds RW Wein, DA MacLean) pp. 1–18. (Wiley: New York, NY, USA)

West, T. A. P., Börner, J., Sills, E. O., & Kontoleon, A. (2020). Overstated carbon emission reductions from voluntary REDD+ projects in the Brazilian Amazon. *Proceedings of the National Academy of Sciences of the United States of America*, *117*(39), 24188–24194. https://doi.org/10.1073/pnas.2004334117

Westerling AL, Hidalgo HG, Cayan DR, Swetnam TW (2006) Warming and earlier spring increase Western US forest wildfire activity. *Science* 313, 940–943. doi:10.1126/SCIENCE.1128834

Westerling, A. L., & Bryant, B. P. (2007). Climate change and wildfire in California. *Climatic Change*, *87*(1 SUPPL). https://doi.org/10.1007/s10584-007-9363-z

Whittaker, R. H. (1975). *Communities and Ecosystems*. New York: MacMillan Publishing.

Wiggins, E. B., Veraverbeke, S., Henderson, J. M., Karion, A., Miller, J. B., Lindaas, J., Commane, R., Sweeney, C., Luus, K. A., Tosca, M. G., Dinardo, S. J., Wofsy, S., Miller, C. E., & Randerson, J. T. (2016). The influence of daily meteorology on boreal fire emissions and regional trace gas variability. *Journal of Geophysical Research: Biogeosciences*, *121*(11), 2793–2810. https://doi.org/10.1002/2016JG003434

Willey, Z., & Chameides, W. L. (2007). *Harnessing farms and forests in the low-carbon economy*. Duke University Press. https://agris.fao.org/agris-search/search.do?recordID=US201300121386

Williams, J. W., Jackson, S. T., & Kutzbach, J. E. (2007). Projected distributions of novel and disappearing climates by 2100 AD. *Proceedings of the National Academy of Sciences of the United States of America*, *104*(14), 5738–5742. https://doi.org/10.1073/pnas.0606292104

Yang, H., Viña, A., Winkler, J. A., Chung, M. G., Huang, Q., Dou, Y., McShea, W. J., Songer, M., Zhang, J., & Liu, J. (2021). A global assessment of the impact of individual protected areas on preventing forest loss. The Science of the Total Environment, 777, 145995. https://doi.org/10.1016/j.scitotenv.2021.145995

Young AM, Higuera PE, Duffy PA, Hu FS (2017) Climatic thresholds shape northern high-latitude fire regimes and imply vulnerability to future climate change. *Ecography* 40, 606–617. doi:10.1111/ECOG. 02205

Zhou, Y., Williams, C. A., Hasler, N., Gu, H., & Kennedy, R. (2021). Beyond biomass to carbon fluxes: application and evaluation of a comprehensive forest carbon monitoring system. *Environmental Research Letters*, *16*(5), 055026. https://doi.org/10.1088/1748-9326/abf06d

Zhu, Z., & Woodcock, C. E. (2014). Continuous change detection and classification of land cover using all available Landsat data. *Remote Sensing of Environment*, *144*, 152–171. https://doi.org/10.1016/j.rse.2014.01.011

Appendix A

Supporting Information for Ch 2: Climate-driven limits to future carbon storage in California's wildland ecosystems

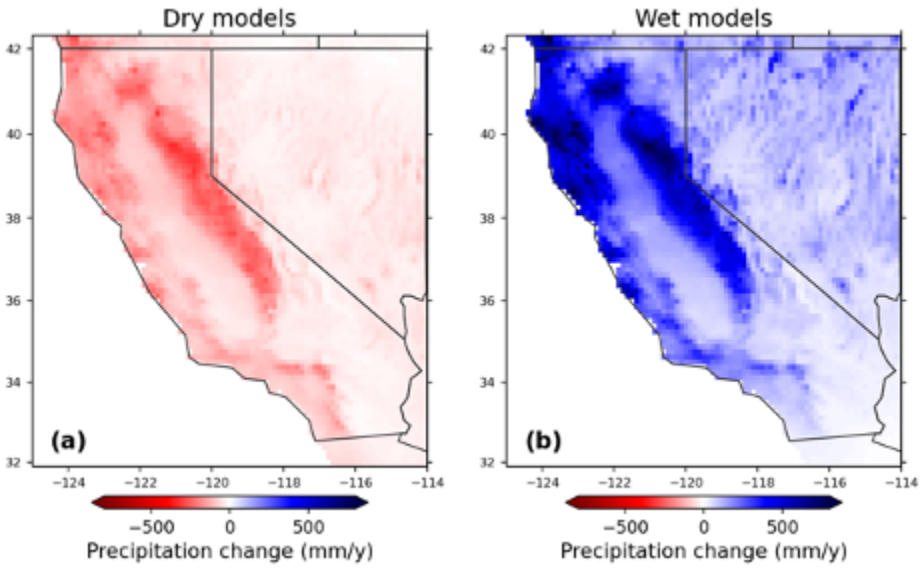

Figure A1. Annual mean precipitation change for the eight driest models (a) and eight wettest models (b) for California which become our "dry" and "wet" scenarios (here showing RCP8.5). These correspond to an average precipitation change of -16% (dry) and +39% (wet). Drying changes are more focused in the Sierra Nevada and Southern Coastal Ranges, while wetting changes are more widespread across the mountains and coasts of northern California.

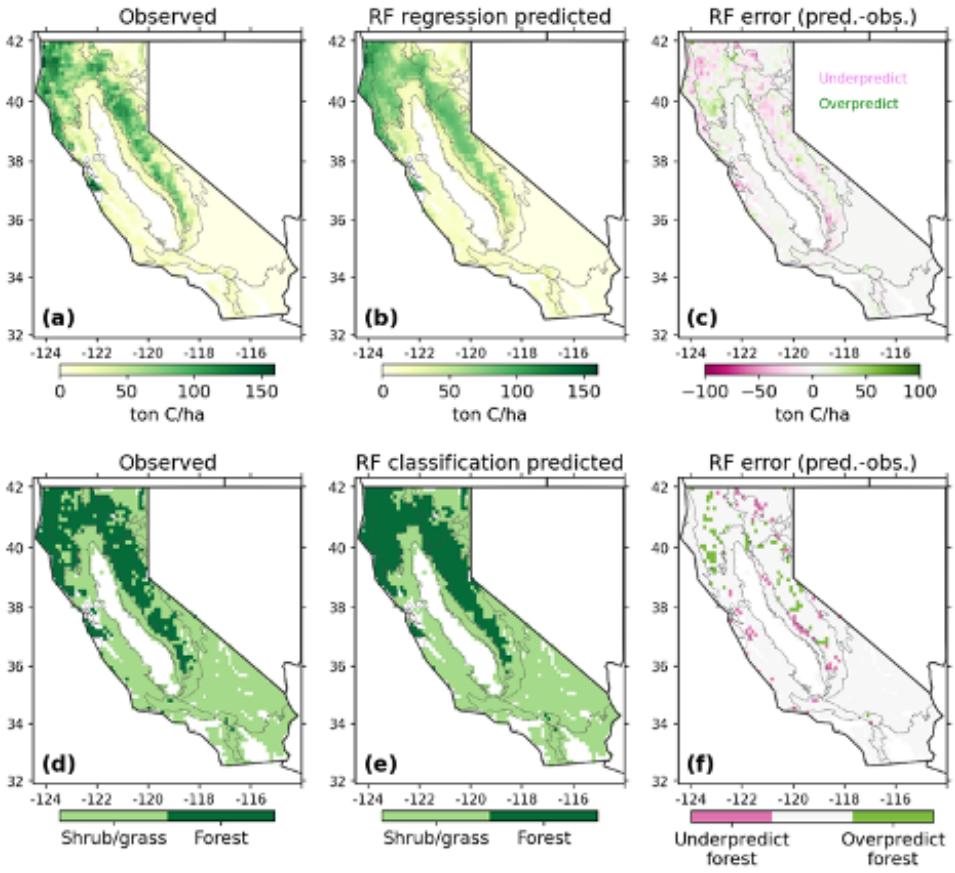
Observed
RF regression predicted
RF error (pred.-obs.)
Underpredict
Overpredict
(a)
(b)
(c)
42
40
38
36
34
32
-124 -122 -120 -118 -116
0 50 100 150
ton C/ha
−100 −50 0 50 100
ton C/ha
Observed
RF classification predicted
RF error (pred.-obs.)
(d)
(e)
(f)
Shrub/grass Forest
Underpredict forest
Overpredict forest

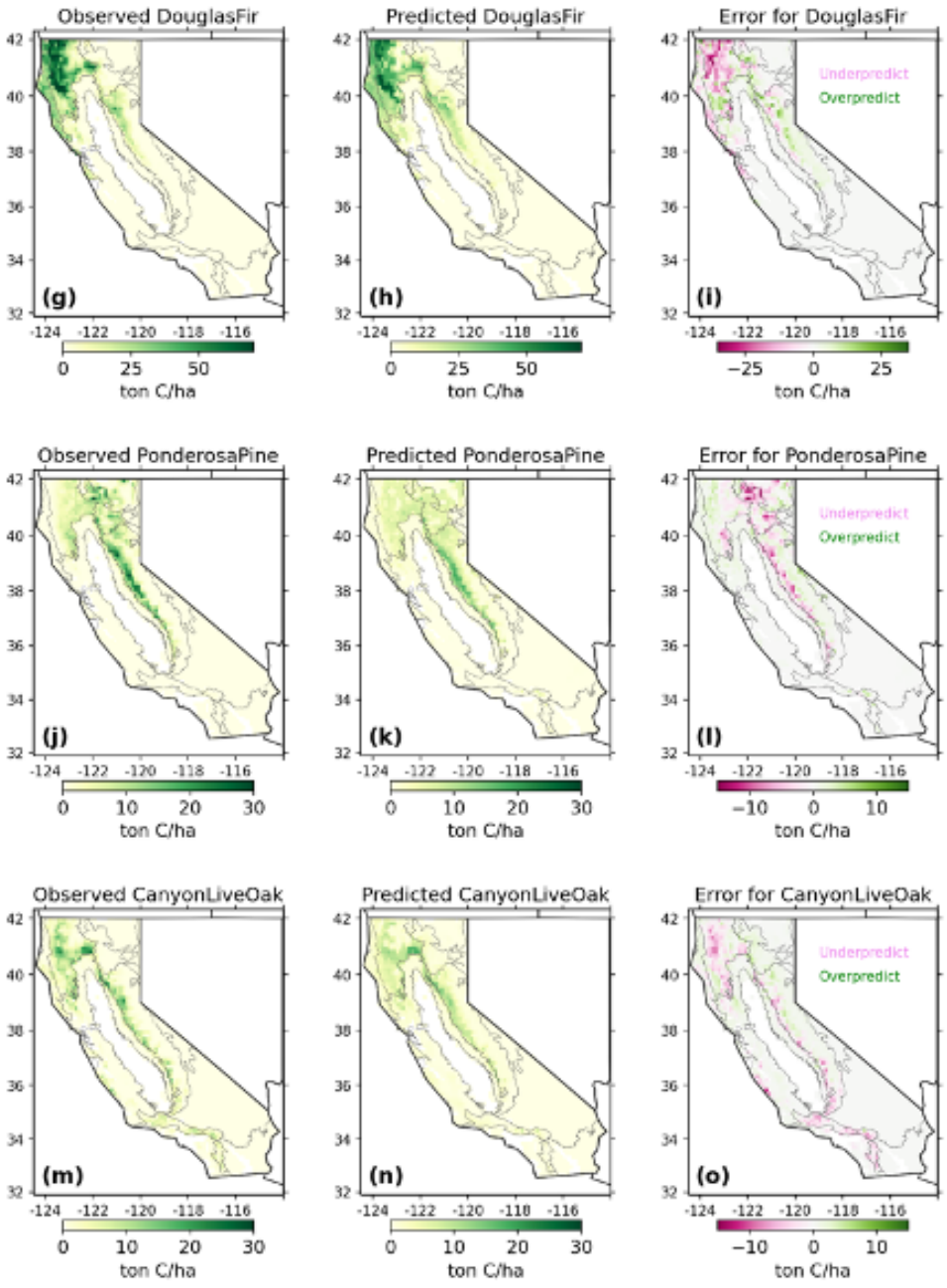
Observed DouglasFir
Predicted DouglasFir
Error for DouglasFir
Underpredict
Overpredict
(g)
(h)
(i)
ton C/ha
Observed PonderosaPine
Predicted PonderosaPine
Error for PonderosaPine
(j)
(k)
(l)
Observed CanyonLiveOak
Predicted CanyonLiveOak
Error for CanyonLiveOak
(m)
(n)
(o)

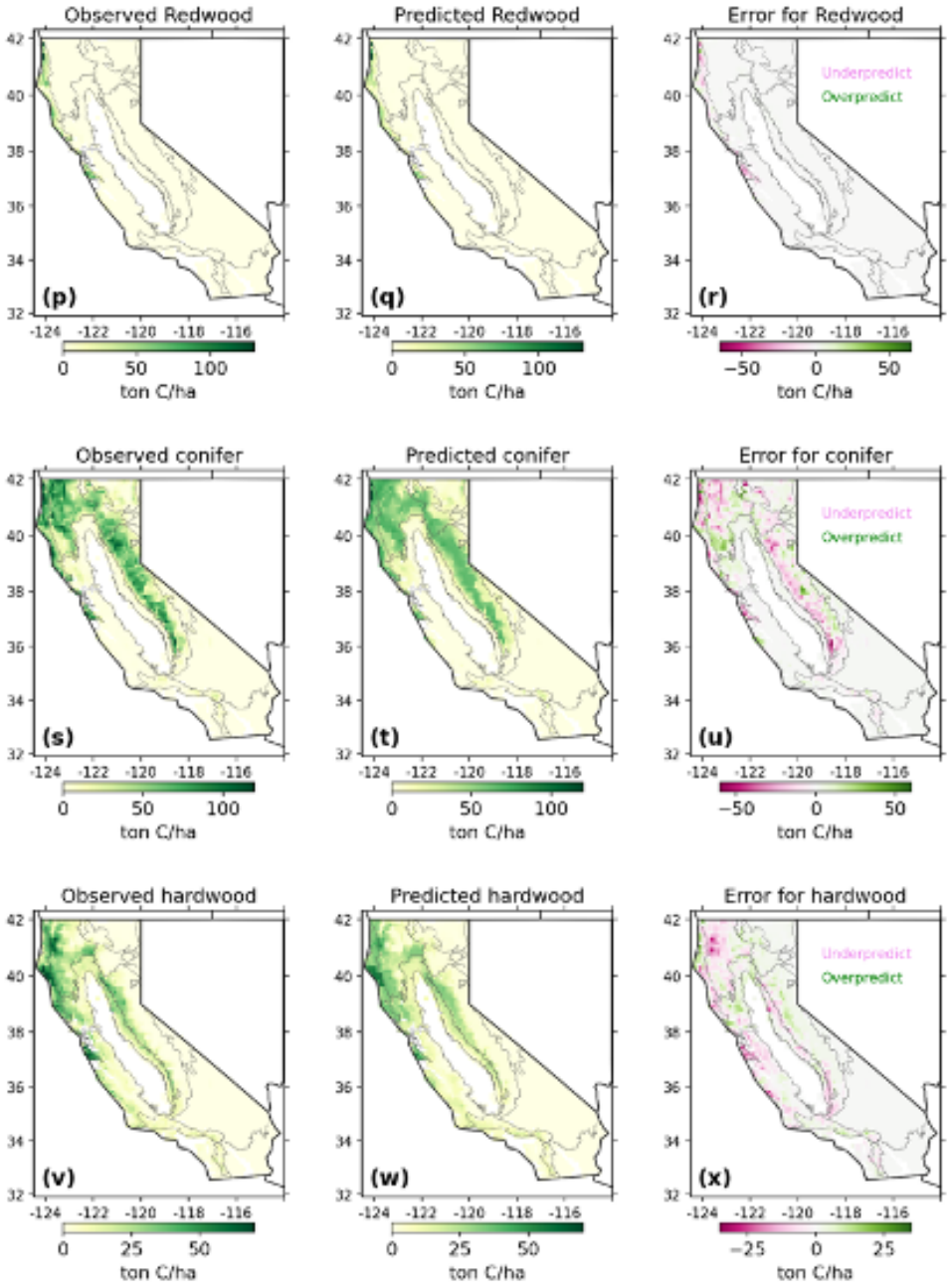

Figure A2. Spatial patterns of residuals across approaches. These include the RF regression of carbon density (a-c), RF classification of vegetation type (d-f), and RF species models (g-x). Note that the "error" column color scale is magnified to highlight areas of over- or underprediction. In many cases (d, l, u), present-day carbon density is higher than predicted based on climate, for example in the foothills of the Sierra Nevada. This pattern may suggest that this region is already exceeding its carbon capacity due to climate change.

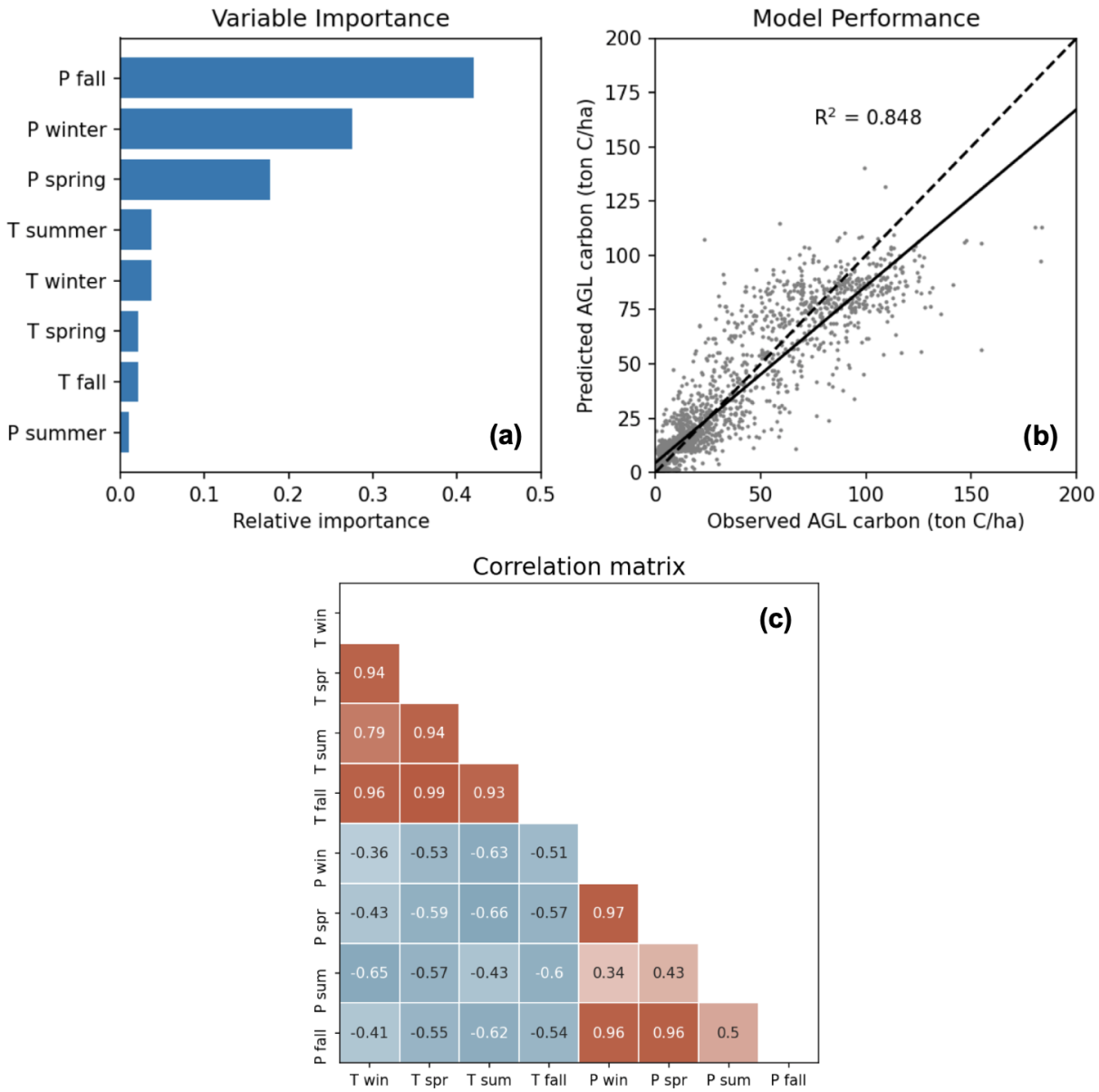

Figure A3. Model details for the aboveground live carbon density RF regression approach. The most important predictors of aboveground carbon were fall, winter, and spring precipitation (a). The random forest model captured the spatial distribution of carbon density, with the out-of-sample predictions explaining 84.8% of the variance in the observations (b). These eight climate variables are highly correlated, but the seasonal attributes still add substantial information (in particular for summer-versus-winter precipitation, for example) (c).

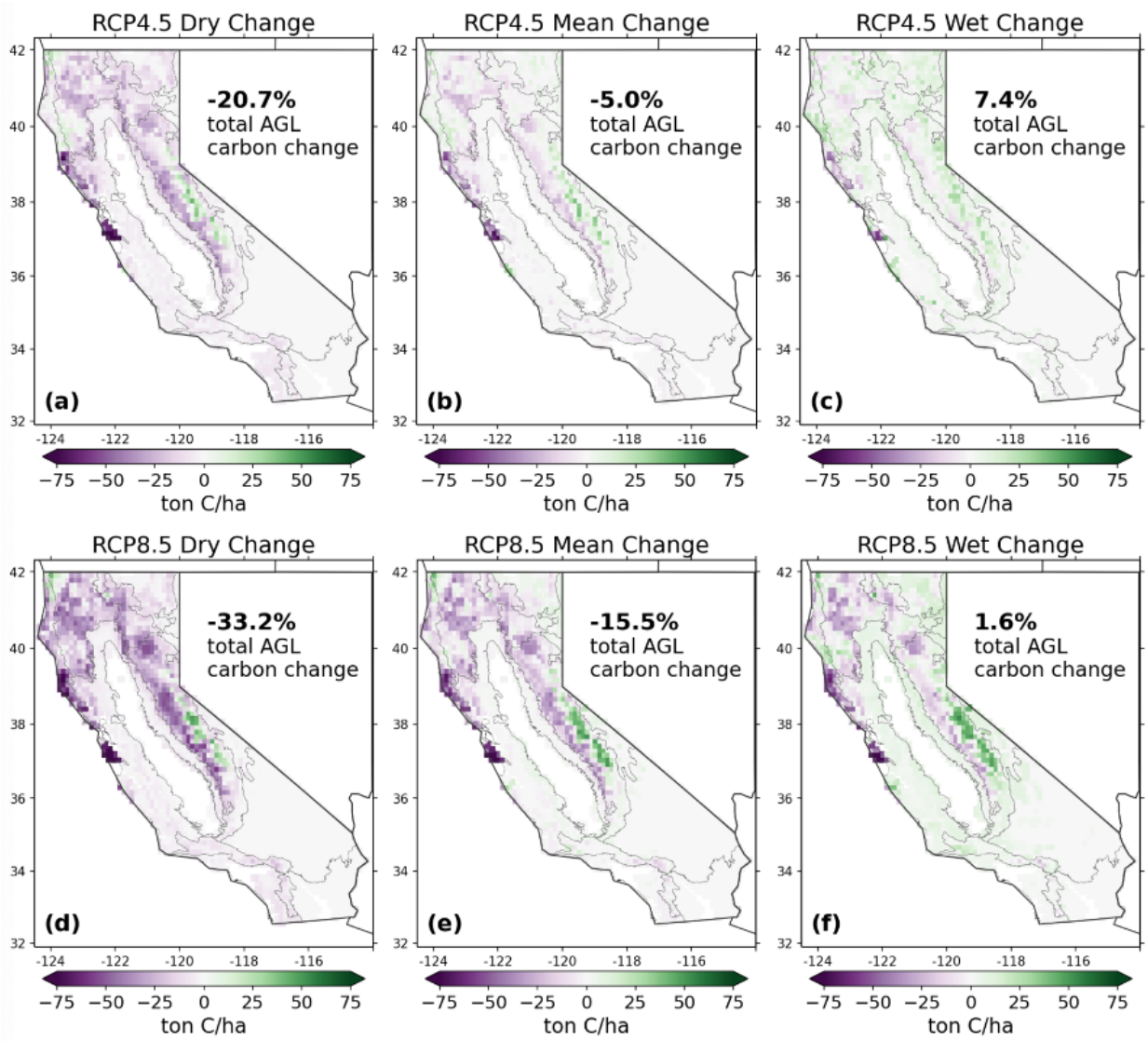

Figure A4. Results from RF regression of aboveground live carbon density for all six scenarios. The greatest difference between results comes from using wet (c, f) versus dry (a, d) climate models, for either RCP4.5 (top row) or RCP8.5 (bottom row) climate change. All scenarios show substantial redistribution of AGL carbon, with losses at low elevation and coastal regions and gains at high elevation.

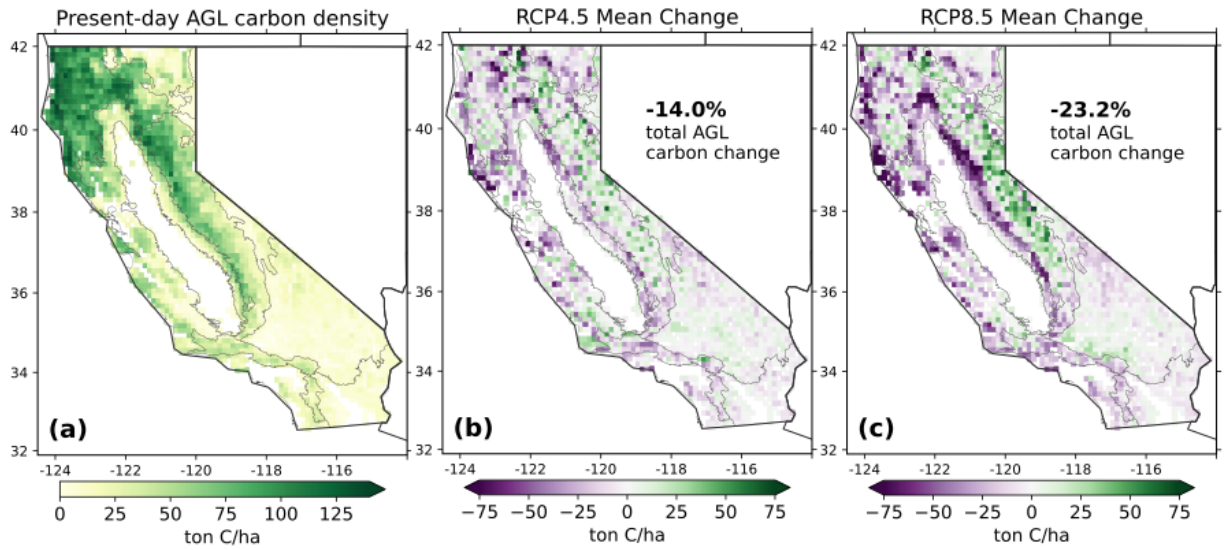

Figure A5. Projected future changes in aboveground carbon storage in the climate analogs approach. In this approach we replaced pixels in the future with the aboveground live carbon density of their corresponding present-day climate analog. Spatial patterns of change are similar to previous approaches, with aboveground live carbon gains at high elevation and largest losses at low elevations.

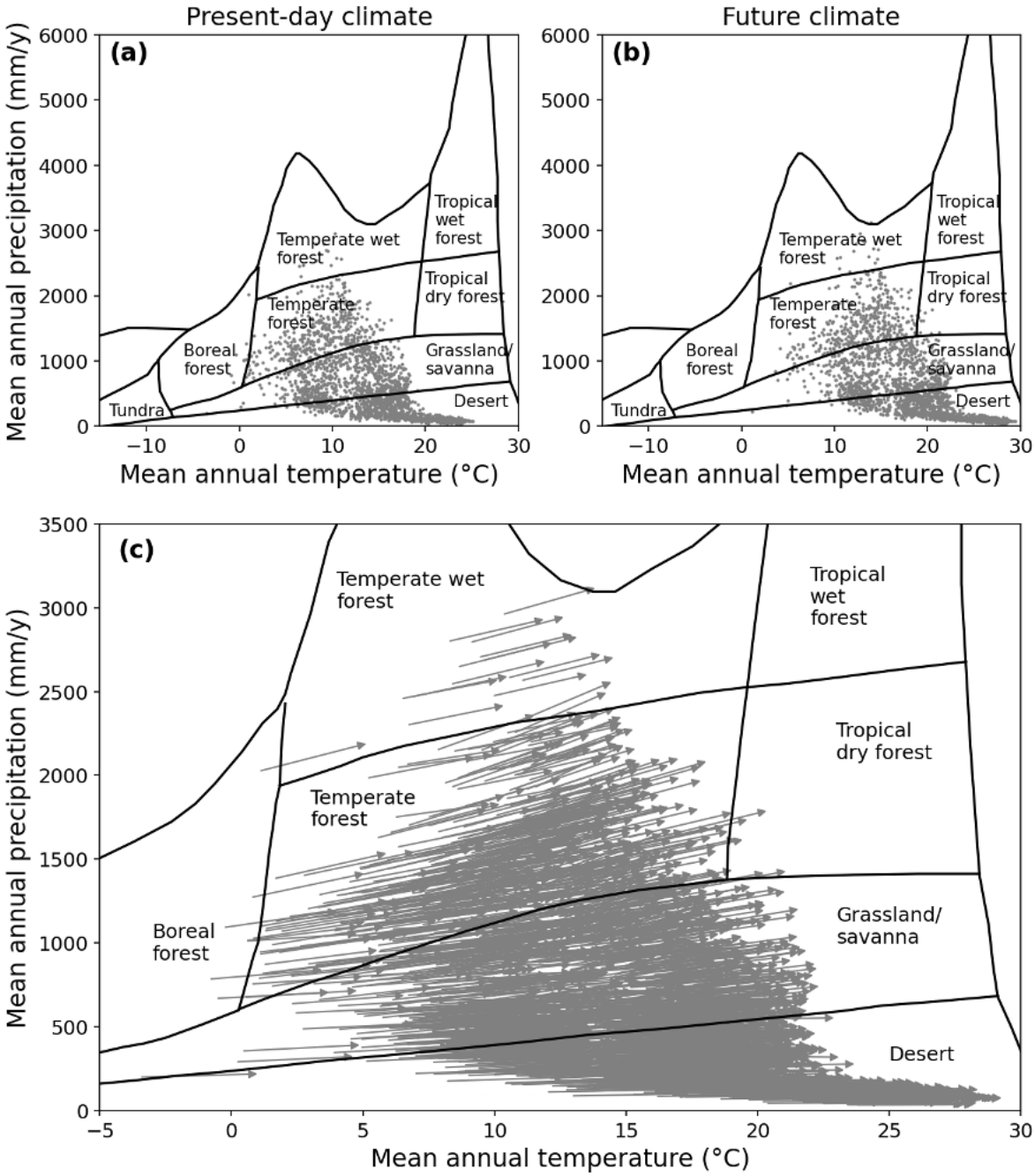

Figure A6. Climate space analysis. California's wildlands are largely desert, grassland/shrublands, and temperate dry forests, with some temperature wet forests in the northwest (a). RCP8.5 climate change will cause large temperature increases, shifting the points substantially to the right (b, c). Biome boundaries were obtained from Chapin et al. (Chapin III et al., 2011).

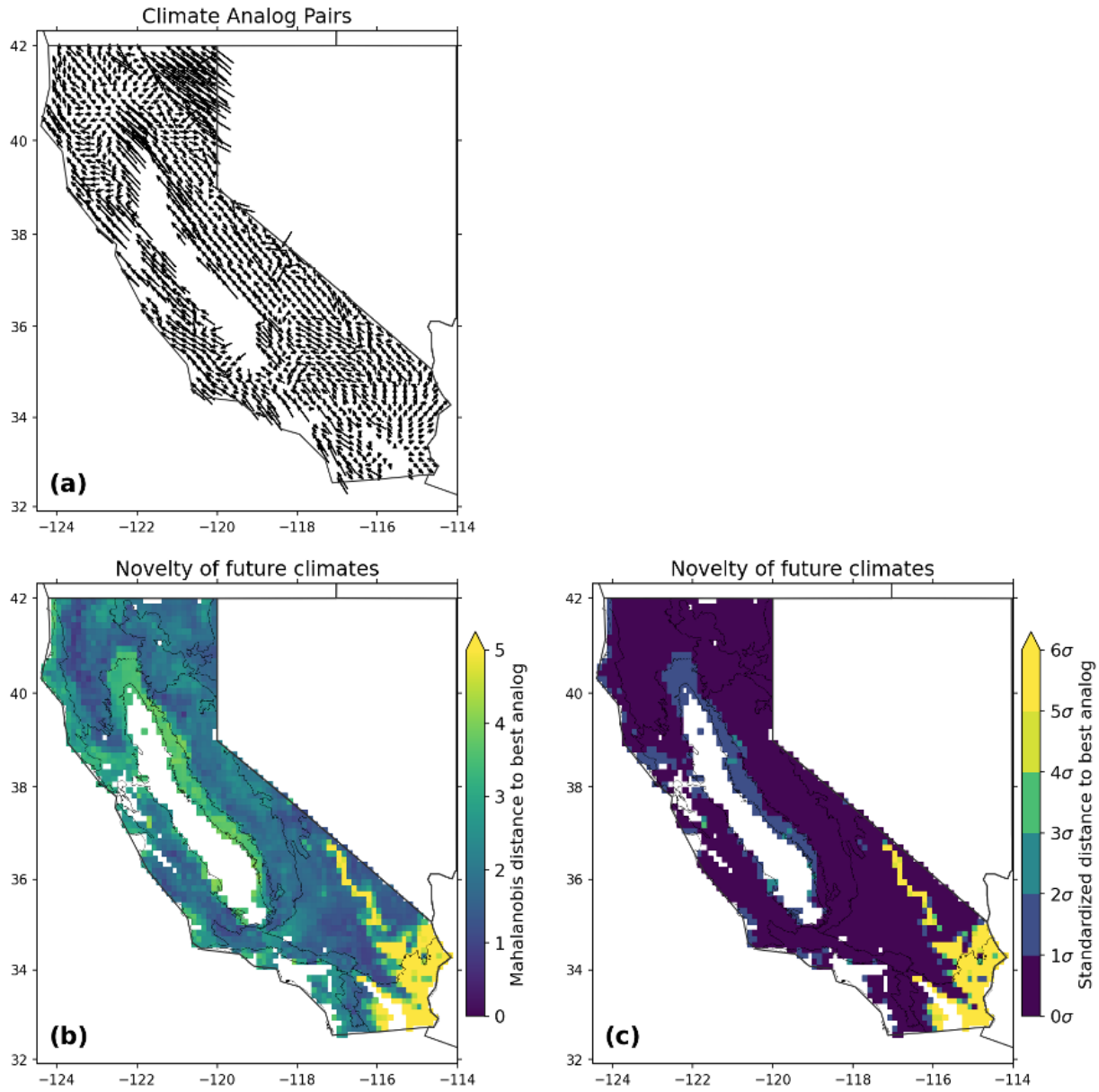

Figure A7. Further analysis from the climate analogs approach. Panel (a) shows the direction and relative magnitude of climate movement. Each arrow terminates at a pixel in the future climate and originates in the direction of the present-day analog. Note that arrow length has been shortened by a factor of 15 for visualization. In general this shows a net northward and upslope movement. Panels (b) and (c) show the novelty of future climates in different units, with (c) interpreting the Mahalanobis distance from (b) as z-scores on a chi-squared distribution with eight degrees of freedom, following the example of Mahony et al., 2017. The southern deserts will have the most novel future climates, as they are already the hottest part of this region and will warm further. The Northern Coast and Sierra Nevada foothills are also indicated as areas of highly novel future climate.

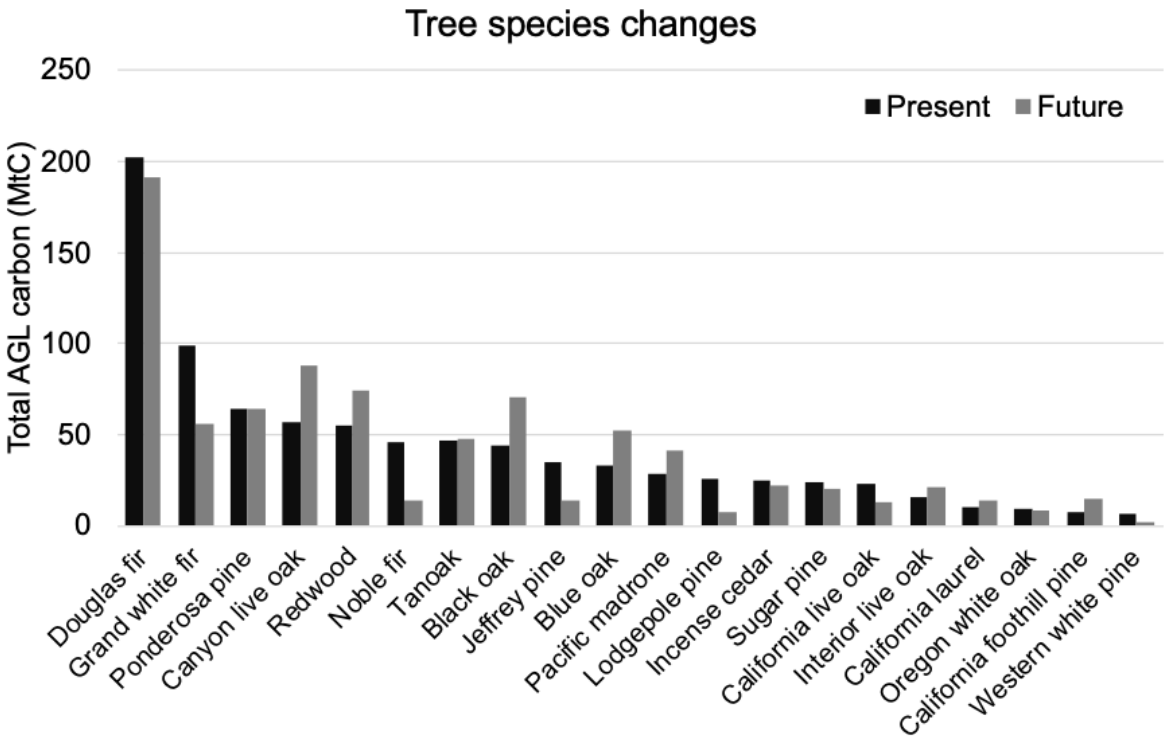

Figure A8. Projected changes to statewide AGL carbon by species for RCP8.5 mean scenario. Conifers such as Douglas fir, grand white fir, noble fir, and Jeffrey pine show the most substantial losses, while oaks such as canyon live oak and black oak are projected to increase in density with climate warming. These values do not reflect migration limitations, which are likely to substantially affect all species, especially larger and slower growing ones.

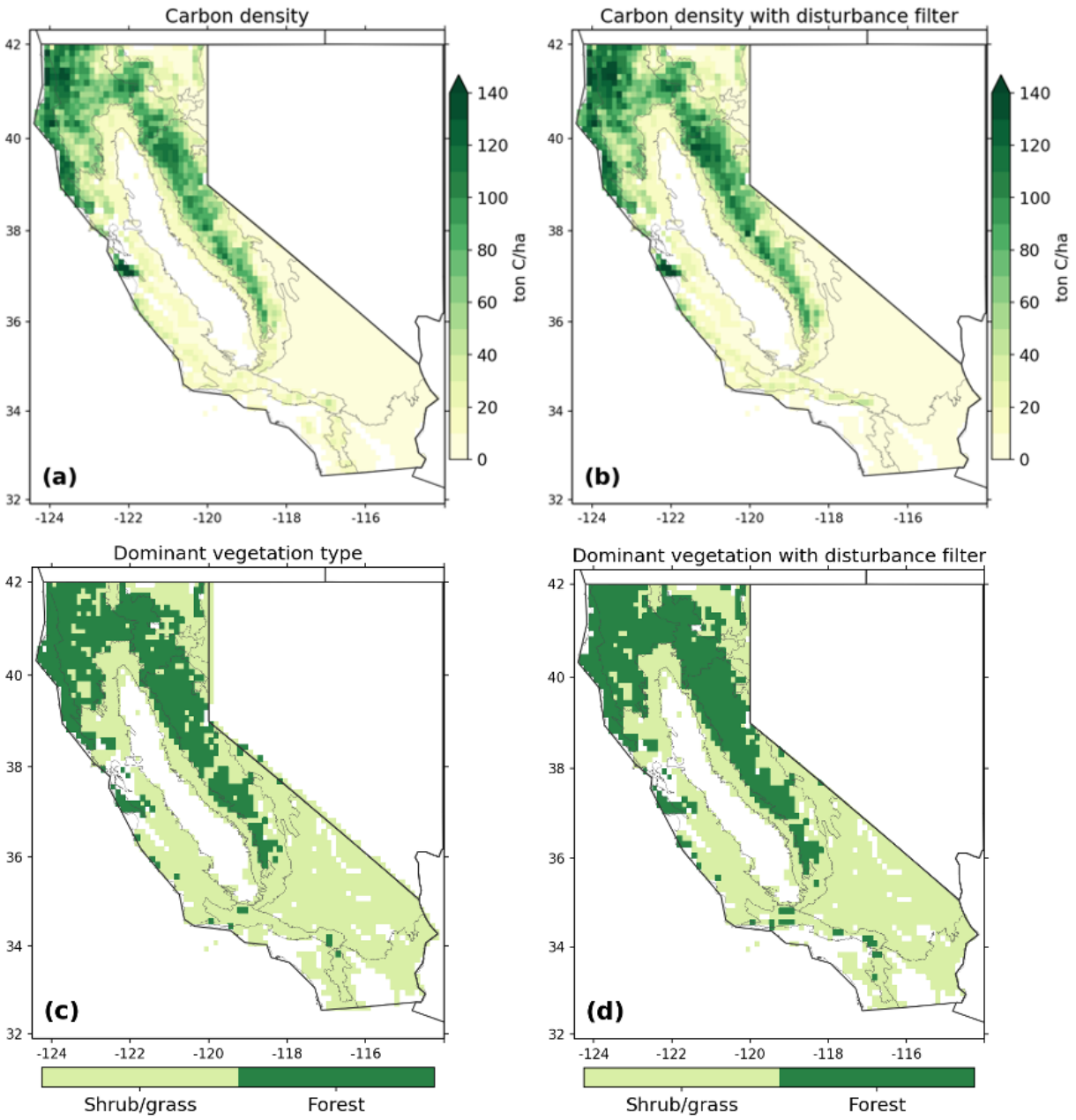

Figure A9. Minimal effect of harvest and fire disturbance history on target datasets. As a supplemental analysis, we explored whether our lack of explicit accounting for disturbance history had a large influence on two of our eighth-degree target datasets or model projections. Filtering out any 30-m pixels with fire or high intensity harvest over 20 years (1995-2014) did result in slightly greater carbon density (b) and forest cover (d) after data were averaged to an eighth-degree resolution. These increases are minimal (3% and 4%, respectively) and did not lead to a consistent directional shift in final projections of carbon change (Table S2), especially given that model fitting further smoothed out fine scale spatial heterogeneity (Fig S3e).

Table A1. Details for the 39 species included in the tree species niche models, including groupings and model performances. RMSE and R^2 describe average performance on out-of-sample data during model validation. Due to decreasing model performance, only species 1-20, which account for 94% of forest carbon, were modeled individually. Projected percent change in AGL carbon is shown for the RCP8.5 mean scenario.

	Scientific name	Common name	Conifer vs hardwood	RMSE validation	R^2 validation	Total carbon (MtC)	Projected % change
1	*Pseudotsuga menziesii*	Douglas-fir	Conifer	6.78	0.76	202.0	-5.2%
2	*Abies grandis/concolor*	grand fir x white fir	Conifer	3.61	0.71	98.6	-43.5%
3	*Pinus ponderosa*	ponderosa pine	Conifer	2.33	0.66	64.2	0.1%
4	*Quercus chrysolepis*	canyon live oak	Hardwood	1.99	0.65	56.8	54.3%
5	*Sequoia sempervirens*	redwood	Conifer	5.81	0.56	55.4	34.3%
6	*Abies procera/shastensis/ magnifica*	noble fir x Shasta red fir	Conifer	2.56	0.70	45.6	-69.3%
7	*Lithocarpus densiflorus*	tanoak	Hardwood	2.86	0.69	46.6	2.3%
8	*Quercus kelloggii*	California black oak	Hardwood	1.42	0.75	44.0	59.2%
9	*Pinus jeffreyi*	Jeffrey pine	Conifer	1.6	0.59	35.1	-60.7%
10	*Quercus douglasii*	blue oak	Hardwood	1.12	0.74	32.6	60.1%
11	*Arbutus menziesii*	Pacific madrone	Hardwood	1.61	0.57	28.0	48.5%
12	*Pinus contorta*	lodgepole pine	Conifer	1.75	0.68	25.6	-72.9%
13	*Calocedrus decurrens*	incense cedar	Conifer	1.11	0.65	25.1	-12.2%
14	*Pinus lambertiana*	sugar pine	Conifer	1.03	0.65	24.2	-15.9%
15	*Quercus agrifolia*	California live oak	Hardwood	1.36	0.64	22.5	-43.8%
16	*Quercus wislizeni*	interior live oak	Hardwood	0.77	0.69	15.6	34.9%
17	*Umbellularia californica*	California laurel	Hardwood	0.62	0.63	10.0	34.1%
18	*Quercus garryana*	Oregon white oak	Hardwood	0.58	0.56	9.6	-10.0%
19	*Pinus sabiniana*	California foothill pine	Conifer	0.31	0.63	7.3	103.1%

20	*Pinus monticola*	western white pine	Conifer	0.34	0.78	6.6	-77.0%
21	*Quercus lobata*	California white oak	Hardwood	0.42	0.19	5.6	
22	*Pinus monophylla*	singleleaf pinyon	Conifer	0.49	0.46	5.8	
23	*Juniperus occidentalis*	western juniper	Conifer	0.25	0.54	4.7	
24	*Acer macrophyllum*	bigleaf maple	Hardwood	0.17	0.65	4.5	
25	*Alnus rubra*	red alder	Hardwood	0.69	0.41	4.3	
26	*Sequoiadendron giganteum*	giant sequoia	Conifer	0.85	0.17	3.8	
27	*Tsuga mertensiana*	mountain hemlock	Conifer	0.32	0.65	3.5	
28	*Picea sitchensis*	Sitka spruce	Conifer	0.72	0.22	2.1	
29	*Tsuga heterophylla*	western hemlock	Conifer	0.43	0.30	2.0	
30	*Pinus attenuata*	knobcone pine	Conifer	0.11	0.39	1.7	
31	*Chrysolepis chrysophylla*	giant chinquapin	Hardwood	0.16	0.37	1.5	
32	*Cercocarpus ledifolius*	curl-leaf mountain mahogany	Hardwood	0.12	0.30	1.5	
33	*Alnus rhombifolia*	white alder	Hardwood	0.09	0.21	1.3	
34	*Pseudotsuga macrocarpa*	bigcone Douglas-fir	Conifer	0.15	0.38	1.2	
35	*Aesculus californica*	California buckeye	Hardwood	0.08	0.37	1.2	
36	*Chamaecyparis lawsoniana*	Port Orford cedar	Conifer	0.32	0.11	1.2	
37	*Juniperus californica*	California juniper	Conifer	0.09	0.31	1.1	
38	*Pinus muricata*	Bishop pine	Conifer	0.20	0.12	0.8	
39	*Populus fremontii*	Fremont cottonwood	Hardwood	0.06	0.17	0.2	

Table A2. Influence of harvest and fire disturbance history on model projections. As a supplemental analysis, we explored whether our lack of explicit accounting for disturbance history had a large influence on two of our eighth-degree target datasets or model projections. Filtering out any 30-m pixels with fire or high intensity harvest over 20 years (1995-2014) did result in slightly greater carbon density and forest cover after data were averaged to an eighth-degree resolution. (Fig S10). These increases are minimal (3% and 4%, respectively) and did not lead to a consistent directional shift in final projections of carbon change, especially given that model fitting further smoothed out fine scale spatial heterogeneity (Fig S3e).

	RCP4.5			*RCP8.5*		
Eco-statistical approach	*Dry*	*Mean*	*Wet*	*Dry*	*Mean*	*Wet*
(1) Regression of carbon density	-20.7%	-5.0%	+7.4%	-33.2%	-15.5%	+1.6%
- after disturbance filter	-21.5%	-4.9%	+7.3%	-32.9%	-14.4%	+2.6%
(2) Classification of dominant veg. type	-17.6%	-6.3%	+1.1%	-27.4%	-18.5%	-15.0%
- after disturbance filter	-16.8%	-7.2%	+2.0%	-26.7%	-16.6%	-12.7%

Appendix B

Supporting Information for Ch 3: Using remote sensing to quantify the additional climate benefits of California forest carbon offsets

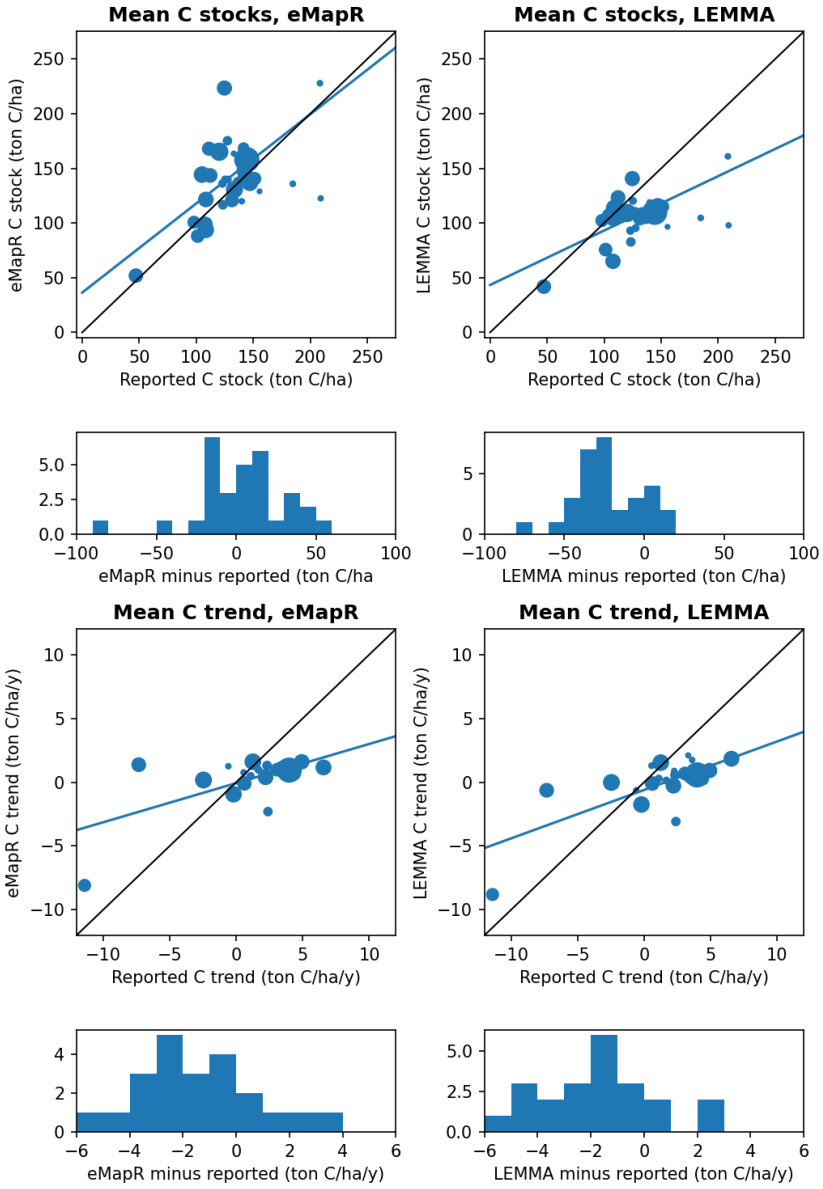

Figure B1. Comparison of remote sensing and reported carbon stocks and trends. eMapR and LEMMA estimates of carbon stocks are not significantly greater or less than reported carbon stocks across the portfolio of projects (top row), but have relatively high root mean square error against reported carbon stocks (30.9 and 29.2 ton C/ha, respectively). There is a slight bias to underestimate carbon stocks at high densities, especially with LEMMA. The largest discrepancies exist in estimations of the carbon accumulation rate over time (bottom half), with eMapR and LEMMA generally estimating lower magnitudes of change. Marker size indicates relative project area.

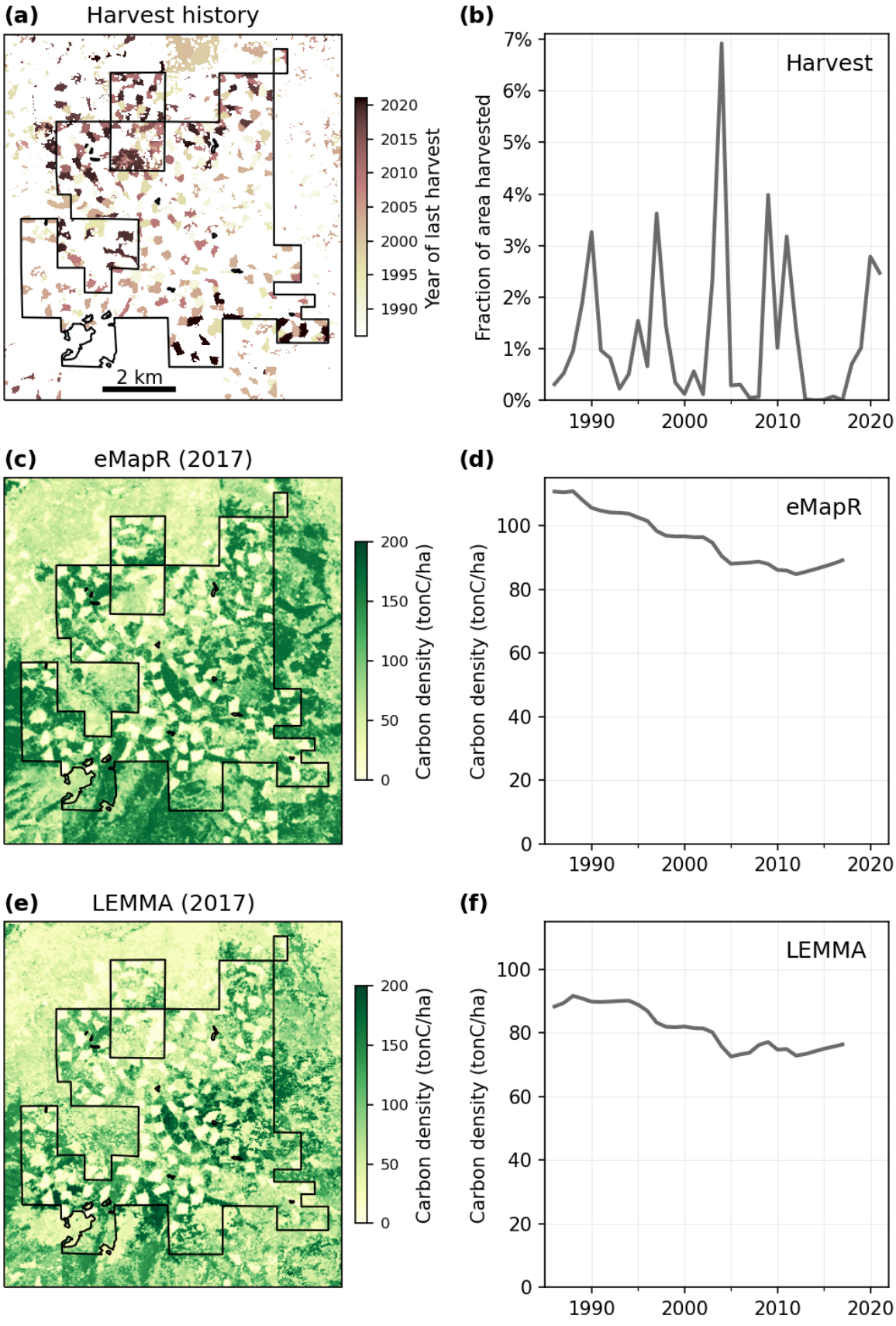
(a) Harvest history
2 km
2020
2015
2010
2005
2000
1995
1990
Year of last harvest
(b)
Harvest
Fraction of area harvested
7%
6%
5%
4%
3%
2%
1%
0%
1990
2000
2010
2020
(c) eMapR (2017)
200
150
100
50
0
Carbon density (tonC/ha)
(d)
eMapR
Carbon density (tonC/ha)
100
80
60
40
20
0
1990
2000
2010
2020
(e) LEMMA (2017)
200
150
100
50
0
Carbon density (tonC/ha)
(f)
LEMMA
Carbon density (tonC/ha)
100
80
60
40
20
0
1990
2000
2010
2020

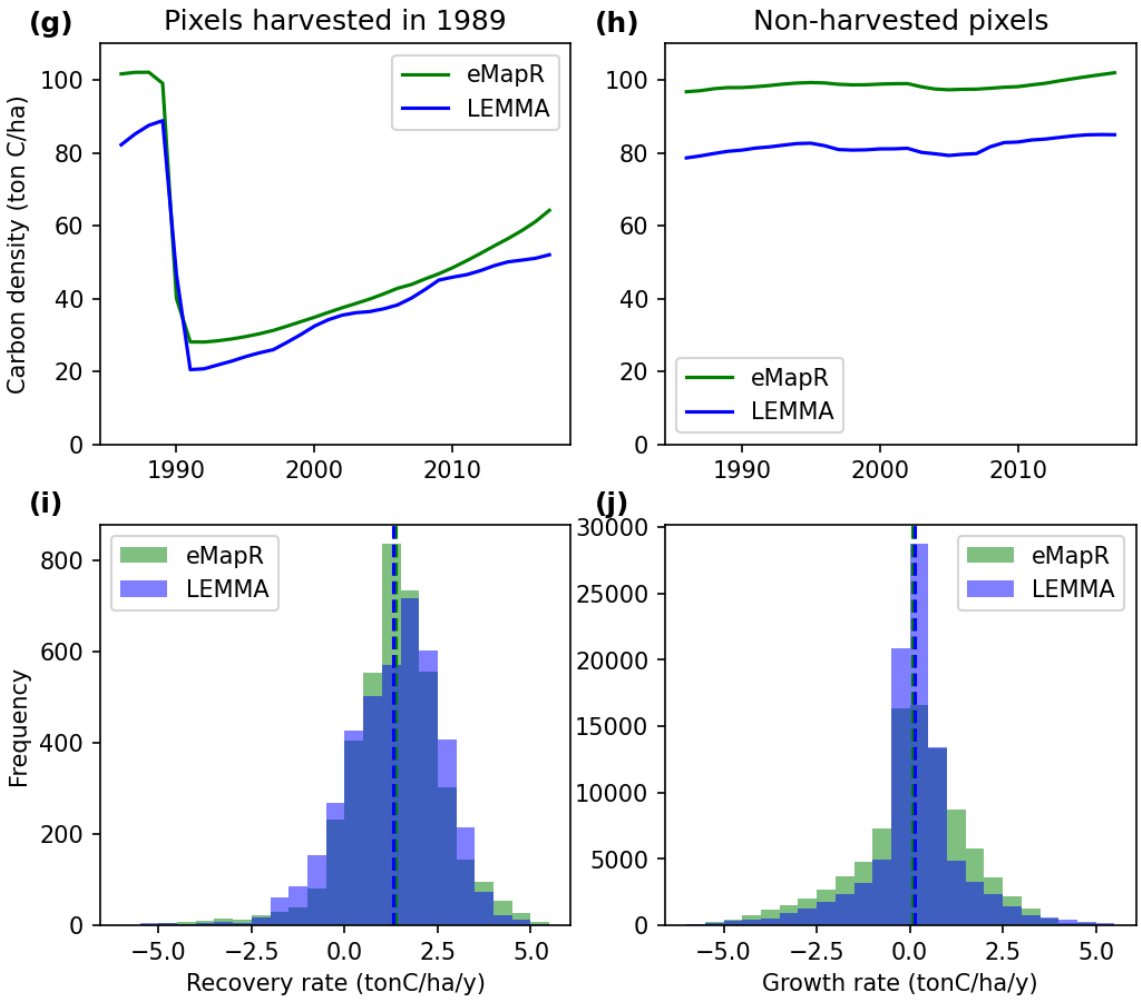

Figure B2. Demonstration of agreement across remote sensing datasets for an example project, CAR1066. The harvest product by Wang et al. 2022 shows an expected pattern of patchwork clearcutting in this area over the available record of 1986-2021 (a). Harvest activity is fairly episodic, ranging from 0% to 7% of the area being cut each year (b). Both eMapR and LEMMA show substantial reductions in aboveground carbon in recently harvested patches (c, e), and loss of carbon in the timeseries aligns with large harvest events, despite the difference in absolute magnitude of carbon stocks between eMapR and LEMMA (d, f). Both eMapR and LEMMA capture steep declines followed by steady recovery for pixels that were harvested in 1989 (g) compared to non-harvested pixels over the record (h). The two carbon datasets agree in terms of rate of change of carbon over time, with approximately normal distributions of carbon sequestration rate across pixels, both for pixels recovering from harvest (i) or undisturbed (j). The means of the eMapR and LEMMA distributions are virtually equivalent as indicated by overlapping green and blue dashed lines.

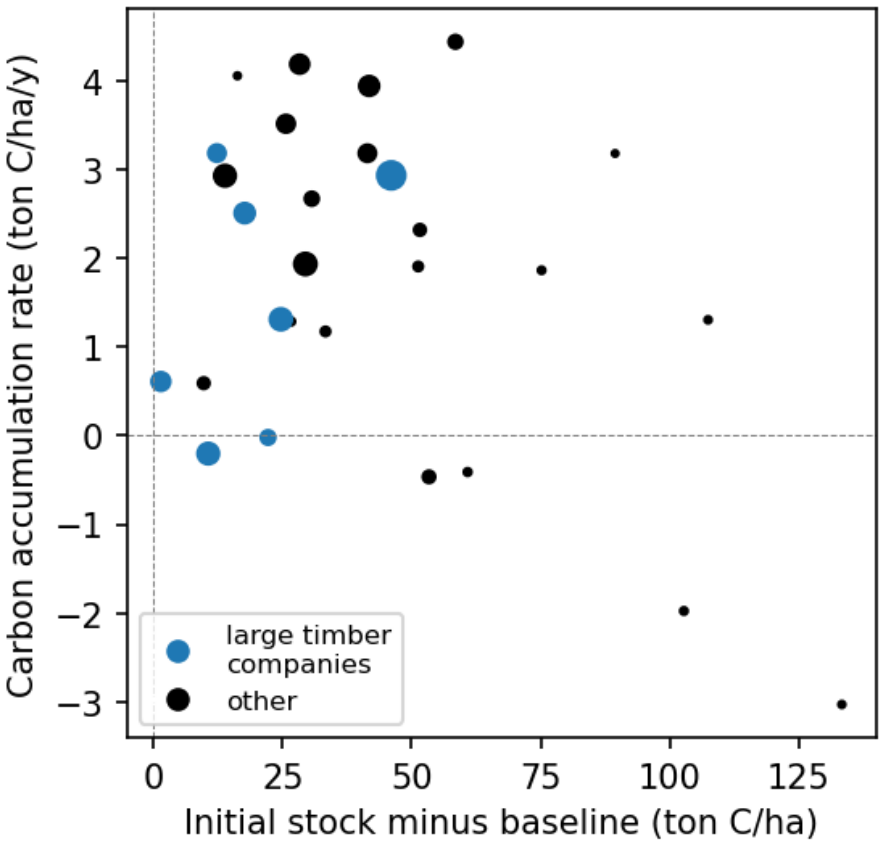

Figure B3. Varying strategies of carbon crediting. Projects receive credits for additional carbon stocks from (1) initial stocking above baseline levels and (2) subsequent incremental increases over time, minus any estimated leakage or secondary effects. This presents a trade-off; projects with lower initial stocks are more likely to have high rates of accumulation such that they are still feasible for substantial crediting long-term. This is particularly the case for projects owned by large timber companies (defined in Table B3). Marker size indicates relative project areas.

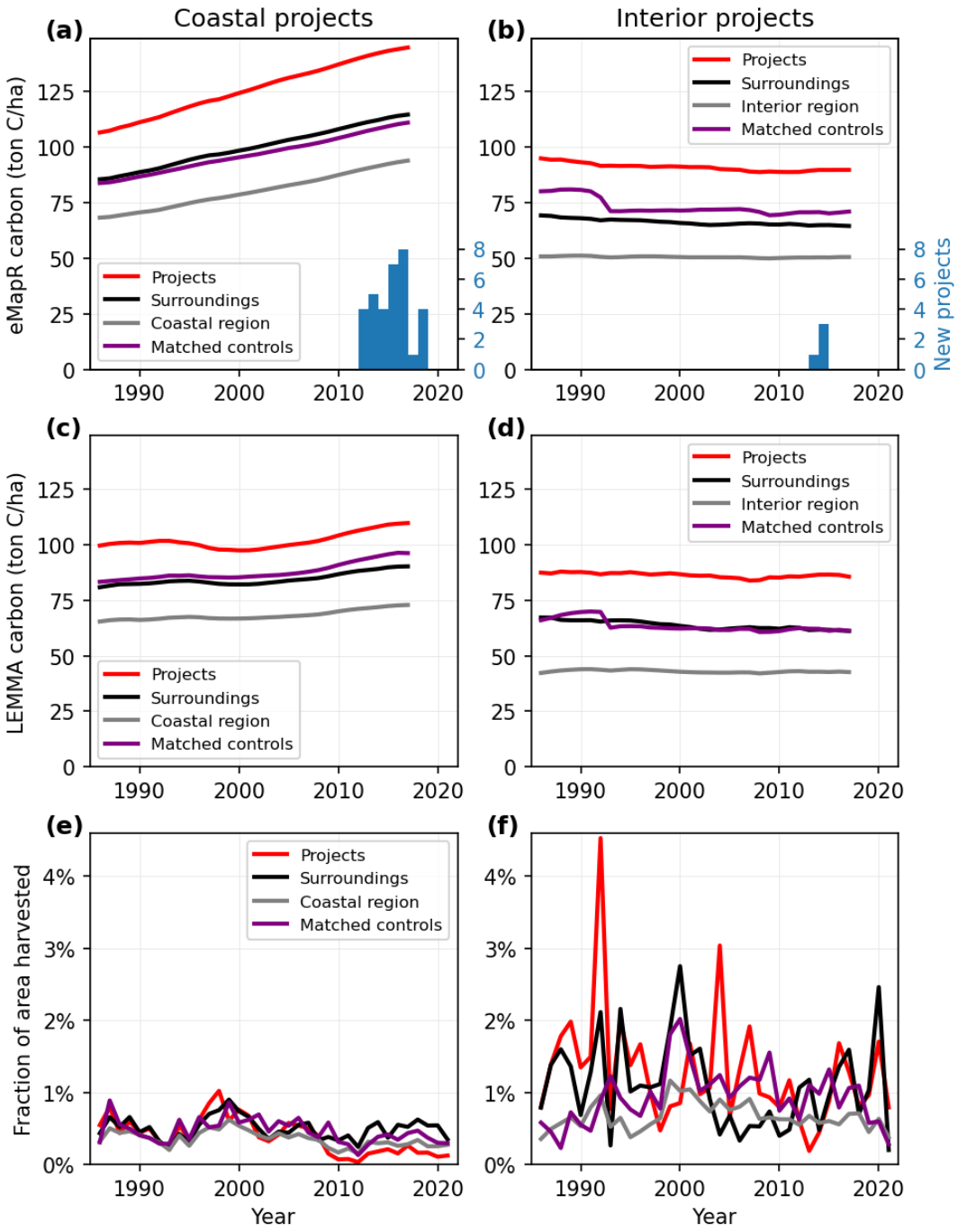

Figure B4. Copy of Fig. 4, with added results for LEMMA carbon timeseries (c, d) and a third system of spatial controls based on covariate matching (purple lines). The LEMMA carbon timeseries shows a slower growth of carbon in the coastal region (c), but similar patterns of projects being relatively carbon-dense and adding carbon at similar rates as the control groups. The third control group - based on Mahalanobis distance matching to other pixels with most similar temperature, precipitation, and productivity in the same region - is shown in purple. This system of controls gave qualitatively similar results to the "surroundings" in black, apart from a decline in carbon in 1993 in the interior controls which is attributable to the 1992 Fountain Fire.

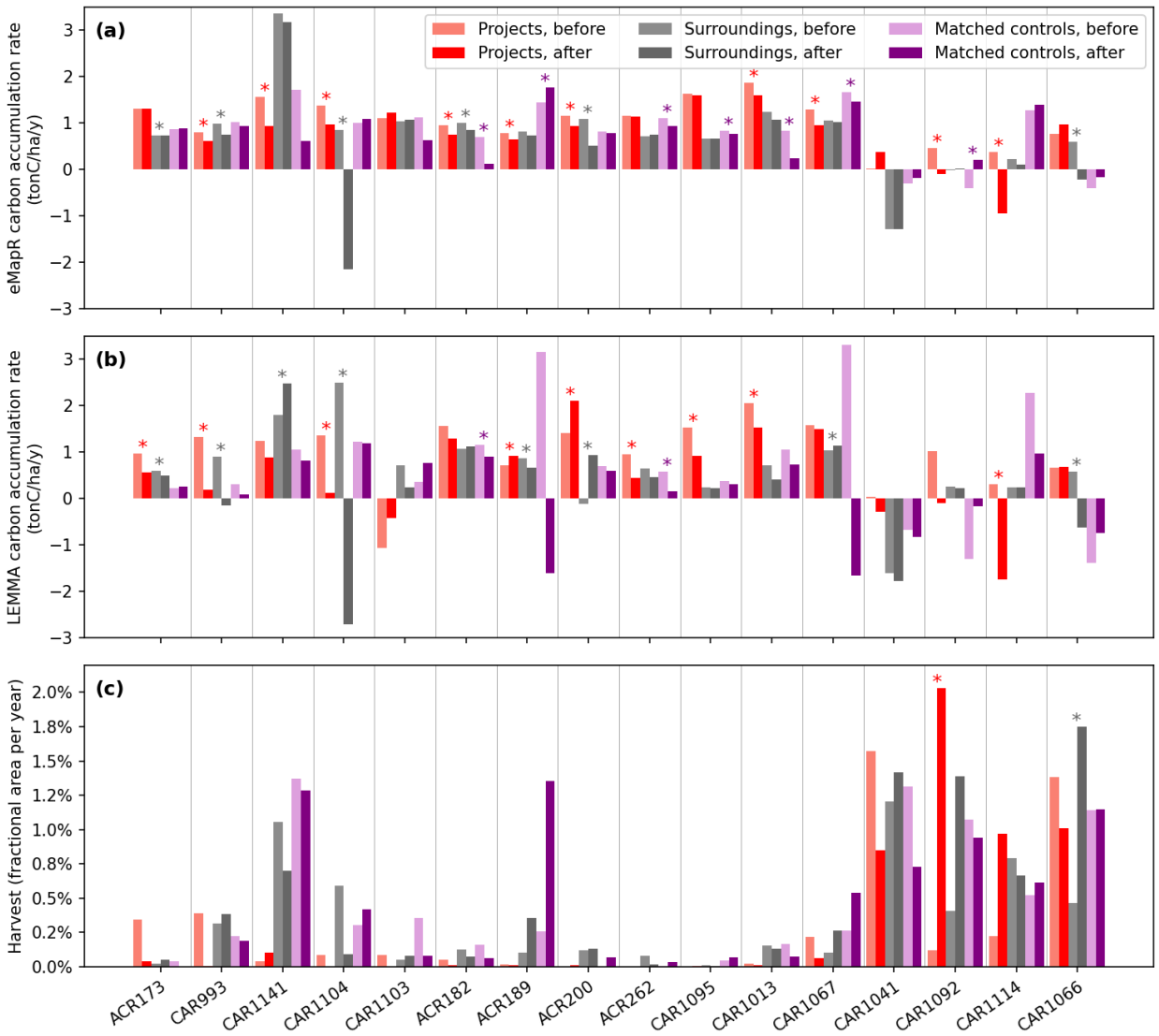

Figure B5: Before-and-after carbon accumulation and harvest rates by project. Asterisks* indicate statistical significance in the pre-to-post-project change, for an equal number of years considered before and after. For the 16 projects that started by 2014 (and excluding CAR1046 which terminated), 12 show a reduction in eMapR carbon accumulation rate after initiation (a), 10 of which are statistically significant (a). Four projects show an insignificant increase. LEMMA results are mostly similar, with predominantly decreases in carbon accumulation rate for projects (b); however one project, ACR200 does show a significant increase according to LEMMA. In terms of harvest, the four Sierra Pacific Industries projects (the four rightmost projects) show relatively high rates of harvest both before and after initiation. One project, CAR1092, has harvested significantly more since it became an offset project; none have harvested significantly less. The two systems of controls (gray and purple) differ in magnitudes of change but agree that the majority of areas show a decrease in carbon accumulation after projects begin.

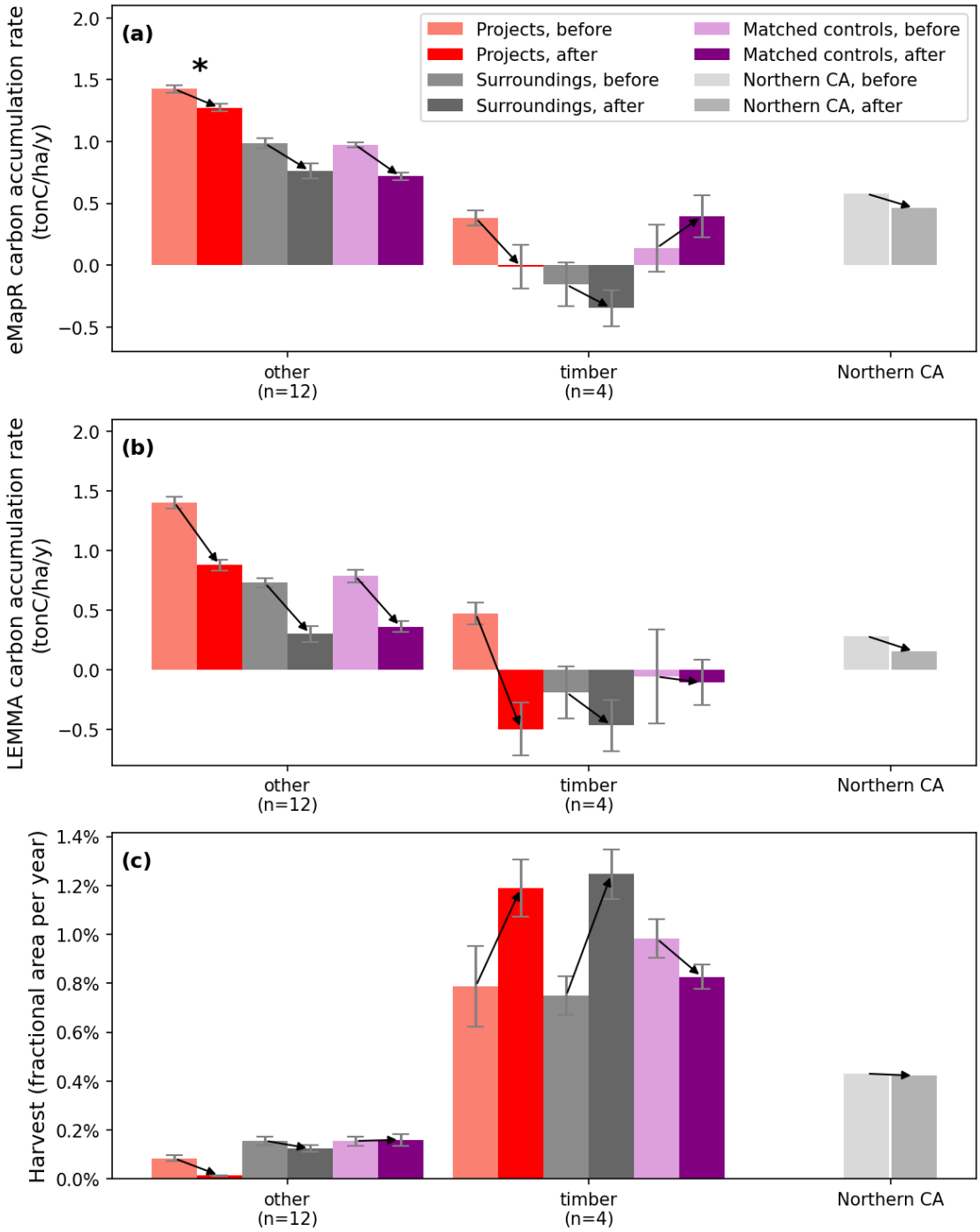

Figure B6: Copy of Fig. 5, with an added panel for LEMMA results (b) and added bars for the third system of controls (purple). At this scale of grouping projects into two landowner categories, eMapR and LEMMA show the same direction of change for all cases – i.e., a decline in carbon accumulation rate. The "matched controls" system performs similarly to the surrounding control areas, with the exception of the statistically insignificant increase in eMapR carbon accumulation and decrease in harvest rates for the timber company (interior) matched controls.

Table B1. Proportion of projects' reported above ground standing live carbon (AGL) to the total standing live pool.

Project ID	Average ratio of AGL to total carbon
ACR173	0.806
ACR182	0.809
ACR378	0.806
CAR1013	0.805
CAR1046	0.789
CAR1102	0.807
CAR1103	0.809
CAR1104	0.808
CAR1141	0.815
CAR1174	0.807
CAR1330	0.804
CAR1368	0.807
CAR993	0.808
Average	**0.806**
Standard deviation	**0.002**

Table B2. Summary of carbon stocks and trends from three datasets. For each project, stocks and accumulation rates are calculated over the time period for which both inventory and eMapR or LEMMA data are available, at most 2012-2017. Therefore projects starting in 2017 or later are reported as n/a.

Project ID	Area (ha)	Mean reported carbon stock (ton C/ha)	Mean eMapR carbon stock (ton C/ha)	Mean LEMMA carbon stock (ton C/ha)	Mean reported carbon accumulation (ton C/ha/y)	Mean eMapR carbon accumulation (ton C/ha/y)	Mean LEMMA carbon accumulation (ton C/ha/y)
ACR173	2246	123.4	115.3	82.1	2.3	1.3	0.7
ACR182	968	139.8	142.7	111.9	0.6	0.8	1.4
ACR189	641	157.1	128.6	96.1	3.3	0.6	0.9
ACR200	714	135.1	163.0	104.3	3.6	0.9	2.0
ACR262	5328	133.1	120.2	103.9	3.5	1.2	0.6
ACR282	6064	113.8	142.8	123.6	0.6	1.4	-0.6
ACR292	2202	127.8	175.4	110.6	1.3	-0.8	-1.2
ACR377	890	183.6	135.6	104.7	-2.0	0.4	-0.1
ACR378	782	207.7	122.6	97.8	-2.8	-0.1	0.2
CAR1013	7913	106.3	143.4	105.3	1.9	1.6	1.6
CAR1041	6863	110.1	121.5	114.1	2.5	0.3	-0.3
CAR1046	4593	98.0	106.0	106.6	-11.4	-1.1	3.4
CAR1066	5053	102.9	87.6	75.3	3.2	0.9	0.7
CAR1067	855	144.6	132.9	106.3	3.6	1.4	1.7
CAR1070	8411	133.7	130.4	106.8	0.3	0.5	-0.4
CAR1092	5917	47.1	51.8	41.6	0.6	0.2	0.6
CAR1095	6642	109.7	98.1	64.5	4.5	1.6	1.0
CAR1098	9624	122.2	164.6	108.4	4.1	1.1	1.7
CAR1099	5480	113.3	167.2	113.9	4.2	1.6	1.4
CAR1100	6439	124.7	221.7	138.6	0.1	3.4	4.1
CAR1102	1422	128.2	139.5	95.2	1.1	0.5	0.3
CAR1103	848	140.9	119.9	118.9	0.9	1.2	-0.3
CAR1104	1416	126.1	139.2	120.0	1.8	1.1	0.5
CAR1114	7837	108.3	94.7	105.9	-0.2	-1.1	-1.1
CAR1139	19418	146.3	157.4	109.4	3.9	1.0	0.7
CAR1140	7156	142.3	146.7	107.6	6.6	1.2	2.0
CAR1141	877	208.5	226.8	159.9	2.3	1.0	1.2
CAR1174	1637	123.8	135.7	93.1	1.6	0.9	-0.1
CAR1180	5005	152.4	140.4	115.1	2.7	0.3	-0.2
CAR1190	3491	141.5	168.2	113.5	0.0	0.3	2.0

CAR1191	8215	147.7	136.8	115.1	0.4	0.2	0.0
CAR1313	749	269.6	191.8	170.6	n/a	n/a	n/a
CAR1329	2547	n/a	n/a	n/a	n/a	n/a	n/a
CAR1330	935	n/a	n/a	n/a	n/a	n/a	n/a
CAR1339	13443	n/a	n/a	n/a	n/a	n/a	n/a
CAR1368	3240	n/a	n/a	n/a	n/a	n/a	n/a
CAR993	3100	136.8	136.7	103.9	4.4	0.7	0.5
Area-weighted average		**125.7**	**137.4**	**105.2**	**1.97**	**0.83**	**0.82**
Standard error		**4.61**	**5.94**	**3.49**	**0.54**	**0.16**	**0.22**

Table B3. Projects' landowner information

Project ID	Area (ha)	Offset Project Operator (OPO)	Category
ACR173	2246	Round Valley Indian Tribes	other
ACR182	968	Forest Carbon Partners, LP	other
ACR189	641	Hanes Ranch Inc.	other
ACR200	714	Edward Miller Trust	other
ACR262	5328	Edward Miller Trust	other
ACR282	6064	Western Rivers Forestry	other
ACR292	2202	Congaree River, LLC	other
ACR377	890	California Timberlands 2, LLC	other
ACR378	782	California Timberlands 2, LLC	other
CAR1013	7913	Sustainable Conservation, Inc.	other
CAR1041	6863	Sierra Pacific Industries	timber
CAR1046	4593	Trinity Timberlands, LLC	other
CAR1066	5053	Sierra Pacific Industries	timber
CAR1067	855	Berry Summit, LLC	other
CAR1070	8411	Yurok Tribe	other
CAR1092	5917	Sierra Pacific Industries	timber
CAR1095	6642	Coastal Forestlands, Ltd.	other
CAR1098	9624	The Conservation Fund	other
CAR1099	5480	The Conservation Fund	other
CAR1100	6439	The Conservation Fund	other
CAR1102	1422	Montesol, LLC	other
CAR1103	848	Ronald Glass	other
CAR1104	1416	GM Gabrych Family LP	other
CAR1114	7837	Sierra Pacific Industries	timber
CAR1139	19418	Usal Redwood Forest Company, LLC	other
CAR1140	7156	Coastal Ridges LLC	other
CAR1141	877	Fred M. van Eck Forest Foundation	other
CAR1174	1637	Eddie Ranch Properties, LLC	other
CAR1180	5005	Mailliard Ranch	other
CAR1190	3491	Mendocino Redwood Company, LLC	timber
CAR1191	8215	Mendocino Redwood Company, LLC	timber
CAR1313	749	Save the Redwoods League	other
CAR1329	2547	Hunter Ranch LLC	other
CAR1330	935	Bohemian Club	other

CAR1339	13443	Green Diamond Resource Company	timber
CAR1368	3240	California Timberlands 2, LLC	other
CAR993	3100	Yurok Tribe	other

Table B4. Additionality criteria per project. We rate each project as passing (✔) or failing (✘) our criteria as established in Table 3.1. While the specific details of any individual project are fairly uncertain and should not be scrutinized, this demonstrates a general pattern that the portfolio of projects does not show strong evidence of sequestering additional carbon. "-" indicates that the project was not evaluated on the given criteria, due to having less than three years since initiation or being outside the domain considered.

Project ID	**1. Pre-project carbon** Historical carbon accumulation rate has been near-zero or negative; flat baseline is a realistic BAU	**2. Pre-project harvest** Project areas were harvested at similar rates as other similar forests over the historical period	**3. Pre-project species** Project areas have similar tree species to nearby forests, or have more high-value species (for Northern Coast)	**4. Post-project carbon** Carbon accumulation rate after project initiation is greater than the pre-initiation and that of similar forests	**5. Post-project carbon** Harvesting rate has decreased relative to pre-project levels and relative to similar forests
ACR173	✘	✔	-	✔	✔
ACR182	✘	✔	✘	✘	✔
ACR189	✘	✔	-	✘	✔
ACR200	✘	✔	✔	✘	✘
ACR262	✘	✔	✘	✘	✘
ACR282	✘	✔	✘	-	-
ACR292	✘	✘	✘	-	-
ACR377	✘	✔	-	-	-
ACR378	✘	✔	-	-	-
CAR1013	✘	✔	✘	✘	✔
CAR1041	✘	✔	-	✔	✔
CAR1046	✘	✘	-	✘	-
CAR1066	✔	✔	-	✔	✔
CAR1067	✘	✔	-	✘	✔
CAR1070	✘	✔	-	-	-
CAR1092	✔	✘	-	✘	✘
CAR1095	✘	✘	-	✘	✘
CAR1098	✘	✔	✘	-	-
CAR1099	✘	✔	✘	-	-
CAR1100	✘	✘	✔	-	-

CAR1102	✘	✔	✘	-	-
CAR1103	✘	✔	-	✔	✔
CAR1104	✘	✔	-	✘	✘
CAR1114	✔	✔	-	✘	✘
CAR1139	✘	✔	✘	-	-
CAR1140	✘	✔	✘	-	-
CAR1141	✘	✔	✔	✘	✘
CAR1174	✘	✔	-	-	-
CAR1180	✘	✘	✔	-	-
CAR1190	✘	✔	✔	-	-
CAR1191	✘	✔	✘	-	-
CAR1313	✘	✔	✔	-	-
CAR1329	✘	✔	-	-	-
CAR1330	✘	✘	✘	-	-
CAR1339	✘	✔	✘	-	-
CAR1368	✘	✔	-	-	-
CAR993	✘	✔	-	✘	✔